**UNIVERSITAT POLITÈCNICA DE VALÈNCIA**

**DEPARTAMENT DE QUÍMICA**


# Isothermal-based DNA biosensors for application in pharmacogenetics

**Ph.D. THESIS**

Submitted by

**Eric Seiti Yamanaka**

Ph.D. Supervisors:

Prof. Dr. Ángel Maquieira Catalá
Prof. Dr. Luis Antonio Tortajada Genaro

**Valencia, May 20th 2020**

Instituto Interuniversitario de Reconocimiento Molecular y Desarrollo Tecnológico

ÁNGEL MAQUIEIRA CATALÁ and LUIS ANTONIO TORTAJADA GENARO, PhD. in Chemistry and professors at the *Universitat Politècnica de València*,

CERTIFY:

That the work "*Isothermal-based DNA biosensors for application in pharmacogenetics"* has been developed by Eric Seiti Yamanaka under their supervision in the Instituto de Reconocimiento Molecular y Desarollo Tecnológico at the *Universitat Politècnica de València*, as a thesis Project in order to obtain the degree of PhD. In Experimental Techniques in Chemistry at the *Universitat Politècnica de València*.

Valencia, May 20th 2020

Prof. Dr. Ángel Maquieira Catalá  Prof. Dr. Luis Antonio Tortajada Genaro

## ACKNOWLEDGEMENTS

Although few names appear in this thesis cover, I consider this work as a compendium of the contribution of many important people, without whom it would not be possible to complete.

Firstly, I would like to thank the *Universitat Politècnica de València*, for having me accepted as a student in one of its doctorate programs, and the *Generalitat Valenciana* for the GRISOLIA/2014/024 PhD grant conceded for the execution of this work. I also acknowledge the *Ministerio de Economía, Industria y Competitividad* for the economic resources provided for this work, by the project MINECO CTQ2013-45875-R.

To my advisors Ángel Maquieira and Luis Tortajada, thank you for the opportunity and the wisdom, patience and motivation while leading this thesis work and helping me to develop myself as a better researcher.

I express my gratitude to Paula Sanchón for her essential work with the ligation set-up experiments; to Javier Carrascosa Rubio for his valuable contributions with the platform manufacturing; to Dr. Francisco Marco and Dr. David Sánchez for the real-time fluorescence measurements in their laboratory; and to my department colleagues: Eva, Enrique, Sergi, Miguel Ángel, Pilar Aragón, Patricia Noguera, Julia, Marichu, Maria José Bañuls, David Giménez, Nuria and Patricia Esteve, for their fellowship and support.

To my laboratory colleagues: Salva Mas, Edurne, Maria José Juárez, Pilar, Gabi, Dani, Miquel, Zeneida, Augusto, Vicky, Rafa and Estrella, thank you so much for the company, the joy of spirit and happiness that you transmitted me every day in the lab. Also, to my DNA-sharing colleagues, Regina, Eli, Salva Mena, Sara Santiago, Sara Martorell, Ana, Carlos and Irene, thank you for your companionship, great scientific contributions and for having the opportunity to learn every day with you. I wish you all the

curiosity, perseverance, strength and patience required in your lives and careers, especially to those who still have a thesis to defend.

Finally, I thank God for my life and for taking care of my soul. I also thank my wife Noelle for standing by my side and supporting me, no matter what the circumstances; and my family: Darwin, Neide and Tiago, who although being very far, always will be my fundamental pillar and examples for life. I hope you are proud of me and I expect to be able to return all the love and inspiration you provide me.

***Thank you all.***

## ABSTRACT

The determination of genetic biomarkers is progressively becoming more extended and popular, being commercialized even in kits for personalized medicine. Establishing specific genotype variations for each patient, such as single nucleotide polymorphisms (SNPs), could be a fundamental tool in the field of diagnosis, prognosis and therapy selection. However, the use of DNA testing is not fully implemented in general healthcare, mainly due to technical and economic barriers associated to the current technologies, which are limited only to specialized centers and large hospitals.

In this thesis, the main goal was to overcome these obstacles by developing simpler, faster and more affordable point-of-care (POC) genotyping systems. Allele discrimination was achieved by employing isothermal enzymatic reactions, like recombinase polymerase amplification (RPA), ligation of oligonucleotides and loop-mediated isothermal amplification (LAMP). These processes were integrated to colorimetric indicators and immunoenzymatic assays, in a microarray format. Using compact discs and polycarbonate chips as platforms, the detection was achieved through widespread electronics, like disc-reader, flatbed scanner and smartphone. To demonstrate their capacities, the resulting systems were applied for identifying SNPs in human samples, associated to therapies for tobacco smoking cessation, major depression disorder and blood clotting-related diseases.

After selecting the proper conditions, all studied strategies discriminated SNPs in samples containing as low as 100 copies of genomic DNA, with an error rate below 15%. Most importantly, the developed methods have reduced assays times varying between 70 and 140 minutes, at

a cost similar to a conventional PCR-based analog, but maintaining or raising amplification efficiency and eliminating the need of specialized temperature cyclers and fluorescence scanners.

In conclusion, the biosensors based in isothermal reactions and consumer electronics devices greatly improve the competitivity of POC DNA analysis. It was demonstrated that the technologies developed in this thesis could support genotyping assays in low-resource areas, such as primary healthcare centers and emerging countries. Through this democratization of genetic testing and by performing adequate association studies, molecular diagnostics and personalized medicine practices could have their application extended to the clinical routine.

## RESUMEN

La determinación de biomarcadores genéticos es cada vez más extensa y popular, estando incluso comercializándose kits para medicina personalizada. Establecer las variaciones específicas en el genotipo de cada paciente, como los polimorfismos de un solo nucleótido (*SNP*) podría ser una herramienta fundamental en el campo del diagnóstico, pronóstico y selección de la terapia. Sin embargo, el uso de pruebas de ADN no se encuentra completamente implementado en la atención médica general, principalmente debido a las barreras técnicas y económicas asociadas a las tecnologías actuales, limitadas solamente a centros especializados y grandes hospitales.

En esta tesis, el objetivo principal fue superar estos obstáculos mediante el desarrollo de sistemas de genotipado *point-of-care* (*POC*), más simples, rápidos y asequibles. La discriminación alélica se logró mediante el uso de reacciones enzimáticas isotermas, como la amplificación de la recombinasa polimerasa (*RPA*), la ligación de oligonucleótidos y la amplificación isotérmica mediada por bucle (*LAMP*). Estos procesos se integraron a indicadores colorimétricos y ensayos inmunoenzimáticos en formato de micromatriz. Utilizando discos compactos y chips de policarbonato como plataforma de ensayo, se ha logrado la detección mediante dispositivos electrónicos de consumo, como un lector de discos, escáner documental y teléfono móvil. Para demostrar sus capacidades, los sistemas resultantes se aplicaron a la identificación de SNPs en muestras humanas, asociados a terapias antitabaquismo, para depresión y enfermedades relacionadas con la coagulación de la sangre.

Tras seleccionar las condiciones adecuadas, todas las estrategias estudiadas discriminaron SNPs en muestras conteniendo tan solo 100 copias de ADN genómico, con una tasa de error inferior al 15%. Más importante, los

métodos desarrollados han reducido los tiempos de ensayo a valores entre 70 y 140 minutos, a un coste similar a un análogo convencional basado en la reacción en cadena de la polimerasa (*PCR*), pero manteniendo o aumentando la eficiencia de amplificación y eliminando la necesidad de termocicladores y escáneres de fluorescencia.

En conclusión, los biosensores basados en reacciones isotérmicas y dispositivos de electrónica de consumo mejoran en gran medida la competitividad del análisis *POC* de ADN. Se ha demostrado que las tecnologías desarrolladas en esta tesis podrían apoyar los ensayos de genotipado en áreas de recursos escasos, como centros de atención primaria y países emergentes. A través de esta democratización de las pruebas genéticas y realización estudios de asociación adecuados, el diagnóstico molecular y las prácticas en medicina personalizada podrían extender su aplicación a la rutina clínica.

## RESUM

La determinació de biomarcadors genètics és cada vegada més extensa i popular, estant fins i tot comercialitzant-se kits per a medicina personalitzada. Establir les variacions específiques en el genotip de cada pacient, com els polimorfismes d'un sol nucleòtid (SNP) podria ser una eina fonamental en el camp del diagnòstic, pronòstic i selecció de la teràpia. No obstant això, l'ús de proves d'ADN no es troba completament implementat en l'atenció mèdica general, principalment a causa de les barreres tècniques i econòmiques associades a les tecnologies actuals, limitades solament a centres especialitzats i grans hospitals.

En aquesta tesi, l'objectiu principal va ser superar aquests obstacles mitjançant el desenvolupament de sistemes de genotipat *point-of-care* (POC), més simples, ràpids i assequibles. La discriminació al·lèlica es va aconseguir mitjançant l'ús de reaccions enzimàtiques isotermes, com l'amplificació de la recombinasa polimerasa (RPA), la lligació de oligonucleòtids i l'amplificació isotèrmica mediada per bucle (LAMP). Aquests processos es van integrar a indicadors colorimètrics i assajos inmunoenzimàtics en format de micromatriu. Utilitzant discos compactes i xips de policarbonat com a plataforma d'assaig, s'ha conseguit la detecció mitjançant dispositius electrònics de consum, com un lector de discos, escàner documental i telèfon mòbil. Per a demostrar les seues capacitats, els sistemes resultants es van aplicar a la identificació de polimorfismes en mostres humanes, associats a teràpies antitabaquisme, per a depressió i malalties relacionades amb la coagulació de la sang.

Després de seleccionar les condicions adequades, totes les estratègies estudiades van ser capaces de discriminar SNPs en mostres contenint tan sols 100 còpies d'ADN genòmic, amb una taxa d'error inferior al 15%. Més

important, els mètodes desenvolupats han reduït els temps d'assaig a valors entre 70 i 140 minuts, a un cost similar a un anàleg convencional basat en la reacció en cadena de la polimerasa (PCR), però mantenint o augmentant l'eficiència d'amplificació i eliminant la necessitat de termocicladors i escàners de fluorescència.

En conclusió, els biosensors basats en reaccions isotèrmiques i dispositius d'electrònica de consum milloren en gran manera la competitivitat de l'anàlisi *POC* del ADN. S'ha demostrat que les tecnologies desenvolupades en aquesta tesi podrien donar suport als assajos de genotipat en àrees de recursos escassos, com a centres d'atenció primària i països emergents. A través d'aquesta democratització de les proves genètiques i realització estudis d'associació adequats, el diagnòstic molecular i les pràctiques en medicina personalitzada podrien estendre la seua aplicació a la rutina clínica.

## RESUMO

A determinação de biomarcadores genéticos está tornando-se cada vez mais extensa e popular, sendo comercializada até em kits para medicina personalizada. O estabelecimento de variações específicas de genotipo para cada paciente, tais como os polimorfismo de nucleotídeo único, pode ser uma ferramenta fundamental no campo do diagnóstico, prognóstico e seleção de terapias. No entanto, o uso de testes de DNA ainda não encontra-se totalmente implementado na área de saúde geral, principalmente devido às barreiras técnicas e econômicas associadas às tecnologias atuais, limitadas apenas a centros especializados e grandes hospitais.

Nesta tese, o principal objetivo foi superar esses obstáculos desenvolvendo sistemas de genotipagem *point-of-care* (POC) de DNA, mais simples, rápidos e acessíveis. A discriminação de alelos foi alcançada empregando reações enzimáticas isotérmicas, como amplificação por recombinase polimerase (*RPA*), ligação de oligonucleotídeos e amplificação isotérmica mediada por loop (*LAMP*). Tais processos foram integrados a indicadores colorimétricos e ensaios imunoenzimáticos, em formato micromatriz. Usando discos compactos e chips de policarbonato como plataforma de ensaio, os analitos foram detectados através de dispositivos eletrônicos de consumo, como leitor de disco, scanner de mesa e smartphone. Para demonstrar suas capacidades, os sistemas resultantes foram aplicados para identificação de polimorfismos em amostras de DNA humano, associados a terapias antitabagismo, para depressão e doenças relacionadas à coagulação do sangue.

Após a seleção das condições adequadas, todas as estratégias estudadas foram capazes de discriminar SNPs em amostras contendo até 100 cópias de DNA genômico, com uma taxa de erro inferior a 15%. Mais

importante, os métodos desenvolvidos reduziram o tempo de ensaio a valores entre 70 e 140 minutos, com um custo similar a um método análogo baseado em reação em cadeia da polimerase (*PCR*), mas mantendo ou aumentando a eficiência da amplificação e eliminando a necessidade de cicladores de temperatura e scanners de fluorescência especializados.

Em conclusão, os biosensores baseados em reações enzimáticas isotérmicas e dispositivos eletrônicos de consumo incrementam grandemente a competitividade da análise *POC* de DNA. Foi demonstrado que as tecnologias desenvolvidas nesta tese poderiam dar suporte a ensaios de genotipagem em lugares com poucos recursos, como centros de atenção primária e países emergentes. Através desta democratização dos testes genéticos e com a realização de estudos de associação adequados, o diagnóstico molecular e as práticas de medicina personalizada poderiam ter sua aplicação extendida à rotina clínica.

## ABBREVIATIONS

| | |
|---|---|
| ANOVA | Analysis of variance |
| APEX | Arrayed primer extension |
| ARMS | Amplification refractory mutation system |
| AS | Allele-specific |
| ASA | Allele-specific amplification |
| ATP | Adenosine triphosphate |
| BD | Blu-ray disc |
| CD | Compact disc |
| CMOS | Complementary metal-oxide semiconductor |
| COC | Cyclic olefin copolymer |
| DNA | Deoxyribonucleic acid |
| dNTPs | Deoxynucleoside triphosphates |
| dUTP | Deoxyuridine triphosphate |
| DOL | Dye-labeled oligonucleotide ligation |
| dsDNA | Double stranded deoxyribonucleic acid |
| DVD | Digital versatile discs |
| EXPAR | Exponential amplification reaction |
| FDA | Food and Drug Administration |
| FRET | Fluorescence resonance energy transfer |
| GWAS | Genome-wide association study |
| HDA | Helicase-dependent amplification |
| HNB | Hydroxynaphtol blue |
| ICAN | Isothermal and chimeric primer-initiated amplification of nucleic acids |
| ISFET | Ion-sensitive field-effect transistors |
| IVD | In vitro diagnostics |
| LAMP | Loop-mediated isothermal amplification |
| LCR | Ligation chain reaction |

| | |
|---|---|
| LNA | Locked nucleic acid |
| MALDI-TOF | Matrix-assisted laser induced - time of flight |
| MDA | Multiple displacement amplification |
| MUT | Mutant |
| NEAR | Nicking and extension amplification reaction |
| NGS | Next-generation sequencing |
| OLA | Oligonucleotide ligation assay |
| PC | Polycarbonate |
| PCR | Polymerase chain reaction |
| PEG | Polyethylene glycol |
| PLA | Polylactic acid |
| PMMA | Poly(methyl-methacrylate) |
| PNA | Peptide nucleic acids |
| POC | Point of care |
| qPCR | Quantitative polymerase chain reaction |
| RCA | Rolling circle amplification |
| RFLP | Restriction fragment length polymorphism |
| RGB | Red-green-blue |
| RNA | Ribonucleic acid |
| RPA | Recombinase polymerase amplification |
| SBE | Single base extension |
| SDA | Strand displacement amplification |
| SERS | Surface-enhanced Raman spectroscopy |
| SMAP | Smart amplification process |
| SMRT | Single molecule real-time sequencing |
| SNP | Single nucleotide polymorphism |
| SSB | Single strand binding protein |
| WGA | Whole genome amplification |
| WT | Wild type |

## LIST OF FIGURES

## LIST OF TABLES

# CONTENTS

# 1 INTRODUCTION

## 1.1 DNA assays in the clinical field

### 1.1.1 Molecular diagnostics and personalized medicine

Diagnosis is a fundamental and critical element of the current healthcare system. It makes possible to determine the nature of illnesses or health conditions, providing valuable insights for all the other stages of medical care, including prevention, prognosis and treatment. While diagnostic procedures in traditional medicine used to rely mainly on medical signs and symptom analysis, modern procedures also make use of laboratory techniques for identifying the causes of a disease, which include chemical, biochemical, immunological, hematological and microbiological tests.

The concept of molecular diagnostics was developed in the mid twentieth century, along with the growing knowledge that had been generated by molecular biology. One of the first so called "molecular diseases" was discovered in 1949 by Pauling and colleagues, who identified a single amino acid modification in the β-globulin chain that causes sickle cell anemia (*1*). Since then, advances in molecular biology and bioanalysis techniques have contributed to establish causality relations between biomolecules and medical conditions (*2*). Molecular diagnostics is currently attracting great attention, due to the vast and valuable information it provides, based on the identification of specific chemical and biological markers in a subject, which can lead to or modulate certain diseases and conditions. It is a versatile tool that supports physicians and healthcare centers, providing fast and accurate data about an individual's biomolecular profile, and also complementing traditional diagnostics and family history (*3*).

Molecular diagnostics are also a key element of personalized medicine, also called precision medicine. This new concept is described as the tailoring of medical treatment to the patient's characteristics, necessities and preferences during all stages of health care, including prevention, treatment and follow-up (*4*). Personalized medicine has a broad range of applications, such as determining a disease predisposition (either genetic or nongenetic among healthy individuals), performing diagnosis, prognosis and guiding the treatment, by anticipating the therapeutic response of the patient (*5*).

A personal healthcare can also be used in the prevention and treatment setting, by identifying high-risk individuals that may develop common diseases, such as diabetes, cancer, cardiovascular disorders, and then selecting the most appropriate preventive or treatment intervention to avoid and control the manifestation (*5*). These practices change the emphasis of medicine from reaction to prevention, helping to avoid adverse drug reactions, increasing patient adherence to treatment, revealing additional or alternative uses for drug candidates and also assisting on the reduction of overall costs in health care (*6*).

### 1.1.2 DNA biomarkers

The molecular information from individuals or patients can substantially contribute to guide prevention and treatment (*7*). Such information is usually associated to biological markers or biomarkers, which are the main object of study in these fields. According to the Biomarkers Definitions Working Group, "a biomarker is a characteristic that is objectively measured and evaluated as an indicator of normal biological

processes, pathogenic processes or pharmacological responses to a therapeutic intervention" (*8*).

Although there are several characteristics and differences between biomarkers, they can be classified in three main groups (*9*): general biomarkers, DNA biomarkers and DNA cancer biomarkers. The term "general biomarker" is used for all other forms of substances, including protein, RNA or metabolites, which can be detected in cells, tissues or biological fluids. Variations in the germline genome sequences are named DNA biomarkers, which are stable over an individual's lifetime and can be measured at any point in time. Finally, DNA tumor biomarkers are specific to cancerous tumors and are typically associated with the presence of a mutation in certain genes.

Each one of the described biomarker categories has its own applicability and advantages. DNA biomarkers are very stable and reproducible, demanding simple and high-speed detection methods, while DNA tumor and general biomarkers can be used to monitor prognostics and therapy, at the cost of more complex and laborious analyses (*9*). Herein we focus on DNA biomarkers, although the knowledge generated by this work can be also extended to oncology applications.

The Human Genome Project, completed in 2003, was a milestone in the DNA biomarker discovery (*10*). After years of sequencing work revealing the entire human genome sequence, the completion of this project opened the way for new opportunities and challenges in genomics.

### 1.1.3 Genomic variations

Humans have a similarity of about 99.9%, with an average nucleotide variation of 0.08% (*11*), which represents a total of 2.4 million base pairs.

Every person presents modifications in specific locations of their DNA, usually referred as variations or alleles. The term “wild type” is generally employed to distinguish the most common variant in a given population group. When the frequency of the minor allele is greater than 1%, the variant is called a polymorphism, while the term “mutation” is usually restricted to changes in DNA which are associated with pathologies (*12*).

The nucleotide sequence of a particular gene or segment is referred as genotype, whereas the term haplotype is usually employed to describe a cluster or set of statistically associated alleles that tend to occur together. Along with environmental and epigenetic factors, the individual’s genotype determines its observable characteristics, called phenotype (*13*).

Genomic variation can be classified in three main categories: single-nucleotide polymorphisms (SNPs) or point mutations, which correspond to a base-pair substitution; insertions or deletions of nucleotides from the regular DNA sequence; and structural rearrangements. SNPs are the most frequent, corresponding to 90% of total genomic variants, occurring approximately every 100-300 base-pairs (*14*).

Genome-wide association studies (GWAS) are used to evaluate the relation of mapped SNPs and common complex conditions in large patient cohorts, like the HapMap Project, initiated in 2003 and completed in 2005 (*15*). This large study provided a genome-wide map of the most common SNPs in different population groups, revealing a significant number of SNPs associated with different health conditions, such as Crohn’s disease, heart diseases, asthma, type 1 and 2 diabetes, rheumatoid arthritis, glaucoma and some types of cancer (*16*). Counterintuitively, most of the SNPs associated to medical conditions were found to be located in non-coding DNA regions, revealing the role of non-genomic factors in those cases. For example, certain

prostate-cancer-related SNPs located in chromosome 8q24 occur at several base-pair distance from any known coding sequence (*17*).

Insertions and deletions can vary in length from a single to thousands of nucleotides. Like SNPs, they can have no effect on the individual phenotype or produce an increased risk for health conditions. A common example of this kind of polymorphisms is called copy-number variations (CNV), which have an increasing number of associations with disorders (*18*). Copy-number variations can also be responsible for the heritability of some diseases that cannot be explained by SNPs (*12*).

Epigenetic factors can also influence DNA expression without modification of the base-pair sequence. For example, cytosine enzymatic methylation or DNA methylation, blocks the transcription of the nucleotide vicinity. Cancers commonly show abnormal DNA methylation patterns, which can be explored to develop drugs that target the affected methylation pathways (*19*). Other structural rearrangements may also have a considerable effect in pathogenesis, although these changes are difficult to measure and their role is still underexplored (*13*).

### 1.1.4 Pharmacogenetics

Pharmacogenetics is one of the fundamental fields in personalized medicine. In this area of study, drug efficacy and toxicity are correlated with inter-individual genetic variants associated to metabolizing enzymes, transporter or target proteins. The modulated expression of these proteins causes variations in pharmacokinetics and pharmacodynamics processes, generating a differential response to the studied therapy (Fig. 1).

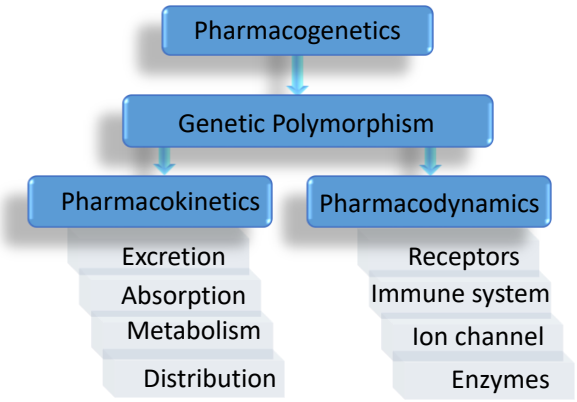


**Figure 1**. Linkage between pharmacogenetics and drug metabolic processes

In 2013, the estimated average cost for developing and approving a new drug was US$1.4 billion (*20*). Since trials represent a significant part of the development expends, identifying genetic biomarkers that determine therapeutic response can be critical to the drug discovery process and development. Moreover, the knowledge of these variations can be used for predicting efficacy and safety, increasing the chance of successful registration and lowering the risk of failure in drug development.

Therapy responses are part explained by the individual genetic background, both in terms of efficacy and toxicity, with 20-40% of the individuals having differences in drug response (*21*). More than 200 drug labels, corresponding to ten percent of the FDA approved drugs, carry pharmacogenetic information (*22*), with metabolizing enzymes accounting for 80% of the data (*23*). One of the most expressive case of pharmacogenetics association is the cardiovascular treatment with oral anticoagulant warfarin. Previous researches identified the major genetic variants that influence the metabolism of the drug (CYP2C9) and the expression of the vitamin K protein epoxy reductase 1 complex (VKORC1), which respond together for 35 to 60% of the required dose variation (*24*).

Another case in which pharmacogenetics plays a key role in treatment with trastuzumab, which is indicated only for patients with overexpression of HER2/neu (about 10%), a protein strongly related to more aggressive types of breast cancer (*25*).

In the Table 1, we list examples of the most relevant genes in pharmacogenetics, which are mainly associated with the drug absorption, transport or metabolism, and can be considered to select the adequate therapy or estimate the drug dosage.

**Table 1.** Genetic polymorphisms that influence drug response in humans (adapted from Roden et al. (26))

| Drug | Variable clinical effect | Gene | Possible mechanism |
|---|---|---|---|
| Azathioprine and mercaptopurine | Increased hematopoietic toxicity; reduced therapeutic effect at standard dose | TPMT | Hypofunctional alleles<br>Wild-types alleles |
| Irinotecan | Increased hematopoietic toxicity | UGT1A1 | Decreased expression due to regulatory polymorphism |
| Fluorouracil | Increased toxicity | DPD | Abrogation of enzymatic activity due to exonic mutation |
| Antidepressants, β-blockers | Increased toxicity; decreased activity | CYP2D6 | Hypofunctional alleles; gene duplication |
| Warfarin | Increased anticoagulant effects | CYP2C9 | Coding region variants causing reduced S-warfarin clearance |
| | Reduced anticoagulant effects | VKORC1 | Variant haplotypes in regulatory regions leading to variable expression |

**Table 1. (cont.)** Genetic polymorphisms that influence drug response in humans (adapted from Roden et al. (26))

| Drug | Variable clinical effect | Gene | Possible mechanism |
|---|---|---|---|
| HIC Protease Inhibitors, digoxin | Decreased CD4 response in HIV-infected patients, decreased digoxin bioavailability | ABCB1 (MDR-1) | Altered P-glycoprotein function |
| Codeine | Decreased analgesia | CYP2D6 | Hypofunctional alleles |
| Omeprazole | Peptic ulcer response | CYP2C19 | Hypofunctional alleles |
| Abacavir | Immunologic reactions | HLA variants | Altered Immunologic response |
| β1-antagonists | Decreased cardiovascular response | β1-adrenergic receptor | Altered receptor function or number |
| B2-antagonists | Decreased bronchodilation | β2-adrenergic receptor | Altered receptor function or number |
| Diuretics | Blood pressure lowering | Adducin | Altered cytoskeletal function by adducing variants |
| QT prolonging drugs | Drug-induced arrythmia | Ion channels (HERG, KvLQT1, Mink, MiRP1) | Exposure of subclinical reduction in repolarizing currents by drugs |
| HMG-CoA reductase inhibitors (statins) | Low density lipoprotein cholesterol lowering | HMGCR | Altered HMG-CoA reductase activity |
| Trastuzumab | Increased toxicity | HER2 /neu | Antibody-dependent cell cytotoxicity and complement-dependent cytotoxicity |

Although great progress has been made in biomarker identification and their correlation to therapy responses and side effects, the application of this knowledge in the routine clinical practice is still limited. Because pharmacogenetics is a recent field, with the exception of few drug-related proteins, the contribution of SNPs to drug effect and toxicity is still not well understood. Moreover, most of the pharmacogenetic studies focus on isolated polymorphisms, neglecting that the drug-response phenotype, like most disease phenotypes, is the result of a complex polygenic set that is also determined by epigenetic factors (*27*).

### 1.1.5 Relevant pharmacogenetic applications

Despite the difficulties related to the association of DNA biomarkers and medical conditions, in some cases the pharmacogenetic background of the disease or health problem is well known. In these cases, the drug selection, as well as dose determination and treatment prognosis, can be highly associated with polymorphisms located in key genes. In the next section we explore some examples of diseases and drugs in which pharmacogenetics can be effectively applied to carry out a personalized treatment.

#### *1.1.5.1 Smoking addiction*

Although 80% of the tobacco smokers wish to quit this habit, only 5 to 10% among them are capable of doing so without relapsing, due to the highly addicting properties of nicotine and low therapy efficacy (*28*). Thus, there is a necessity for effective measures and therapies to treat this addiction and avoid relapses during the quitting process. The vulnerability for developing a smoking addiction depends on a series of environmental and

genetic factors, being the heredity responsible for at least 50% of the predisposition (*29*). Consequently, recent pharmacogenomics researches focus on identifying genes related to highly successful therapies, offering the possibility of a personal treatment of individual addicted patients (*30*). Below we discuss some relevant SNPs related to smoking cessation therapies, describing their mechanisms and effects.

The OPRM1 gene codifies the μ-opioid receptor, a protein strictly related with the susceptibility to the addiction with several drugs, like heroin, cocaine, alcohol and nicotine. This protein acts as a primary receptor for these drugs, modulating their effect on the nervous system (*31*). Some polymorphisms present in this gene are related with sensitivity variations to nicotine, due to the structural differences they produce. The rs1799971 or A118G polymorphism is located in the first exon of OPRM1 gene and is characterized by an adenine-guanine substitution, which leads to an asparagine-aspartic acid amino acid substitution in the position 40 of the protein. This alteration induces the loss of an N-glycosylation site in the extracellular region, causing a lower affinity to nicotine (*32*). In consequence, mutant homozygous individuals (GG genotype) have a greater resistance to nicotine and alcohol than wild-type homozygous for this polymorphism, therefore being more prone to suffer from addiction. On the other hand, individuals with at least an adenine allele tend to be more responsive to addiction treatment, like alcoholism therapy with naltrexone (*33*).

The ankyrin repeat and kinase domain containing 1 (ANKK1) codifies for a protein from the serine/threonine kinase family, which is distinguished by a highly homologous amino-terminal domain. This kinase takes part in a signaling path closely related with the dopamine receptor codified by the DRD2 gene (*34*). A low density of this receptor is associated with a higher risk of addiction to nicotine or cocaine, due to high dopamine

levels in the organism (*35*). The rs1800497, also called Taq1A, is a C/T polymorphism in the exon 8 of ANKK1 gen and causes an amino acid change at the 713 position (Glu713Lys) of the C-terminal domain, affecting protein-protein interactions (*34*). Some evidences show that the rs1800497 is responsible for differential responses to the bupropion therapy in smoker patients (*36*).

The CHRNA5 gene codes for the α5 subunit of the acetylcholine neuronal nicotinic receptor. This kind of receptor is formed by two alpha, one beta, one gamma and one delta subunits, and is expressed in the central and peripheral nervous system. Specifically, the α5 subunit of this receptor is present in many nicotinic receptors, including α4β2α5, which contributes to nicotine-induced dopamine release (*37*). The rs16969968 polymorphism causes an aspartic acid to asparagine mutation, which affects the nicotine-receptor linkage. The wild-type allele is related with a higher risk of dependence, being stronger in homozygous individuals, rather than heterozygous ones (*38*).

#### *1.1.5.2 Major depressive disorder*

Major depression is a highly prevalent and often chronic disorder with an estimated lifetime prevalence of 16.2% (*39*). Although antidepressant drugs are beneficial to some patients, current treatments for depression remain sub-optimal (*40, 41*). Several weeks of treatment are required before full clinical improvement is observed and, during this therapeutic delay, patients may experience worsening symptoms and therefore withdraw from treatment prematurely. Antidepressants are also associated with side-effects that can reduce compliance in many patients. Thus, given the time-lag in the therapeutic effects and the switching of one treatment to another due to side-

effects or a lack of antidepressant response, achieving remission from depression can take several rounds of different treatments.

In consequence, it is estimated that up to 50% of patients with a major depressive episode fail to achieve remission with first line antidepressant treatment (*42*). Moreover, the probability of achieving remission decreases when additional treatments are required following the failure of a first line treatment (*40, 43, 44*). For that reasons, there is a considerable need to increase efforts in maximizing clinical outcomes in major psychiatric disorders. In this context, the identification of genetic factors underlying drug response is among the most promising areas of research in molecular medicine.

In 2007, by comparing the data of 1,816 patients of the STAR*D cohort (Sequenced Treatment Alternatives to Relieve Depression), a new marker (rs1954787) in the GRIK4 gene, which codes for the kainic acid-type glutamate receptor KA1, was identified by Paddock and colleagues (*45*). The effect size of the GRIK4 marker alone was modest, but homozygote carriers of the treatment-response-associated marker alleles of both the GRIK4 and HTR2A genes were 23% less likely to experience nonresponse to treatment relative to participants who did not carry any of these marker alleles (*45*).

The trait was corroborated by a meta-analysis 2014 study, which concluded that subjects possessing the C allele or CC genotype of the GRIK4 polymorphism rs1954787 are more likely to respond to antidepressant treatment relative to subjects harboring the T allele and TT genotype (*46*).

#### *1.1.5.3 Cardiovascular diseases*

Warfarin is a member of the vitamin K antagonists (coumarins), employed as an excellence anticoagulant, especially indicated to atrial

fibrillation patients. It presents a chiral structure, with the S isomer having 4 times more activity than the R one (*47*). This drug needs to be administered during large duration periods, which can lead to an increasing risk of losing sensitivity to the drug with the time. Moreover, the drug's efficacy depends highly on maintaining the adequate levels of anticoagulant action, leading to a very narrow therapeutic index, which is a measure of security for a drug therapy. With drug levels lower than the therapeutic dose, the risk of developing clots increases, while if the dose is too high the patient can suffer from hemorrhages in various organs (*48*).

In order to determine the adequate doses for therapy with warfarin, it is necessary to identify the genetic markers that cause variability between individuals. The P450 cytochromes are a very important group of enzymes, since they act in the metabolism of most of the drugs that enter the organism. Particularly, the CYP2C9 cytochrome has a high importance in the metabolism and inactivation of the S-warfarin. Therefore, polymorphisms in the coding gene for this cytochrome give rise to protein structures with variable levels of catalytic activity. The highest activity was found to be related with the wild-type CYP2C9*1 allele (Arg144/Tyr356/Ile359/Gly417), with CYP2C9*2 (Arg144Cys) and CYP2C9*3 (Ile359Leu) being other common variants. Only 2% of the Caucasian population is wild-type homozygous, while 20% is *1*2 heterozygous. The *3 allele is much less frequent, even in heterozygosis with the wild-type allele (*48*).

Another important gene of the warfarin action mechanism is the one that encodes vitamin K epoxide reductase (VKOR), the main target enzyme of the coumarins. This enzyme is responsible for the hydroquinone vitamin K regeneration from 2,3-epoxyde vitamin K. It acts as a cofactor and is essential to the activation from the coagulant-dependent factors of the vitamin K.

Single nucleotide variants present in the VKORC1 gene can modulate the enzyme activity and are used to determine the adequate dose depending on the genotype profile. Rieder and colleagues analyzed the 10 most frequent SNPs in this gene, identifying a low dose (A) and a high dose haplotype group (B). The resulting mean maintenance doses were 2.7 ± 0.2 mg/day for A/A individuals, 4.9 ± 0.2 mg/day for A/B and 6.2 ± 0.3 mg/day for B/B patients (*49*).

Due to the highly valuable information generated by biomarkers such as SNPs, great efforts are being made in order to develop viable methods for detecting and validating these variations. In the next section, we discuss the current technologies for sensing DNA and genetic polymorphisms.

## 1.2 Biosensors for DNA detection

### 1.2.1 Biosensing concept

During the XX century, research involving biomolecules and bioprocesses demonstrated the fundamental importance of many substances and life cycles. Such great impact generated a demand for effective, fast and feasible analytical technologies. Within this context, Clark Jr. and Lyons designed in 1962 what are currently known as the first biomolecule-based sensor (*50*), which was applied to continuously determine glucose and urea concentrations in blood. Another so-called “bio-selective sensor” was developed in 1977, where living bacterial cells were employed to selectively metabolize L-arginine producing ammonia, which was detected by a gas-sensing ammonia electrode (*51*). These pioneer systems, currently named biosensors, were highly selective and allowed real-time monitoring of the target analyte.

Although there are many interpretations for the term biosensor, the IUPAC defines it as a self-contained integrated dispositive, capable to provide qualitative and/or quantitative analytical information about a sample using a biological recognition element (biochemical receptor) (*52*). A biosensor is mainly composed by a biological recognition element in direct contact with a transduction element. The analyte recognition event produces a variation in one or various physicochemical properties of the vicinity, such as pH, heat, electronic transfer, electric potential, mass, light absorption, etc. This effect is detected by the transductor and converted in a secondary measurable signal, mainly electrical, which is processed in order to be adequately analyzed (Fig. 2) (*53*, *54*).

Combining the selectivity of the biological recognition element and the sensitivity of the transducers/detectors, biosensors are capable of detecting and differentiating constituents of complex matrices, in order to provide unambiguous identification and accurate quantification. The main advantages offered by biosensors over conventional analytical techniques are their competitive cost and analysis time, ease of use, miniaturization, portability and the ability to measure analytes in complex matrices with minimal sample preparation (*55*).

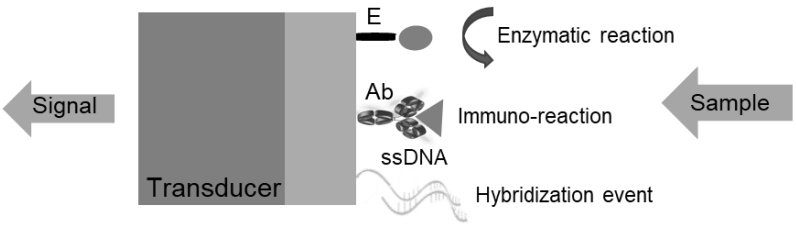


**Figure 2.** Schematic representation of the biosensing principle

Due to the high variety of available biosensors, they can be classified accordingly to different criteria (Table 2), such as the analyte-receptor type of interaction (biocatalytic or bioaffinity), nature of the recognition element (nucleic acids, proteins, biomimetic elements, tissues, whole organisms, etc.), assay format (homogeneous or heterogeneous), detection method (direct or indirect) and transduction system (generally optical, electrochemical or piezoelectric). In the following sub-sections, we describe the main elements and methods employed in DNA biosensors, exploring their advantages and limitations.

**Table 2.** Elements for biosensors classification

<table>
<tr><th>Type of biointeraction</th><th>Interaction detection</th></tr>
<tr><td>Catalytic<br>Affinity</td><td>Direct<br>Indirect</td></tr>
<tr><th>Biorecognition element</th><th>Transduction system</th></tr>
<tr><td>Protein<br>Enzyme<br>Antibody<br>Cellular receptor</td><td>Potentiometric<br>Amperometric<br>Impedimetric</td></tr>
<tr><td>DNA<br>RNA<br>Peptide nucleic acid (PNA)<br>Aptamer</td><td rowspan="2">Fluorescence<br>Colorimetry<br>Infrared spectrometry<br>SERS<br>Refraction spectrometry<br>Fiber optic<br>Interferometry<br>Polarization<br>Surface plasmon resonance</td></tr>
<tr><td>Supramolecular elements<br>Cells or cellular organelles<br>Tissues<br>Bacteria<br>Virus<br>Phages</td></tr>
<tr><td>Biomimetic element<br>Molecular imprinted polymer</td><td>Quartz crystal microbalance<br>Acoustic waves<br>Magnetoelastic</td></tr>
</table>

### 1.2.2 Assay format

The physical phase where the interaction takes place greatly affects the reaction yields and product detection. In homogeneous assays the recognition event and detection occur in the same phase, generally in solution. These methods are characterized by their simplicity and time effectiveness, allowing one-step detection and ease of automation for high-throughput analysis. In heterogeneous assays, the analyte and receptor are in different phases, usually with the receptor immobilized in a solid support. The most significant example of heterogeneous biosensor is the microarray (Fig. 3). This format combines spatially-separated spots, each one containing an individual molecular receptor, within a small area, generating a very high-resolution assay. This design allows the recognition of multiple analytes, by immobilizing different receptors on the same sensing surface. For this reason, the multiplex capacity is the main feature of this format.

In both cases, the interaction can be detected directly or indirectly. Direct or label-free detection is based on the changes of physicochemical properties in the sensor microenvironment, generated by the bio-interaction, such as mass, refraction index, luminescent waves or electric impedance. In indirect detection it is necessary to mark the reaction products, with enzymes, enzymatic cofactors, radioactive elements, fluorophores, chemiluminescent molecules or metallic particles being the most common labels. In contrast, direct detection allows real-time analysis and a simpler format, labelling the targets usually enhances sensitivity and increases the multiplex capacity, at the cost of a higher analysis time, complexity and cost (*56*).

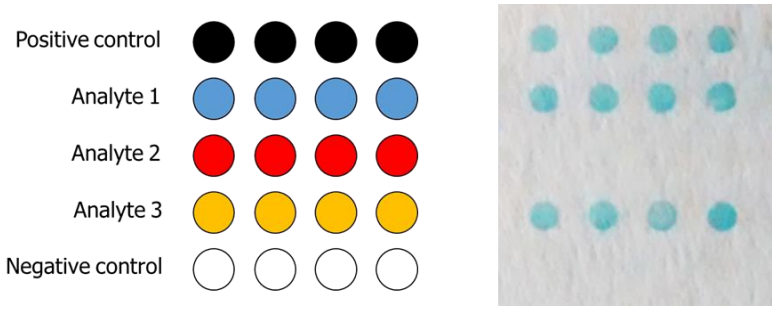


**Figure 3**. Schematic representation and image of a biomolecular microarray

### 1.2.3 Biorecognition elements

The choice of the sensing element of a biosensor will depend on a number of factors, like selectivity, assay format, detection technique, automation degree, storage, operational and environmental stability (*57*). In DNA biosensing, most methods rely on the recognition of the target by hybridization with nucleic acid probes. Since this kind of bond is highly stable, selective and reversible, the analyte can be directly detected in solution or immobilized in a surface, allowing its separation from the other sample components (*58*).

In alternative to naturally occurring nucleic acids, other synthetic recognition elements were developed (*59*). Aptamers are artificially synthesized single stranded oligonucleotides, obtained by *in vitro* selecting specific sequences of DNA or RNA from a large sequence library against a target, using the technique called systematic evolution of ligands by exponential enrichment (SELEX) (*60*). Due to this highly selective isolation process, aptamers are capable of recognizing a large range of molecules with high specificity and affinity, by tridimensional folding of their sequence (*61*). The advantages of aptamer-based biosensors (aptasensors) are their high affinity, simple sample preparation and versatility, with the capability of

recognizing inorganic ions, small organic molecules, large biomolecules or even whole cells, being compatible with different detection methods (*62–64*).

On the other hand, PNAs are synthetic molecules, similar to regular nucleic acids, where the phosphate-sugar backbone is replaced by a 2-(N-aminoethyl)-glycine chain, united by peptide bonds (*65*). Another alternative is the replacement of the natural nucleotide by a 2′-O,4′-C-methylene-β-D-ribofuranosyl nucleotide, forming a locked nucleic acid (LNA) (*66*). These chemical modifications enhance the hybridization affinity, making these synthetic nucleic acid more selective to the complementary base pair (*67*), although their application can be hindered by the higher costs and purification issues by the formation of aggregates.

### 1.2.4 Supports

Although hybridization in solution is quicker and simpler than solid-phase reactions, a separation step is usually required before detection when analyzing multiple targets or complex matrices, which favors heterogeneous assays in these cases. Three types of solid supports are employed in optical biosensors. The first one is the inert type, that has the only purpose to serve as a merely support for handling the planar sensor. The second one is the optical waveguide surface, which is used in surface plasmon resonance assays. The last type is composed by active 2D-3D supports, such as metal, inorganic or organic films, beads and nanoparticles, that can actively take part of a spectroscopic measurement (*68*).

The sensitivity and selectivity of a heterogeneous biosensor are highly dependent on the characteristics of the assay surface. In the case of DNA microarrays, the main properties that affect their performance are the structural and chemical homogeneity, hydrophobicity or hydrophilicity and

space between probes (*69*). Other factors that must be considered are the surface area, biocompatibility, mechanical and optical features.

The most common materials for the biosensor supports are silicon, glass and other types of silicates, synthetic polymers, metals, oxides and carbon (graphite, fullerenes, graphene, diamond, etc.). Herein we highlight the synthetic polymeric materials, which were developed as an alternative to more stablished substrates, such as glass and silicon. They present good mechanical properties, transparency and low background signals (*70*). Synthetic polymers are usually more affordable, chemically versatile and more suitable for mass production microfabrication techniques (*71*).

Microfluidics is a field of research that has vastly developed the automation of biosensing technologies. By fabricating assay platforms with micrometric or nanometric channels, chambers and valves, it is possible to greatly reduce reagent consumption, the amount of sample, assay times, making molecular recognition methods more portable and efficient (*72*, *73*).

Thermoplastic materials, such as polystyrene (PS), poly(methyl-meth-acrylate) (PMMA), polycarbonate (PC) and cyclic olefin copolymer (COC) are among the most employed materials for producing microfluidic chips. The most factor for making these materials more viable for composing microfluidic chips is the development of low-cost and scalable microfabrication techniques, such as hot embossing, injection molding, microthermoforming, photolithography and laser ablation (*74*).

### 1.2.5 Oligonucleotide probe immobilization

Although in situ synthesis is an interesting strategy, the most common solution for analyzing multiple targets simultaneously (multiplex analysis) is the immobilization of different recognition elements on the same surface.

After the recognition event, the other components of the sample can be washed away, avoiding interference. The main application of this principle are DNA microarrays, which are made of glass, plastic, or silicon supports and are constituted of tens to thousands of 10-100 µm reaction spots, where individual oligonucleotide sequences are immobilized (*75*).

In order to increase sensitivity and selectivity, it is necessary to improve the stability, amount and orientation of the immobilized biomolecule, while minimizing non-specific adsorption (*76*). For this reason, depending on the application, the choice of the immobilization technique is extremely important. In DNA biosensors, the main immobilization approaches are electrostatic, covalent attaching and affinity-based interaction (*77*) (Fig. 4). In the following paragraphs we describe the most common methods that apply these immobilization strategies, which are summarized in Table 3.

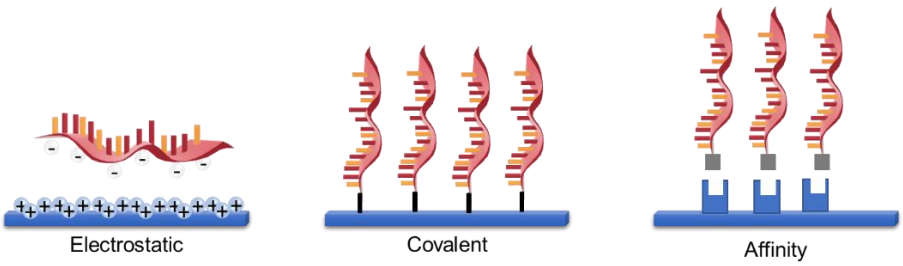


**Figure 4.** Immobilization methods for DNA probes in functionalized surfaces

Electrostatic immobilization is based in the interaction between the negatively-charged phosphate DNA backbone and a positively charged surface. By this approach, researchers achieved the immobilization of oligonucleotide probes on various types of materials, specially glass (*78*, *79*).

After contacting of the surface with the probe solution, the unabsorbed DNA can be removed by rinsing.

While physical adsorption provides simple and rapid immobilization, with minimum chemical reagent consumption, it relies mainly on electrostatic interaction, being highly influenced by changes in the medium conditions, such as pH, ionic strength and temperature. Additionally, the random orientation of the immobilized probes on the surface can also influence the hybridization yield (*80*).

The second approach for DNA probe immobilization is the covalent attachment on activated surfaces. This is a more stable and selective approach for immobilizing DNA probes than physical adsorption, although it frequently requires their chemical modification. In this category, one of the most applied methods is the chemisorption of thiol-modified probes, which have great affinity with noble metals. Based on this principle, the sulfur-metal covalent bonds are used for immobilizing DNA in gold surfaces (*81*).

Other popular mechanism for covalent immobilization is the activation of carboxylated surfaces with 1-ethyl-3-(3-dimethylaminopropyl)-carbodiimide (EDC), followed by binding of aminated probes, which can be optionally combined with N-hydroxysuccinimide (NHS) (*82*). This method presents a high versatility, since it can be adapted for a large number of functional groups (*80*).

Another alternative for DNA probe immobilization is the use of affinity-mediated attachment, such as avidin-biotin or streptavidin-biotin interaction. Biotin is a small molecule with a very high affinity to avidin or streptavidin, forming a complex that is resistant to different stringent conditions (*83*). Thus, by employing biotin-modified DNA probes, it is possible to achieve highly stable and specific immobilization with avidin-(streptavidin) molecules on surface (*84*). Avidin and streptavidin are large

tetrameric proteins with four identical binding sites, which provides a high immobilization yield. Among these two, streptavidin is more usually employed, due to its lower nonspecific binding, consequence of a lower isoelectric point (5 vs 10.5 of avidin) (*76*). In addition, these proteins can be easily immobilized on the sensing surface by adsorption (*85*); or alternatively by chemical bonding on activated surfaces (*86, 87*).

**Table 3.** Methods for oligonucleotide probe immobilization

| Immobilization method | Surface property | Probe modification | Reference |
|---|---|---|---|
| Electrostatic | Amine | - | (*88*) |
| | Nitrocellulose | - | (*89*) |
| | Poly(L-lysine) | - | (*90*) |
| | PAAH | - | (*91*) |
| | Diazonium ion | - | (*92*) |
| Chemisorption | Gold | Thiol | (*93*) |
| Covalent | Silicate | Silane | (*94*) |
| | Carboxyl (with EDC) | Amine | (*95*) |
| | Aldehyde | Amine | (*96*) |
| | Epoxy | Amine | (*97*) |
| | Isothiocyanate | Amine | (*98*) |
| | Maleimidie | Thiol | (*99*) |
| | Mercaptosilane | Thiol | (*100*) |
| Affinity | Streptavidin | DNA-biotin | (*101*) |
| | Avidin | DNA-biotin | (*81*) |

PAAH: polyallylamine hydrochloride

EDC: 1-ethyl-3-(3-dimethylaminopropyl)carbodiimide

### 1.2.6 Transduction systems

Transductors are the elements that convert variations in physicochemical properties into measurable analytical signals, in order to identify and quantify a biorecognition event. While there are many types of transduction systems, choosing an adequate one is determined by particular

demands and features of the final application. Nevertheless, the most common transduction systems are electrochemical, piezoelectrical and optical (*102*).

Electrochemical transductors are based in current, potential or impedance changes, produced by the interaction between the analyte and bioreceptor. Due to the simplicity of their components, electrochemical transductors are very affordable, fast and easily miniaturizable. For oligonucleotide detection, the most common electrochemical techniques are amperometry, which is based in electric current variations, and conductometry, which uses conductance changes to detect the biorecognition event (*103*). The main signaling strategies for electrochemically detecting DNA are based on the direct or catalyzed oxidation of DNA bases, reporter molecules and enzymes, or by charge transport reactions (*104*).

On the other hand, piezoelectrical or mass transduction systems measure mass changes generated by the formation of the analyte-bioreceptor complex. The piezoelectric crystals employed in these systems vibrate at a specific frequency, which is proportional to an applied electric current and the crystal's mass. By measuring oscillation variations generated by the biorecognition process, it is possible to determine the additional mass of the crystal (*78*). The main advantages of piezoelectric transduction are its label-free capacity and high sensitivity, at the cost of a higher price and limited multiplex capabilities (*76*, *105*).

Finally, optical transducers are based in the measurement of variations in light properties as a consequence of the analyte and bioreceptor interaction. These variations are caused by different phenomena, like fluorescence, absorption, interferometry, luminescence, scattering, reflection or refraction in the recognition region (*53*). Due to variety of light features that can be measured, optical devices offer the largest number of subcategories among the three main groups of transducers. Optical methods

are also the main category explored in this thesis due to the versatility they provide.

Among the optical detection biosensors, the most common principle is fluorescence, due to its simplicity, sensitivity and speed. It is based on the use of polyaromatic hydrocarbons or heterocycle-based fluorophores that have a higher fluorescent emission in the presence of the target DNA. By employing different wavelength dyes, it is possible to detect multiple DNA sequences (*106*), which was explored in the development of massively parallel assay chips (*107*).

The change in the local refraction index is an optical measurement explored in surface plasmon resonance (SPR). This technique is highly specific, fast and label-free, allowing real-time analysis with multiple usages of the sensing surface (*105*), being previously applied for mutation detection (*108, 109*).

Conjugating sequence-specific oligonucleotide probes with nanoparticles is also an effective way for allowing colorimetric detection of DNA targets, which is simple, harmless and relatively inexpensive (*110*). By exploring the aggregation of oligonucleotide probe-functionalized gold nanoparticles after hybridization with the target, a colorimetric measurement can be applied for detecting SNPs (*111*, *112*).

Other expressive optical techniques used for DNA sequence detection are fiber optics, that can be used in an array format to create a low-area biosensor for individually monitoring multiple probes (*113*) and for SNP detection (*114*); and surface-enhanced Raman spectroscopy (SERS), which employs precisely fabricated surfaces in order to produce a specific scattering pattern, being capable of determine single nucleotide polymorphisms (*115–117*).

## 1.3 SNP genotyping methods

As seen in previous sections, SNPs are important biomarkers for determining genetic diseases, medical conditions or therapy response. Therefore, SNP detection technologies have been crucial tools in the development of personalized medicine. They can be used in entire genome scanning studies for discovering unknown disease-related polymorphisms or, on the other hand, screening (genotyping) individuals in order to verify the presence of previously cataloged variations. Selectivity and sensitivity are most important factors in SNP detection methods, since a single nitrogenous base difference must be detected in a full or partial genome sequence, often with low amounts of sample. In addition, other critical aspects must be considered, like the assay robustness, speed and cost, depending on the application.

In the following section, we explore the main strategies for discriminating SNPs, as well as the most important technologies currently available for identifying and quantifying this kind of DNA variation. The majority of the approaches can be classified in four main mechanisms: hybridization, primer extension, oligonucleotide ligation and enzymatic cleavage (*118*). These principles are reliable and well developed, being applied in the vast majority of the genotyping technologies.

### 1.3.1 Discrimination mechanisms

#### *1.3.1.1 Hybridization*

The DNA hybridization is characterized by the selective pairing of a synthetic DNA oligonucleotide to a biological DNA target sequence. This

process forms the basis for most modern DNA analysis, having as main advantages its simplicity, high multiplexing capacity and robustness. Unlike enzymatic-based methods, hybridization is a biophysical phenomenon, which is efficient in variable medium conditions and is the simplest of the discriminating strategies. However, it generally does not provide sufficient sensitivity for practical use, and must be coupled with a signal amplification technique or highly sensitive detectors (*119*).

In allele-specific hybridization, the polymorphism is recognized by oligonucleotide probes that anneal with the target sequence only when they match perfectly (Fig. 5). Under optimized conditions, a single nucleotide difference is sufficient for limiting the hybridization only to one of the two allele-specific probes. As the oligonucleotide probe is the key element in this mechanism, a successful discrimination relies strongly on the probe design, meaning oligonucleotide sequence and length, as well as the SNP location and hybridization conditions (*118*). Currently, more advanced designing algorithms, as well as probe chemical modifications and the use of enhancement moieties, like DNA minor groove binders, allow the hybridization assays to be highly specific to the target SNPs (*120*).

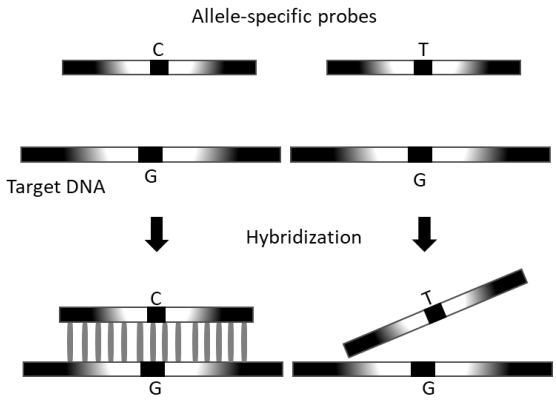


**Figure 5.** Single nucleotide polymorphism genotyping by hybridization

#### *1.3.1.2 Primer extension*

This strategy relies on the specificity of a DNA polymerase to selectively incorporate one or more nucleotides in a primer sequence. It is a very robust and flexible mechanism, with simple probe design and assay optimization. In order to reach the adequate sensitivity, primer extension methods are usually performed after a polymerase chain reaction (PCR) amplification step, which greatly increases the number of target copies. For this reason, a purification step is generally required, so that residual primers and dNTPs from the PCR reaction are removed from the medium. In addition, variables as nucleotide labelling and chemical modifications can be implemented for allowing different assay platforms and detection techniques.

Although there are several variations of the primer extension process, the majority of methods can be classified in two categories: allele-specific extension and single base extension (SBE) (Fig. 6). In the former group, the extension is performed with allele-specific primers, with a single base change in their 3'-end that is complementary to the SNP site. On the other hand, single base extension uses a common primer with the 3'-end adjacent to the SNP and dideoxynucleotides (ddNTPs), which are selectively incorporated to the primer and terminate the extension process (*121*).

The first primer extension category is called allele-specific extension, being first reported by Richard Gibbs (*122*), who observed amplification yield differences between 3'-end matched and mismatched forward primers in a PCR reaction, with combination with a common reverse primer. This strategy made possible to discriminate single nucleotide polymorphisms based in the presence or absence of the amplification product. Currently, this method is

called allele-specific PCR and can be combined with capillary electrophoresis and fluorescence for SNP genotyping (*123, 124*).

Additionally, allele-specific extension can be performed without the reverse primer, which reduces the amplification yield but increases selectivity. Some examples of this kind of approach involve the use of fluorogenic primers (*125*) or tagged primers, followed by capture in microbeads (*126*) or microarrays (*127*).

The second primer extension category is single base extension (SBE), also called minisequencing. The methods comprised in this group explore the use of a common primer with its 3'-end adjacent to the SNP site, where a dideoxynucleotide (ddNTPs) is incorporated and blocks the polymerase from continue extending (*128*). Subsequently, the identity of the incorporated base is determined by different detection methods. In Table 5, techniques based in SBE are summarized, according to their main features. While more sophisticated detection methods, such as mass spectrometry coupled with matrix-assisted laser induced time of flight (MALDI-TOF), provide highly accurate label-free assays, simpler techniques like fluorescence and photometric measurements can be employed for a higher cost-effectiveness and increased multiplex capacity.

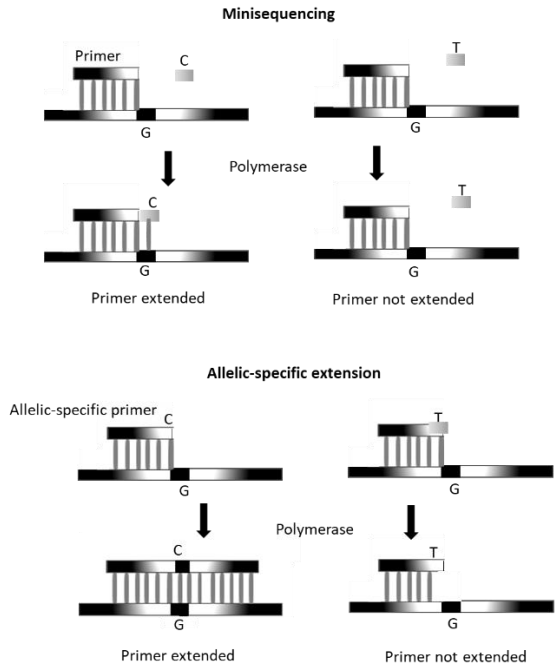


**Figure 6.** Single nucleotide polymorphism genotyping by allele-specific extension

**Table 4**. Primer extension SNP genotyping methods

| Technique | Principle | Detection | Comment | Reference |
|---|---|---|---|---|
| PinPoint™ assay | SBE with unlabeled ddNTPs | MALDI-TOF MS | Simplest technique, reduced accuracy due to low spectral peak resolution. | (*129*, *130*) |
| MassEXTEND™ | Mixture of regular dNTPs and unlabeled ddNTPs | MALDI-TOF MS | Increased mass difference of extended products, with higher resolution | (*131*) |
| GOOD™ assay | Phosphorothioate-modified primers, α-S-ddNTPs | MALDI-TOF MS | Short charge-tagged extension fragments increase spectral resolution and eliminate the need of sample purification | (*132*, *133*) |
| SPC-SBE | Biotin-labeled ddNTPs and capture of extended products by streptavidin-coated beads | MALDI-TOF MS | Increased specificity by the isolation of extension products | (*134*) |
| SNaPshot™ | SBE with fluorescent labeled ddNTPs | Capillary array electrophoresis and fluorescence | Decreased detection complexity and increased multiplex capacity by 5'-end tails | (*135*) |
| Homogeneous extension and solid-phase detection | Tagged primers and capture of extension products in a solid support | Fluorescence scanning | High extension efficiency by performing reaction in solution. Increased multiplex capacity by immobilized products | (*136*) |
| Arrayed primer extension (APEX) | 5'-end immobilized primers. Extension in solid-phase | Fluorescence scanning | Increased specificity and multiplex capacity. Decreased extension efficiency, leading to lower sensitivities | (*137*, *138*) |
| Solid-phase amplification and extension | 5'-end immobilized primers. PCR and extension performed in solid-phase | Fluorescence scanning | Improved specificity by primer-primer interaction reduction. Decreased extension efficiency, leading to lower sensitivities | (*139*) |

### *1.3.1.3 Oligonucleotide ligation*

DNA ligase is highly efficient enzyme for repairing nicks in DNA molecules, by regenerating missing phosphodiester bonds. This ligation process occurs only when two oligonucleotides are annealed to a target template in adjacent positions. As this phenomenon is strictly dependent on the perfect alignment of target and complementary strands, the reaction can be applied for SNP genotyping purposes, by determining if the ligation product was formed in the presence of allele-specific probes (*140*) (Fig. 7). This discrimination method is called oligonucleotide ligation assay (OLA), being performed with two allele-specific probes and a common probe. Most OLA methods employ allele-specific probes with their 3'-end at the SNP site, since ligases are more sensitive to mismatches at this position (*118*).

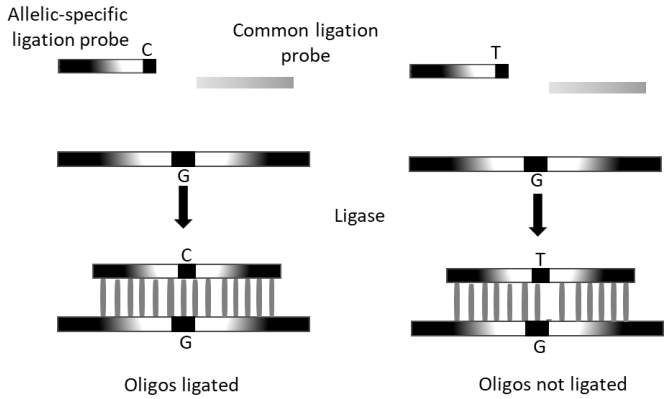


**Figure 7.** Single nucleotide polymorphism genotyping by allele-specific ligation

Enzymatic ligation has the highest specificity among the allele discrimination mechanisms, but requires a high number of modified probes and previous amplification for reaching adequate sensitivity (*120*). Eggerding and colleagues reduced assay time and manipulation by performing PCR and

ligation in one step (*141*). This method, called coupled amplification and oligonucleotide ligation (CAL) used high melting temperature primers and low $T_m$ ligation probes. After template denaturation, higher temperature steps were used for primer hybridization and extension, while in a second phase, the temperature was lowered, allowing ligation to occur. A real-time variation of the CAL method is the dye-labeled oligonucleotide ligation (DOL), in which the allele-specific probes are labeled with fluorescence acceptor dyes, while the common probe is coupled to a donor dye. Detecting the ligation products can be carried out in real time by measuring the increase in fluorescence resonance energy transfer (FRET) produced by closed proximity of the ligated probes (*142*).

Besides combining PCR and ligation, polymerase-free ligation can be performed replacing PCR amplification by a process ligation chain reaction (LCR). In this method, two oligonucleotide probe pairs (one for each strand) are joined by a thermostable ligase and used as new ligation templates in consecutive denaturing/annealing cycles, exponentially increasing the number of target copies (*143*).

Another way to avoid PCR is to use the ligation mechanism to circularize padlock probes. This kind of probe is comprised by a linear oligonucleotide sequence designed to have both ends complementary to the DNA template, forming a closed structure after hybridization (*144*). If correctly ligated, the padlock probe will form a circular strand, that can be amplified by rolling cycle amplification (*145*–*147*).

A high-throughput variation of this method is called molecular inversion probe technique (MIP), which employs a single base extension of a modified padlock probe prior to the ligation. The reaction is followed by degradation of non-ligated probes, linearization and PCR amplification of the

joined probes with sequence tagged primers, generating amplicons that are hybridized to a fluorescence detection microarray (*148–150*).

#### *1.3.1.4 Enzymatic cleavage*

Enzymatic cleavage is a mechanism based on the ability of restriction enzymes to recognize specific sequences and structures in DNA, cleaving both strands at or near a particular position. Since the recognition is highly affected by allelic polymorphisms, the process can be explored to discriminate SNPs located in restriction enzyme sites. This technique, called restriction fragment length polymorphism (RFLP), is carried out by incubating a PCR amplicon with the corresponding enzyme, which cleaves the DNA if the polymorphism is present, generating shorter length strands, which are separated and visualized by electrophoresis (*151*) .

Since RFLP relies only on the specificity of the restriction enzymes to cleave the target sequence, the method does not require oligonucleotide probes. However, as each restriction enzyme can recognize a unique DNA sequence, the method throughput is limited. On the other hand, it is mandatory that the SNP is located in a specific restriction enzyme sequence, which narrows the scope of possible polymorphisms that can be detected by this method (*118*).

For SNPs genotyping purposes, the most popular application is the invasive cleavage. It was developed in 1999 as the Invader® assay and uses a flap endonuclease called cleavase to recognize a triplex structure, formed by the target DNA, an invader probe and an allele-specific signaling probe (*152, 153*). The invader probe is complementary to the 3'-end of the polymorphic site, while the signaling probe has two regions: one complementary to the 5'-end of the SNP, including the polymorphic base, and

a non-complementary 5' arm, also called flap segment. The cleavase recognizes the structure only when the target strand, invasive probe and allele-specific probe overlap, cleaving the probe and releasing the flap segment (Fig. 8). A size analysis can determine if this sequence was released, either by electrophoresis or mass spectrometry. However, as the signaling probe can be modified with haptens or dyes, the detection can be performed with enzyme-linked immunoassay or fluorescence resonance energy transfer (FRET). (*153*). With this modification, an invasion cleavage FRET-based method was automated and applied for genotyping 36 SNPs and one insertion polymorphism, with simultaneous analysis of 384 individuals (*154*).

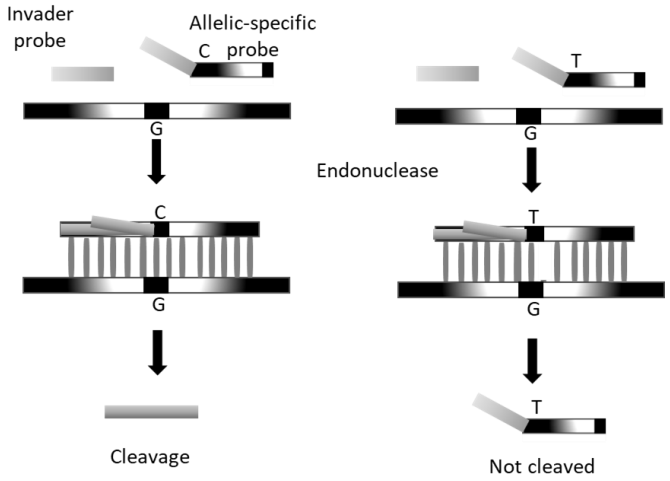


**Figure 8.** Single nucleotide polymorphism genotyping by invasive cleavage

In order to increase sensitivity, Hall and colleagues developed a modified signaling probe, in which the cleaved flap segment serves as an invader probe for a second cleaving reaction. This strategy increased the number of labeled cleaved product by three orders of magnitude, from $10^4$ to $10^7$ per target sequence per hour (*155*), avoiding the requirement of high

template DNA amounts or a previous PCR step. Also, Hsu and colleagues reduced the assay time, employing different fluorophore labels for the signaling probes, which allows the simultaneous detection of both alleles in the same reaction (*156*). As a major drawback, the high number of modified probes required for the described methods generates a cost increase by the labelling process, and significant effort in oligonucleotide designing and optimization.

More recent applications make use of the enzymatic cleavage in microsphere and microarray formats, increasing the multiplexing capacity (*157*, *158*). Also, alternative assay platforms were more recently developed to reduce the assay cost, by miniaturization (*159*) and electrochemical detection (*160*).

### 1.3.2 Genotyping technologies

Currently, the technologies available for genome variation detection and quantification can be grouped into three main categories: next-generation sequencing (NGS), polymerase chain reaction (PCR) and microarray-based methods. Each of these approaches shows different advantages, disadvantages and technical features, which will be further discussed.

#### *1.3.2.1 Next-generation sequencing*

Until the 1970s, determining a DNA sequence was very difficult and laborious. However, in 1976-1977, two different rapid sequencing methods were simultaneously developed. The first one, developed by A. Maxam and W. Gilbert, was based in the chemical modification of the target DNA, followed by cleavage in specific positions (*161*). The other technique, created

by F. Sanger, used consecutive chain-termination reactions in order to determine the nucleotide at each position (*162*). Due to its lower complexity, high efficiency, lower amounts of radioactive and toxic reagents, the Sanger method has become more popular and is still frequently used nowadays.

The original Sanger method makes use of regular dNTPs and ddNTPS that are incorporated in a target primer. The labeled ddNTPs terminate the replication, generating different size fragments that are further separated and visualized in a denaturing polyacrylamide gel. By comparing the positions in which each base is observed, the target sequence can be inferred. The Sanger technique is currently considered the gold standard of DNA sequencing and was exclusively used for decades for determining genome sequences of various sources. However, the high cost and relatively low throughput associated to this method hindered its application for routine translational research.

After the completion of the Human Genome Project, researchers and diagnostics companies have been specially interested in developing more affordable and faster sequencing alternatives, called next-generation sequencing (NGS) techniques. Unlike Sanger sequencing, which requires homogeneous DNA as template, NGS methods may be applied for heterogeneous samples and allow the simultaneous analysis of more than 10 million randomly selected DNA molecules (*163*, *164*). As a disadvantage, these methods have a higher error rate compared to traditional sequencing, usually associated to signal reading, enzyme fidelity and imperfect deprotection, which is specially problematic when dealing with low-frequency polymorphisms (*119*).

All NGS methods share the capability of performing massively parallel sequencing, through assaying in microfluidic platforms, generating gigabases of nucleotide data in a single run. They differ from each other

mainly by the recognition mechanism and detection strategy. Here we explore the most representative NGS techniques and their applications.

#### *1.3.2.2 Pyrosequencing*

Pyrosequencing is a sequencing-by-synthesis method, relying on chemiluminescence detection. It is based in the release of pyrophosphate molecules when a nucleotide is incorporated to DNA strands by a polymerase. In this process, the target DNA is end-repaired and ligated to adapter oligonucleotides immobilized on magnetic beads. The immobilized strands are then amplified by digital PCR and the beads are transferred to picoliter wells in a microfluidic chip. The extension reaction occurs when deoxynucleotides are sequentially injected through the microfluidic chip, one at a time. With the aid of an enzyme cascade system, formed by ATP sulfurylase and luciferase, the released pyrophosphate is converted to ATP, which is used to produce visible light. Free unincorporated nucleotides are then degraded by apyrase. As the light intensity generated is proportional to the number of extended nucleotides, the addition of separated unmodified dNTPs in a defined order allows to infer which base was incorporated (*165*, *166*).

A sequencing capacity of 400-600 million bases per run is achievable by pyrosequencing, with 400-700-base read lengths, which is higher than most sequencing techniques (*167*). However, the main limiting factors associated with the technique are the complex template preparation, limited multiplex capacity and higher error rates when sequencing long homopolymers (>8 bases) (*121*, *168*).

### *1.3.2.3 Sequencing-by-synthesis*

The Illumina™ method (*169*) relies on an engineered polymerase for incorporating fluorescence-labeled nucleotides in a reversible dye-termination mechanism. The studied DNA fragments are ligated to adapter oligonucleotides and hybridized to immobilized forward and reverse universal primers, which are attached to microbeads. Amplification is carried out by digital PCR, generating clusters of tethered amplicons. Next, the four types of reversible terminator nucleotides are sequentially flowed into the microfluidic chip. After washing away non-incorporated nucleotides, fluorescence scanning can be performed and the fluorescent dyes are cleaved off from the extended sequences, allowing the next round of nucleotide incorporation.

Illumina is currently the leader in throughput (1.5 Tb), sequencing error rate and cost per read ($2 per $10^6$ bases). However, it is one of the slowest NGS techniques, with a reading rate of approximately 150 nt per day (*119*). Illumina has developed benchtop sequencing systems with lower throughput (<15 gigabases), called MiSeq™ and NextSeq™. The former was the first NGS system to receive clearance from de Food and Drug Administration (FDA) for in vitro diagnostics (IVD) (*170*), being the base platform for a FDA cleared cystic fibrosis variant genotyping assay (*171*).

### *1.3.2.4 pH-monitored synthesis*

Differently from the previously described technologies, which are based in spectrophotometric measurements, the Ion Torrent™ sequencing system is based on the detection of protons, released during each nucleotide incorporation event (*172*). The assay is carried out in miniaturized pH sensors,

which are microwells containing ion-sensitive field-effect transistors (ISFET). Emulsion PCR products from the DNA template are placed in the microwells and nucleotides are sequentially added to the sensors, one at a time, producing localized pH changes when extension occurs.

Due to the nature of the sensor, the main advantages of the Ion Torrent system are its high reading speed (approximately 100 nt per hour), associated with the fast response of the ISFET, and lower equipment cost, since an electrochemical sensor is used instead of an optic system (*119*). However, the method presents higher error rates, associated with homopolymer regions, which generate non-proportional pH changes, and base misincorporation due to the presence of only one nucleotide type in each cycle (*119*, *168*). Also, as a lower throughput is achieved with this method, its cost per read is relatively higher than Illumina, with approximately $10 per $10^6$ reads (*119*).

#### *1.3.2.5 Single molecule real-time sequencing (SMRT)*

This Pacific Biosciences technology is a sequencing-by-synthesis technique, which relies on the real-time detection of fluorophore-labeled nucleotides in a zero-mode waveguide well (*173*). This nanoscale reaction well contains an immobilized sequencing complex at its bottom, formed by a DNA polymerase molecule, the target DNA and a complementary sequencing primer. The ZMW is designed in order to create a zeptoliter-sized observation zone, where the sequencing complex is located, allowing the detection of a single nucleotide when it is bond to the primer. As the nucleotides are fluorescently labeled in the gamma-phosphate position, they are naturally cleaved after extension, allowing the next round of incorporation. Thus, primer extension and fluorescence measurement are done simultaneously,

with a continuous reading of 75 reads per second, allowing real-time monitoring of the DNA synthesis. Each type of nucleotide is labeled with a different fluorescence tag, making possible to call the extended base according to the color generated in the ZMW.

The main advantage of this technique is its very high read lengths of 10,000 nt in average and a maximum of roughly 40,000 nt, while other methods are usually limited to 300 nt. On the other hand, higher intrinsic error rates are observed with SMRT, in addition to a higher cost of roughly $300 per $10^6$ bases (*119*).

#### *1.3.2.6 Nanopore-based sequencing*

The Oxford Nanopore sequencing method is distinct from other technologies in the way DNA sequences are analyzed. Instead of using polymerase-based extension, the target DNA is threaded and pulled through an enzyme nanopore embedded in a synthetic membrane. Different nucleotides generate specific electric current variations, which are measured and used to infer the identity of the base (*174*, *175*).

Genia Technologies has also developed an NGS method based in nanopore reading. However, this method uses a tethered polymerase molecule in the nanopore complex to extend a primer. The dNTPs are modified with polyethylene glycol-based tags with different sizes, which are cleaved in the extension process and generate specific electric currents through the nanopore (*176*).

### *1.3.2.7 PCR-based techniques*

DNA replication was a well-known process in 1983, when the polymerase chain reaction (PCR) was developed (*177*). This technique consisted in an enzyme-driven, primer-mediated and temperature-dependent DNA replicating process, which revolutionized molecular biology due to its efficiency and velocity. By employing PCR, the identification of a known polymorphism was accelerated from a scale of months to hours. It explored the use of a DNA polymerase for adding deoxynucleotides to previously designed primers, which recognized a specific target sequence in the desired genome. The process consisted of a repetition of temperature cycles: an initial thermal aperture step at 95 °C, followed by an annealing step at the primers melting temperature, and an extension step at the enzyme optimal activity temperature. After the first cycle, the original DNA and generated strands could be used as new targets, allowing the number of copies to grow exponentially.

A main problem, associated with the high temperatures of the denaturation step, was the activity decrease of the polymerase, which demanded the constant addition of enzyme after a certain number of cycles. This problem was solved by employing a thermo stable enzyme from *Thermus aquaticus* (Taq polymerase) (*178*), making the reaction very efficient and facilitating the automation of the process.

A variation of the original reaction is called multiplex PCR, which carried out with the addition of two or more primer-pairs in the same test-run. This allows the operator to simultaneously replicate several target genes in a single tube, reducing the assay time and reagent consumption. However, proper primer designing and screening are essential for selectively amplify all

targets at similar yield. Also, selecting an adequate detection method is important to identify the mixed amplification.

Another very useful variation of this reaction is real-time PCR or quantitative PCR (qPCR), developed by Higuchi et al. (*179*). This technique is based on the fluorescence detection of the PCR products in real time, allowing the analyst to continuously monitor the reaction and avoiding post-amplification analysis. Generally, the labelling of the amplification products can be carried out by intercalating dyes, such as SYBR Green I, which binds to double-stranded DNA and generate a non-specific fluorescent signal (Light Cycler assay); or with the use of fluorescent probes that produce a fluorescence signal only when specifically hybridized to the target cDNA (TaqMan assay). Also, after amplification the resulting products can be analyzed by a melting curve, determining the melting temperature of the amplicons.

The polymerase chain reaction has been the main solution for solving problems associated with low amount of template DNA or low-frequency mutations, since it can amplify in several times the region of interest. The technologies based in PCR have the advantages of high DNA quantifying accuracy, high molecular sensitivity and ease of use. On the other hand, multiple targets are difficult to analyze with this approach, since a high number of primers can generate primer-dimers that produce false negative or positive results.

One of the early PCR-based technique is the amplification refractory mutation system (ARMS). It relies on the high sensitivity of polymerases to mismatches at the 3'-end of primers, only extending properly when complementarity is present at that position (*180*). This mechanism is suitable when the mutation is present at 50% or 0% frequency (*181*), but is not as consistent with lower frequencies, such as somatic mutations, where the

polymorphism can be present at a concentration as low as 5%. Since some mismatches are more thermodynamically destabilizing or more easily recognized by the DNA polymerase, this can lead to false positive amplification of the untargeted polymorphism. The optimization of primer design and medium conditions can contribute to mitigate this problem. Furthermore, additional mismatches can be introduced in the ARMS primers near the 3'-end, providing improved specificity in exchange of a lower amplification yield.

Blocking oligonucleotides are also an option for suppress the amplification of an allele, in a technique called blocker PCR. These blockers are designed to hybridize to a specific polymorphic site, avoiding primer annealing and preventing amplification. Blocker PCR has the advantage of providing compound specificity through multiple amplification cycles, since the blocker is not extended and continuously prevents primer annealing. The first reported case of blocker PCR uses a peptide nucleic acid (PNA) oligonucleotide, which cannot be extended or digested by DNA polymerases (*182*). The PNAClamp is an IVD method for guiding cancer therapy, based on the analysis of EGFR, KRAS, BRAF, PI3K and IDH1 genes (*183*). Other approaches of this technique are xeno nucleic acids (XNA), which have improved binding affinity than PNA (*184*), and the Selector assay by Biocept, employing more affordable 5' phosphorothiate-modified DNA blockers (*185*).

#### *1.3.2.8 Hybridization techniques*

The allele-specific hybridization is the basis of several homogeneous genotyping methods, which are usually distinguished by the way the hybridization event is detected. Some authors employed Cy5-labeled and

fluorescein-labeled oligonucleotides (primers and/or probes) that when hybridized to the target sequence are in fluorescence resonance energy transfer. By using a melt curve analysis, an increase in fluorescence is observed, as the labeled oligonucleotides denature and separate from each other (*186*, *187*).

Other significant hybridization-based genotyping methods use different types of mechanisms. For instance, in the 5' nuclease assay, a fluorogenic probe, labeled with a reporter fluorescence dye and a quencher, anneals to the target DNA product and is cleaved during PCR amplification, generating a fluorescence signal (*188*).

Molecular beacons are also a very popular type of hybridization probe. These are partially self-complementary oligonucleotides that form a stem-loop structure in normal conditions, but can linearly anneal to a target ssDNA in optimal conditions. By labeling the ends of the beacon with a fluorescent dye and quencher, one can infer the presence of a polymorphism by analyzing the fluorescence generated in the hybridization event (*189*, *190*).

Another example are the light-up probes, developed by Svanvik and colleagues (*191*), which are peptide nucleic acids (PNA) linked to an asymmetric cyanine dye. When correctly hybridized, the dye binds to the target DNA, increasing the fluorescence signal, in a more simple and selective way than FRET-based probes.

#### *1.3.2.9 Microarray-based methods*

Array-based genotyping techniques are a special subgroup of the hybridization methods, which make use of spatial arrangement in order to highly increase the multiplexity of the analysis. This is achieved by oligonucleotides probes immobilized in a solid platform, that hybridize to the

target labeled amplification products. This format allows the parallel analysis of multiple genes, since each oligonucleotide probe has a unique sequence that must be complementary to the target. The hybridization stability and efficiency depend mostly on the probe design (length and sequence, melt temperature, polymorphism position, flanking sequences) (*192*), but also on the medium stringency and presence of stabilizing/destabilizing additives.

In the pioneer GeneChip array technology (Affymetrix), 25 nt allele-specific probes are synthesized in solid-phase by photolithography to form a probe array (*107*, *193*). The target regions are amplified from genomic DNA and submitted to an enzymatic cleavage, tagging and hybridization to the probe array under stringent conditions, followed by washing and fluorescent reading. Multiple probes with different bases at a single position are employed for increasing genotyping accuracy, a technique referred as tiling strategy (*194*, *195*). In this method, a single array can hold millions of probes, to perform $10^4$ to $10^5$ SNPs simultaneously.

Although microarrays should theoretically provide reliable quantitative information about nucleic acid concentration, a substation quantitation bias occurs between different platforms, genes and even across microarray chips from the same manufacturer (*196*). This happens mainly due to variations in probe density, hybridization yield, non-specific cross hybridization and quantum yield differences by neighboring fluorophores (*119*). For that reason, microarray techniques usually provide relative concentration results, rather than absolute values.

#### *1.3.2.10 Final remarks*

Technologies such as those described above are very useful for new biomarker discovery or large association studies, due to their high accuracy

and/or large multiplexing capacity. While next-generation sequencing techniques provide accurate base-calling of target SNPs, the high costs and elevated analysis times associated to these methods reduce their cost-effectiveness for a higher number of samples. Thus, they are not as suitable in the field of applied pharmacogenetics, in which a smaller number of known SNPs has to be genotyped in a shorter period of time. On the other hand, hybridization and PCR-based techniques can sacrifice accuracy to generate a higher multiplexed capacity, usually requiring a previous amplification step prior or simultaneously to the discrimination process. In both cases, high specialization, reagent and equipment costs are the critical limiting factors for implementing them to the clinical practice.

There is still a lack of methods capable of low to medium-throughput SNP detection in a large set of clinical samples, in an affordable way but maintaining sensitivity and selectivity. Thus, an important demand for techniques that can meet these requirements is currently observed. In the next section we discuss the possibilities for developing lower-cost genotyping methods by exploring different reactions and detection equipment, which can be applied to the pharmacogenetics clinical routine.

## 1.4 Integrated systems for DNA assays

### 1.4.1 Point-of-care systems

Current research addresses that DNA sequencing and genotyping methods should be both cost-effective and easily accessible. Due to their high complexity, most of the genetic variation detection technologies are restricted to very well equipped private and public organizations, having a turnaround time from 2 to 7 days, which can delay treatment choice, minimal dose

prediction and close monitoring of the patient (*197*). Consequently, there is a need to develop faster systems that offer easy operation, high throughput and low cost, in order to respond more rapidly to the increasing need for genetic testing.

Point-of-care (POC) alternatives can contribute to solve this demand, reducing the assay complexity and costs, but also maintaining the adequate accuracy level. By focusing on very specific biomarkers and simplifying the analysis technique and platform, POC analysis sacrifices throughput and sophistication in order to solve punctual demands in a fast and affordable way, such as diagnosing a genetic disease or identifying pathogens, as well as determining the most effective therapy. Thus, the simplicity, faster assay times, stability of reagents, portability and overall safety are the main features of medical philosophy (*197*). However, in order to be a highly effective POC technology, a method should follow recommendations as the ASSURED criteria, establish by the World Health Organization, standing for: Affordable, Sensitive, Specific, User-friendly, Rapid and robust, Equipment-free and Delivered to those in need (*198*).

One of the main challenges for implementing POC genotyping technologies in the clinical practice is the integration of three testing phases into a single device, including nucleic acid extraction, amplification, and detection. Currently, most genotyping methods employ a PCR amplification step, followed by the SNP discrimination assay. However, besides being the most used and well-studied amplification reaction, PCR has its own limitations, such as false-negative occurrence and inhibition by medium conditions (*199*). Moreover, the high temperatures related to the thermal aperture stages, promote the formation of air bubbles, which can compromise the liquid flow in applications such as microfluidics. Most importantly, the requirement of a precise thermal cycling unit greatly hinders its application

in POC solutions because the assay protocol is longer and needs particular equipment as thermocyclers (*200*).

### 1.4.2 Isothermal assays

In order to overcome the limitations of PCR amplification, research in POC-based analysis is increasingly focusing in isothermal alternatives. Instead of relying on precise cycling, these techniques employ other enzymes and proteins present in *in vivo* DNA/RNA synthesis (*201*), with the objective of performing amplification at a constant temperature, without the need of thermal cycling equipment.

Differently from PCR, enzyme activity and kinetics are the main limiting factors of isothermal techniques, rather than thermal cycling rates (*202*). This allows the amplification reaction to be performed in microchambers with no fluid motion, which greatly simplifies the platform design and reduces the energy consumption, in comparison with the rapid heating, cooling or re-circulation required in miniaturized PCR devices (*203*).

The choice of the isothermal reaction depends on the application and target of interest. Different features, such as operating temperature, amplification time, number of oligonucleotides, tolerance to inhibitors, denaturation requirement, among others, must be considered in order to explore the full potential of each technique. Herein we describe the main DNA isothermal amplification reactions, focusing on their application for SNP genotyping. These techniques were grouped in terms of the replication mechanism, which can be based on the displacement of extended sequences (SDA, MDA, RCA and LAMP) or dsDNA enzymatic aperture (RPA and HDA). RNA-based technologies and pathogen detection techniques were reviewed elsewhere (*204–207*) and are not in the scope of this work.

### *1.4.2.1 Strand displacement amplification (SDA)*

This method was first described in 1992 by Walker and colleagues (*208*) and relies on the activity of a restriction endonuclease and a strand displacing DNA polymerase. After an initial denaturation step, SDA primers containing restriction sites are annealed to the target ssDNA and extended. Subsequently, the annealing and extension of bumper primers displace the extension product and regenerates the original dsDNA sequence. A second round of extension and displacement with the reverse primers generates an amplicon which is flanked by restriction sites. The endonuclease is then used to nick these sites, leaving a free 3'-end which can be further elongated, displacing the complementary strand for subsequent nicking/displacing cycles (Fig. 9). This exponential process can be used to achieve a $10^7$-fold amplification yield, within 2 hours at 37 °C (*209*).

In SDA, extension and nicking reactions occur concurrently in a single step, meaning that the operator intervention is limited to reagent mixing, an initial denaturing step and the addition of enzymes at 37 °C. Although this simple protocol is suitable for POC use, SDA is not frequently mentioned in the literature, probably due to its relatively slow amplification time and the reaction sensitivity to background DNA in low-stringency conditions, which causes non-specific primer binding and co-amplification of untargeted products (*200*).

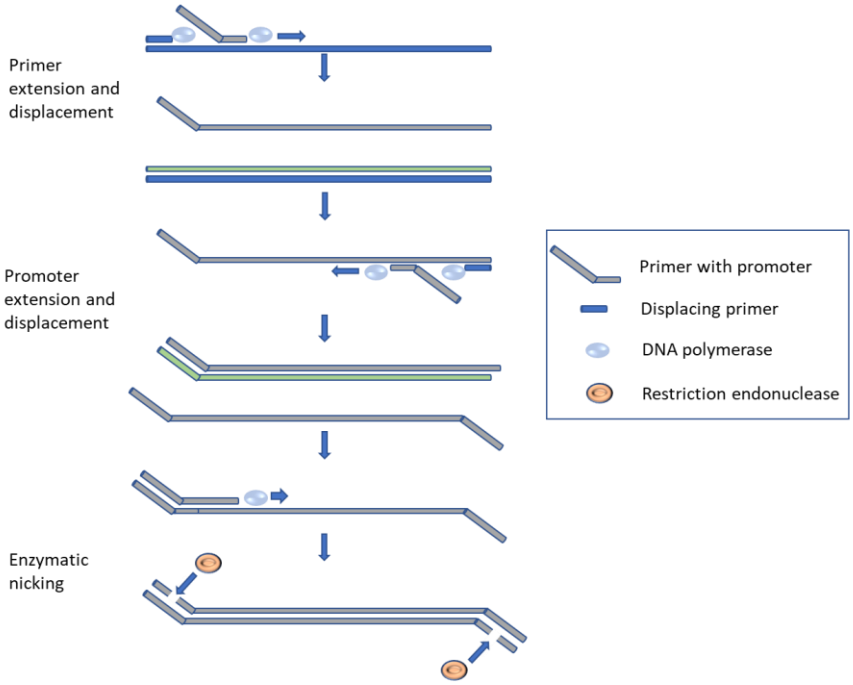


**Figure 9.** Schematic representation of the strand displacement amplification (SDA) mechanism

### *1.4.2.2 Rolling circle amplification (RCA)*

The strand displacement activity of some polymerases is also a key mechanism in rolling circle amplification (*210*). In this method, a high processivity polymerase (e.g. Φ29 polymerase) is used for continuously extending a primer from a circular DNA template, at a constant temperature between 30 and 60 °C (Fig. 10). Due to the strand displacement effect, the resulting product is a long DNA molecule with tandem repeats of the original template, reaching up to 0.5 megabases (*147*). This extension process continues until an external factor, such as nucleotide depletion, stops the reaction.

RCA can be applied for linear or exponential amplification, differing by the number of primers. In linear RCA, a single primer is annealed and extended from the original template, whereas exponential amplification can be achieved by incorporating a secondary primer that targets the first primer product at regular intervals, initiating additional elongation events and hyper-branching in the DNA replication (*211*).

While RCA requires a circular single stranded DNA as template, a large number of relevant DNA targets is composed by double stranded linear sequences, limiting the direct application of the RCA. In order to solve this problem, padlock probes can be used to anneal and circularize to the linear DNA, being further sealed by a ligase alone or in combination with a DNA polymerase. As this circularizing step is strictly sequence-dependent, it can achieve single-base accuracy for identifying SNPs (*145*, *212*). However, as this circularization process demands additional enzymes and adds up complexity to the assay, it hinders the method's application for POC devices.

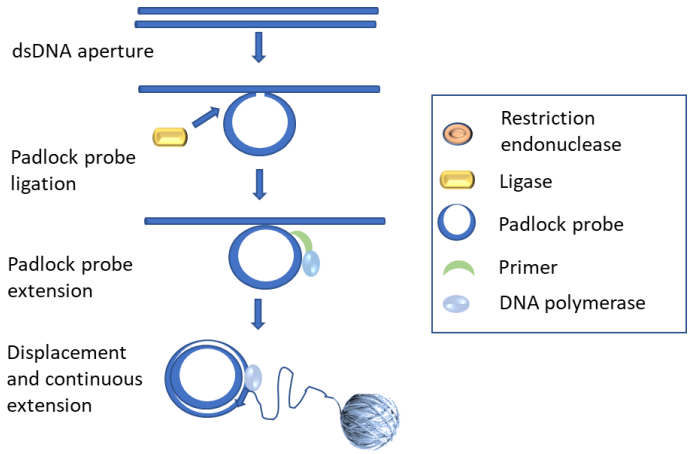


**Figure 10.** Schematic representation of the rolling circle amplification (RCA) mechanism

### *1.4.2.3 Multiple displacement amplification (MDA)*

The high processivity of Φ29 polymerase is also explored MDA, which employs multiple oligonucleotide hexamers that hybridize with random sequences in a genome sequence. The extension of this hexamers generates branched structures that can be targeted by new primers, initiating exponential amplification (*213*) (Fig. 11).

Due to the random nature of MDA primers, the reaction is generally applied in whole genome amplification (WGA), or to obtain larger amounts of genomic material from single cells, for sequencing or mutation analysis purposes (*146*, *214*, *215*).

Although this technique has shown to be very sensitive, capable of detecting DNA from a single-cell, only about 30% of the resulting product is specific, since all DNA in the sample is amplified (*216*). A higher selectivity can be achieved by reducing amplification reaction volumes which was explored by Marcy et al (*217*), using nanoliter microreactors. Another limiting of this technique is that MDA is a self-inhibiting reaction, reaching a plateau at 0.7 – 1.0 μg/μL of amplified DNA (*215*).

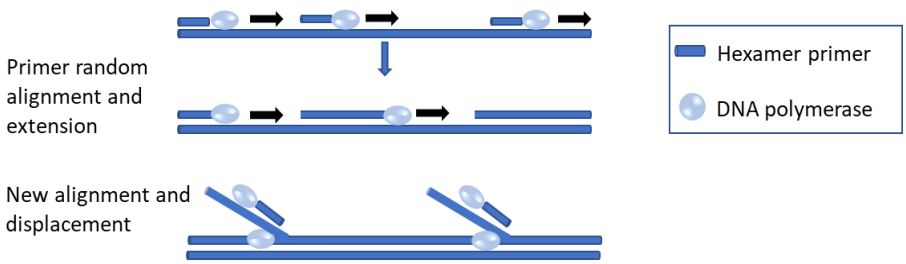


**Figure 11.** Schematic representation of the multiple strand displacement amplification (MDA) mechanism

#### *1.4.2.4 Loop-mediated isothermal amplification (LAMP)*

This reaction was first described by Notomi and colleagues (*218*), who employed two sets of primers and a DNA polymerase with strand displacement activity to amplify the target region by a factor of $10^6$, in less than an hour, at around 60 °C. The first primer pair anneals to inner sequences in the target DNA, being extended by the DNA polymerase. Subsequently, the second primer pair anneals to outer regions of the target and is extended, detaching the just-synthesized strands generated by the inner primers (Fig. 12). This process creates a stem-loop structure that is self-complementary in both ends, which is used as template for new elongation steps by self-priming and inner primer annealing, creating a mixture of stem-loop DNAs with different stem lengths and cauliflower-like structures with inverted repeats of the original template.

The main advantages of LAMP are high selectivity, high amplification efficiency and detection versatility. The carefully designed primers target multiple specific sequences, while a high-processivity enzyme (Bst polymerase) provides a high amplification yield. In addition, the high amounts of pyrophosphate generated by the DNA polymerization tend to precipitate with magnesium ions present in the medium, allowing the reaction to be monitored by the increase of turbidity (*219*), real-time transmittance (*220*) or absorbance (*221*).

The LAMP has been investigated for SNP detection in the past two decades. The reaction was used to perform genotyping assays, by combining it to microarrays (*222*), allele-specific amplification (*223, 224*), strand-displacement probes (*225*), PNA blocking probes (*226*) and endonuclease reaction (*227, 228*). Despite these efforts, this technique still has a great

potential for application in POC genotyping methods, since its detection versatility and specificity are excellent, when compared to other techniques.

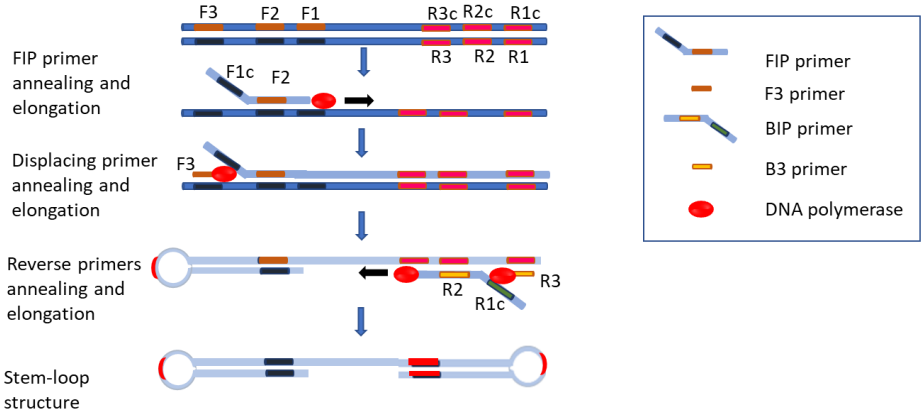


**Figure 12.** Schematic representation of the loop-mediated isothermal amplification (LAMP) mechanism

### *1.4.2.5 Recombinase polymerase amplification (RPA)*

Differently from the previously described techniques, which use thermal aperture steps or denaturation equilibrium to anneal the primers, RPA mimics DNA replication/synthesis mechanisms in order to achieve low and constant temperature amplification. The reaction was first described by Piepenburg et al. (*229*) and employs single strand binding proteins and a polymerase in order to stabilize and extend nucleic acid sequences at low temperatures. However, the annealing step is carried out by a recombinase enzyme, which forms a complex with the primer and scans the target dsDNA. The recombinase then inserts the primer at the complementary sequence and displaces the opposite strand, which is stabilized by single strand binding proteins. After recombinase disassembling, the primer 3'-end can be extended

by the polymerase and be targeted by reverse primers, leading to exponential amplification (Fig. 13).

Due to the enzymatic insertion process, the operational temperature in RPA is low (37-42 °C), when compared to other isothermal methods. Along with these favorable thermal features, the procedural simplicity and very rapid amplification times (20-40 min) turn this recent method into a leading technology for integration with POC devices (*230*).

On the other hand, the medium components necessary to carry out the amplification make this technology incompatible with current available intercalating dyes, molecular beacons and TaqMan probes (*200*). Thus, other detection tools must be employed to identify the amplification products, like modifying the medium conditions (*231*), purifying the amplicons (*232*), or attaching labels to the products (*233*). Additionally, the low temperature required to initiate amplification can lead to unspecific results at room temperature, which can be reduced by controlling preparation conditions, working at low set-up temperatures and adding magnesium only when the reaction is ready to start.

Few examples of SNP detection applications are found in the literature, with most of the published works involving pathogen detection (*230*, *234*, *235*). These works explore the rapid amplification speed and low temperature of RPA to create a faster and precise response to diagnosis in clinical practices. However, there is still a lack of genotyping and personalized medicine applications, offering opportunities for research in this area.

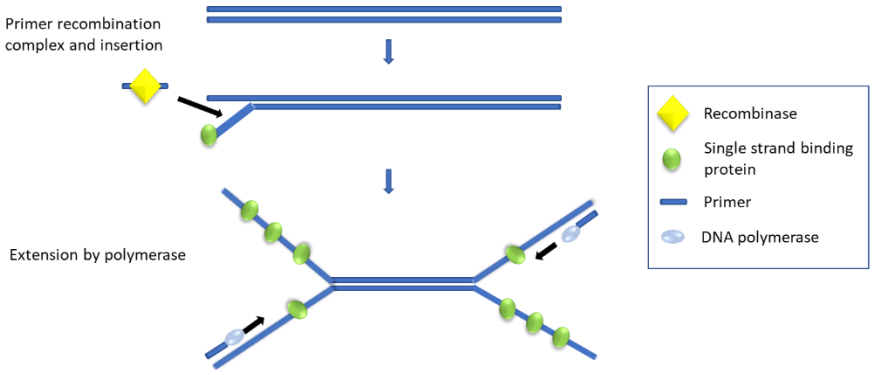


**Figure 13**. Schematic representation of the recombinase polymerase amplification (RPA) mechanism

### *1.4.2.6 Helicase-dependent amplification (HDA)*

The HDA is one of the isothermal techniques that mimics *in vivo* DNA replication mechanisms in order to achieve favorable primer extension conditions (*236*). In this method, a DNA helicase is employed to unwind the double-stranded DNA template, allowing primers to anneal and be elongated by a polymerase enzyme. After extension, the generated amplicons can be used as templates for new unwinding/annealing/elongation steps, allowing exponential amplification at 60-65 °C (Fig. 14).

Improvements in helicase activity were obtained by optimizing enzyme concentrations, addition of crowding agents and employing restriction endonucleases that target upstream regions (*200*). Also, the employment of single strand binding proteins (SSBs) enhances processivity and amplification speed, allowing amplification of 2.3 kb DNA fragments, in comparison with the original 400 bp (*237*).

HDA has interesting features for POC applications, due to its simplicity: a single pair of primers, a couple of enzymes and compatibility

with fluorescence detection techniques, makes the reaction protocol very similar to PCR (*238*, *239*). The technique was employed for SNP detection by different authors (*240*, *241*). On the other hand, HDA speed can be a limitation for POC applications for low amounts of template DNA (< 100 copies) (*242*), requiring exhaustive optimization of the assay.

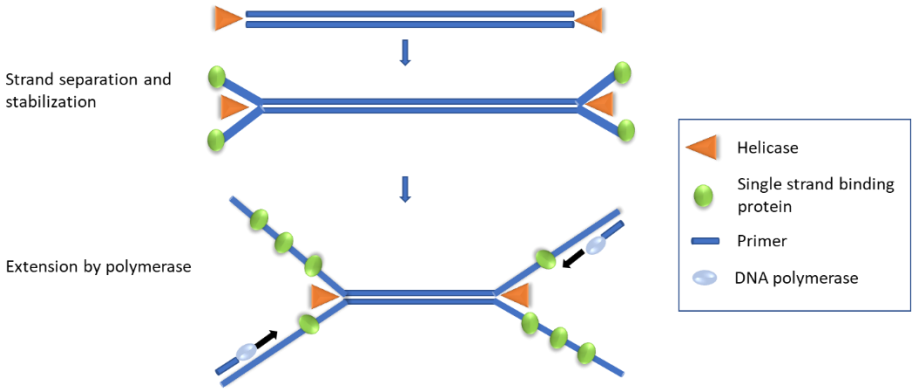


**Figure 14.** Schematic representation of the helicase dependent amplification (HDA) mechanism

### *1.4.2.7 Other techniques*

The isothermal exponential amplification reaction (EXPAR) has a unique mechanism that employs a functional oligonucleotide, rather than primers, to produce amplification. This strand is designed with two repetitions of a sequence complementary to the target, separated by an endonuclease nicking site (*243*). After hybridization to the target and extension, the functional oligonucleotide can be nicked by the endonuclease and reextended by the polymerase, displacing a 10-20 intermediate oligonucleotide sequence that can act as a primer. This nicking/extension/displacing cycling process

continues exponentially, showing an amplification yield higher than $10^6$, occurring at 60 °C in less than 10 min (*243*).

The main restriction of EXPAR is its limitation to target regions having close native nicking-enzyme recognition sites (*244*). Nicking and extension amplification reaction (NEAR) is a refinement of EXPAR, using the insertion of adjacent nicking-enzyme recognition sites into the target regions to allow subsequent amplification. The reaction is similar to SDA, employing enzymes to generate a starting point from which polymerase can initiate extension. However, the nicking enzyme used in NEAR only nicks a single strand of the DNA duplex, avoiding the use of modified nucleotides to prevent double strand nicking.

The smart amplification process version 2 (SMAP2, also named SmartAmp2) employs self-priming loop structures and enzymes that are similar to those used in LAMP (*245*). However, the reaction also relies on background suppression in order to achieve ultra-high selectivity. Instead of symmetrical primers used in LAMP, SMAP2 flanking primers are designed with two different tail sequences, in order to reduce unspecific annealing. The polymerase employed in SMAP2, Aac polymerase, has a high fidelity and strand displacement activity, which avoid the incorporation of unmatched nucleotides and facilitate primer binding by displacing previously synthesized strands. Also, the technology employs a mismatch repair protein (*Thermusaquaticus* MutS) to irreversibly bind to any mismatched duplex, inhibiting their extension. With these modifications, the SMAP2 is a very suitable method for SNP detection (*246–251*), since a positive amplification in optimized conditions will most certainly indicate the presence of the target polymorphism.

As the main limitations presented by SMAP2, this technology requires a complex design of folding primers, optimization and evaluation to

achieve the adequate selectivity. Furthermore, this technology is not as much explored as more developed reactions like LAMP and SDA, meaning that fewer studies were published and until this date there is not an available kit for research or diagnostic use.

In a recent technology, called isothermal and chimeric primer-initiated amplification of nucleic acids (ICAN), the reaction is carried out by using 5'-DNA-RNA-3' chimeric primers, a thermostable RNAseH and *Bca*BEST polymerase, which presents strand displacement activity (*252*). Following template thermal aperture, the chimeric primers are extended by the polymerase and the products are nicked at the penultimate 3'-RNA position, leaving a shorter annealed primer and a single DNA strand with a 5'-end RNA residue that can be displaced by the subsequent extension step. This extension/nicking process occurs at 55 °C and repeats until the primer is sufficiently shortened, allowing new primers to anneal and restart the cycle.

One of the main advantages of this method is the simplicity of the assay design, as only a primer pair is required per target and the amplification products are similar to those from PCR, allowing the assay result reading by conventional techniques. Also, ICAN presents a sensitivity that is 25 times higher than PCR-based methods (*253*) and can be applied to detect both DNA, RNA and hybrid targets as well.

To the date, very few studies on ICAN have been published, all of them in the first decade of the 2000's. Perhaps this low dissemination can be related to the absence of commercial kits or to the relatively long amplification times required (60-110 min). Among these publications, only one was applied to SNP detection (*254*). This work employed quenched chimeric DNA-RNA probes labels, that were nicked by the RNAseH when correctly hybridized, allowing fluorescence detection.

### 1.4.3 Consumer electronic devices for analytical uses

Over the last two decades, creative solutions have been developed in order to overcome the high cost, complexity and analysis times required in standard laboratory genetic testing. Advances in biotechnology, nanotechnology, microfluidics and electronics have contributed to miniaturize and make molecular analysis more portable than ever in history.

By one side, isothermal amplification and other enzymatic approaches, discussed previously, provide the biochemical background to require less bulky and sophisticated equipment. On the other hand, new microfluidic assay platforms facilitate the miniaturization, efficiency and automatization, by integrating sample pretreatment, reactions, separation and detection in a single microfabricated chip. By combining isothermal amplification and fully enclosed microfluidic structures, it is possible to lower equipment requirements, while still reducing contamination risk, the amount of required DNA sample and reagent consumption (*255*).

At the same time, new information processing and image capturing technologies have spread worldwide and continue to develop. A current sample of these advances are the consumer electronic devices, which are equipment that is used on a daily basis for entertainment, communication or office routine purposes. Some examples are the digital cameras, scanners, computers, console games, music and video players, recorders and, most recently, smartphones, which can practically integrate all the previously mentioned devices in a single piece of equipment. By exploring the high image resolution, storage capacity and processivity of these tools, affordable and easy-to-use methods can be developed, employing optical readable platforms to support the biomolecular assay.

Consumer electronic equipment has been adapted as point-of-care imaging platforms for sequence-specific diagnostics with demonstrated sensitivity (*256*, *257*). In this section, we discuss some promising devices that show great potential for detecting SNP discriminating reactions, focusing mainly on optical detection and exploring the main features and applications for each type of device.

### *1.4.3.1 Compact disc technology*

Compact discs are composed by a transparent plastic substrate, usually polycarbonate (PC), covered by a thin metallic reflective aluminum, silver or gold layer, which is protected by a polymeric lacquer (generally polymethyl methacrylate, PMMA). Both PC and PMMA are transparent to visible light and present low optical distortion, high mechanical resistance, decent thermal stability and high hydrophobicity, providing viable surfaces for performing bioassays (*74*).

The information is stored over a in the form of pits, that are created over the metallic layer during the fabrication process (normal discs) or generated in the recording process (recordable discs). On average, each pit has a 125-nm depth, a 500-nm width and between 830 and 3500-nm length. The pits are arranged on the disc surface along a single continuous spiral that constitutes the data track, which is scanned from the inside to the outside by a laser beam in the reading process. This information is read by an optical pick-up system, that captures the reflected and diffracted light by the metallic layer and the pits to an optoelectronic sensor (photodiode), generating binary information (Fig. 15).

The first commercial compact discs and players were marketed in the 1990-decade. Also, in this period, digital versatile discs (DVD) were

developed, having as main advantages the faster reading speeds and higher storage capacities. This was achieved by reducing pit dimensions and spacing between tracking lines, demanding a higher frequency laser (650 nm emission). Afterwards, the Blu-ray disc (BD) was developed, improving data storage capacity even more, by using smaller pits and a better resolution laser (405 nm).

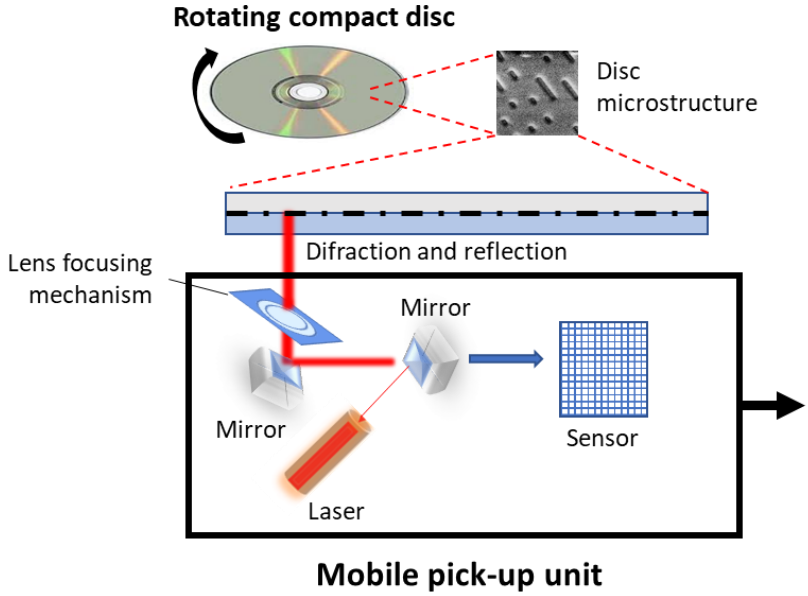


**Figure 15.** Schematic representation of the compact disc reading mechanism

Polymeric materials like those found in compact discs have demonstrated to be a good alternative to more traditional ones, like glass, silicon and silicon oxide, for application in biosensor platforms. There is a significant number of researches that use polymeric platforms in a circular shape as analytical support, which can be classified by two different approaches (Fig. 16). The first one uses microfluidic centrifugal platforms

(lab-on-a-disc) to perform the assay, that is read by conventional laboratory detectors (photometers, fluorimeters, etc.) adapted to the circular geometry. The second approach uses the audio-video disc technology both for carrying out the assay and reading the optical results (driver/recorder).

Centrifugal or lab-on-a-disc platforms are usually consisted by millimetric-thick polymeric discs with a net of microchannels, chambers and valves, which allow the integration of several DNA analysis steps, such as extraction, amplification, hybridization and detection. Moreover, due to the circular shape of these structures and their carefully designed layout, the liquid flow can be controlled inside the platform by rotating the disc and applying different spinning rates.

The application of lab-on-a-disc technologies for biosensing has been reviewed by several authors (*258–261*). The first published study that employed disc-shaped structures for SNP discrimination was developed by Shi *et al*. for genotyping methylenetetrahydrofolate reductase (MTHFR) alleles (*262*), which used a restriction endonuclease assay and a radial capillary array microplate to perform the fragment separation by electrophoresis. Other SNP genotyping microfluidic-based methods employ fluorescence detection for reading allele-specific hybridization assays with synthetic oligonucleotides (*263*), end-point PCR products (*264–266*) or real-time allele-specific PCR products (*267*).

On the other hand, a standard disc drive is a small high-precision optical instrument which well developed and present in most places, and could serve as a very robust tool for biorecognition detection (*268*, *269*). This technology not only can lower the detection costs but also simplify the data acquiring, since disc readers are highly compatible with computer hardware (*270*).

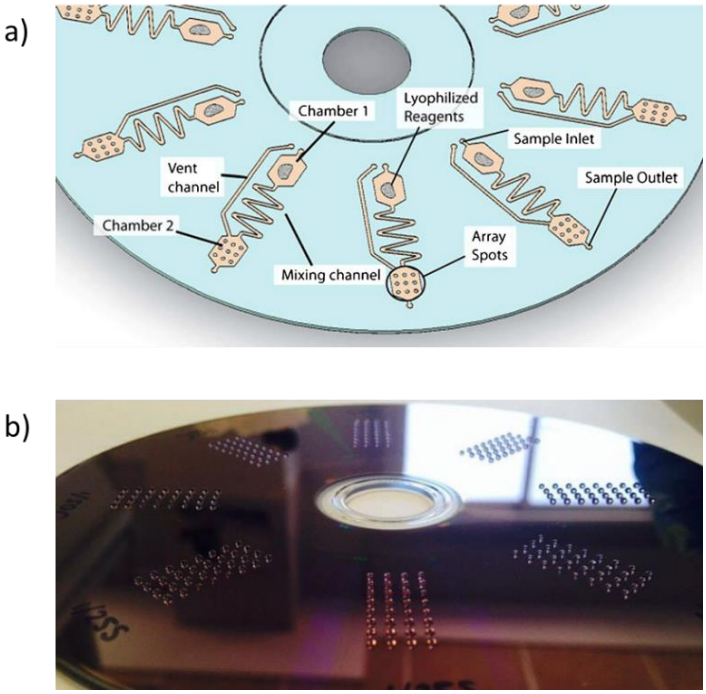


**Figure 16**. Examples of disc-based platforms for nucleic acid analysis platforms. a) microfluidic disc for DNA amplification and hybridization; b) Blu-ray disc for microarray DNA analysis. Reprinted by permission from Royal Society of Chemistry: RSC Advances, Tortajada-Genaro et al., 2015; and Springer Nature: Microchimica Acta, Díaz-Betancor et al., 2019. References (*271*) and (*272*).

The first application of compact discs as an analytical support was explored by Kido and colleagues (*273*), who used it to identify pesticides by immunorecognition and fluorescence detection. Few years later, the disc driver was incorporated for reading the assay, using the platform for detecting nucleic acids (*274*) and molecular screening (*275*).

Since the creation of this analytical tool, the research group where this thesis is being developed has accomplished numerous advances in the platform for detecting nucleic acids (*272*, *276–278*). Disc-based methods have shown to be adequately sensitive for detecting foodborne pathogens and

genetically modified organisms (*220*, *271*, *279–281*). Also, our group has recently demonstrated that the discrimination of SNPs in clinical genomic samples is also viable using CD-based methods (*282*, *283*). Therefore, the audio-video compact disc technology can be of high valor to the POC healthcare context, since it can greatly improve analysis costs and response times, while maintaining the analytical quality.

#### *1.4.3.2 Smartphone-based technologies*

Smartphones are unique electronic equipment, with a built-in LED flashlight as illumination source, multiple complementary metal-oxide semiconductor (CMOS) high-resolution cameras, a high storage capacity and high-performance processors, which allow bioassay detection by combining them with sensing platforms. These devices also integrate a handful of connectivity technologies, such as infrared, Bluetooth, wi-fi, near field communication (NFC) and global positioning system (GPS). Also, various types of attachments can be coupled with the mobile phones, such as lenses, filters, alternative light sources and diffraction gratings, allowing this instrument to serve as a measurement system for multiple purposes (*257*).

In the past two decades, much progress in the imaging hardware have been achieved, with resolution doubling every two years and recently reaching more than 40 mega-pixels (*284*). For biosensing imaging, the most important component of smartphone cameras is their CMOS sensor, which presents a high sensitivity and framerate, compactness and low power consumption (*285*). This piece of hardware is composed by a pixel sensor array and optical filters for color transmission and to block ultraviolet and infrared light. The light is captured by the array of pixels, which proportionally convert it into variable voltages. The color information is

generated from a red-green-blue (RGB) filter pattern, composed by a repetitive 2x2 grid, with two green pixels for every blue and red filter (*286*). The analysis of the digital images acquired with a smartphone in means of grayscale or RGB intensity, allows the quantification of spectrophotometric assays, with a low-cost and easy-to-use platform.

Due to their still unmatched features as consumer electronics, smartphones have been extensively studied in the last decade for biosensing purposes, acting as a point-of-care detector and data processor. Applications of this equipment are found in colorimetric, surface plasmon resonance, luminescence, electrochemical and microscopy-based biorecognition methods (*285*, *287–291*).

Smartphones have been combined with isothermal amplification in many POC DNA detection assays. Some examples are illustrated in the Figure 17. Most of the published studies are concentrated in the fluorescence detection of pathogen-targeted LAMP products with different platforms, such as microfluidic polymeric chips (*292*), hybrid polymer-paper chips (*293*) or more extravagant solutions, like a self-heating coffee mug (*294*) or a modified pipette tip, which serves as support for performing extraction, amplification and detection (*295*). Also, a lab-on-a-chip device was developed by Sayad *et al*., which integrates all the steps for detecting *Escherichia coli*, *Salmonella spp* and *Vibrio cholerae* in a microfluidic disc, taking advantage of the calcein fluorescence in the presence of LAMP byproducts (*296*).

The LAMP versatility for detection methods was explored in smartphone DNA sensing with an acoustic wave detector (*297*), and colorimetric assays, by coupling the amplification reaction with gold nanoparticle hybridization (*298*), quenched fluorophore primers (*299*, *300*), a pH indicator (*301*) and hydroxynaphtol blue (HNB), a magnesium indicator (*302*).

RPA is the second most studied reaction for POC detection of low amounts of DNA with a smartphone. This strategy was combined with quantum dot barcodes and fluorescence detection (*303*), a two-step RPA and LAMP amplification with solution detection with HNB (*304*) and fluorescence detection in a modified 3D printer (*305*). A single study using rolling circle amplification (RCA) was published, using magnetic particles with fishhook probes, that serve as centers for target micro RNA hybridization and extension (*306*).

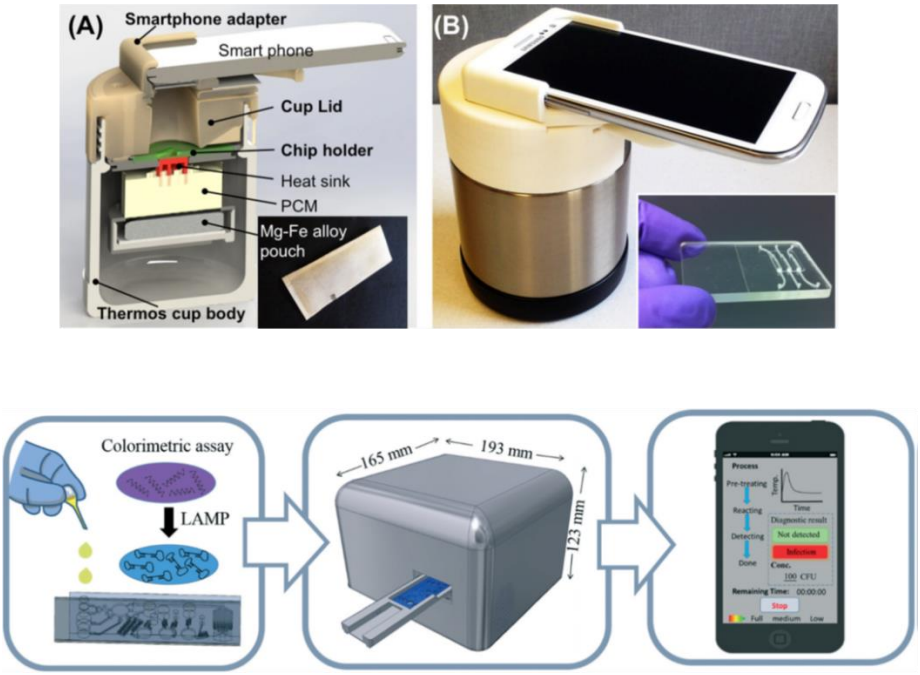


**Figure 17.** Smartphone-based DNA isothermal biosensing technologies. Reproduced by permission of The Royal Society of Chemistry. References (*294*) and (*302*).

The first published study involving smartphone detection with SNP discrimination was described by Michikawa *et al.*, who developed a visible

microarray by allele-specific extension of immobilized LNA primers with biotin-dUTP labels, staining the labeled products with streptavidin-alkaline-phosphatase conjugates (*307*). In another study, PCR amplification was followed by bead separation and an endonuclease nicking and HRP staining in order to produce a colorimetric product (*308*). An urease-mediated assay was also developed, based on the sequestering of silver atoms by mismatched dsDNA, activating the enzyme and generating a pH change by conversion of urea in carbon dioxide and ammonia (*309*).

Fluorescence-based mutation detection methods were published by various groups, majorly in the probe array format. Sequence-specific hybridization was coupled with RCA amplification, for detecting KRAS mutations (*310*), and RGB FRET analysis by capturing Cy3 and Cy5 synthetic targets with quantum dot probes (*311, 312*). An homogeneous assay was also developed by Yu *et al.*, using hybridization with quenched molecular beacons for detecting mRNA single-base variations (*313*).

A luminescence measurement system for detecting MTHFR polymorphisms was developed by Spyrou *et al.*, combining a two-step PCR/allele-specific extension and hybridization of the products with probes immobilized in a lateral-flow membrane, followed by enzymatic staining with HRP and a chemiluminescent substrate (*314*). Another interesting method employed the ligation of immobilized targets and amplification by RCA, producing microarrays that were visualized by breathing vapor condensation (*315*).

#### *1.4.3.3 Other devices*

Flatbed scanners are also a widespread equipment, created for producing high quality images within a very short time. From an analytical

point of view, these devices offer a large detection area (>600 $cm^2$) and high resolution (>600 dpi), combined with a highly reproducible positioning and illumination. They are also very compact and affordable, supporting connection with computers by wi-fi or USB (*286*).

The flatbed scanner was the first consumer electronic device to be applied for POC SNP detection (*111*). These authors used the equipment for capturing images of gold-nanoparticle-conjugated oligonucleotide microarrays, stained by silver reduction. The method reached single nucleotide selectivity and a sensitivity two magnitude orders higher than an analogous fluorophore system. This same strategy was employed by other groups for detecting pathogens in food samples (*316*, *317*).

Enzymatic staining by alkaline phosphatase system was employed by Petersen *et al*. for visualizing a 10 SNP microarray, which was read by a scanner (*318*). In another study, a paper-based breast cancer panel with 10 SNP was developed, with previous PCR amplification of the target DNA with biotinylated dUTP. The products were added to the paper support containing immobilized probes and anti-biotin antibodies conjugated to gold nanoparticles, producing colored spots that were read by the flatbed scanner (*319*).

A very creative alternative for POC SNP electrochemical detection was developed by Xiang and Lu (*320*), who adapted a home glucose meter to detect DNA in concentrations as low as 40 pM, with single nucleotide specificity. Instead of using PCR to replicate the nucleic acid, it relied on the enzymatic signal amplification. The target DNA was captured by magnetic beads with immobilized probes and hybridized to invertase-conjugated recognition probes. After magnetic separation of the products, the conversion of sucrose into glucose by the invertase generated an electric signal that was measured by the device.

## 1.5 Final remarks

Currently, the paradigm of healthcare procedures is progressively becoming more personalized and molecular-analysis-based. Moreover, at the present, the commercially available technologies for performing genetic analysis have poor capacity for application in more simple environments, with lower resource availability. For these reasons, there is an important demand into developing simple, low/medium-throughput and low-cost POC methods to support the increasing demand for genetic testing.

The solutions presented in this thesis are based, by one side, on the simplicity and selectivity of isothermal enzymatic reactions, which could minimize or eliminate the problems related to PCR. On the other hand, we propose the employment of simple platforms and consumer electronic devices to facilitate and lower the costs of the assay reading steps, allowing fast and easy-to-use detection. With the aid of these principles and technologies, pharmacogenetics could be more effectively supported and precision medicine could become more available to the general public.

## 1.6 References


1. L. Pauling, H. A. Atano, S. J. Singer, I. C. Wells, *Science.* **110**, 543–548 (1949).
2. M. Debnath, G. B. K. S. Prasad, P. S. Bisen, *Molecular diagnostics: Promises and possibilities* (2010).
3. A. Kesari, A. Dalal, G. Lal, S. N. Pandey, *Biomed Res. Int.* **2013**, 1–2 (2013).
4. U.S. Food and Drug Administration, *FDA's Role in a New Era of Medical Product Development* (2013). Available in: https://www.fdanews.com/ext/resources/files/10/10-28-13-Personalized-Medicine.pdf. Accesed in 02/05/2020.
5. I. S. Chan, G. S. Ginsburg, *Annu. Rev. Genomics Hum. Genet.* **12**, 217–244 (2011).
6. Personalized Medicine Coalition, *The Case for Personalized Medicine* (2014). Available in: http://www.personalizedmedicinecoalition.org/Userfiles/PMC-Corporate/file/pmc_the_case_for_personalized_medicine.pdf. Accessed in 02/05/2020.
7. C. Katsios, D. H. Roukos, *Per. Med.* **7**, 347–350 (2010).
8. A. J. Atkinson *et al.*, *Clin. Pharmacol. Ther.* **69**, 89–95 (2001).
9. A. Ziegler *et al.* , *Hum. Genet.* **131**, 1627–1638 (2012).
10. F. S. Collins, M. Morgan, A. Patrinos, *Science.* **300**, 286–290 (2003).
11. M. Przeworski, R. R. Hudson, A. Di Rienzo, *Trends Genet.* **16**, 296–302 (2000).
12. W. G. Feero, A. E. Guttmacher, F. S. Collins, *N. Engl. J. Med.* **362**, 2001–2011 (2010).
13. L. Feuk, A. R. Carson, S. W. Scherer, *Nat. Rev. Genet.* **7**, 85–97 (2006).
14. K. R. Crews *et al.*, *Clin. Pharmacol. Ther.* **92**, 467–475 (2012).
15. International HapMap Consortium, *Nature*. **426**, 789–796 (2003).
16. D. A. Peiffer, K. L. Gunderson, in *DNA Microarrays for Biomedical Research: Methods and Protocols* (2009), vol. 529, pp. 51–61.
17. L. A. Hindorff *et al.*, *Proc. Natl. Acad. Sci. U. S. A.* **106**, 9362–9367 (2009).
18. E. H. Cook, S. W. Scherer, *Nature*. **455**, 919–923 (2008).
19. M. Esteller, *N. Engl. J. Med.* **358**, 1148–1159 (2008).
20. J. A. DiMasi, H. G. Grabowski, R. W. Hansen, *J. Health Econ.* **47**, 20–33 (2016).
21. K. J. Karczewski, R. Daneshjou, R. B. Altman, *PLoS Comput. Biol.* **8** (2012).
22. U. M. Zanger, *Front. Pharmacol.* **1**, 1–2 (2010).
23. M. L. Brandi *et al.*, *J. Pharmacogenomics Pharmacoproteomics*. **03** (2012).
24. D. Voora *et al.*, *Pharmacogenomics*. **6**, 503–513 (2005).
25. J. S. Ross, in *Essentials of Genomic and Personalized Medicine* (Academic Press, 2010), pp. 532–547.
26. D. M. Roden *et al.*, *Ann. Intern. Med.* **145**, 749–757 (2016).
27. M. Eichelbaum, M. Ingelman-Sundberg, W. E. Evans, *Annu. Rev. Med.* **57**, 119–137 (2006).

28. M. K. Ho, R. F. Tyndale, *Pharmacogenomics J.* **7**, 81–98 (2007).
29. W. R. True *et al.*, *Addiction*. **92**, 1277–1287 (1997).
30. G. R. Uhl, *Pharmacogenomics*. **10**, 1123–1125 (2009).
31. Y. Zhang *et al.*, *J. Biol. Chem.* **280**, 32618–32624 (2005).
32. L. Zhang, K. S. Kendler, X. Chen, *Behav. Brain Funct.* **2**, 28 (2006).
33. R. F. Anton *et al.*, *Arch. Gen. Psychiatry*. **65**, 135–144 (2008).
34. W. Huang *et al.*, *Neuropsychopharmacology*. **34**, 319–330 (2009).
35. J. H. Baik, *Front. Neural Circuits*. **7**, 1–16 (2013).
36. S. P. David *et al.*, *Nicotine Tob. Res.* **9**, 1251–1257 (2007).
37. L. J. Bierut *et al.*, *Am. J. Psychiatry*. **165**, 1163–1171 (2008).
38. S. F. Saccone *et al.*, *Hum. Mol. Genet.* **16**, 36–49 (2007).
39. R. C. Kessler *et al.*, *Evidence-Based Eye Care*. **4**, 186–187 (2003).
40. T. E. Schlaepfer *et al.*, *J. Psychopharmacol.* **26**, 587–602 (2012).
41. E. Vieta, F. Colom, *Ann. Med.* **43**, 512–530 (2011).
42. M. H. Trivedi *et al.*, *Am. J. Psychiatry*. **163**, 28–40 (2006).
43. A. Fekadu *et al.*, *J. Affect. Disord.* **116**, 4–11 (2009).
44. D. Warden *et al.*, *Curr. Psychiatry Rep.* **9**, 449–459 (2007).
45. S. Paddock *et al.*, *Am. J. Psychiatry*. **164**, 1181–1188 (2007).
46. D. M. Kawaguchi, S. J. Glatt, *Pharmacogenomics*. **15**, 1451–1459 (2014).
47. M. Ufer, *Clin. Pharmacokinet.* **44**, 1227–1246 (2005).
48. F. Kamali, H. Wynne, *Annu. Rev. Med.* **61**, 63–75 (2010).
49. M. J. Rieder *et al.*, *N. Engl. J. Med.* **352**, 2285–2293 (2005).
50. L. C. Clark, C. Lyons, *Ann. N. Y. Acad. Sci.* **102**, 29–45 (1962).
51. G. A. Rechnitz *et al.*, *Anal. Chim. Acta*. **94**, 357–365 (1977).
52. D. R. Thévenot *et al.*, *Biosens. Bioelectron.* **55**, 201 (1996).
53. T. Vo-dinh, B. Cullum, *Fresenius J. Anal. Chem.* **366**, 540–551 (2000).
54. D. R. Thévenot *et al.*, *Biosens. Bioelectron.* **16**, 121–131 (2001).
55. I. Palchetti, M. Mascini, *Analyst*. **133**, 846–854 (2008).
56. S. Cosnier, P. Mailley, *Analyst*. **133**, 984–991 (2008).
57. S. Bobade, D. R. Kalorey, S. Warke, *Biosci. Biotechnol. Res. Commun.* **9**, 132–137 (2016).
58. V. Perumal, U. Hashim, *J. Appl. Biomed.* **12**, 1–15 (2014).
59. S. A. Benner, *Acc. Chem. Res.* **37**, 784–797 (2004).
60. C. Tuerk, L. Gold, *Science.* **249**, 505–510 (1990).
61. B. Van Dorst *et al.*, *Biosens. Bioelectron.* **26**, 1178–1194 (2010).
62. N. K. Navani, Y. Li, *Curr. Opin. Chem. Biol.* **10**, 272–281 (2006).
63. D. I. Li, S. Song, C. Fan, *Acc. Chem. Res.* **43**, 631–641 (2010).
64. M. Famulok, G. Mayer, *Acc. Chem. Res.* **44**, 1349–1358 (2011).
65. P. E. Nielsen, *Curr. Med. Chem.* **8**, 545–550 (2012).
66. J. Wengel *et al.*, *Nucleosides and Nucleotides*. **18**, 1365–1370 (1999).
67. B. Vester, J. Wengel, *Biochemistry*. **43**, 13233–13241 (2004).
68. S. M. Borisov, O. S. Wolfbeis, *Chem. Rev.* **108**, 423–461 (2008).
69. S. J. Oh *et al.*, *Omi. A J. Integr. Biol.* **10**, 327–343 (2006).
70. S. A. Soper *et al.*, *Anal. Chem.*, in press, doi:10.1021/ac0029511.
71. C. Liu, *Adv. Mater.* **19**, 3783–3790 (2007).
72. G. M. Whitesides, *Nature*. **442**, 368–373 (2006).

73. J. Wu *et al.*, *Microchim. Acta*. **181**, 1611–1631 (2014).
74. H. Becker, C. Gärtner, *Anal. Bioanal. Chem.* **390**, 89–111 (2008).
75. J. Wang, *Nucleic Acids Res.* **28**, 3011–3016 (2000).
76. A. Sassolas *et al.*, *Chem. Rev.* **108**, 109–139 (2008).
77. W. H. Scouten, J. H. T. Luong, R. Stephen Brown, *Trends Biotechnol.* **13**, 178–185 (1995).
78. X. C. Zhou, L. Q. Huang, S. F. Y. Li, *Biosens. Bioelectron.* **16**, 85–95 (2001).
79. S. D. Conzone, C. G. Pantano, *Mater. Today*. **7**, 20–26 (2004).
80. J. I. A. Rashid, N. A. Yusof, *Sens. Bio-Sensing Res.* **16**, 19–31 (2017).
81. Y. Sakao *et al.*, *Colloids Surfaces B Biointerfaces*. **40**, 149–152 (2005).
82. F. T. Huey *et al.*, *Anal. Chim. Acta*. **551**, 23–29 (2005).
83. M. Wilchek, E. A. Bayer, O. Livnah, *Immunol. Lett.* **103**, 27–32 (2006).
84. M. Wilchek, E. A. Bayer, *J. Clin. Chem. Clin. Biochem.* **27**, 889–890 (1989).
85. X. Fang *et al.*, *J. Am. Chem. Soc.* **121**, 2921–2922 (1999).
86. S. Pan, L. Rothberg, *Langmuir*. **21**, 1022–1027 (2005).
87. A. Dupont-Filliard *et al.*, *Anal. Chim. Acta*. **449**, 45–50 (2001).
88. S. K. Chiu *et al.*, *Biochem. J.* **374**, 625–632 (2003).
89. B. A. Stillman, J. L. Tonkinson, *Biotechniques*. **29**, 630–635 (2000).
90. S. Chu *et al.*, *Science.* **282**, 699–705 (1998).
91. T. De Lumley-Woodyear, C. N. Campbell, A. Heller, *J. Am. Chem. Soc.* **118**, 5504–5505 (1996).
92. A. Csaki *et al.*, *Nucleic Acids Res.* **29**, e81 (2001).
93. A. B. Steel, T. M. Herne, M. J. Tarlov, *Anal. Chem.* **70**, 4670–4677 (1998).
94. A. Kumar *et al.*, *Nucleic Acids Res.* **28**, e71 (2000).
95. D. H. Jung *et al.*, *Langmuir*. **20**, 8886–8891 (2004).
96. F. Fixe *et al.*, *Nucleic Acids Res.* **32**, e9 (2004).
97. M. Beier, J. D. Hoheisel, *Nucleic Acids Res.* **27**, 1970–1977 (1999).
98. R. Benters *et al.*, *Nucleic Acids Res.*, 30, e10 (2002).
99. Y. H. Rogers *et al.*, *Anal. Biochem.* **266**, 23–30 (1999).
100. N. Gajovic-Eichelmann, E. Ehrentreich-Förster, F. F. Bier, *Biosens. Bioelectron.* **19**, 417–422 (2003).
101. C. R. Sabanayagam, C. L. Smith, C. R. Cantor, *Nucleic Acids Res.* **28**, 33e (2000).
102. R. Singh *et al.*, *Sensors Actuators, B Chem.* **197**, 385–404 (2014).
103. E. Palec, *Talanta*. **56**, 809–819 (2002).
104. T. G. Drummond, M. G. Hill, J. K. Barton, *Nat. Biotechnol.* **21**, 1192–1199 (2003).
105. V. Kumar Khanna, *Biotechnol. Adv.* **25**, 85–98 (2007).
106. D. Shalon, S. J. Smith, P. O. Brown, *Genome Res.* **6**, 639–645 (1996).
107. H. Matsuzaki *et al.*, *Genome Res.* **14**, 414–425 (2004).
108. G. Feriotto *et al.*, *Hum. Mutat.* **18**, 70–81 (2001).
109. T. Jiang *et al.*, *Biosens. Bioelectron.* **20**, 1939–1945 (2005).
110. F. R. R. Teles, L. P. Fonseca, *Talanta*. **77**, 606–623 (2008).
111. T. A. Taton, C. A. Mirkin, R. L. Letsinger, *Science*. **289**, 1757–1760 (2000).
112. A. Charrier *et al.*, *Biosens. Bioelectron.* **22**, 1881–1886 (2007).
113. J. A. Ferguson *et al.*, *Nat. Biotechnol.* **14**, 1681–1684 (1996).

114. J. H. Watterson, *Nucleic Acids Res.* **32**, e18 (2004).
115. K. Kneipp *et al.*, *Phys. Rev. E - Stat. Physics, Plasmas, Fluids, Relat. Interdiscip. Top.* **57**, 6281–6284 (1998).
116. M. B. Wabuyele, F. Yan, T. Vo-Dinh, *Anal. Bioanal. Chem.* **398**, 729–736 (2010).
117. S. M. Yoo *et al.*, *Chem. - A Eur. J.* **17**, 8657–8662 (2011).
118. S. Kim, A. Misra, *Annu. Rev. Biomed. Eng.* **9**, 289–320 (2007).
119. D. Khodakov, C. Wang, D. Y. Zhang, *Adv. Drug Deliv. Rev.* **105**, 3–19 (2016).
120. P. Y. Kwok, X. Chen, *Curr. Issues Mol. Biol.* **5**, 43–60 (2003).
121. B. Sobrino, M. Brión, A. Carracedo, *Forensic Sci. Int.* **154**, 181–194 (2005).
122. R. A. Gibbs, *Nucleic Acids Res.* **17**, 2437–2448 (1989).
123. I. Medintz *et al.*, *Genome Res.* **11**, 413–421 (2001).
124. J. L. McClay *et al.*, *Anal. Biochem.* **301**, 200–206 (2002).
125. L. Ugozzoli *et al.*, *Genet. Anal. Biomol. Eng.* **9**, 107–112 (1992).
126. S. Bortolin *et al.*, *Clin. Chem.* **50**, 2028–2036 (2004).
127. T. Pastinen *et al.*, *Genome Res.* **10**, 1031–1042 (2000).
128. B. P. Sokolov, *Nucleic Acids Res.* **18**, 3671 (1990).
129. L. A. Haff, I. P. Smirnov, *Genome Res.* **7**, 378–388 (1997).
130. P. Ross *et al.*, *Nat. Biotechnol.* **16**, 1347–1351 (1998).
131. A. Braun, D. P. Little, H. Köster, *Clin. Chem.* **43**, 1151–1158 (1997).
132. S. Sauer, *Nucleic Acids Res.* **30**, e22 (2002).
133. S. Sauer, I. G. Gut, *Rapid Commun. Mass Spectrom.* **17**, 1265–1272 (2003).
134. S. Kim, *Nucleic Acids Res.* **30**, e85 (2002).
135. J. J. Sanchez *et al.*, *Forensic Sci. Int.* **137**, 74–84 (2003).
136. J. B. Fan *et al.*, *Genome Res.* **10**, 853–860 (2000).
137. J. M. Shumaker, A. Metspalu, C. T. Caskey, *Hum. Mutat.* **7**, 346–354 (1996).
138. T. Pastinen *et al.*, *Genome Res.* **7**, 606–614 (1997).
139. M. H. Shapero *et al.*, *Genome Res.* **11**, 1926–1934 (2001).
140. U. Landegren *et al.*, *Science*, **241**, 1077-1080 (1988).
141. F. A. Eggerding, *Genome Res.* **4**, 337–345 (1995).
142. X. Chen, K. J. Livak, P. Y. Kwok, *Genome Res.* **8**, 549–556 (1998).
143. F. Barany, *Genome Res.* **1**, 5–16 (1991).
144. M. Nilsson *et al.*, *Science.* **265**, 2085–2088 (1994).
145. P. M. Lizardi *et al.*, *Nat. Genet.* **19**, 225–232 (1998).
146. F. A. Faruqi *et al.*, *BMC Genomics*. **2** (2001).
147. J. Banér *et al.*, *Nucleic Acids Res.* **26**, 5073–5078 (1998).
148. J. Baner, *Nucleic Acids Res.* **31**, e103 (2003).
149. P. Hardenbol *et al.*, *Nat. Biotechnol.* **21**, 673–678 (2003).
150. P. Hardenbol *et al.*, *Genome Res.* **15**, 269–275 (2005).
151. D. Botstein *et al.*, *Am. J. Hum. Genet.* **32**, 314–331 (1980).
152. V. Lyamichev *et al.*, *Nat. Biotechnol.* **17**, 292–296 (1999).
153. R. W. Kwiatkowski *et al.*, *Mol. Diagnosis*. **4**, 353–364 (1999).
154. C. A. Mein *et al.*, *Genome Res.* **10**, 330–343 (2000).
155. J. G. Hall *et al.*, *Proc. Natl. Acad. Sci.* **97**, 8272–8277 (2000).
156. T. M. Hsu *et al.*, *Clin. Chem.* **47**, 1373–1377 (2001).

157. K. V. N. Rao, *Nucleic Acids Res.* **31**, e66 (2003).
158. Y. Chen *et al.*, *Anal. Chem.* **77**, 2400–2405 (2005).
159. S. Nomura *et al.*, *J. Biochem. Biophys. Methods*. **70**, 787–795 (2007).
160. Q. Liu *et al.*, *Ann. Clin. Lab. Sci.* **45**, 128–133 (2015).
161. A. M. Maxam, W. Gilbert, *Proc. Natl. Acad. Sci.* **74**, 560–564 (1977).
162. F. Sanger, S. Nicklen, R. Coulson, *Proc. Natl. Acad. Sci.* **74**, 5463–5467 (1977).
163. E. L. van Dijk *et al.*, *Trends Genet.* **30**, 418–426 (2014).
164. M. Eisenstein, *Nat. Biotechnol.* **30**, 1023–1026 (2012).
165. M. Ronaghi *et al.*, *Anal. Biochem.* **242**, 84–89 (1996).
166. M. Ronaghi, M. Uhlén, P. Nyrén, *Science*. **281**, 363–365 (1998).
167. H. Fakhrai-Rad, N. Pourmand, M. Ronaghi, *Hum. Mutat.* **19**, 479–485 (2002).
168. W. Shen *et al.*, *TrAC - Trends Anal. Chem.* **69**, 1–13 (2015).
169. A. Oliphant *et al.*, *Biotechniques*. **32**, S56–S61 (2002).
170. C. Sheridan, *Nat. Biotechnol.* **32**, 111–112 (2014).
171. D. S. Grosu *et al.*, *Expert Rev. Mol. Diagn.* **14**, 605–622 (2014).
172. J. M. Rothberg *et al.*, *Nature*. **475**, 348–52 (2011).
173. J. Eid *et al.*, *Science (80-. ).* **323**, 133–138 (2009).
174. H. Bayley, S. Howorka, S. Cheley, *Nat. Biotechnol.* **19**, 636–639 (2001).
175. J. Clarke *et al.*, *Nat. Nanotechnol.* **4**, 265–270 (2009).
176. S. Kumar *et al.*, *Sci. Rep.* **2**, 1–8 (2012).
177. K. B. Mullis, F. A. Faloona, *Methods Enzymol.* **155**, 335–350 (1987).
178. R. K. Saik *et al.*, *Science.* **239**, 487–491 (1988).
179. R. Higuchi *et al.*, *Nat. Biotechnol.* **10**, 413–417 (1992).
180. C. R. Newton *et al.*, *Nucleic Acids Res.* **17**, 2503–2516 (1989).
181. R. K. Bai, L. J. C. Wong, *Clin. Chem.* **50**, 996–1001 (2004).
182. H. Ørum *et al.*, *Nucleic Acids Res.* **21**, 5332–5336 (1993).
183. Y. Nagai *et al.*, *Cancer Res.* **65**, 7276–7282 (2005).
184. Q. Wang *et al.*, *Theranostics*. **3**, 395–408 (2013).
185. A. V. *et al.*, *J. Mol. Diagnostics*. **17**, 832–833 (2015).
186. M. J. Lay, C. T. Wittwer, *Clin. Chem.* **43**, 2262–2267 (1997).
187. P. S. Bernard *et al.*, *Am. J. Pathol.* **153**, 1055–1061 (1998).
188. K. J. Livak, *Genet. Anal. - Biomol. Eng.* **14**, 143–149 (1999).
189. L. G. Kostrikis *et al.*, *Science.* **279**, 1228–1229 (1998).
190. W. D. K. Shusta, E. V. Raines, R. T. Pluckthun, *Nat. Biotechnol.* **16**, 291–294 (1998).
191. N. Svanvik, *et al.*, *Anal. Biochem.* **287**, 179–182 (2000).
192. B. J. Conner *et al.*, *Proc. Natl. Acad. Sci. U. S. A.* **80**, 278–282 (1983).
193. G. C. Kennedy *et al.*, *Nat. Biotechnol.* **21**, 1233–1237 (2003).
194. D. G. Wang *et al.*, *Science.* **280**, 1077–1082 (1998).
195. R. Mei *et al.*, *Genome Res.* **10**, 1126–1137 (2000).
196. A. C. Eklund, Z. Szallasi, *Genome Biol.* **9** (2008).
197. S. B. Haga, *Expert Rev. Mol. Diagn.* **16**, 949–960 (2016).
198. M. Urdea *et al.*, *Nature*. **444 Suppl**, 73–79 (2006).
199. J. J. Maurer, *Annu. Rev. Food Sci. Technol.* **2**, 259–279 (2012).

200. P. Craw, W. Balachandran, *Lab Chip*. **12**, 2469–2486 (2012).
201. P. Gill, A. Ghaemi, *Nucleosides, Nucleotides and Nucleic Acids*. **27**, 224–243 (2008).
202. G. Münchow, K. S. Drese, in *Microfluidic Technologies for Miniaturized Analysis Systems* (2007), pp. 523–567.
203. P. J. Asiello, A. J. Baeumner, *Lab Chip*. **11**, 1420–1430 (2011).
204. L. Yan *et al.*, *Mol. Biosyst.* **10**, 970–1003 (2014).
205. V. P. Dave *et al.*, *Lab. Investig.* **99**, 452–469 (2019).
206. J. Zhong, X. Zhao, *Food Anal. Methods*. **11**, 1543–1560 (2018).
207. X. Ding *et al.*, *Anal. Chem.* **91**, 655–672 (2019).
208. G. T. Walker *et al.*, *Proc. Natl. Acad. Sci. U. S. A.* **89**, 392–396 (1992).
209. G. T. Walker *et al.*, *Nucleic Acids Res.* **20**, 1691–1696 (1992).
210. A. Fire, S. Q. Xu, *Proc. Natl. Acad. Sci. U. S. A.* **92**, 4641–4645 (1995).
211. E. A. Mothershed, A. M. Whitney, *Clin. Chim. Acta*. **363**, 206–220 (2006).
212. L. Mahmoudian *et al.*, *Anal. Chem.* **80**, 2483–2490 (2008).
213. F. B. Dean *et al.*, *Proc. Natl. Acad. Sci. U. S. A.* **99**, 5261–5266 (2002).
214. C. Spits *et al.*, *Nat. Protoc.* **1**, 1965–1970 (2006).
215. S. Hosono *et al.*, *Genome Res.* **13**, 954–964 (2003).
216. A. Raghunathan *et al.*, *Appl. Environ. Microbiol.* **71**, 3342–3347 (2005).
217. Y. Marcy *et al.*, *PLoS Genet.* **3**, 1702–1708 (2007).
218. T. Notomi *et al.*, *Nucleic Acids Res.* **28**, e63 (2000).
219. Y. Mori *et al.*, *Biochem. Biophys. Res. Commun.* **289**, 150–154 (2001).
220. S. Santiago-Felipe *et al.*, *Biosens. Bioelectron.* **79**, 300–306 (2016).
221. M. Goto *et al.*, *Biotechniques*. **46**, 167–172 (2009).
222. N. Nakamura *et al.*, *Anal. Chem.* **79**, 9484–9493 (2007).
223. Y. Yuan *et al.*, *Sci Rep*. **4**, 5395 (2014).
224. L. Zhang *et al.*, *Anal. Chem.* **86**, 10461–10466 (2014).
225. Y. S. Jiang *et al.*, *Anal. Chem.* **87**, 3314–3320 (2015).
226. M. Itonaga *et al.*, *PLoS One*. **11**, e0151654 (2016).
227. Y. Higashimoto *et al.*, *J. Clin. Microbiol.* **46**, 2665–2670 (2008).
228. Y. Lu *et al.*, *Biosens. Bioelectron.* **90**, 388–393 (2017).
229. O. Piepenburg *et al.*, *PLoS Biol.* **4**, 1115–1121 (2006).
230. M. D. Moore, L. A. Jaykus, *Future Virol.* **12**, 421–429 (2017).
231. G. C. Luo *et al.*, *Anal. Biochem.* **575**, 36–39 (2019).
232. M. A. Londoño, C. L. Harmon, J. E. Polston, *Virol. J.* **13**, 1–9 (2016).
233. J. Li, J. Macdonald, F. Von Stetten, *Analyst*. **144**, 31–67 (2019).
234. R. K. Daher *et al.*, *Clin. Chem.* **62**, 947–958 (2016).
235. I. M. Lobato, C. K. O'Sullivan, *TrAC - Trends Anal. Chem.* **98**, 19–35 (2018).
236. M. Vincent, Y. Xu, H. Kong, *EMBO Rep.* **5**, 795–800 (2004).
237. Y. J. Jeong, K. Park, D. E. Kim, *Cell. Mol. Life Sci.* **66**, 3325–3336 (2009).
238. W. H. A. Chow *et al.*, *J. Mol. Diagnostics*. **10**, 452–458 (2008).
239. N. Ramalingam *et al.*, *Microfluid. Nanofluidics*. **7**, 325–336 (2009).
240. A. Sedighi, C. Oberc, V. Whitehall, P. C. H. Li, *Nano Res.* **10**, 12–21 (2017).
241. Y. Li *et al.*, *Clin. Chim. Acta*. **412**, 79–85 (2011).
242. Y. Tong, B. Lemieux, H. Kong, *BMC Biotechnol.* **11** (2011).
243. J. Van Ness, L. K. Van Ness, D. J. Galas, *Proc. Natl. Acad. Sci. U. S. A.* **100**,

4504–4509 (2003).
244. H. Jia, Z. Li, C. Liu, Y. Cheng, *Angew. Chemie - Int. Ed.* **49**, 5498–5501 (2010).
245. Y. Mitani *et al.*, *Nat. Methods*. **4**, 257–262 (2007).
246. K. Tatsumi *et al.*, *J. Mol. Diagnostics*. **10**, 520–526 (2008).
247. N. Rashwan *et al.*, *PLoS Negl. Trop. Dis.* **10**, 1–16 (2016).
248. Y. Kawai *et al.*, *Biologicals*. **36**, 234–238 (2008).
249. K. Tsunekawa *et al.*, *Biomed Res. Int.* **2014**, 964635 (2014).
250. K. Yoshida *et al.*, *AAPS J.* **15**, 618–622 (2013).
251. J. Watanabe *et al.*, *Biotechniques*. **43**, 479–484 (2007).
252. M. Shimida *et al.*, *Rinsho Byori, Japanese J. Clin. Pathol.* **50**, 528–532 (2002).
253. N. Urasaki *et al.*, in *International Research Conference on Huanglongbing* (2008), p. 124.
254. H. Mukai *et al.*, *Mol. Cell. Probes*. **22**, 333–337 (2008).
255. L. M. Zanoli, G. Spoto, *Biosensors*. **3**, 18–43 (2013).
256. S. A. Boppart, R. Richards-Kortum, *Sci. Transl. Med.* **6** (2014).
257. M. Zarei, *TrAC - Trends Anal. Chem.* **91**, 26–41 (2017).
258. M. Madou *et al.*, *Annu. Rev. Biomed. Eng.* **8**, 601–628 (2006).
259. D. D. Nolte, *Rev. Sci. Instrum.* **80** (2009), doi:10.1063/1.3236681.
260. R. Gorkin *et al.*, *Lab Chip*. **10**, 1758–1773 (2010).
261. R. Burger *et al.*, *Curr. Opin. Chem. Biol.* **16**, 409–414 (2012).
262. Y. Shi *et al.*, *Anal. Chem.* **71**, 5354–5361 (1999).
263. C. Li *et al.*, *Electrophoresis*. **30**, 4270–4276 (2009).
264. R. Peytavi *et al.*, *Clin. Chem.* **51**, 1836–1844 (2005).
265. L. Wang, P. C. H. Li, *Anal. Biochem.* **400**, 282–288 (2010).
266. A. Sedighi, P. C. H. Li, in *Microarray Technology. Methods in Molecular Biology* (2016), vol. 1368, pp. 133–141.
267. O. Strohmeier *et al.*, *Microchim. Acta*. **181**, 1681–1688 (2014).
268. H. Z. Yu, Y. Li, L. M. L. Ou, *Acc. Chem. Res.* **46**, 258–268 (2013).
269. E. E. Te Hwu, A. Boisen, *ACS Sensors*. **3**, 1222–1232 (2018).
270. S. Morais, R. Puchades, Á. Maquieira, *Anal. Bioanal. Chem.* **408**, 4523–4534 (2016).
271. L. A. Tortajada-Genaro *et al.*, *RSC Adv.* **5**, 29987–29995 (2015).
272. Z. Díaz-Betancor *et al.*, *Microchim. Acta*. **186**, 570 (2019).
273. H. Kido, A. Maquieira, B. D. Hammock, *Anal. Chim. Acta*. **411**, 1–11 (2000).
274. I. Alexandre *et al.*, *Biotechniques*. **33**, 435–439 (2002).
275. J. J. La Clair, M. D. Burkart, *Org. Biomol. Chem.* **1**, 3244–3249 (2003).
276. S. Morais *et al.*, *Chem. Commun.*, 2368–2370 (2006).
277. M. J. Bañuls *et al.*, *Bioconjug. Chem.* **19**, 665–672 (2008).
278. J. Tamarit-López *et al.*, *Bioconjug. Chem.* **22**, 2573–2580 (2011).
279. T. Arnandis-Chover *et al.*, *Talanta*. **101**, 405–412 (2012).
280. L. A. Tortajada-Genaro *et al.*, *J. Agric. Food Chem.* **60**, 36–43 (2012).
281. S. Santiago-Felipe *et al.*, *Sensors Actuators, B Chem.* **204**, 273–281 (2014).
282. L. A. Tortajada-Genaro *et al.*, *Anal. Bioanal. Chem.* **408**, 2339–2345 (2016).
283. L. A. Tortajada-Genaro *et al.*, *Analyst*. **144**, 707–715 (2019).

284. A. Ozcan, *Lab Chip*. **14**, 3187–3194 (2014).
285. J. C. Contreras-Naranjo, Q. Wei, A. Ozcan, *IEEE J. Sel. Top. Quantum Electron.* **22** (2016).
286. E. Petryayeva, W. R. Algar, *RSC Adv.* **5**, 22256–22282 (2015).
287. K. Yang *et al.*, *Lab Chip*. **16**, 943–958 (2016).
288. D. Zhang, Q. Liu, *Biosens. Bioelectron.* **75**, 273–284 (2016).
289. A. Roda *et al.*, *Comprehensive Anal. Chem*., 77, 237-287 (2017).
290. D. Quesada-González, A. Merkoçi, *Biosens. Bioelectron.* **92**, 549–562 (2017).
291. J. Liu *et al.*, *Biosens. Bioelectron.* **132**, 17–37 (2019).
292. R. D. Stedtfeld *et al.*, *Lab Chip*. **12**, 1454–1462 (2012).
293. M. Dou *et al.*, *Biosens. Bioelectron.* **87**, 865–873 (2017).
294. S. C. Liao *et al.*, *Sensors Actuators, B Chem.* **229**, 232–238 (2016).
295. J. Hui *et al.*, *Lab Chip*. **18**, 2854–2864 (2018).
296. A. Sayad *et al.*, *Biosens. Bioelectron.* **100**, 96–104 (2018).
297. G. Papadakis *et al.*, *ACS Sensors*. **4**, 1329–1336 (2019).
298. J. R. Choi *et al.*, *Lab Chip*. **16**, 611–621 (2016).
299. A. Priye *et al.*, *Sci. Rep.* **7**, 1–11 (2017).
300. A. Priye, C. S. Ball, R. J. Meagher, *Anal. Chem.* **90**, 12385–12389 (2018).
301. K. Kaarj, P. Akarapipad, J. Y. Yoon, *Sci. Rep.* **8**, 1–11 (2018).
302. Y. D. Ma *et al.*, *Lab Chip*. **19**, 3804–3814 (2019).
303. K. Ming *et al.*, *ACS Nano*. **9**, 3060–3074 (2015).
304. J. Song *et al.*, *Clin. Chem.* **63**, 714–722 (2017).
305. K. Chan *et al.*, *Anal. Biochem.* **545**, 4–12 (2018).
306. W. Lu *et al.*, *Analyst*. **143**, 5046–5053 (2018).
307. Y. Michikawa *et al.*, *Sensors*. **8**, 2722–2735 (2008).
308. X. Zhang *et al.*, *Genet. Test. Mol. Biomarkers*. **22**, 719–723 (2018).
309. M. G. Wolfe, M. M. Ali, J. D. Brennan, *Anal. Chem.* **91**, 4735–4740 (2019).
310. M. Kühnemund *et al.*, *Nat. Commun.* **8**, 1–8 (2017).
311. M. O. Noor, U. J. Krull, *Anal. Chem.* **86**, 10331–10339 (2014).
312. K. Malhotra, M. O. Noor, U. J. Krull, *Analyst*. **143**, 3049–3058 (2018).
313. H. Yu, Y. Tan, B. T. Cunningham, *Anal. Chem.* **86**, 8805–8813 (2014).
314. E. M. Spyrou *et al.*, *Anal. Bioanal. Chem.* **408**, 7393–7402 (2016).
315. L. Xie *et al.*, *Sci. Rep.* **4**, 1–6 (2014).
316. X. Wang *et al.*, *Int. J. Food Microbiol.* **253**, 66–74 (2017).
317. V. Srinivasan *et al.*, *J. Microbiol. Methods*. **139**, 15–21 (2017).
318. J. Petersen *et al.*, *Anal. Biochem.* **360**, 169–171 (2007).
319. A. Galaziou, T. K. Christopoulos, P. C. Ioannou, *Anal. Bioanal. Chem.* **411**, 3769–3776 (2019).
320. Y. Xiang, Y. Lu, *Anal. Chem.* **84**, 1975–1980 (2012).

# 2 OBJECTIVES

The **general objective** of this thesis is the development of new analytical tools for performing point-of-care DNA biosensing, based on isothermal enzymatic SNP discrimination and detection by consumer electronic devices, in order to support pharmacogenetics.

In order to achieve this general goal, the following **specific objectives** must be accomplished:

1. To set-up isothermal discrimination assays, based on recombinase-polymerase amplification (RPA), loop-mediated isothermal amplification (LAMP) and ligation, for differentiating single base polymorphisms;
2. To combine the reaction with biosensing platforms, employing direct fluorescent or colorimetric detection, microarray hybridization and enzymatic staining; and integrating it with simple, effective and affordable supports, such as polymeric chips, 3D-printer structures and compact discs;
3. To develop techniques for reading the assay, employing a compact disc reader, a flatbed scanner, a smartphone and other consumer electronic devices.
4. To verify the performance of the developed POC biosensors, by carrying out genotyping assays associated with the personalized treatment of tobacco addiction, major depressive disorder and cardiovascular diseases.

These goals were achieved through the exploration of different strategies. The experiments and obtained results are organized in the next chapters, presented in the format of indexed journal articles.

# 3 EXPERIMENTAL RESULTS

# Chapter 1. Allele-specific recombinase polymerase amplification and colorimetric microarray detection

In this first chapter, the favourable features of recombinase polymerase amplification were exploited for performing isothermal amplification at low temperature and short response times. The reaction was combined to microarray hybridization and enzymatic immunostaining in order to perform a SNP genotyping method for smoking cessation-related genes, meaning that it could be used for selecting adequate therapies according to the resulting genotype. The most important challenge was the achievement of an extremely high selectivity, by selecting the assay reagents and adjusting the medium conditions. The application of 3D-printing was also exploited for creating a versatile and miniaturized amplification platform, allowing the execution of multiple low-volume simultaneous RPA reactions. The assay was detected using digital versatile disc (DVD) and reader, as this consumer electronic device presents a well-developed, widespread and cheap technology that can be used for optical detection.

Microchim Acta (2017) 184:1453–1462
DOI 10.1007/s00604-017-2144-0

ORIGINAL PAPER

# Low-cost genotyping method based on allele-specific recombinase polymerase amplification and colorimetric microarray detection

Eric Seiti Yamanaka[1] · Luis A. Tortajada-Genaro[1,2] · Ángel Maquieira[1,2]



## 3.1 Abstract

The costs of current genotyping methods limit their application to personalized therapy. The authors describe an alternative approach for the detection of single-point-polymorphisms using recombinant polymerase amplification as an allele-specific technique. The use of short and chemically modified primers, and locked nucleic acids allowed for a selective isothermal amplification of wild-type or mutant variants at 37 °C within 40 min. An amplification chip containing 100 wells was manufactured with a 3D printer and using thermoplastic polylactic acid. The platform reduces reagent consumption and allows parallelization. As a proof of concept, the method was applied to the genotyping of four SNPs that are related to the treatment of tobacco addiction. The target polymorphisms included rs4680 (COMT gene), rs1799971 (OPRM1 gene), rs1800497 (ANKK1 gene), and rs16969968 (CHRNA5 gene). The genotype populations can be well discriminated.

Keywords: pharmacogenomics, SNP genotyping, isothermal amplification, micro-well plate, microchip; tobacco addiction; 3D-printer, COMT gene, OPRM1 gene, ANKK1 gene, CHRNA5 gene.

## 3.2 Introduction

Pharmacogenomics is currently considered one of the most active areas of the personalized medicine paradigm. However, numerous barriers have been encountered to launch DNA variation analyses, such as single-nucleotide polymorphisms (SNPs), in health systems (*1*). Among other factors, available platforms have a marked technological limitation. Most genomic findings have been obtained from high-throughput technologies, such as Illumina and Affimetrix platforms. However, the incorporation of these methods into primary care centers is limited, and cost is the main drawback (*2–4*). Dramatically cutting the turnaround times of these platforms is an important goal for implementing SNP testing into clinical scenarios. Therefore, the novel generation of simple diagnostic tools is absolutely necessary for the real adoption of personalized medicine (*5*, *6*).

A large family of high-potential methods to be developed in simple systems is that based on allele-specific (AS) amplification (*7*). Polymerase chain reaction (PCR) uses primer pairs, deliberately designed at SNP sites. Primers have a single-base variation at the 3’ end (allele-specific primers), so extension and amplification reactions take place with only perfectly-matched sequences of target regions. This approach has been successfully used as a pharmacogenomic tool combined with several detection systems (*8–10*). Nevertheless, these techniques require particular thermal cycling, consequently there are several limitations for their future integration as point-of-care devices. PCR demands an accurate temperature control system to

quickly heat/cool reaction solutions. The high temperature reached (up to 95 °C) leads to variations in the volume reaction due to water evaporation and gas bubble formation, which renders accurate process control necessary.

Several new technologies have emerged to improve DNA-based analyses (*11*). Many efforts have been made that focus on developing low-cost systems to be used for point-of-care applications or in small laboratories located at the physician's office or in primary health centers.

A revolution in the development of new methods is currently being witnessed, and is associated with the application of isothermal solutions for microanalyses (*12*). These approaches are based on using proteins that separate DNA strands instead of thermal approaches so that target nucleic acids are synthesized at constant temperature. Nevertheless, the application of isothermal amplification for SNP genotyping is still minimum (*13, 14*). Among isothermal reactions, recombinase polymerase amplification (RPA) has many interesting properties; e.g., short reaction times (20-60 min), robustness and low energy requirements (close to room temperature) (*15*). Recently, our research group has demonstrated that polycarbonate-based substrates can be used to support RPA assays in chip (*16*), micro-reactors (*17*), or dynamic formats (*18*). A well array chip has been described to process miniaturized RPA assays, applied for pathogen detection in under 30 min (*19*). The chip was manufactured from a silicon substrate by a complex fabrication technique, including photolithography and chemical treatment, and is only available in specialized laboratories.

The capability of RPA technology for SNP genotyping remains an unsolved issue. A recent study evaluated the influence of sequence mismatches on the amplification specificity of closely-related pathogens (*20*). A proof of concept assay describes the discrimination of a single-point mutation of the HRAS gene (*21*). To this end, DNA extracted from cell lines

was selectively amplified and genetic variants were distinguished by measuring the wavelength shift on silicon micro-ring resonators. However, this technology is far from being adopted generally in health centers.

In the present study, the capability of allele-specific RPA (AS-RPA) is evaluated and a low-cost method is developed for the SNP genotyping of clinically relevant polymorphisms. In a first approach, amplification is performed in conventional polypropylene vials in a single format (detection of a single polymorphism). The advantages of this disposable format are its low cost and compatibility with a huge number of laboratory equipment. However, lab-on-a-chip or μ-total analysis systems offer important advantages for diagnostic devices, such as high-throughput and miniaturization, among others (*22*).

There are many ways to microfabricate plastic-based materials; e.g. laminate, embossing or injection molding. Additive manufacturing is being examined given its growing interest in the microfluidics field (*23*). It is capable of producing customized structures that range from a few microns to several centimeters in a single step. The main limitations of 3D printers are related to spatial resolution, dimensional fidelity, surface quality, biocompatibility, optical transparency, among others (*24*). Advantages include low infrastructure costs and easy manufacturing compared to photolithography or soft lithography approaches. In order to evaluate the potential of this technology, a well array chip for performing AS-RPA was designed and developed with a commercial 3D printer. The objective was to demonstrate RPA's capability as a genotyping method and to compare its performance in an advanced platform compared to the standard format (vials).

As proof of concept, the solution was applied as a pharmacogenomics tool to treat smoking cessation and the highly addictive properties of nicotine (*25*, *26*). In such diseases, the benefits of personalized medicine based on

genotype populations has been demonstrated. However, the high cost of current genotyping technologies, compared to the cost of ineffective or erroneous treatment, compromises the application of the test. Therefore, the approach was designed by following the analytical quality and health system sustainability goals.

## 3.3 Material and methods

### Target genes

The target polymorphisms for the tobacco use disorder were rs4680 (COMT gene), rs1799971 (OPRM1 gene), rs1800497 (ANKK1 gene) and rs16969968 (CHRNA5 gene). The wild-type variants are G, A, G, and G, and the mutant variants are A, G, A, and A, respectively. The pharmacogenomic information about these variants is included as Supplementary Material (Tables SI.1, SI.2 and SI.3). The human beta actin (ACTB) gene was selected as an endogenous control. The list of oligonucleotides for the genotyping of each SNP is found in Table SI.4.

### Patient samples and reference discrimination method

Subjects (n=17) were recruited for the present study according to ethics and with informed consents. Buccal smear samples were collected using sterile swabs. They were submitted to digestion and purification steps with a PureLink Genomic DNA Mini Kit (Invitrogen, Thermo Fisher Scientific, USA, www.thermofisher.com). The isolated DNA extracts were eluted from the spin-columns of the kit with Tris-HCl buffer (10 mMTris, pH 8.6) and stored at -20 °C until analyzed.

Allele-specific PCR in a single format was applied as the reference genotyping method. Briefly, the extracted genomic DNA (4 ng) was amplified using two PCR master mixes (Biotools, Spain, www.biotools.eu) and employing 300 nM of each variant primer pair (reverse and allele-specific forward). To confirm amplification, products were diluted in 0.5x SyBR Safe (Invitrogen, Thermo Fisher Scientific, USA) and submitted to fluorescence measurements in a plate reader (Victor 3TM V1420, PerkinElmer, Finland, www.perkinelmer.com). Genotypes were also verified by 3% agarose gel electrophoresis, followed by dying with an intercalating agent (Real Safe, Durviz, Spain, www.durviz.com) and visualization under UV light.

**Fabrication of structured platforms**

The 100-well array chip was modeled with the Autodesk Inventor Professional 2015 software (Autodesk, USA, www.autodesk.com) and fabricated with a 3D printer (Ultimaker 2 Extended, UltimakerB.V., the Netherlands, www.ultimaker.com). Polylactic acid (PLA) filament (RS Pro, Spain; 2.85 mm diameter, www.rs-online.com) was employed as the printing material. Fabrication was carried out using a 0.4 mm diameter nozzle at 210 °C and a bed operation temperature of 60 °C. In order to evaluate the best printing conditions, prototypes were fabricated with different layer thicknesses (up to 0.2 mm) and at various printing speeds (up to 300 $mm.s^{-1}$). Subsequently, printed structures were cleaned with a 30-minute ultrasonic bath and dried with compressed air.

The fabrication quality of the PLA-chips was monitored by optical microscopy imaging. Surface pictures were captured (1.2x magnification) by an Olympus SZ61 stereo microscope (Olympus Co., Japan, www.olympus.com). Images were analyzed with the Image J software to

provide an estimated roughness for each sample. Surface hydrophobicity was estimated from the contact angle data. Measures of the deionized water droplets (4 μL) were taken using a Dino-Lite Digital Microscope (AnMo Electronics Co., Taiwan, www.dino-lite.com) at the 1.3-megapixel resolution.

A mass loss study was also done to evaluate possible sample evaporation on the platform. The chip was loaded with 10 RPA samples (4 μL each) and placed in an oven at 37 °C. Mass measurements of the set were periodically taken during 4 h and compared with those of an unloaded reference chip.

**Assay protocol: amplification**

The amplification step was performed using a TwistAmp Basic RPA kit (TwistDx, UK, www.twistdx.co.uk). Eight allele-specific mixes (2 per SNP) were prepared with rehydration buffer, 14 mM of magnesium acetate, 480 nM of allele-specific forward primer and reverse digoxigenin-labeled primer, and the enzyme pellet. Mineral oil (8%) was also added to minimize sample evaporation. Solutions were loaded onto the 100-well array chip and the DNA template (2.56 ng) was added to allow the simultaneous amplification of eight different allelic variants for 10 patient samples and controls (human ACTB gene). The chip was then covered with a polyester plate sealer (Corning, USA, www.corning.com) and gently vortexed to mix reagents and samples. Amplification was carried out in a heating oven (Memmert UF30, Germany, www.memmert.com) at 37 °C for 40 min.

The AS-RPA reactions were also performed in 0.2 mL-polypropylene vials (Labbox, Spain, www.labbox.com) and polycarbonate home-made array chips. These chips were fabricated using a computer numerical control

drilling machine (Bungard CCD, Karo 5410, Germany, www.bungard.de). The feed speed and rotational rate of the drill were respectively 2,000 $mm \cdot s^{-1}$ and 48,000 rpm. The diameter of each well was 5 mm and their depth was 1.1 mm. The composition of the RPA mixtures was the same as that previously described, but volumes were 25 µL and 4 µL per reaction for vials and chips, respectively. The heating system used was a thermocycler (TC-4000, Techne, UK, www.techne.com) and an oven, respectively.

**Assay protocol: detection and data analysis**

The AS-RPA products were detected by a hybridization assay on polycarbonate chips, adapted from reference (*10*). Briefly, the mixtures of the wild-type or mutant products for all four SNPs were prepared from the respective single RPA solutions. For this purpose, 2 µL of each amplification product were diluted in 16 µL of hybridization buffer composed of NaCl 225 mM, sodium citrate 22.5 mM, 10% formamide and 2.5x Denhardt's solution, pH 7. Subsequently, mixtures were heated at 95 °C for 10 min for denaturation and transferred to the chips with the immobilized probes in the microarray format. After 60 min of incubation at 37 °C, chips were washed with diluted hybridization buffer. The immunoreaction protocol with enzymatic labelling was followed to develop the duplex of the probe-RPA product, as described in reference (*10*). The oxidized form of 3,3',5,5'-tetramethylbenzidine (substrate of horse-radish-peroxidase) produced a blue precipitate over the positive or control spots. Chips were then read with a desktop scanner (Epson Perfection 1640SU Office, Epson, Japan, www.epson.com).

**Discrimination index**

The resulting gray-scale images (Tagged Image File Format, color depth 16 bit) were processed by an in-house software for the microarray analysis. The optical intensity signals of each spot and local background were quantified by generating a data matrix of the signal-to-noise ratios. The genotype determination rule was constructed according to the replicated responses of the specific probes for each polymorphism. A discrimination index was calculated from the signal of the wild-type (WT) and mutant (MUT) variants according to this equation: (WT − MUT)/(WT + MUT). The Statgraphics Centurion statistical package for Windows v.16 was used for the data analysis.

## 3.4 Results

**RPA capability as a genotyping tool**

The use of RPA as an allele-specific amplification technique was analyzed by considering the role of each element in the process. A recombinase (T4 uvsX) recognizes targeted DNA templates and specific primers at a high affinity and catalyzes subsequent homologous pairing and strand exchange (*20*). Polymerase produces the correct elongation of the perfect-annealed primer/template, and is the key reaction in the DNA duplication process (*27*). Furthermore, the Pol I large fragment (Bsu polymerase) lacks exonuclease activity (3’→5’) that may modify the target nucleotide. Therefore, we expected the presence of mismatches on their 3'-extreme to hamper the nonspecific reaction due to the combined action of two enzymes, even at a low working temperature.

Complementarily, oligonucleotide sets were carefully selected to satisfactorily amplify/detect the given template region. The in-silico design restrictions were primer length, absence of secondary structures, and primer/template duplex stability. Both these last parameters were estimated from the thermodynamic models available for DNA duplexes (*28*). Although the recommended length for RPA primers should be 30-35 bases long according to the manufacturer's instructions, shorter primers (19–21 mer) were chosen to improve selectivity. The free energy (ΔG) values for the self-annealing and hairpin structures were restricted to 1.0 $Kcal.mol^{-1}$ (the equivalent to melting temperatures < 50 °C). The selected oligonucleotides produced primer/template duplexes with changes in free energy (ΔG) of -25.6±0.2 $Kcal.mol^{-1}$ (the equivalent to a melting temperature of 75.4±0.1 °C) for totally complementary primers. The duplexes between the template and mismatched primers were less stable (-24.0±0.6 $Kcal.mol^{-1}$, 72.7±0.6 °C).

The experiments focused on evaluating discrimination capability using the designed primers that differentiated at their 3'-endnucleotide. Figure 18a shows the kinetic curve to perform amplification in a homogeneous format (reaction volume of 25 μL). The expected positive signals were observed after 10-20 min following typical logistic regression (maximum response after 60 min). Under the selected conditions, a different behavior was observed depending on the added primer. Extension by polymerase was efficient when the 3' terminal base of a primer matched its target, whereas extension was inefficient or nonexistent when the terminal base was mismatched. These effects agree with the previously reported results about the reduction or inhibition of the RPA reaction due to the presence of a mismatch in the primer/template duplex (*20*).

Conventional and chemical-modified primers, locked nucleic acids (LNA), were compared for AS-RPA. Figure 18b shows that nonspecific

amplification took place for the mismatched duplexes between the primer and templates. Nevertheless, the amplification yield was significantly higher for the totally complementary duplexes (ANOVA, p-value<0.001). With the LNA primers, differences were more marked, and even nonspecific amplification was similar to the negative controls. These experiments demonstrated that the presence of this nucleoside at the 3' terminal base improved allelic discrimination.

A multiplex reaction was studied for the simultaneous amplification of more than one target in a single reaction. However, reaction yields were not satisfactory and there were sensitivity losses. One system displayed dominating and/or inhibiting activity over other primers and amplicons, and even genotyping capability was lost. These results agreed with conventional RPA behavior and can be associated with their high sensitivity to the total primer concentration (*16*).

(a)

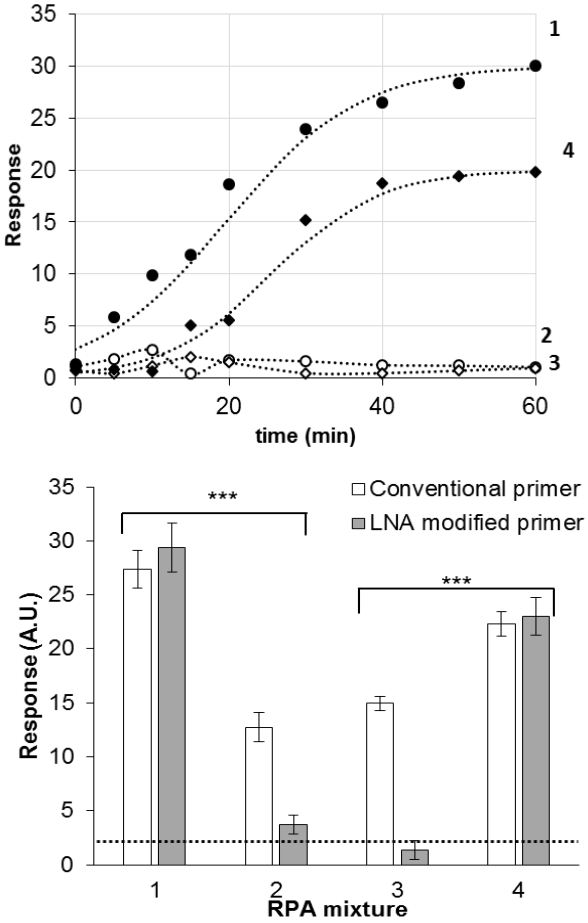


(b)

***Figure 18.*** (a) Amplification kinetic curves of rs1799971 (OPRM1 gene) depending on the RPA mixture: logistic regressions y = 30 / (1+exp(-2.28 – 0.12 t), R= 0.977 for the wild-type and y = 20 / (1+exp(-3.64 – 0.15 t)), R= 0.977 for the mutant variant. (b) Response depending on the primer nature and RPA mixture: statistical comparison compared to the perfect-match duplex (*** $p<0.001$). Mixture 1: wild-type template DNA and wild-type FP). Mixture 2: wild-type template DNA and mutant FP. Mixture 3: mutant template DNA and wild-type FP. Mixture 4: mutant template DNA and mutant FP. Four replicates

**Design and fabrication of well array chip**

The amplification assays, described in the previous section, were performed in 0.2-mL polypropylene vials. The next step was to reduce the reaction volume by performing the assay in a well array chip. This kind of platforms improves amplification capabilities, particularly high-throughput (*29*). Fused filament fabrication was chosen as the additive manufacturing technology, with a biocompatible polymer, e.g., PLA, as the thermoplastic material. This technique was selected because it produces innovative bioanalytical platforms that can be customer-designed and fast prototyped by a 3D printer.

The first experiments focused on designing an array chip with 100 wells. The well dimensions (2.5 mm × 2.5 mm × 4 mm) were chosen to perform RPA in a reduced volume (<5 µL). Edge-to-edge spacing (distance between wells) was 1 cm for RPA-mixture dispensation by a multi-channel micropipette. The deposition of filament layers, one on top of the other, built up the bottom and the walls of the chip. This additive technique produced grooved structured surfaces on chip walls to study the effect of the 3D printing parameters on chip quality (Supplementary Material/Figure SI.1). By increasing printing layer separation, groove thickness changed from 71±2 µm (0.06 mm) to 238±5 µm (0.2 mm). With a 0.02-mm layer height, the surface became irregular and did not produce visible grooves. Surface roughness, expressed in Rq, varied from 53.8 µm (0.02 mm) to 76.6 µm (0.2 mm). The effect of printing speed and working temperatures during the deposition process were negligible. The selected values were a layer height of 0.1 mm and a print speed of 50 $mm.s^{-1}$, which resulted in a fabrication time of 480 $min.unit^{-1}$. Figures 19a and 19b show the optical microscope images of the PLA-chips produced under the selected conditions. Sealing, performed with

a polyester adhesive film and by adding mineral oil, was effective for the tested range (up to 37 ºC and 4 h), with null leaking and evaporation (p-value< 0.001).

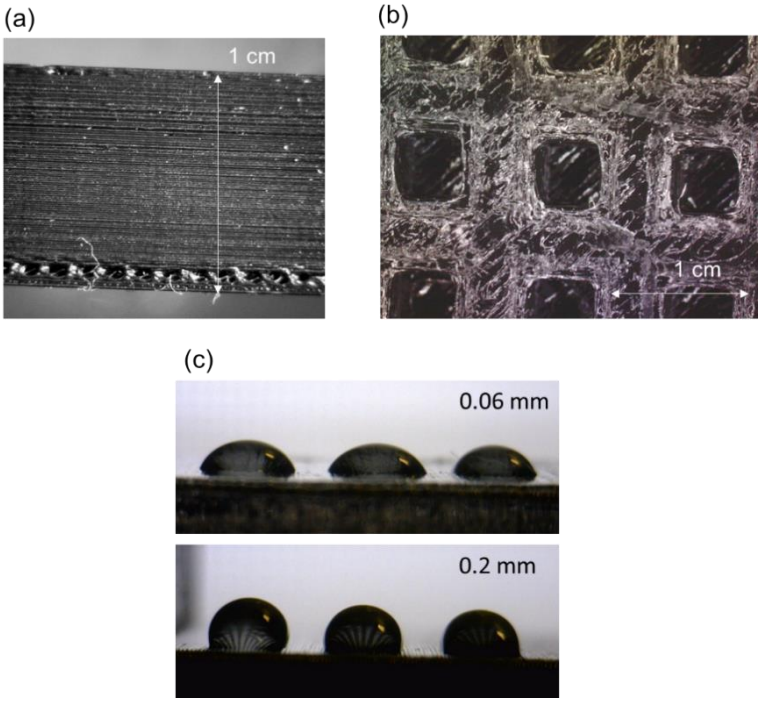


**Figure 19.** (a) Optical microscope image of the chip wall. (b) Optical microscope image of chip wells (top view). (c) Effect of printing layer height on the PLA contact angle

The hydrophilic/hydrophobic nature of the reaction vessel can affect the easy-filling of wells. Hence the wettability of the raw PLA-chips was estimated and the contact angle of well surfaces was measured. The results were 97±4 ° and 77± 2 ° for the wall and the bottom surface, respectively. These values indicated how the patterned topography modified the interfacial tension between the liquid and thermoplastic compared to the base material

(PLA, contact angle of about 80 °). Two chemically modified chips (UV/ozone irradiation and PEG passivation) were tested. The surface topographies, estimated by microscope image analyses, were comparable to those from the raw chip (p-value > 0.05). After applying soft UV/ozone irradiation, the contact angle was 71±2 °. This lower value indicated that some photo-oxidized polar groups on the surface were formed, consequently fiber adhesion increased (higher surface energy). Addition of PEG also produced a coating over all the active surfaces, and hydrophilicity increased (62±3 °). Regardless of the surface treatment, reagent solutions were easily loaded in wells.

The effect of the unpolished surfaces and chemical treatment on the amplification yield was studied. Replicate RPA reactions were performed using genomic DNA for native/mutant patients (order of magnitude: 103 pg of gDNA). Effective amplification was achieved in all the wells of the raw and chemically modified PLA-chips. Nevertheless, the PEG coating was chosen because this treatment can help block chip surfaces, and prevent nonspecific signals and sample losses through protein and amplification product adsorption (*30*).

**Comparison of amplification platforms**

The RPA performances for the reactions run in the PLA-3D printed chip were compared with two previously reported platforms (Table 5). The first reference platform was polypropylene vials (0.2 mL) (individual or tube strips), which are widely used for DNA amplification in conventional thermal cyclers. The second was micro-reactors fabricated in polycarbonate (PC) substrate by drilling because they are a low-cost alternative for reduced volume amplifications performed in ovens or other cheap thermal systems

(*17*). The analysis of variance (ANOVA) indicated that the responses for three platforms were comparable, with p-values of 0.63 for the negative controls, 0.27 for the reference gene (ACTB gene) and 0.23 for the target genes. The platform cost for 100-plex reactions using the current 3D-printed chips was the equivalent to those of the polypropylene vials. Nevertheless, the main advantages of this approach stemmed from volume reduction and the cost of the reagent; reagent consumption (and the amount of DNA) decreased by about 6-fold. Other advantages were reduced size, which was compatible with portable heating systems (i.e. miniaturized Peltier-based devices), and facilitated their adaptation for field or doctor office applications (*11*, *12*). These performances confirmed PLA-additive manufacturing to be a strategy for the rapid versatile low-cost prototyping of bioanalytical devices. The assay costs of each platform were estimated, considering their material, equipment and processing expenses (3D printing or CNC milling), as well as their number of parallel assays. The estimated platform cost per assay for the 3D printed PLA chip was similar to polystyrene vials, while 4-times lower than for the polycarbonate milled chips.

Our approach based on reaction vessels was compared with microfluidic chips in virtue of their high applicability as point-of-care systems (*31*). The microfluidic platforms, generally based on poly(methyl-methacrylate) (PMMA) or similar polymers, allow a higher degree of assay integration and lower reaction volumes (nanoliter scale). In exchange, the PLA multi-well chip presents easier manipulation, no fluidic control equipment requirements and a simpler fabrication process with a 16-fold lower cost.

This study can open up ways to test PLA-microfluidic devices, e.g., integration of RPA amplification and real-time detection, prior to their mass production in other thermoplastics, such as PC (e.g., injection molding).

**Table 5.** Characteristics of the tested amplification platforms

| |  PLA chip |  PP vial |  PC chip |
|---|---|---|---|
| Response negative control | 3 ± 2 a.u. | 4 ± 1 a.u. | 4 ± 1 a.u. |
| Response reference gene | 37 ± 3 a.u. | 41 ± 2 a.u. | 39 ± 3 a.u. |
| Response target genes | 34 ± 3 a.u. | 37 ± 1 a.u. | 35 ± 1 a.u. |
| Fabrication technique | 3D printing | Molding | Molding + Milling |
| Platform dimensions | 52 mm × 52 mm × 10 mm | 100 × (20 mm, ϕ 7 mm) | 30 mm × 30 mm × 12 mm |
| Material thermal conductivity | 0.13 $W \cdot m^{-1} \cdot K^{-1}$ | 0.20 $W \cdot m^{-1} \cdot K^{-1}$ | 0.19 $W \cdot m^{-1} \cdot K^{-1}$ |
| Number of simultaneous samples | 100 | 1 | 9 |
| Reaction volume per assay | 4 μL | 25 μL | 4 μL |
| DNA amount per assay | 2.56 ng | 16 ng | 2.56 ng |

a.u.: arbitrary units. Data from three replicated assays

## Analytical performance of the genotyping assay

Having demonstrated that AS-RPA can be used for SNP genotyping in a single format, the capabilities of a multiplex detection method were studied. Among the techniques currently available (i.e. optical, electrochemical, etc.), AS-RPA on PLA chips combined to a hybridization assay on PC chips was tested. This detection approach showed excellent performance to simultaneously identify several PCR products (*10*).

The AS-RPA products from the target genes related to the tobacco use disorder were simultaneously determined. Selectivity was estimated from cross-reactivity experiments by hybridizing products from single

amplification assays on a chip that contained probes for the five studied genes (four target genes and a control gene) (Figure 20). Positive responses were obtained only for the specific probe, and were negative for the remaining ones. Sensitivity was determined by preparing heterozygous mixtures with increasing percentages of wild-type DNA compared to the mutant type (Supplementary Material). Mismatched DNA was detected up to 5-10 %, which indicated that the system was capable of discriminating both genotypes selectively. Intra-day repeatability and inter-day reproducibility, expressed as the relative standard deviation of spot intensities for the replicated assays (five replicates), were 13 % and 17 %, respectively. The ANOVA test showed that the end-point responses were comparable for the four studied genes (p-value > 0.05).

Our detection method of AS-RPA products displayed comparable performance to others previously described for AS-PCR, such as capillary electrophoresis (*8*), real-time fluorescence (*32*), the fluorescent-based droplet technique (*9*) and hybridization to covalently immobilized probes in fluorescent magnetic beads (*33*).

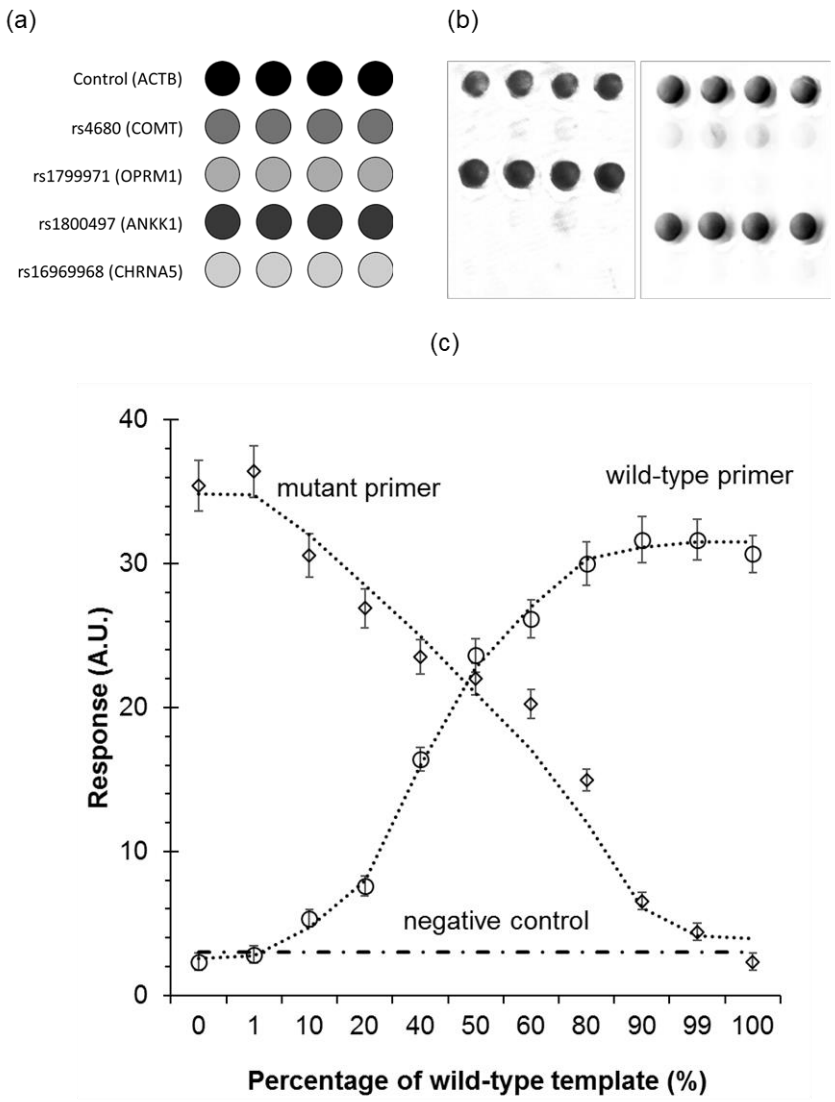


**Figure 20.** (a) Probe layout of a microarray chip (b) Microarray images obtained for the amplification products: rs1799971 (left) and rs1800497 (right) (c) Assay response depending on the percentage of wild-type template compared to the total template for both RPA mixtures (wild-type FP and mutant FP). Logistic regressions: y = 32 / (1+exp(2.43 – 0.07 t), R= 0.982 for the wild-type and y = 37 / (1+exp(-2.80 + 0.05 t), R= -0.935 for the mutant.

**Analysis of patient samples**

The applicability of chip-based AS-RPA for genotyping screening in tobacco cessation treatment, or for drugs used in nicotine dependence, was investigated. As a biological sample, buccal swab extracts were selected. In a clinical scenario, the use of buccal swabs is noninvasive, less stressful and a much easier technique to collect DNA samples. Moreover, sample storage does not require refrigeration and DNA extraction is a much simpler process than blood samples. As a detection strategy, a desktop scanner was used for chip reading. Then the procedure was performed using low-resource laboratory materials and equipment (i.e. a primary health center). The analysis time was 210 min (DNA extraction: 50 min, amplification: 60 min, hybridization-detection: 100 min).

The absorption measurements indicated that a sufficient amount of high quality amplifiable human DNA was isolated from all the tested samples. The reference (ACTB gene) and targeted regions were amplified and submitted to on-chip hybridization. Figure SI.3 illustrates some examples of the microarray images. Presence of mutated variants in rs4680 and rs1799971 was detected. A subsequent comparison of the acquired chip signals with patient stratification based on the reference method clearly demonstrated perfect matching. The clinical implications of the provided genotyping results are a review of drug treatment, including anti-depressives or nicotine replacement products (e.g. patch). Functional polymorphisms in dopamine pathways (rs4680) are associated with the use of bupropion to mitigate lapsing to smoking following a quit attempt (*34*). Better prolonged abstinence rates have been reported after the nicotine replacement therapy tailored to

each smoker, and based on either genotype in the opioid receptor (rs1799971) (*26*).

Presence of mutant alleles was detected for 70.6 % (rs4680), 52.9 % (rs1799971), 41.2 % (rs1800497), and 41.2 % (rs16969968) of the smoker patients. A discrimination factor for genotype assignment was calculated from the signal-to-noise ratios recorded in the microarray images (Figure 21). Each call type within each target polymorphism statistically and significantly differed from the others (p-values <0.0001). Homozygous genotypes led to discrimination factors above 0.3 and under −0.3 for the wild-type and the mutant, respectively. An intermediate discrimination factor (between −0.3 and +0.3) was calculated for each heterozygous genotype. The genotype assignments, listed in Supplementary Material, agreed with those obtained by the reference method (100 % coincidence).

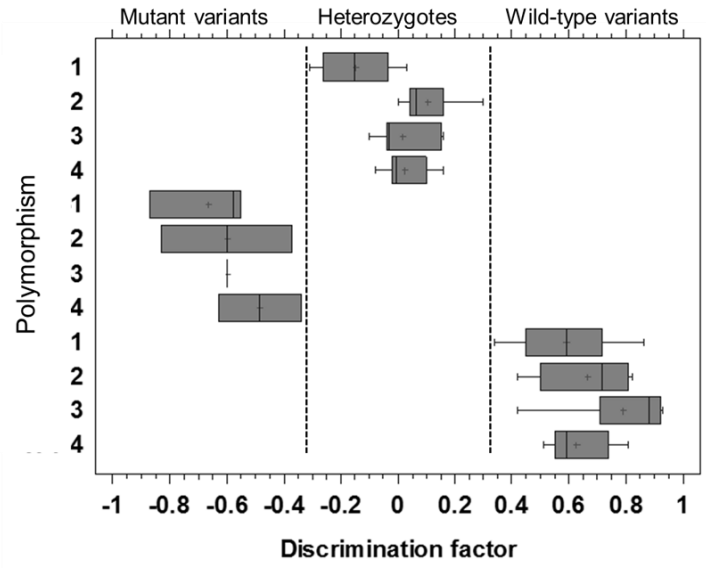


**Figure 21.** Boxplots of the discrimination factors classified according to the polymorphism and population group. 1: rs4680, 2: rs1799971, 3: rs1800497, and 4: rs16969968

## 3.5 Conclusions

In the last few decades, patient genome information has been proposed to select individual clinical care, particularly drug treatment decisions. However, the impact of personalized medicine is low compared to the research advances made. The results reported herein study demonstrate how pharmacogenomics knowledge combined with emerging analytical methodologies can benefit clinical practice more broadly. Although more in-depth research must be conducted, the combination of two innovative solutions was a success. Firstly, the advantages of the isothermal amplification reaction were incorporated to acquire the demanded copy number for sensitive SNP loci detection. The best features were their fast-response (4-fold compared to the PCR), low temperature (37 °C) and few design restrictions. However, the reduced multiplexing capabilities forced single parallelized reactions. Secondly, we employed additive manufacturing based on using a 3D printer as the chosen technology to create a customer-tailored platform for high-throughput analyses. The 100-well PLA-chip design considerably reduced reagent consumption and avoided expensive manufacturing processes or complex pumping systems associated with some DNA detection instruments. In fact, the assay can be performed with standard materials (i.e. pipettes, oven) found in clinical laboratories. The present work demonstrates that PLA is an adequate material for performing enzymatic reactions in a static format. The following step is to achieve better point-of-care performance and the next challenge is to develop microfluidic devices fabricated with this material that integrate all DNA assay steps, from extraction to detection. The advantages include the method's flexibility and accessibility compared to other micro-prototyping or micro-fabrication techniques.

Regarding the clinical impact, today pharmacogenomics is applied mainly to certain treatments in psychiatry, oncology and cardiology. One main reason is the cost-effectiveness of genotyping methods. In addition, only some diseases apply to this approach because their treatment generally involves expensive pharmaceutical products or drugs with highly probable adverse effects. With our approach, personalized therapies based on incorporating genetics into patient stratification can be offered, and even for relatively less-impact treatments. The methodology's cost-effectiveness, flexibility and portability will support the well-known genetic marker for predicting drug responses. In the particular case of tobacco addiction, genotyping information will help predict the degree of success in smoking cessation.

**Acknowledgements**

The authors acknowledge the financial support received from the Generalitat Valenciana (GVA-PROMETEOII/2014/040 Project and GRISOLIA/2014/024 PhD grant) and the Spanish Ministry of Economy and Competitiveness (MINECO CTQ2013-45875-R project).

## 3.6 References


1. T. A. Manolio *et al.*, *Genet. Med.* **15**, 258–267 (2013).
2. S. A. Scott, *Clin. Pharmacol. Ther.* **93**, 33–35 (2013).
3. N. Limaye, *Appl. Transl. Genomics*. **2**, 17–21 (2013).
4. N. S. Abul-Husn *et al.*, *Pharmgenomics. Pers. Med.* **7**, 227–240 (2014).
5. K. Knez *et al.*, *Analyst*. **139**, 353–370 (2013).
6. W. Shen *et al.*, *TrAC - Trends Anal. Chem.* **69**, 1–13 (2015).
7. C. A. Milbury, J. Li, G. M. Makrigiorgos, *Clin. Chem.* **55**, 632-640 (2009).
8. M. Asari *et al.*, *Anal. Biochem.* **386**, 85–90 (2009).
9. C. Taira *et al.*, *Clin. Chim. Acta*. **424**, 39–46 (2013).
10. L. A. Tortajada-Genaro *et al.*, *Anal. Bioanal. Chem.* **408**, 2339–2345 (2016).
11. C. F. Woolley, M. A. Hayes, *Analyst*. **139**, 2277–2288 (2014).
12. P. Craw, W. Balachandran, *Lab Chip*. **12**, 2469–2486 (2012).
13. L. Zhang *et al.*, *Anal. Chem.* **86**, 10461–10466 (2014).
14. F. Chen *et al.*, *Anal. Chem.* **87**, 8718–8723 (2015).
15. J. Li, J. Macdonald, *Biosens. Bioelectron.* **64**, 196-211 (2015).
16. S. Santiago-Felipe *et al.*, *Sensors Actuators, B Chem.* **204**, 273–281 (2014).
17. S. Santiago-Felipe *et al.*, *Microchim. Acta*. **183**, 1195–1202 (2016).
18. L. A. Tortajada-Genaro *et al.*, *RSC Adv.* **5**, 29987–29995 (2015).
19. Z. Li *et al.*, *PLoS One*. **11**, 1–15 (2016).
20. R. K. Daher *et al.*, *Mol. Cell. Probes*. **29**, 116–121 (2015).
21. Y. Shin *et al.*, *Lab Chip*. **13**, 2106–2114 (2013).
22. P. N. Nge, C. I. Rogers, A. T. Woolley, *Chem. Rev.* **113** , 2550-2583 (2013).
23. N. Bhattacharjee *et al.*, *Lab Chip*. **16**, 1720-1742 (2016).
24. S. Waheed *et al.*, *Lab Chip*. **16** (2016), pp. 1993–2013.
25. L. J. Bierut *et al.*, *Hum. Mol. Genet.* **16**, 24–35 (2007).
26. M. J. Carpenter *et al.*, *Drugs*. **73**, 407-426 (2013).
27. C. Moody, H. Newell, H. Viljoen, *Biochem. Eng. J.* **112**, 193–201 (2016).
28. R. A. Dimitrov, M. Zuker, *Biophys. J.* **87**, 215–226 (2004).
29. C. Zhang, D. Xing, *Nucleic Acids Res.* **35**, 4223–4237 (2007).
30. B. Liu *et al.*, *Anal. Chem.* **85**, 10045–10050 (2013).
31. J. Wu *et al.*, *Microchim. Acta*. **181**, 1611–1631 (2014).
32. J. Li *et al.*, *Nat. Med.* **14**, 579–584 (2008).
33. R. Shen *et al.*, *Mutat. Res. - Fundam. Mol. Mech. Mutagen.* **573**, 70-82 (2005).
34. S. P. David *et al.*, *Addiction*. **108**, 2202–2211 (2013).

# Chapter 2. Allele-specific ligation and recombinase polymerase amplification for the detection of single nucleotide polymorphisms

The previous chapter described the capacity of RPA to perform SNP discrimination using PCR-like primers, maintaining selectivity and greatly reducing reaction times. However, our experience with RPA showed that this reaction produces preferential amplification when trying to perform genotyping assays with multiple primer pairs. Thus, this chapter presents a strategy to increase the RPA multiplex capacity, by performing a previous bar-code probe allele-specific ligation step before amplification. Subsequently, RPA was used for targeting the universal sequences in the ligation products and replicating them to adequate amounts of cDNA. An optical point-of-care array detection step was developed, using a Blu-ray disc and reader to increase the throughput, since this platform has a resolution greater than DVDs.

# Triplex allele discrimination by ligation, universal recombinase polymerase amplification and optical array detection

*Yamanaka, Eric Seiti; Maquieira, Ángel, Tortajada-Genaro, Luis A.*

## 3.7 Abstract

A point-of-care genotyping method is proposed for overcoming the technical requirements and complexity associated with the current single nucleotide polymorphism (SNP) detection technologies. In order to perform the allele discrimination, multiple bar-code-probes target the sample DNA and are united by a ligase. Two shared pairs of primers are then used to target complementary sequences present in the probes, using recombinase polymerase amplification (RPA) to perform replication at constant temperature. The amplicons are labelled with 11-digoxigenin-dUTP during the amplification and are subsequently hybridized with bar-code oligonucleotide microarrays on a Blu-ray disc, followed by immunostaining based in a phosphatase alkaline substrate. A triplex method was obtained, with an excellent selectivity and a 10 template copies detection limit, with a maximum inter-assay error rate of 19%. The genotyping capability of the method was demonstrated by application in genotyping assays related with the treatment with anticoagulants like warfarin and other coumarin derivates.

*Keywords*

Single nucleotide polymorphism; ligation; recombinase polymerase amplification; microarray; point-of-care; Blu-ray; compact disc

## 3.8 Introduction

Personalized medicine procedures can vastly improve response times for diagnosing and selecting the adequate therapy, based on the patient's single nucleotide polymorphisms (SNPs) and other genetic variants (*1*). However, there is a current challenge in implementing these practices, related to the scarce accessibility to genetic information caused by technological and economic barriers. Although new generation sequencing methods are commercially available, these technologies are still expensive and unaffordable in most clinical realities (*2*). In that sense, great efforts are being made into developing more cost-effective technologies, more portable, with faster response times and easier operation.

Isothermal approaches are a viable solution for reaching an adequate sensitivity in point-of-care DNA testing devices. By replicating nucleic acids at constant temperature and eliminating the requirement of precision control equipment, these methods are potential alternatives to polymerase chain reaction (PCR) (*3*).

One of the most promising techniques in this group is the recombinase polymerase amplification (RPA), which has a very simple primer design, rapid reaction times (< 20 min) and requires only a single incubation step. This method operates at a low and constant temperature (35-42 °C), by combining enzymes to facilitate primer pairing to one of the target strands, while stabilizing the remaining one with single strand binding proteins (SSBs) (*4*). Therefore, by adequately integrating analysis steps, RPA allows the miniaturization of the assay platform and simplification of the

materials and immobilization techniques employed to the assay platform (*3*, *5*). RPA products have been detected with several platforms (*6*), like microtiter plates (*7*), microdevices (*8*), microarrays (*9*) and other fast-response and equipment-free approaches (*10*).

Despite these features, RPA has a limited capacity for simultaneous amplification of multiple primer pairs (*6*). Therefore, a possible improvement to this technique would be to combine it with a ligase-mediated discrimination, which has an excellent genotyping performance (*11*). The reaction is usually performed after an amplification step to reach the sufficient sensitivity, being followed by different quantification techniques, such as capillary electrophoresis (*11–13*), chemiluminescence (*14*), bead-based colorimetric detection (*15*), chip-based fluorescence (*16*), real-time fluorescence (*17*) and chip-based reflection (*18*). Ligation reactions were also performed along isothermal amplification techniques, like rolling circle amplification (RCA) (*19*, *20*) and loop-mediated isothermal amplification (LAMP) (*21*).

The aim of this work is to increase the multiplex capacity of RPA-based discrimination by performing a previous enzyme-mediated ligation step before amplification, in a similar approach to that found in ligation-PCR methods (*13*, *18*). When the target polymorphism is present, a ligase enzyme unites SNP-specific probes containing a common amplification tail and a hybridization bar-code, while primers designed to target these tails enable the replication of all the formed ligation products by universal RPA. 11-digoxigenin-dUTP is used to label the amplification products, which are then hybridized to bar-code microarrays printed on a Blu-ray disc. An enzymatic reaction step, based on alkaline phosphatase-conjugated antibodies, is used for staining the captured products. After washing the unhybridized and

unstained components, the assay is read by a modified Blu-ray disc drive, providing the information for determining the sample genotype.

The expected benefits associated to this format are a high-throughput capability, flexible hybridization conditions, a wide working range and remarkable assay selectivity and sensitivity (*22*, *23*). In order to evaluate the developed system, it was applied to the genotyping of single nucleotide polymorphisms (SNPs) used to avoid adverse effects and determine the therapy efficacy with anticoagulants like warfarin and other coumarin derivates (*24*, *25*).

## 3.9 Materials and methods

### Probes and primers

The oligonucleotides used in this study were designed in order to maximize the assay general selectivity (Table 6). The aims were to design unique sequences to avoid non-specific targeting and maximize the melting temperature between polymorphisms, while reaching an adequate amplification by RPA and a selective hybridization with the microarray probes. Four oligonucleotides were employed for each gene, three ligation probes (wild-type and mutant left probe and common right probe) and a single capture probe. Only three primers were utilized to amplify all ligation products, two different forward primers (wild-type and mutant) and a common reverse one. All oligonucleotides were purchased from Eurofins (Luxemburg).

**Ligation-RPA protocol**

Two reaction mixtures were prepared using SNP-specific ligation probes (wild-type or mutant) at 50 nM and 30 ng of genomic DNA in Tris-EDTA buffer (Trizma-base 10 mM, EDTA 1 mM, pH 8). After an annealing step (5 min, 98°C and 30 min, 65ºC), the ligase (Salsa Ligase-65, MRC-Holland, The Netherlands) was added, followed by two incubation steps for ligation (54°C, 15 min) and enzyme deactivation (98°C, 5 min). A ligation control was analyzed in parallel to the genomic DNA samples. This control was a $10^{-6}$-diluted amplicon, obtained from the PCR amplification of a pair of forward and reverse primers (3-5' sequences were CCTGAAAAACAACCATTGGCCA and TCGTCCGACCGTAACCTGC-TATCTCAAGTGATCCACCCACCT, respectively).

A TwistAmp Basic RPA kit (TwistDx, UK) was employed for performing universal RPA. Two amplification mixtures (12.5 μL) were prepared with a rehydration buffer, 14 mM of magnesium acetate, 200 nM of the wild-type or mutant universal forward primer, 200 nM of the universal reverse primer, 10 μM of digoxigenin dUTP and 1.25 μL of the ligation product. The solutions were incubated at 37ºC for 40 min in an oven. Amplification controls were analyzed in parallel to the ligation products.

**Hybridization protocol**

A multi-sample microarray platform, based on Blu-ray technology (disc and reader), was developed for simultaneously detect the ligation-RPA products generated in the previously described protocol. Gene-specific and control biotinylated probes were immobilized on a 36-sample layout over the

surface of a Blu-ray disc, using streptavidin physisorption as anchoring technique, according to a previously described protocol (*26*).

The ligation-RPA product (6 μL) was mixed with a hybridization solution (21 μL), composed of SSC buffer 3× (sodium citrate 45 mM, NaCl 450 mM, pH 7), 20% formamide, and 2.5× Denhardt's reagent. A positive hybridization control (labelled amplification product of ACTB gene) also was added (3 μL). The sample was denatured at 92°C for 10 min and transferred to the array surface. The disc was incubated at 37°C for 45 min in a conventional oven, gently washed with successively diluted SSC buffers (0.1× and 0.01×) and dried by centrifugation.

**Staining and reading protocol**

A labelling solution was made with 5 mg/mL rabbit anti-digoxigenin monoclonal antibody (Invitrogen, USA) and 10 mg/mL alkaline phosphatase-conjugated goat anti-rabbit antibody (Abcam, UK), in phosphate buffer saline buffer with 0.5% Tween-20 (PBS-T). The solution was dispensed over the arrays and the disc was incubated for 20 min at ambient temperature. After washing with PBS-T and water, 1 mL of Fast Red/naphtol (4-chloro-2-methylbenzenediazonium/3-hydroxy-2-naphthoic acid 2,4-dimethylanilide phosphate) (Sigma, MI, USA) was dispensed and maintained over the disc for 10 min at ambient temperature, generating intense pink spots.

The disc was read by a Blu-ray drive (405 nm laser), generating a 16-bit monochromatic image (tagged image file, TIF format). An in-home software was used for converting the light intensity absorbed by the spots in optical density intensities. The data of each spot was expressed in terms of signal-to-noise ratios (SNR), considering the spot intensity and background variation.

**Table 6.** Oligonucleotide sequences employed in the ligation SNP discrimination and RPA amplification method

| Gen | Function | Sequence (5'-3') | Length (nt) | %GC | Tm (ºC) |
|---|---|---|---|---|---|
| **Ligation** | | | | | |
| *CYP2C9*2* | LLP-A | ACTTCGTCAGTAACGGAC- | 18 | 50 | 53.8 |
| | | CGGGCTTCCTCTTGAACAC**A** | 20 | 55 | 60.5 |
| *rs1799853* | LLP-B | GAGTCGAGGTCATATCGT- | 18 | 50 | 53.8 |
| | | CGGGCTTCCTCTTGAACAC**G** | 20 | 60 | 62.5 |
| | RLP | [P]-GTCCTCAATGCTCCTCTTCCC- | 21 | 57 | 63.2 |
| | | CGTTCTAGCCTAACCGCCTTGA- | 22 | 55 | 64.2 |
| | | GTCTGCCTATAGTGAGTC | 18 | 50 | 53.8 |
| *CYP2C9*3* | LLP-A | ACTTCGTCAGTAACGGAC- | 18 | 50 | 53.8 |
| | | GCTGGTGGGGAGAAGGTCAA**T** | 21 | 57 | 63.2 |
| *rs1057910* | LLP-B | GAGTCGAGGTCATATCGT- | 18 | 50 | 53.8 |
| | | GCTGGTGGGGAGAAGGTCAA**G** | 21 | 62 | 65.3 |
| | RLP | [P]-GTATCTCTGGACCTCGTGCAC- | 21 | 57 | 63.2 |
| | | GCGATTCATAGACCCGTTTCCG- | 22 | 55 | 64.2 |
| | | GTCTGCCTATAGTGAGTC | 18 | 50 | 53.8 |
| *VKORC1* | LLP-A | ACTTCGTCAGTAACGGAC- | 18 | 50 | 53.8 |
| | | AGACCTGAAAAACAACCATTGGC | 25 | 44 | 64.1 |
| | | C**A** | | | |
| *rs9923231* | LLP-B | GAGTCGAGGTCATATCGT- | 18 | 50 | 53.8 |
| | | AGACCTGAAAAACAACCATTGGC | 25 | 48 | 65.8 |
| | | C**G** | | | |
| | RLP | [P]-GGTGCGGTGGCTCACGCCTA- | 20 | 70 | 66.6 |
| | | ATAGCAGGTTACGGTCGGACGA- | 22 | 55 | 64.2 |
| | | GTCTGCCTATAGTGAGTC | 18 | 50 | 53.8 |
| **Amplification** | | | | | |
| | U-FP-A | ACTTCGTCAGTAACGGAC | 18 | 50 | 53.8 |
| | U-FP-B | GAGTCGAGGTCATATCGT | 18 | 50 | 53.8 |
| | U-RP | GACTCACTATAGGCAGAC | 18 | 50 | 53.8 |
| **Hybridization** | | | | | |
| *CYP2C9*2* | u-probe | [BtnTg]TTTTTTTTTT- | 22 | 55 | 64.2 |
| | | TCAAGGCGGTTAGGCTAGAACG | | | |
| *CYP2C9*3* | u-probe | [BtnTg]TTTTTTTTTT- | 22 | 55 | 64.2 |
| | | CGGAAACGGGTCTATGAATCGC | | | |
| *VKORC1* | u-probe | [BtnTg]TTTTTTTTTT- | 22 | 55 | 64.2 |
| | | TCGTCCGACCGTAACCTGCTAT | | | |

LLP: left ligation probe; RLP: right ligation probe; U-FP: universal forward primer; U-RP: universal reverse primer; p: probe; [P]: 5'-phosphate group; [BtnTg]: biotin TEG; Tm: melting temperature.

**Sample analysis**

In order to evaluate the analytical capacity of the developed method, it was employed for genotyping SNPs associated with the efficacy and adverse effects of anticoagulant drugs (*24*). The selected polymorphisms were rs1057910, rs1799853 and rs9923231 located in the CYP2C9 and VKORC1 genes.

Two individuals were selected for the study, according to ethical guidelines. Genomic DNA samples were collected from buccal smear using swabs and isolated using an extraction kit (Purelink Invitrogen, USA). The samples were diluted to 4 ng/μL (approximately 1300 copies/μL) and analyzed with the previously described genotyping protocol.

The discrimination factor (DF) for determining the sample genotype was based on the response for wild-type (WT) and mutant (M) alleles, using the equation (WT+M)/2. For values FD>1.5, 0.5<FD<1.5 and FD<0.5, the sample genotype was considered as wild-type, heterozygous and mutant, respectively.

## 3.10 Results and discussion

**Oligonucleotide selection and selectivity studies**

The main objective of this research was to develop a highly selective and rapid method for genotyping several SNPs, employing a ligase-mediated discrimination and universal isothermal amplification. Most of the method selectivity relies on the oligonucleotide thermodynamic features, the medium conditions and the enzymes capacity for ligating or extending the correct bases. Therefore, the first challenge was to design probes and primers with

minimum homology to other genes, reduced cross hybridization with the other sequences, and absence of secondary structures. The polymorphisms were targeted by the 3' end of a left ligation probe, with the right ligation probe 5' end adjacent to this position. Both ligation probes had amplification tails, which were complementary to the RPA primers. Finally, a bar-code sequence was also inserted in the right ligation probe, between the ligation sequence and amplification tail, targeting a gene-specific immobilized probe (Figure 22). A detailed description of the selected oligonucleotides can be found in the Supplementary Information.

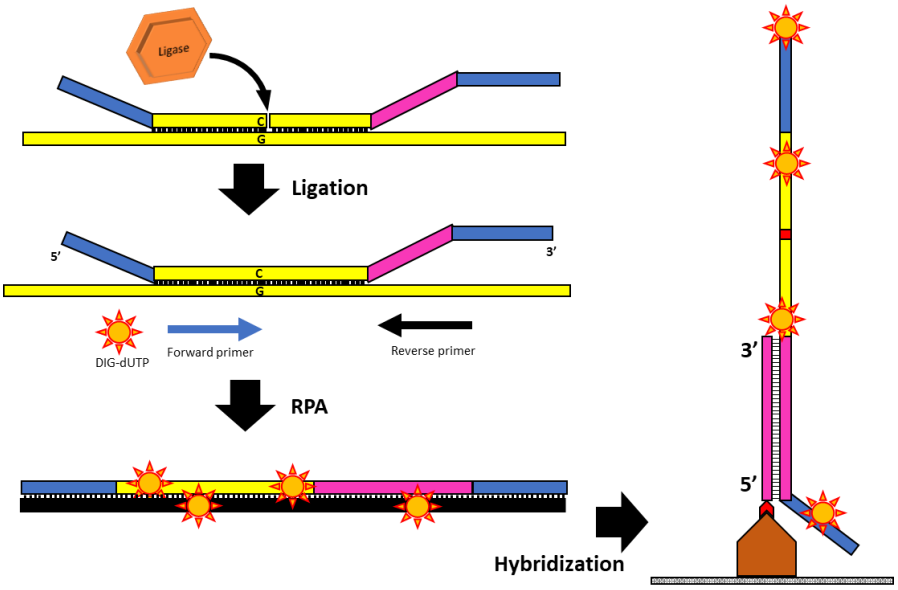


**Figure 22.** Illustrated mechanism of the ligation-RPA-hybridization protocol employed in this work

An initial study was carried out to evaluate the correct design of the ligation probes, amplification primers and immobilized probes. Artificial double-stranded DNA sequences, containing the target sequences for

rs9923231 ligation and universal amplification, were used as positive controls (Supplementary Information). A no-template control (NTC) and bacterial DNA (*Salmonella enterica*) samples were employed as negative controls. A non-human and rs1057910 oligonucleotide sequences were employed as negative hybridization controls. All samples were submitted to analysis using the described ligation-RPA-hybridization protocol, showing target probe signals 7.7 higher for positive samples than for negative ones (Figure 23).

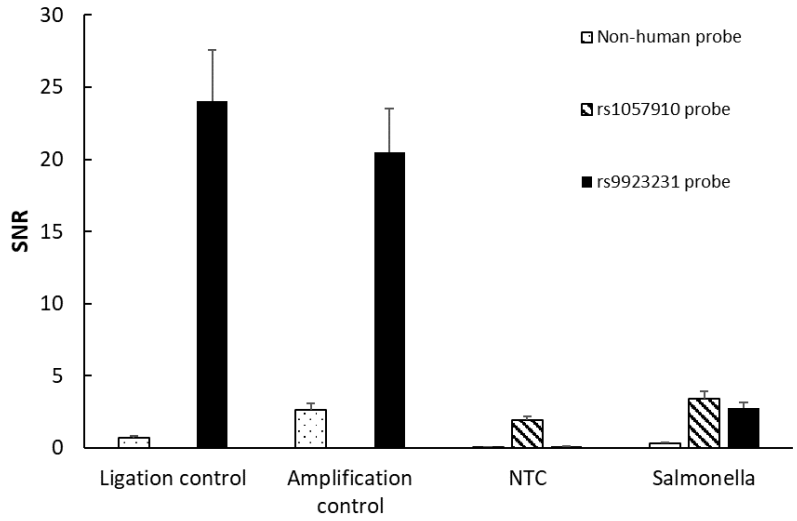


**Figure 23.** Evaluation of oligonucleotide probes and primers for the ligation-universal RPA method, using synthetic DNA targets and unmatched DNA templates. Oligonucleotide set: VKORC1 (rs9923231). Templates: $10^4$ copies of double-stranded DNA. Non-human probe and genomic DNA from Salmonella enterica.

**Optical detection set-up**

The strategy proposed for detection was the labelling of the discrimination products with digoxigenin during amplification, followed by hybridization with immobilized probes and immunostaining by phosphatase-conjugated antibodies. The following experiments were performed in order to achieve higher spot intensities and a selective labelling protocol.

The microarray printing conditions were evaluated in order to achieve an adequate spot intensity. Microarray replicates (n=4) were printed on a Blu-ray disc using different biotinylated capture probe concentrations and spot volumes from 5 to 40 nL. The ligation control ($10^4$ copies) was subjected to the analysis protocol, with subsequent measurement of the resulting signal-to-noise ratios (Fig. 24a). Better results were obtained with 20 nL spots with 200 nM probe concentration (SNR = 33±6), while higher volumes and concentrations did not significantly improve the signals.

Two approaches were tested for labelling the amplification products: 5'-digoxigenin-modified reverse primers and 11-digoxigenin dUTP. A ligation control and no-template control were ligated using the described protocol and the products were amplified using labeled primers and dUTP. As seen in Figure 24b, the assay using labeled dUTP produced selective responses to the target sequence only in the presence of the ligation control, while the use of labeled primers generated signals for the target and a non-complementary human probe, even in the absence of template DNA. This unspecific response could be partially explained by a hybridization of unreacted labeled primers with non-complementary probes, which would demand more stringent hybridization conditions. The digoxigenin-dUTP was selected as labeling approach, since it showed to be more selective and has a

higher versatility for being incorporated in various amplification products, while labeled primers are unique for a specific target sequence.

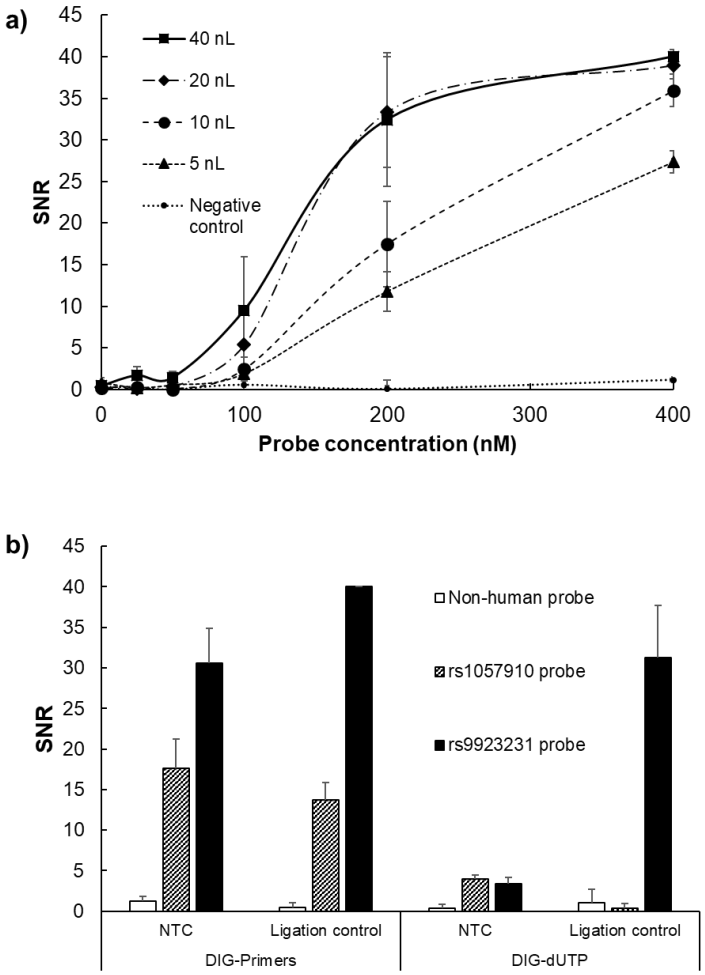


**Figure 24.** Microarray printing parameters and digoxigenin labelling evaluation. a) spot volume and probe concentration effect over the target optical intensity; b) selectivity comparison between digoxigenin primers and digoxigenin dUTP during the amplification step. Target ligation product from rs9923231. 4 replicates per assay, negative control probes from Salmonella enterica and rs1057910

**Genomic DNA analysis**

The conditions for selectively obtaining the allele-specific products by ligation and RPA, using genomic DNA samples, were determined. Two different enzymes were evaluated for application in the developed method: SALSA Ligase-65 (MRC-Holland, Netherland) and Ampligase (Lucigen-Epicentre, USA) (Figure 25a). The first enzyme is used in multiplex ligation-dependent probe amplification (MLPA), while the second ligase has been used in several ligase-based methods (*11, 17*). A genomic DNA sample and no-template control were submitted to ligation using both enzymes, with subsequent amplification and hybridization of the ligation products. Negative results (SNR <3) were obtained with the absence of oligonucleotides or non-complementary DNA templates. Both enzymes produced detectable products from 0.1 units per reaction in the presence of genomic DNA. However, the assays with SALSA Ligase-65 produced more reproducible and intense signals, which lead to the choice of this enzyme for developing the genotyping method.

The conditions for adequately amplifying the genomic ligation products with RPA were also tested. The effects of universal primer concentration and amount of ligation product were evaluated by performing ligation-RPA reactions with dilutions of a genomic DNA ligation product and no-template control (Figure 25b). A minimum primer concentration of 100 nM was sufficient for amplifying 1/5 and 1/10 dilutions, while lower amounts (1/20 and 1/40) required the use of 200 nM. This lower amplification efficiency could be due to a lower number of initial template copies or a inhibiting effect of the matrix components. All samples presented a positive amplification signal at 400 nM, in less than 40 min, which is consistent with other previous RPA studies (*27, 28*). As this concentration did not produced

false-positives, it was selected for the developed method, with the aim of assuring an adequate sensitivity.

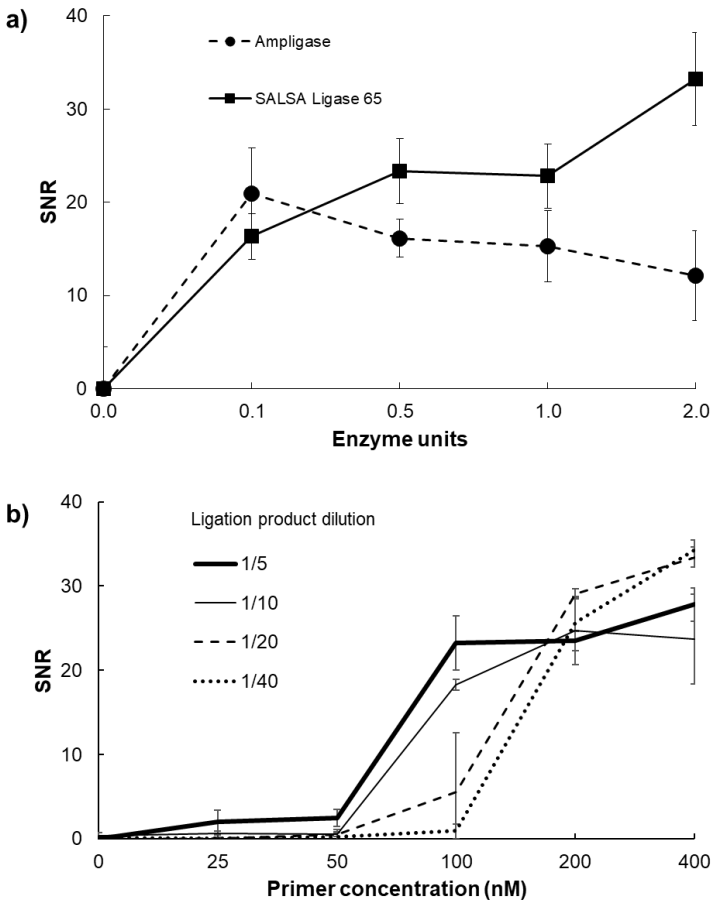


**Figure 25.** Medium conditions selection for the universal amplification of ligation products with RPA. a) Ligase enzyme nature and amount effect on response intensities; b) Effect of the primer concentration and ligation product dilution on the RPA yield. Target polymorphism: mutant allele from rs9923231. Genomic DNA from a Sanger-sequenced mutant individual ($10^4$ copies).

**Performance evaluation**

The analytical capacities of the ligation-RPA method were evaluated through genotyping assays of Sanger-sequenced DNA samples. A sensitivity assay was performed by analysis of successively diluted samples of genomic DNA (Figure 26). A minimum of 10 copies per assay was successfully detected with the method, with a maximum signal obtained from 1000 copies and above. Although sensitivity is not usually a great concern in genotyping systems, the detection of low-frequency polymorphisms could be performed with the developed method without prior enrichment processes. Also, a repeatability experiment was performed by replicated analysis (n=5), showing that the system presents 6% and 19% intra-assay and inter-assay error rates, respectively.

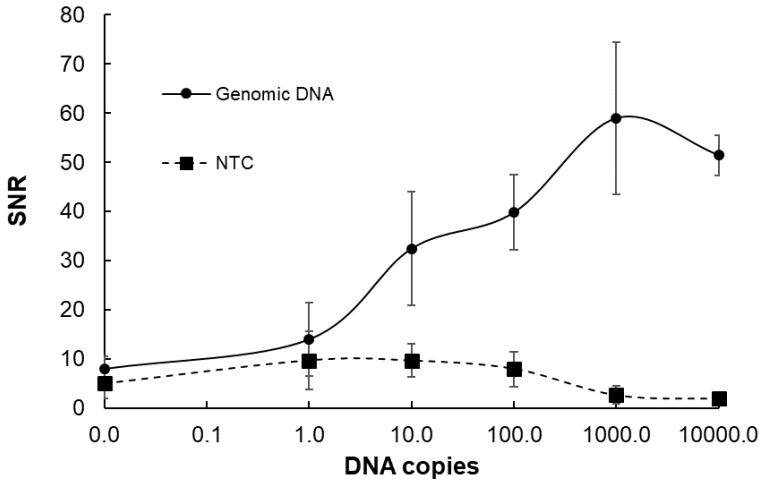


**Figure 26.** Sensitivity evaluation with successive dilutions of genomic human DNA

In order to demonstrate the multiplex capacities of the developed method, a selectivity study was carried out, using rs1799853, rs1057910 and rs9923231, located in the CYP2C9 and VKORC1 genes; as model polymorphisms, due to their association to dosage selection of coumarin-type drugs, with high clinical annotation levels of evidence. Thus, a cross-reactivity assay was performed by simultaneously analyzing multiple genes with combinations of the target ligation probes (Figure 27). Two individual samples were sequenced using the Sanger method. Next, they were submitted to ligation and amplification using different oligonucleotide compositions: single-plex mixes with only a pair of ligation probes, duplex mixes with two pairs and a complete mix, containing all ligation probes for three different alleles. Target signals were clearly distinguished from untargeted probes, in the presence of the corresponding polymorphism. The response profiles matched with the Sanger-sequenced individual genotypes for all ligation mixes, independently from the number of parallel genes.

Based on the favorable allele-discrimination results achieved, this method could be employed for rapid determination of haplotypes in pharmacogenetics. In the particular case of coumarin and anticoagulant therapies, the detection of mutant haplotypes is important for selecting the adequate drug doses, providing a more effective treatment (*24*).

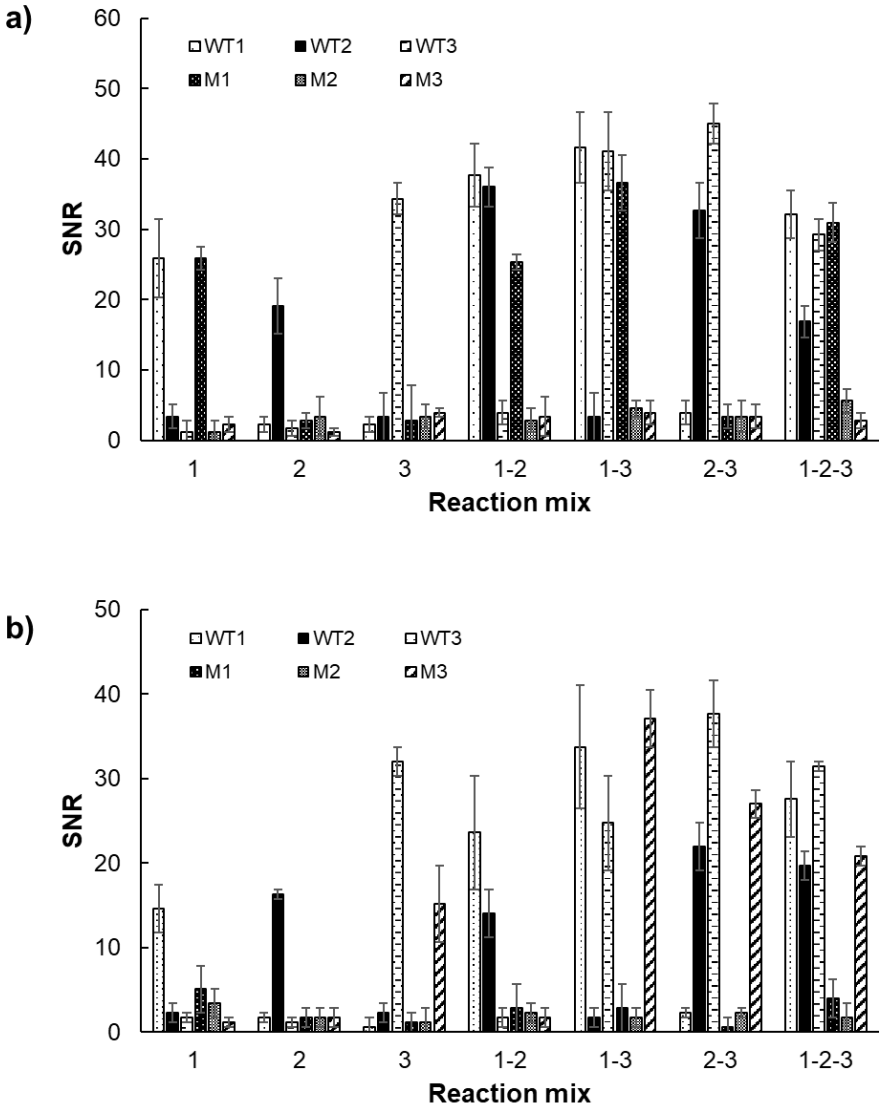


**Figure 27.** Genotype analysis with single, duplex and triplex discrimination mixes. Template DNA: 104 copies. Mixes: 1 rs1799853, 2 rs1057910, 3 rs9923231.

## 3.11 Conclusions

With the increasing demand for more affordable and practical solutions to perform genetic testing, isothermal enzymatic reactions are a potent alternative for reducing costs and technical requirements. These features open the path for creating integrated, miniaturized and automatized systems for point-of-care DNA analysis.

In the developed method, the high selectivity of ligases and energy reduction provided by primer recombination and extension create a path for simplifying single nucleotide polymorphism discrimination. By one side, the high multiplex capacity of the SALSA Ligase-65 contributed for discriminating multiple polymorphisms simultaneously. On the other hand, the universal amplification using a single shared primer pair reduces the assay complexity, avoiding the optimization steps related to multiplex primer extension. Finally, the alkaline phosphatase-based immunostaining technique provided an affordable, sensitive and selective detection, by combination with Blu-ray disc platform and reader.

Although further validation research must be performed with clinical samples, the developed method shows great potential for application in pharmacogenetics and other fields of personalized medicine. By adaptation within an integrated platform, it can be converted into a simple, cost-effective and robust device for onsite SNP detection in less specialized environments, such as primary healthcare centers and low-resource areas.

**Acknowledgements**

The authors acknowledge the financial support received from the Generalitat Valenciana (GRISOLIA/2014/024 PhD Grant and GVA-FPI-

2017 PhD Grant) and the Spanish Ministry of Economy and Competitiveness (MINECO Project CTQ2016-75749-R).

## 3.12 References


1. I. S. Chan, G. S. Ginsburg, *Annu. Rev. Genomics Hum. Genet.* **12**, 217–244 (2011).
2. S. A. Scott, *Clin. Pharmacol. Ther.* **93**, 33–35 (2013).
3. M. C. Giuffrida, G. Spoto, *Biosens. Bioelectron.* **90**, 174–186 (2017).
4. O. Piepenburg *et al.*, *PLoS Biol.* **4**, 1115–1121 (2006).
5. Y. Zhao *et al.*, *Chem. Rev.* **115**, 12491–12545 (2015).
6. I. M. Lobato, C. K. O'Sullivan, *TrAC - Trends Anal. Chem.* **98**, 19–35 (2018).
7. S. Santiago-Felipe *et al.*, *Anal. Chim. Acta*. **811**, 81–87 (2014).
8. G. Choi *et al.*, *Lab Chip*. **16**, 2309–2316 (2016).
9. S. Martorell *et al.*, *Anal. Biochem.* **544**, 49–56 (2018).
10. Z. A. Crannell, B. Rohrman, R. Richards-Kortum, *PLoS One*. **9**, e112146 (2014).
11. A. A. Gibriel, O. Adel, *Mutat. Res. - Rev. Mutat. Res.* **773**, 66-90 (2017).
12. W. Shen *et al.*, *TrAC - Trends Anal. Chem.* **69**, 1–13 (2015).
13. J. P. Schouten, *Nucleic Acids Res.* **30**, e57 (2002).
14. H. Q. Wang *et al.*, *Anal. Chem.* **83**, 1883–1889 (2011).
15. X. Chen, A. Ying, Z. Gao, *Biosens. Bioelectron.* **36**, 89–94 (2012).
16. J. Ritari *et al.*, *PLoS One*. **7**, e34211 (2012).
17. Y. Sun *et al.*, *Biosens. Bioelectron.* **74**, 705–710 (2015).
18. L. A. Tortajada-Genaro *et al.*, *Analyst*. **144**, 707–715 (2019).
19. J. Pickering, *Nucleic Acids Res.* **30**, e60 (2002).
20. H. Y. Heo *et al.*, *Biosens. Bioelectron.* **78**, 140–146 (2016).
21. W. Du *et al.*, *Chem. Commun.* **52**, 12721–12724 (2016).
22. C.-X. Li *et al.*, *Hum. Mutat.* **29**, 306–314 (2008).
23. P. Wang *et al.*, *Biosens. Bioelectron.* **26**, 3719–3724 (2011).
24. A. S. Tseng *et al.*, *Cardiovasc. Drugs Ther.* **32**, 121-126 (2018).
25. A. Alfirevic, M. Pirmohamed, *Trends Pharmacol. Sci.* **38**, 100-109 (2017).
26. L. A. Tortajada-Genaro *et al.*, *Anal. Bioanal. Chem.* **408**, 2339–2345 (2016).
27. S. Santiago-Felipe *et al.*, *Sensors Actuators, B Chem.* **204**, 273–281 (2014).
28. E. S. Yamanaka, L. A. Tortajada-Genaro, Á. Maquieira, *Microchim. Acta*. **184**, 1453–1462 (2017).

# Chapter 3. Polymorphism genotyping based on loop-mediated isothermal amplification and smartphone detection

In this chapter we studied the performance of loop-mediated isothermal amplification (LAMP) for genotyping SNPs related to major depression therapy, due to the fast amplification times and detection versatility that are inherent to this reaction. Two strategies were developed in order to achieve the adequate selectivity and exploit different detection principles: the first is a fast method with fewer steps, using allele-specific primers and a colorimetric indicator in solution; the second is an array-based hybridization method employing allele-specific probes, which has a higher multiplex potential. In both systems, the detection was carried out using a smartphone, making use of the sophisticated imaging and processing features of this device.


Contents lists available at ScienceDirect

Biosensors and Bioelectronics

journal homepage: www.elsevier.com/locate/bios

# Polymorphism genotyping based on loop-mediated isothermal amplification and smartphone detection

*Eric Seiti Yamanaka, Luis A. Tortajada-Genaro, Nuria Pastor, Ángel Maquieira*

This article was published in **Biosensors and Bioelectronics, 2018, 109, 177-183**



## 3.13 Abstract

The genotyping of a single-nucleotide polymorphism (SNP) is addressed through methods based on loop-mediated isothermal amplification (LAMP) combined with user-friendly optical read-outs to cover the current demand for point-of-care DNA biomarker detection. The modification of primer design and reaction composition improved the assay selectivity yielding allele-specific results and reducing false-positive frequency. Furthermore, the reduced cost, ease of use and effectiveness of colorimetric detection (solution and hybridization chip formats) were availed for the image capture by a smartphone, reaching high sensitivity. In order to evaluate their discriminating capacities, LAMP-based methods were applied to human samples to genotype an SNP biomarker (rs1954787) located in the *GRIK4* gene and related to the treatment response to anti-depressants drugs. Sensitive (limit of detection: 100 genomic DNA copies), reproducible (<15% error),

fast (around 70 min) and low-cost assays were accomplished. Patient subgroups were correctly discriminated, agreeing with reference sequencing techniques. The achieved analytical performances using the developed amplification-detection principles confirmed the approach potential for point-of-care optical DNA testing.

**Keywords**

Single-nucleotide polymorphism; loop-mediated isothermal amplification; point-of-care optical testing; smartphone; pharmacogenomics.

## 3.14 Introduction

Rapid advances made in DNA biomarkers research are providing us with a better understanding of disease mechanisms and drug action, which can lead to offering new personalized medicine opportunities (*1*). The key step for implementing such systems in clinical routine is to employ highly efficient testing methods, which have to be accurate and sensitive enough to detect even minority variants, but also practical and economically feasible. In recent years, several studies have examined the capabilities of point-of-care (POC) genetic testing (*2*). These tests generally include a cost-effective field-portable device, along with an accurate, sensitive and simple DNA assay.

Amplification reactions are central to DNA-based diagnostic methods because sensitivity and selectivity depend on the effective increment in the copy number for the target region (*3*). The most widely used amplification method is polymerase chain reaction (PCR), but it has some limitations for POC applications: a specific instrument for strict temperature control, susceptibility to amplification yield variations related to reaction conditions or the formation of air bubbles in miniaturized devices (*4*).

Scientific advances have led to several enzymatic reactions run at constant temperature that can be used as an alternative to PCR-based amplification. Some recent reviews summarize isothermal amplification reactions and their use as analytical tools (*5*–*7*)).

Loop-mediated isothermal amplification (LAMP), developed by Notomi and colleagues (*8*), is the most extensively studied isothermal amplification technique. The main advantages over other approaches are its high amplification yield, good tolerance to inhibitors, short time and compatibility with several detection principles. The conventional approach relies on four primers to recognize six different sequences of the target DNA, which also leads to very high specificity. The action of a highly strand-displacing DNA polymerase (Bst polymerase) generates large amounts of dumbbell-like structures under isothermal conditions (60–65°C). In virtue of these features, LAMP-based methods have been extensively applied to diagnose infectious diseases by detecting bacteria, viruses and parasites (*9*, *10*).

In the last few years, several studies have demonstrated LAMP's capability to discriminate single-base variations, such as single nucleotide polymorphisms (SNPs) and somatic point detection. These methods are based on allele-specific hybridization (*11*, *12*) and amplification using allele-specific primers (*13*, *14*) or a blocking agent (*15*). However, these methods usually rely on naked-eye visualization or carry out the detection with expensive and bulky laboratory equipment (e.g. electrochemical stations, real-time turbidimeter or fluorometer). With the adequate integration to user-friendly detection technologies, these LAMP variants are appealing to develop POC testing. Examples of candidate clinical challenges are to select the correct oncological treatment with monoclonal antibodies (*16*), and to adjust drug doses in neuropathies and psychiatric disorders (*17*, *18*).

We herein explored these discrimination principles to develop high-performance POC systems. The first method involved the allele-specific oligonucleotide hybridization of the LAMP products in the stem-loop region (LAMP-ASO). The second was based on the annealing selectivity of allele-specific inner primers (3'AS-LAMP), while discrimination in the third approach relied on DNA synthesis from a dumbbell-like starting structure (5' AS-LAMP). The key conditions to obtain adequate amplification yield, improve the discrimination factor and reduce false-positive frequency, were investigated. To this end, modifications in the primer/probe design, and variations in the amplification or hybridization mix composition, were included.

Detection of allele specific products in POC scenarios also requires alternative detectors to previous LAMP approaches. In line with this, the features of consumer electronic devices are excellent as they are ubiquitous, low-cost, compact and high-performance products that can benefit advanced analytical measurements (*19–22*). The sensing devices described for diagnostic purposes include compact disc drivers (*23*), flatbed scanners (*24*) and mobile phones (*25*, *26*), among others. In this study, we explored the colorimetric detection of the developed homogeneous and heterogeneous LAMP assays supported by smartphone technology due to its widespread presence, portability and capacity to transmit data at a user-friendly interface. This integrated system also fulfils WHO requirements, and corresponds to the acronym "ASSURED": affordable, sensitive, specific, user-friendly, rapid and robust, equipment-free, and delivered to those who need it.

## 3.15 Material and methods

### Primers and probes

LAMP primers and probes were designed for the target SNP according to the thermodynamic parameters described in the literature (*8*, *27*) The complete design strategy and oligonucleotide sequences can be found in the Supplementary Material. All the oligonucleotides used in this study were purchased from Eurofins (Luxembourg).

### LAMP combined with allele-selective oligonucleotide hybridization: LAMP-ASO method

In this approach, isothermal amplification was followed by hybridization to the specific probes immobilized on planar polycarbonate chips (25 × 75 mm). Non-allele selective LAMP amplification was carried out in 200 µL propylene phials with primers that enclosed the polymorphic site. Each reaction (12.5 µL) was composed of 1× isothermal amplification buffer (20 mM Tris-HCl, 10 mM $(NH_4)_2SO_4$, 50 mM KCl, 2 mM $MgSO_4$, 0.1% Tween 20, pH 8.8), 1.5 M betaine, further 6 mM $MgSO_4$, 1.2 mM dNTPs, 10 µM digoxigenin-11-deoxyuridine triphosphate (DIG-dUTP), 0.2 µM of outer primers, 1.2 µM of inner primers, 0.32 U/µL Bst polymerase 2.0 (New England Biolabs, USA) and 0.32 ng/µL (approximately 100 copies per µL) of the studied DNA. Vials were incubated at 62°C for 60 min (digital heat block, VWR). Amplification products were then hybridized with the allele-specific oligonucleotide probes immobilized on chips in a microarray format. Probe arraying, hybridization and colorimetric staining were performed according to the protocol developed in previous works (*24*, *28*). The resulting

hybridization products anchored to the surface were recognized by horseradish peroxidase-conjugated antibodies and stained by 3,3',5,5'-tetramethylbenzidine to produce a precipitate.

A digital imaging technique was used to record the LAMP-ASO results. Array images were captured by a smartphone (MotoG first generation, Motorola) using a homemade capture chamber (8.0 x 6.7 x 4.4 cm). This chamber had a frontal rectangular aperture for the smartphone camera, a lateral hole to illuminate the array by an external optical fiber light source (20W power, 3,000 K color temperature, LE.5209 model, Euromex, Holland), and an inferior aperture to insert the assay chip. The image was captured after adjusting both focus and exposure (75% saturation) and was converted into a tagged image file format on a 16-bit (0-65,535) greyscale with the ImageJ software (National Institutes of Health, USA). Images were analyzed and the resulting spot intensities were expressed in signal-to-noise ratio terms.

**Allele-specific LAMP: 3'AS-LAMP and 5' AS-LAMP formats**

Two homogeneous amplification formats were assayed using allele-specific primers (see Supplementary Material). In each case, discrimination was achieved using two reaction mixtures to amplify the wild-type variant (wild-type primers) or the mutant variant (mutant primers). For 3' AS-LAMP format, the polymorphism was located at the 3'-end of the forward inner primer (FIP), leading two allele-specific primers and a reverse inner primer common to both reaction mixtures. Therefore, the reaction mixture composition varied from the previously described non-selective LAMP by using each FIP primer, 1.25 M betaine and 300 μM hydroxynaphtol blue. In the 5' AS-LAMP format, the polymorphism was located at the 5'-end of both FIP and BIP, and the difference in mixture composition was the betaine and

dyer concentrations, which were 0.75 M and 300 μM, respectively. On-chip amplification was carried out with a rhombic chamber chip (reaction volume 10 μL, Zeonor material) supplied by microfluidic ChipShop (Germany). Inlets and outlets were connected directly to Tygon tubing. Chips were loaded with the amplification samples and were incubated at 62°C for 60 min.

Smartphone imaging enabled end-point direct colorimetric detection. For this purpose, the reaction chip with a reference color palette was placed in the previously described detection assembly. The AssayColor software (Alidans, Italy), installed in the smartphone, was used to capture and analyze images. This scientific application, developed for the Android operating system, provided color intensities in the red, green and blue channels (RGB) for each LAMP product. The R/G intensity ratio was selected as an analytical signal.

**Sample analysis**

Subjects (n=15) were recruited according to ethics with informed consents. DNA extracts were obtained from the buccal smear samples with the Purelink Genomic DNA mini kit (Thermo Fisher Scientific, USA). Purified products were eluted with Tris-HCl buffer (Tris 10 mM, pH 8.6) and their genomic DNA content was quantified in a NanoDrop 2000 spectrophotometer (Thermo Fisher Scientific, USA). A 260/280 nm absorbance ratio above 1.8 was considered to determine adequate purity. Extracts were diluted to 4 ng/μL and stored at -20°C until further use. Subsequently, samples were submitted to the LAMP-ASO, 3'AS-LAMP and 5'AS-LAMP methods. A no-template control and a *Salmonella typhimurium* DNA extract were used to check for false-positive assays. A discrimination index was calculated from the signal of the wild-type (WT) and mutant

(MUT) responses according to the following equation: (WT − MUT)/(WT + MUT). The genotype was assigned according to discrimination thresholds (TT higher than +0.33, TC between +0.33 and -0.33, and CC lower than -0.33).

**Genotyping validation**

Two techniques were used to confirm patients' genotypes: Sanger sequencing and allele-specific PCR.

For Sanger sequencing, each PCR reaction was carried out in a mixture (12.5 µL) that contained 1x amplification buffer, 3 mM $MgCl_2$, 200 µM dNTPs, 300 nM of the forward and reverse primers, 0.5 units of Taq polymerase (Biotools, Spain) and 20 ng of genomic DNA per reaction. Amplification was carried out in a UnoCycler thermal cycler (VWR, USA) according to the following program: initial denaturation at 95°C for 5 min, followed by 35 amplification cycles of denaturation (95°C for 30 s), annealing (60°C for 30 s) and elongation (72°C for 30 s), and a final extension step at 72°C for 5 min. The resulting amplification products were diluted, extended with fluorescent dideoxynucleotides (Big Dye Terminator Cycle Sequencing Kit v3.1, Thermo Fisher Scientific, USA), and analyzed in a fluorescence-capillary sequencer (ABI 3130xl Genetic Analyzer, Applied Biosystems, USA).

Allele-specific PCR (AS-PCR) was based on the use of two forward primers that differed at the 3'-end nucleotide and were complementary to the wild-type or mutant variant. An additional mismatch at the penultimate nucleotide was included. The amplification conditions were identical to those previously described for PCR, except for the use of the allele-specific primers and an annealing temperature of 62°C. End-point fluorescence was measured

to confirm amplification. Products were diluted in 0.5× SYBR Safe (Invitrogen, USA) on a 96-well black polystyrene plate and analyzed in a plate reader (Victor 3TM V1420, Perking Elmer, Finland) at excitation and emission wavelengths of 485 and 535 nm, respectively.

The Statgraphics Centurion statistical package for Windows v.16 was used for the data analysis.

## 3.16 Results and discussion

### ASO-LAMP set-up

SNP discrimination was performed with the combination of isothermal DNA amplification and hybridization with allele-selective probes in a solid-phase format.

The first step was the oligonucleotide design (primers and probes). There were two design options according to the target polymorphism location in the LAMP product loop-structure: central position (double-strand region) or loops (single-strand regions). The second option was chosen to improve the hybridization yield to the array probe (Fig. 28a). A thermodynamic analysis was used to select the candidate probes that maximized the hybridization of perfect-match pairs (wild-type or mutant) and hampered the coupling of mismatched products (wild-type product/mutant probe or mutant product/wild-type probe). An additional design restriction was the central position of the polymorphic mismatch in the probe to increase assay selectivity. The selected sequences produced wide variation in standard free energies, expressed as the difference between the single-base mismatch ($\Delta G^{o}_{mutant}$) and the perfect match ($\Delta G^{o}_{wild\text{-}type}$). Estimated values were 3.3-4.5 kcal/mol.

The LAMP reaction was optimized to selectively amplify the targeted region using the designed non-allele-specific primers. Reagent concentrations (enzyme, inner primers and outer primers), amplification temperature and reaction time were studied by the fluorescence analysis (see the Supplementary Material). Negative controls (non-human DNA) produced a signal comparable to the background, while the amplification of the human DNA template generated a significantly distinguishable signal (Fig. 28b). The wild-type and mutant templates produced similar amplification curves, and the time selected for the end-point analysis was 60 min. The amplification factor was $(2.6\pm0.8)\times10^8$, which gave a 23-fold higher yield than a typical PCR using the same external primers and the amount of the initial DNA template.

The next experiments focused on the selective hybridization to the probes anchored to the plastic chip, by directly dispensing the end-point LAMP product on the probe arrays. This approach is simpler and more efficient than combining PCR-based methods with microarray detection because an intermediate (thermal or chemical) denaturalization step is generally required (*1*, *24*). The probe immobilization parameters (concentration, drop volume, and surface treatment) and the hybridization variables (buffer composition, time and washing cycle) were studied to balance yield and selectivity, as described in the Supplementary Material. The most critical variable to achieve selective hybridization was buffer composition, particularly formamide concentration (Figure 28c). Under the optimal conditions (1x sodium saline citrate buffer, 30% formamide), a detectable signal was obtained for the perfect-matched duplexes (wild-type and mutant homoduplex), while a background-equivalent response was acquired for the mismatch hybrids.

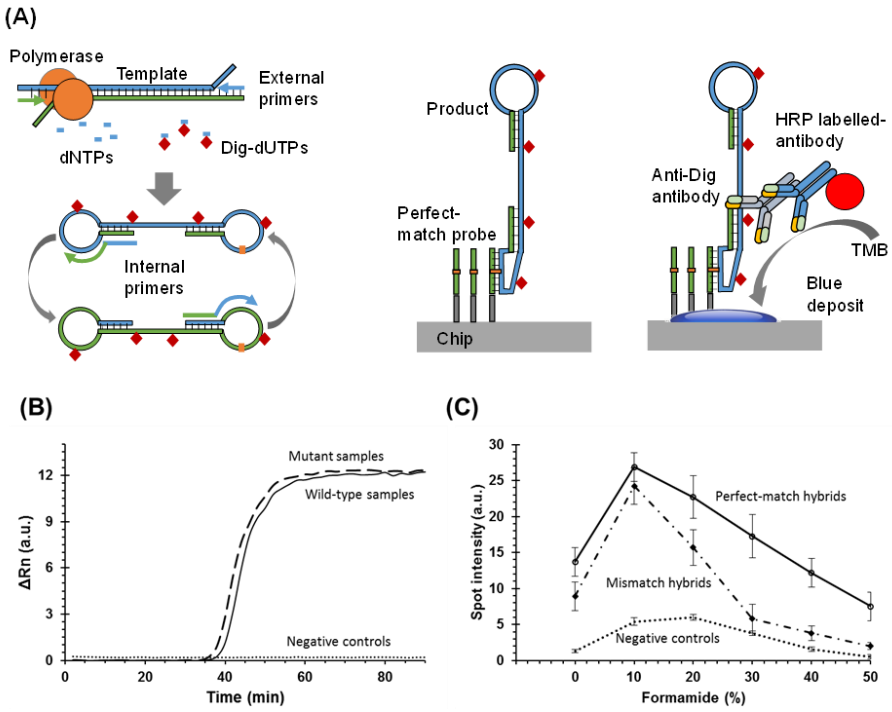


**Figure 28.** ASO-LAMP assay: (A) Scheme of ASO-LAMP format. (B) Kinetic profile of the LAMP amplification (three replicates): wild-type sample, mutant sample and negative template control. DNA template: 2000 copies. Replicate errors:< 10%. (C) Effect of formamide percentage in the hybridization buffer composition on the spot intensity responses for homoduplex and heteroduplex (LAMP product-probe). Target SNP: rs1954787 located in the GRIK4 gene

**AS-LAMP set-up**

In the preliminary studies, a non-specific amplification signal was generated for the non-matched primer-template pairs. The LAMP assays generated false-positives due to the formation of unexpected primer structures, as observed in other studies (*10, 29*). Therefore, several modifications were made to increase assay selectivity in the AS-LAMP formats. Firstly, an additional mismatch was deliberately added to the penultimate nucleotide of the allele-specific primers. Major destabilization of the hybridization process was estimated for the mismatch probes, where the calculated variation of the standard free energies was about 1.2 - 2.8 kcal/mol. Secondly, the effect adding betaine to the amplification mix was evaluated. This amino acid analogue is often used for destabilizing dsDNA and for reducing the sequence composition influence on the melting temperature. The experiments showed that adding betaine eliminated the false-positive results associated with the mismatch hybrids (Fig. 29). However, increasing the betaine concentrations also led to the undesired inhibition of the perfect-matched duplexes. The inhibition effect was more prominent in the 5' allele-specific format than in the 3' one. This could be explained by the lesser stability of the associated perfect-match hybrids (about 5 kcal/mol) and a different number of allele-specific primers (two in the 5' format and one in the 3' format). In summary, the results at the selected values (1.25 M for 3'AS-LAMP and 0.75 M for 5'AS-LAMP) showed better amplification selectivity compared to conventional conditions.

Amplification kinetics was studied to verify the discrimination capacity and the assay turnout time for the LAMP reactions. Both the allele-specific methods showed adequate selectivity as the real-time signals for the no-template control and the non-human DNA extract (*Salmonella* culture)

were similar to the background. When the perfectly matched primers were used, amplification started at 40 min for the 3’ and 5’ allele-specific approaches, while the mismatched primers generated a signal after a delay that went beyond 30 min in both cases. It is worth noting that the stability difference between the previously described matched and mismatched duplexes was also reflected in the amplification kinetic profiles. Longer delays for the mismatched pairs were found in the 3’ format. After considering the results, a 60-minute amplification time was selected for the following experiments to prevent the formation of non-specific products during the assay.

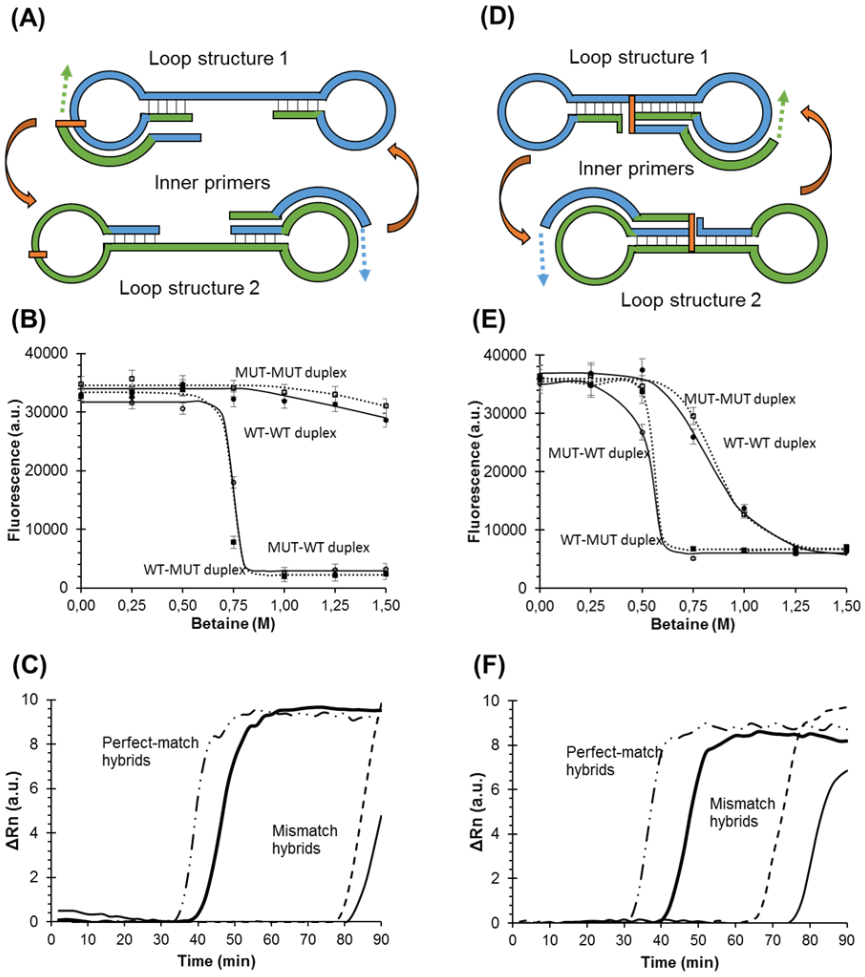


**Figure 29.** AS-LAMP assay: (A) Scheme of 3'AS-LAMP format. (B) Betaine effect on the selectivity of 3'AS-LAMP method. (C) Kinetic profile of 3'AS-LAMP method. (D) Scheme of 5'AS-LAMP format. (E) Betaine effect on the selectivity of 5'AS-LAMP method. (F) Kinetic profile of 5'AS-LAMP method. Data adjusted to a four-parameter logistic model (regression coefficient: 0.994–0.999); DNA template: 2000 copies. WT: wild-type and MUT: mutant. Replicate errors:< 10%. Target SNP: rs1954787 located in the GRIK4 gene.

**Smartphone detection**

The detection of the previously described allele-selective products was achieved with conventional laboratory instruments; i.e. fluorescence qPCR thermocycler, fluorescence spectrophotometer or fluorescence scanner. The next challenge was to adapt the methods for colorimetric detection using a smartphone (complementary metal–oxide–semiconductor, CMOS sensor) suitable for point-of-care testing. An integrated detection device was assembled for chip reading, which comprised a light source, a dark chamber and the smartphone aligned to the chip (Fig. 30). To guarantee inter-assay measurement robustness, a color pattern (a violet to blue scale) was photographed together with the assay platforms. The specific measuring conditions were optimized to digitalize the array profile by the smartphone camera, as the Supplementary Material describes. Image resolution, expressed as pixel width, was 17 μm.

For the LAMP-ASO approach, a colorimetric detection method for the probe-LAMP product hybrids based on an immunorecognition step (digoxigenin/primary antibody/secondary antibody system) and enzymatic staining (horseradish peroxidase/colorimetric substrate system) was studied. If hybridization was positive, a blue precipitate was generated on the spot by attenuating the captured optical density (reflection-mode detection). The intensity of each array spot (400 μm diameter) was calculated as the average of 448 pixels. A perfect-match interaction (LAMP product/probe) produced signals up to 56,000 a.u. in 16-bit greyscale units, while the chip background values were in the range of 7,000±400 a.u.. Therefore, the spot intensities discriminated positive and negative recognition events depending on the probe/product pair. Statistical significance was calculated by a Student's *t*-test, and p-values were $<0.05$ in all cases. This study demonstrates, for the

first time, the colorimetric detection of allele-specific hybridization LAMP products, which produces excellent versatility and is a key factor to make a simpler reader-suitable method for POC applications.

For the AS-LAMP approaches, the addition of a magnesium indicator (hydroxynaphtol blue) was evaluated (*30*). Along with the capacity of the isothermally amplifying double strand DNA, a very high yield is an interesting advantage that LAMP offers over conventional PCR and other isothermal amplification methods, as it allows a subsequent direct colorimetric detection with a smartphone. This staining method was simple and did not require any additional devices (i.e. ultraviolet source, wavelength filters, magnification lens). Detection was achieved with no post-amplification steps. To improve the recorded responses (scattered light), the concentration of hydroxynaphtol blue was gradually increased and the light intensity for the RGB channels was recorded (Fig. 30). Concentrations above 300 µM provided a significant signal of red channel for the positive amplifications compared to the negative controls (test t: $t=2.25$, $p<0.05$). From the obtained results, the proposed modification of ASA-LAMP approaches showed excellent signal discrimination, which indicates its potential as a polymorphism biomarker analysis tool.

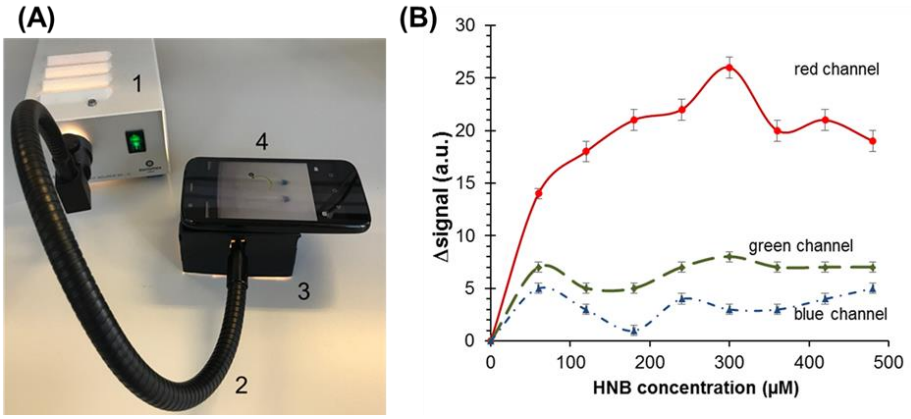


**Figure 30.** Smartphone detection of end-point AS-LAMP products for different concentrations of colorimetric dye (hydroxylnaphtol blue, HNB): (A) Photograph of the detection device: (1) cold light source; (2) adjustable optical fiber; (3) capture chamber; (4) smartphone. (B) Recorded signal variation according to the dyer concentration. DNA template: 1300 copies. Target SNP: rs1954787 located in the GRIK4 gene.

## Comparing methods

The main features and analytical performances of the three methods were subsequently compared (Table 7). Analytical sensitivity and reproducibility were calculated from the consecutive dilutions of a genomic human DNA template. Although naked-eye color observation was possible to visualize positive amplification (violet to sky blue), the use of an imaging/sensing device guaranteed reliable measurements when smaller amounts of the target SNP were present in the sample and color change was subtle. The estimated limit of detection was 100 copies for the all LAMP-smartphones-based methods. Thus, the required amount of genomic DNA was smaller than previous LAMP approaches (*12*, *15*) some genotyping assays (*31*) and sequencing techniques (*32*). Assay repeatability, calculated

from replicates, yielded error rates under 15% in all the formats, which were lower than those obtained by naked eye visualization and similar to other SNP methods that have been applied to human samples.

The technical requirements for developing point-of-care systems were also evaluated. The estimated reagent cost of LAMP-ASO was 2.65-fold higher than the AS variants, mainly because of immunoreagent prices. Compared with the corresponding PCR approaches, LAMP assays were more expensive (about 1.5-fold), mainly due to the cost of enzymes (Bst polymerase *versus* Taq polymerase). In contrast, the LAMP approaches only required a low-cost heating system (62°C; i.e. heater) compared to the conventional thermal cycler used in PCR-based methods, along with a cheaper and more practical detector. The LAMP methods also worked in shorter analysis times than their equivalent PCR approaches. The AS-LAMP formats were the quickest (70 min) compared to LAMP-ASO (140 min), AS-PCR (120 min) or PCR-ASO (190 min), mostly because of the shorter amplification times in the LAMP-based methods. Hence these results are similar, or better, than those obtained for previous LAMP approaches (*10*, *15*, *33*).

**Table 7.** Comparison of general characteristics and analytical performances between the developed SNP discrimination methods and PCR-based methods

| Discrimination strategy | LAMP-ASO | 3' AS-LAMP | 5' AS-LAMP | PCR-ASO | AS-PCR |
|---|---|---|---|---|---|
| Amplification mixtures | 1 | 2 | 2 | 1 | 2 |
| Primers | 4 | 5 | 5 | 2 | 3 |
| Array probes | 2 | - | - | 2 | - |
| Amplification factor ($10^7$) | 34 ± 2 | 14 ± 2 | 27 ± 3 | 8.6 ± 0.3 | 1.4 ± 0.3 |
| Allele-specific oligonucleotide | Probe | BIP | FIP and BIP | Probe | FP |
| Number of steps [a] | 4 | 3 | 3 | 4 | 3 |
| Detection method | Microarray | Colorimetric | Colorimetric | Microarray | Fluorescent |
| Sensitivity (copies) | 50 | 100 | 100 | 200 | 200 |
| Analysis time (min) | 140 | 70 | 70 | 190 | 120 |
| Estimated cost [b] | 3.9 | 1.5 | 1.5 | 3.5 | 1 |
| Required equipment | ++ | + | + | +++ | +++ |

[a] ASO techniques: extraction/amplification/hybridization/detection, AS techniques: extraction/amplification/ detection

b Normalized to AS-PCR assay cost

c +: few; ++: medium; +++: high.

## Patient sample analysis

Psychiatric pharmacogenetics is a candidate field for developed POC genotyping methods (*34*). As proof of concept, the genotyping of the rs1954787 polymorphism, located in the *GRIK4* gene, was selected to determine the genetic predisposition of antidepressant treatment from the human DNA (n=15) extracted from buccal swabs. Only by following the developed methodology were signals sufficiently different to achieve a specific response profile depending on the genetic variant. Figure 31 shows the subsequent discrimination graph. The three methods provided the same

genotypes for all patients, except for patient 8 in the LAMP-ASO approach. Nevertheless, the homogeneous approaches (3' AS-LAMP and 5' AS-LAMP methods) provided clearer discrimination factors than the solid hybridization format (LAMP-ASO) due to their lower signals for the mismatched reaction mixtures. Among the analyzed samples, six patients (40%) were identified as being mutant homozygous (CC) which can be related to a better chance of positive responses to depression treatment (*35*). There were also six heterozygous patients (40%), who were expected to give a normal response for drugs like citalopram. Finally, the results indicated that three (20%) subjects presented a homozygous wild-type genotype (TT), which indicates a higher risk of a non-response. Another comparison of the reference results (Sanger sequencing and AS-PCR) revealed a perfect correlation with the genotypes determined by the LAMP-based assays.

The clinical implications of this *in vitro* diagnostic assay were analyzed. Major depressive disorder affects were about 10-15% of the population (annually), with a degree of uncertainty about the individual efficacy of the antidepressant treatment (*36*). The discrimination of specific polymorphisms can enable quick personalized patient management with a strong effect on therapy. Clinical trials have identified an association of rs1954787 with therapy effectiveness, and have reported that CC homozygotes are more likely to respond to treatment than TT homozygotes. Therefore, a simple low-cost genotyping tool can support the better dosing of antidepressants.

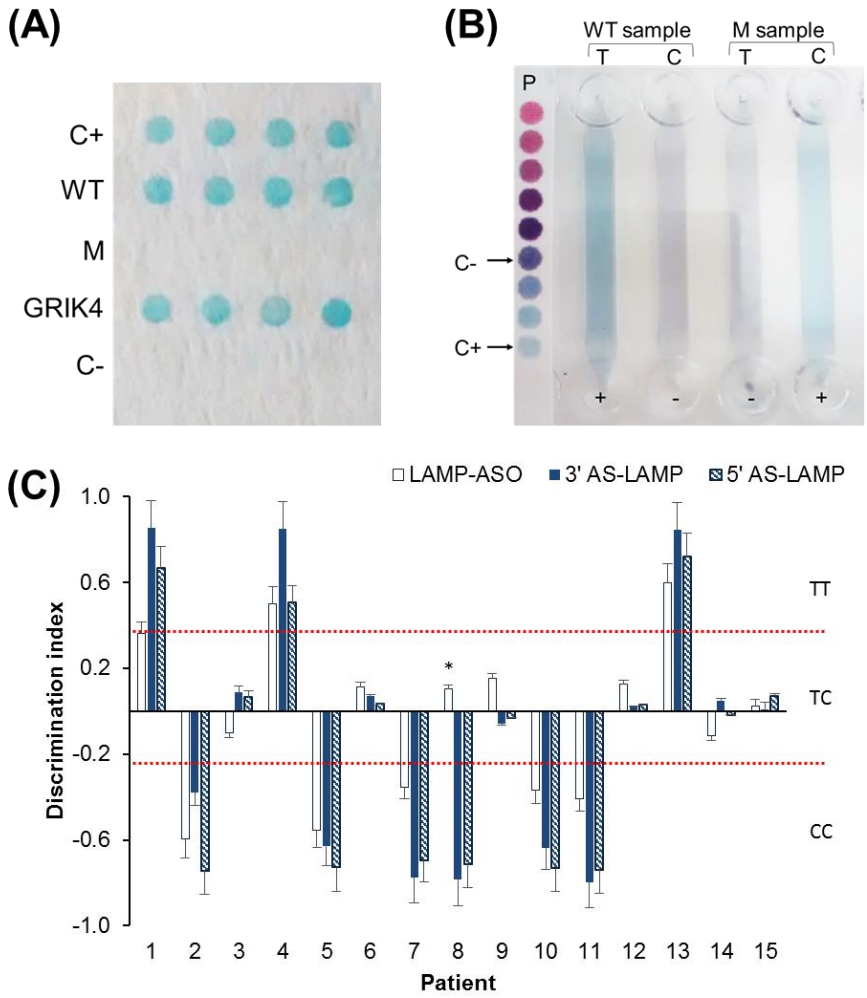


**Figure 31.** Genotype analysis of rs1954787 polymorphism using the proposed LAMP-based methods combined with smartphone detection. (A) Planar chip of ASO-LAMP method: wild-type human DNA extract. (B) Microfluidic chip of AS-LAMP method: wild-type and mutant human DNA extracts. The image includes the color pattern (P) used for smartphone detection. (C) Genotyping analysis for 15 patients using LAMP-ASO, 3' and 5' ASLAMP methods. C+: positive control, C-: negative control, WT: wild-type, M: mutant, GRIK: non-allele-specific probe.

## 3.17 Conclusion

This research confirms the excellent features of LAMP as a viable alternative to current methodologies whose aim is genotyping purposes in order to overcome the associated technical barriers. This study particularly supports the oligonucleotide design and the selection of reaction conditions for colorimetric detection in both homogeneous and heterogeneous formats. An accurate control of these experimental variables is required because false-positive results are more frequent than for PCR-based methods. Our results endorse the technical capabilities of smartphones as analytical readers for molecular diagnostic systems. Despite having a worse optical resolution than benchtop instruments, CMOS sensor chips incorporated into phone cameras offer adequate imaging features and widespread availability, which make them ideal detectors for cost-effective assays. Compared to other electronic devices, smartphone technology has additional advantages, such as assay reader, given its capability to transmit data, ubiquity and users' familiarity to handle it.

The achieved LAMP discrimination process and low-cost detector combination shows excellent performance and a wide dynamic range, which allows the technique to be extrapolated other target genetic biomarkers. This offers researchers the chance to develop integrated systems, which enable quicker monitoring of genetic predispositions to develop certain diseases or to predict genomic-related responses to drug therapies.

**Acknowledgements**

The authors acknowledge the financial support received from the Generalitat Valenciana (Project GVA-PROMETEOII/2014/040 and

GRISOLIA/2014/024 PhD grant) and from the Spanish Ministry of Economy and Competitiveness (MINECO CTQ2013-45875-R Project).

## 3.18 References


1. C. F. Woolley, M. A. Hayes, *Analyst*. **139**, 2277–2288 (2014).
2. M. G. Dobson, P. Galvin, D. E. Barton, *Expert Rev. Mol. Diagn.* **7**, 359-370 (2007).
3. S. K. Vashist *et al.*, *Trends Biotechnol.* **33** (2015), pp. 692–705.
4. H. Deng, Z. Gao, *Anal. Chim. Acta*. **853**, 30-45 (2015).
5. P. Craw, W. Balachandran, *Lab Chip*. **12**, 2469–2486 (2012).
6. L. Yan *et al.*, *Mol. Biosyst.* **10**, 970–1003 (2014).
7. J. Li, J. Macdonald, *Biosens. Bioelectron.* **64**, 196-211 (2015).
8. T. Notomi *et al.*, *Nucleic Acids Res.* **28**, e63 (2000).
9. M. Parida *et al.*, *Rev. Med. Virol.* **18**, 407–421 (2008).
10. J. T. Connelly, J. P. Rolland, G. M. Whitesides, *Anal. Chem.* **87**, 7595–7601 (2015).
11. Y. S. Jiang *et al.*, *Anal. Chem.* **87**, 3314–3320 (2015).
12. N. Nakamura *et al.*, *Anal. Chem.* **79**, 9484–9493 (2007).
13. L. Zhang *et al.*, *Anal. Chem.* **86**, 10461–10466 (2014).
14. S. Yongkiettrakul *et al.*, *Parasitol. Int.* **66**, 964–971 (2017).
15. M. Itonaga *et al.*, *PLoS One*. **11**, 1–12 (2016).
16. R. E. Shackelford *et al.*, *Genes Cancer*. **3**, 459–66 (2012).
17. A. Chan, M. Pirmohamed, M. Comabella, *Ann. Neurol.* **70**, 684–697 (2011).
18. S. P. Hamilton, *Biol. Psychiatry*. **77**, 29-35 (2015).
19. H. Kido, A. Maquieira, B. D. Hammock, *Anal. Chim. Acta*. **411**, 1–11 (2000).
20. A. Maquieira, in *Biosensors and molecular technologies for cancer diagnostics*, K. Herold, E. Rasooly, Eds. (CRC Press, 2012), 417–440.
21. A. Ozcan, *Lab Chip*. **14**, 3187–3194 (2014).
22. D. Quesada-González, A. Merkoçi, *Biosens. Bioelectron.* **92**, 549–562 (2017).
23. S. Morais, L. Tortajada-Genaro, Á. Maquieira, *Expert Rev. Mol. Diagn.* **14**, 773-775 (2014).
24. L. A. Tortajada-Genaro *et al.*, *Anal. Bioanal. Chem.* **408**, 2339–2345 (2016).
25. A. Roda *et al.*, *TrAC - Trends Anal. Chem.* **79**, 317-325 (2016).
26. S. Kanchi *et al.*, *Biosens. Bioelectron.* **102**, 136-149 (2018).
27. L. A. Tortajada-Genaro, R. Puchades, Á. Maquieira, *J. Pharm. Biomed. Anal.* **136**, 14–21 (2017).
28. E. S. Yamanaka, L. A. Tortajada-Genaro, Á. Maquieira, *Microchim. Acta*. **184**, 1453–1462 (2017).
29. D.-G. Wang *et al.*, *Molecules*. **20**, 6048–6059 (2015).
30. F. Zhang *et al.*, *Chem. Commun.* **50**, 14382–14385 (2014).
31. A. A. Gibriel, O. Adel, *Mutat. Res. - Rev. Mutat. Res.* **773**, 66-90 (2017).

32. S. Goodwin, J. D. McPherson, W. R. McCombie, *Nat. Rev. Genet.* **17**, 333-351 (2016).
33. M. Safavieh *et al.*, *ACS Biomater. Sci. Eng.* **2**, 278–294 (2016).
34. E. Milanesi *et al.*, *Genet. Res. (Camb).* **97**, e14 (2015).
35. S. Horstmann *et al.*, *Neuropsychopharmacology*. **35**, 727–740 (2010).
36. D. M. Kawaguchi, S. J. Glatt, *Pharmacogenomics*. **15**, 1451–1459 (2014).

# Chapter 4. Detection of genotyping assays based on loop-mediated isothermal amplification and consumer electronic devices

While in the previous chapter we focused in the set-up and application of the LAMP for genotyping major depression-related SNPs, in this chapter we dedicate our efforts to the detection of the developed assay with different consumer electronic devices. A model allele-specific hybridization assay was selected for creating colored microarray chips. Several daily-use devices were then applied for creating images from the model microarrays. The assay and ambient conditions were adjusted for obtaining better signal-to-noise ratios, increasing the discrimination capacity of the general analysis. The devices were compared regarding their main features and analytical performance.


# Consumer electronics devices for DNA genotyping based on loop-mediated isothermal amplification and array hybridization

*Luis A. Tortajada-Genaro, Eric Seiti Yamanaka, Ángel Maquieira*

This article was published in **Talanta, 2019, 198, 424-431**



## 3.19 Abstract

Consumer electronic technologies offer practical performances to develop compact biosensing systems intended for the point-of-care testing of DNA biomarkers. Herein a discrimination method for detecting single nucleotide polymorphisms, based on isothermal amplification and on-chip hybridization, was developed and integrated into user-friendly optical devices: e.g., USB digital microscope, flatbed scanner, smartphone and DVD drive. In order to adequately identify a single base change, loop-mediated isothermal amplification (LAMP) was employed, with high yields (8 orders) within 45 min. Subsequently, products were directly hybridized to the allele-specific probes attached to plastic chips in an array format. After colorimetric staining, four consumer electronic techniques were compared. Sensitive

precise measurements were taken (high signal-to-noise ratios, 10-□m image resolution, 99% scan-to-scan reproducibility). These features confirmed their potential as analytical tools, are a competitive alternative to fluorescence scanners, and incorporate additional advantages, such as user-friendly interface and connectivity for telemedicine needs. The analytical performances of the integrated platform (assay and reader) in the human samples were also excellent, with a low detection limit (100 genomic DNA copies), and reproducible (<15%) and cheap assays (< 10 €/test). The correct genotyping of a genetic biomarker (single-nucleotide polymorphism located in the GRIK4 gene) was achieved as the assigned genotypes agreed with those determined by using sequencing. The portability, favorable discriminating and read-out capabilities reveal that the implementation of mass-produced low-cost devices into minimal-specialized clinical laboratories is closer to becoming a reality.

*Keywords*
Single-nucleotide polymorphism; Isothermal DNA amplification; Point-of-care testing; Smartphone; Scanner; Compact disc.

## 3.20 Introduction

Advanced molecular technologies are a growing field in the healthcare system that address both diagnostics and treatment selection (*1*). Current analytical methodologies enable measurements, basically in laboratories with specialized infrastructure and classical instruments (biochemical analyzers, DNA sequencers, scanners, etc.). Alternative systems

are needed to broaden the clinical facilities available to incorporate diagnostic tools. Point-of-care (POC) approaches offer fast, robust and reliable results and reduce medical costs, mislabeling and mishandling (*2*). Thanks to these characteristics, POC tests are used for the prevention, control of disease outbreaks and monitoring health conditions, extending the medical scenarios to be addressed (*3*).

The recent advances made in materials, microfluidics and instrumentation have improved the performances of POC systems (*4*). Particularly, the availability and affordability of consumer electronic, or home electronic, equipment, are increasing the possibilities of innovative solutions. They include devices used for entertainment, communications and home-office activities, such as smartphones, scanners, and compact disc drives. These hand-held optoelectronic devices have the potential to make biosensing more accessible to society (*5*). Two categories can be defined depending on the employed sensing principle. The first is composed of digital imaging devices, which consists of an array of pixel sensors that converts light intensity into electrical current (charge coupled device or a complementary-metal-oxide-semiconductor). The optical sensors installed in smartphones (*6*), documental scanners (*7*), or similar devices, provide images of the assay platform, generally a planar or microfluidic chip, with enough quality to obtain analytical information (*8*). In case of smartphones, custom-made attachments are used to hold the sample and auxiliary optical modules (*9*). The second category is based on compact disc technology, where assays are performed on the optical disc surface and a disc drive acts as the optical scanner (*10–13*).

Consumer electronic equipment has been adapted as imaging platforms for genetic diagnoses with demonstrated sensitivity (*14*). To reach the copy number required for molecular detection, a common challenge is the

DNA amplification process (e.g. polymerase chain reaction, PCR). In POC approaches, one important component is the heat system for performing a precise fast thermal cycling (*15*). In recent years, alternative methods have been explored using isothermal amplification techniques and simple heaters (*16*, *17*). Among the available options, the loop-mediated amplification method (LAMP) is the most popular solution (*18*). This reaction amplifies DNA at constant temperatures by using the Bst polymerase large fragment, which presents great strand displacement activity and enzymatic processivity. LAMP also provides higher amplification yields than PCR in shorter incubation times.

Regarding applications, consumer electronic devices have been employed for detecting specific target (e.g. disease biomarker and infectious pathogen) (*19*–*22*). However, several diagnostic and prognostic applications demand the simultaneous detection of multiple regions or variants (e.g. differentiation among similar pathogen strains or detection of point-mutations). In order to increase multiplexing capabilities, a common strategy is multiple parallel assays performed in microreactors on chips (*23*). Another alternative is the combination with a hybridization assay using probes immobilized on a chip surface, followed by adequate labelling and the optical detection of the corresponding array. In a recent paper, we demonstrated the potential of this approach combined to smartphone based-detection (*24*). However, other consumer electronic devices are also potentially compatible to be used as readers of array-based assays. A scientific challenge for low-cost diagnostic community is an evaluation of their suitability and limitations, considering specific spectral responsivity, integration capabilities and associated data quality (*25*).

In this research, our goal was to explore the analytical capabilities of different consumer electronic techniques leverages for imaging of array chips

of nucleic acids. The compared devices were smartphone, flatbed scanner, USB digital microscope and compact disc drive. Therefore, the study was to stablish the feasible requirements to transform each equipment into analytical reader of results generated by a highly sensitive and specific isothermal DNA assay. As proof of concept, the final POC integrated systems (biosensing assay and readers) were intended to be applied to the accurate low-cost discrimination of clinically relevant genetic variants.

## 3.21 Material and methods

### Primers and probes

The studied biomarker was the single nucleotide polymorphism (SNP) associated with the pharmacogenomics of anti-depressants drugs (rs1954787, g.285909T>C, located in the *GRIK4* gene). LAMP primers and probes were selected according to the thermodynamic parameters associated with the perfect-match and mismatched duplexes (Supplementary Material). All the oligonucleotides used in this study were purchased from Eurofins (Luxembourg).

### LAMP combined with allele selective hybridization

Genomic DNA amplification was carried out in 200-µL polypropylene vials. Each reaction (12.5 µL) was composed of 1× isothermal amplification buffer (20 mM Tris-HCl, 10 mM $(NH_4)_2SO_4$, 50 mM KCl, 2 mM $MgSO_4$, 0.1% Tween 20, pH 8.8), 1.5 M betaine, additional 6 mM $MgSO_4$, 1.2 mM dNTPs, 10 µM digoxigenin-11-deoxyuridine triphosphate (DIG-dUTP), 0.2 µM of outer primers, 1.2 µM of inner primers, 0.32 U/µL

Bst polymerase 2.0 (New England Biolabs, USA) and 0.32 ng/µL of DNA. Vials were incubated at 62°C for 60 min (digital heat block, VWR, USA).

An allele-selective hybridization assay led to the discrimination of the amplified products. Assays were performed on polycarbonate planar slides (detection device: chip-based sensors) or on the bottom layer of DVD discs (detection device: DVD drive). Probe arraying and the hybridization of the amplification products were performed according to the protocol developed in previous work (*26*). The array layout contained 4 replicates per probe and 10 arrays per chip. Regarding chip staining, the digoxigenin-labelled duplexes were recognized by horseradish-peroxidase-conjugated anti-digoxigenin antibodies, and were stained by deposition of 3,3',5,5'-tetramethylbenzidine (ep(HS)TMB, SDT reagents, Germany).

**Array imagining**

Four different consumer electronic technologies were examined to image the arrays according to the following protocols:

*USB digital microscope*. The profile intensities were measured by a portable microscope (Dino-Lite AM4013MZT, AnMo Electronics Co., Taiwan) based on a color CMOS system (resolution 1.3 Megapixel, maximum frame rate: 30 fps). Images were captured by vertically positioning the equipment over the array at a 5-centimetre distance and employing the microscope internal LED as the light source (maximum illumination 18,500 lux). The DinoCapture 2.0 software was employed to record the image at the 1.3-megapixel resolution.

*Smartphone.* Array images were also captured by a smartphone (MotoG first generation, Motorola, EEUU) using a home-made chamber (8 x 6.7 x 4.4 cm) (*24*). The device specifications were typical of a mid-range

phone (display 4.5”, processor 1.2 GHz quad core, RAM 1 GB, rear camera 5-megapixel CMOS). The reading chamber had a frontal rectangular aperture for the smartphone camera, a lateral hole used to illuminate the array by an external optical fiber light source (power 20W, LE.5209 model, Euromex, Holland), and an aperture for inserting the assay chip. After adjusting the focus and exposure (75% level), images were captured. The system did not require any connection to the telephone network.

*Flatbed scanner.* An office scanner (Perfection 1640SU Office, Epson, Japan), which incorporated a CCD image sensor, was also employed in the reflectance mode. The array support was positioned over the equipment bed and scanning was carried out at a 1,600 dpi (dots per inch) resolution using the Epson scan default software (disabled auto-correction functions).

*Compact disc drive.* The DVD-supported microarrays were directly read by a digital versatile disc (DVD) drive (LG DVD GSA-H42N, LG Electronics Inc., USA), which incorporated a data acquisition board model (DT9832A-02-OEM; Data Translation, Marlboro, MA, USA) (*13*). The standard disc drive acted as a miniature high-precision optical device that consists of laser diodes, collimating lenses, diffraction gratings and a photodiode. The focus and tracking mechanism was responsible for spinning the disc and moving the optical pickup head unit. The reading conditions were adjusted by a custom software: rotation speed of 4× (13.46 m/s) and 21 dB gain at a detection rate of 1,700 mega-samples/s. Thus, the array image was formed from the data captured in each radius.

The ImageJ free-access software (National Institutes of Health, USA) was used to process the images in the tagged image file format (TIF) and on a 16-bit grey-scale (65,535 intensity values). The software provided the spot and surrounding background intensities. Signal-to-noise ratios were

calculated as the net spot signal, divided by the background standard deviation.

**Sample analysis**

The performances of the POC systems for clinical routine were evaluated by applying SNP genotyping methods. Human subjects (n=15) were recruited for the present study according to ethics guidelines. Buccal smear samples were collected by a minimally invasive method. DNA extracts were obtained using a Purelink Genomic DNA mini kit (Thermo Fisher Scientific, USA). The genomic DNA content was quantified with a NanoDrop 2000 spectrophotometer (Thermo Fisher Scientific, USA). Extracts were diluted to 4 ng/µL (1,300 copies) and analyzed as described in previous sections. The analysis was declared valid if the amplification and hybridization controls provided a correct response. The genotype decision rule was constructed based on the signal-to-noise ratio associated with the wild-type (T) and mutant (C) probes.

**Genotyping validation**

Sanger sequencing was used to determine patient genotypes (blind samples). Each PCR reaction (12.5 µL) contained 1x amplification buffer, 3 mM $MgCl_2$, 200 µM dNTPs, 300 nM of forward and reverse primers, 0.5 units of Taq polymerase (Biotools, Spain) and 4 ng of DNA. The amplification was carried out in a thermal cycler (UnoCycler, VWR): initial denaturation at 95°C for 5 min, followed by 35 amplification cycles of denaturation (95°C for 30 s), annealing (60°C for 30 s) and elongation (72°C for 30 s), and a final extension step at 72°C for 5 min. The resulting amplification products were diluted, extended with fluorescent dideoxynucleotides (Big Dye Terminator Cycle Sequencing Kit v3.1, Thermo Fisher Scientific, USA), and analyzed in a fluorescence-capillary sequencer (ABI 3130xl Genetic Analyzer, Applied Biosystems, USA).

The Statgraphics Centurion statistical package for Windows v.16 was used for the data analysis.

## 3.22 Results and discussion

**Selection of model assay selection**

As reference assay for the evaluation of devices, the allele-specific oligonucleotide hybridization of LAMP products on a planar chip was chosen. This method has demonstrated as promising POC approach in clinical application (*24*, *27*, *28*). Their advantages are isothermal process, biosensing assay in solid-phase format, direct hybridization of amplified products, compatible to low-cost materials and high selectivity for the discrimination of single-nucleotide variations. In order to improve the signal-to-noise ratios

compared to the results described in a previous paper (*24*), the optimization experiment were performed (Supplementary Material). A colorimetric staining of chips was selected because it was simple and all the studied devices read them on a common detection principle basis. The assay output was chips with specific hybridization patterns (blue spots, $\lambda_{max}$ = 650 nm), depending on the genetic profile.

**Set-up of detection systems**

The next challenge was to select the biosensing measurement conditions to quantify the array spot intensities using consumer electronic devices as user-friendly optical read-out. Such electronic or digital equipment is intended for everyday use, typically in homes or offices. Thus, their conversion into a DNA detection platform required reviewing their capabilities and exploiting the feasibility of their components.

A set of standard chips containing nine replicated positive spots and six replicated negative spots was imaged (spot diameter: 150-600 μm, center-to-center spot-distance: 150-600 μm). Four technologies were tested: USB digital microscope, documental scanner, smartphone and compact disc (Table 8). Also, required detection assembly, auxiliary components, experimental imaging conditions and data processing methods were examined.

**Table 8.** Optimization of DNA array signal reading using the studied devices.

| Device | Parameter | Range | Selected |
|---|---|---|---|
| Microscope | Chip distance | 1.5 – 10.0 cm | 5.0 cm |
| | LED lighting | Internal/External | Internal |
| | Relative exposure | 10-100% | 60% |
| Scanner | Capture mode | Reflectance | Reflectance |
| | Exposition | Document/Photo | Photo |
| | Resolution | 50 – 2,400 dpi | 1,600 dpi |
| Smartphone | Chip-phone distance | 2.0 – 8.0 cm | 4.4 cm |
| | With, without Dark chamber | With | With |
| | Type of light | Flash/LED/Cold light | Cold light |
| | Light angle | -15º – 120º | 90º |
| DVD reader | Rotation speed | 1× – 32× | 8× |
| | Gain | 10 – 40 dB | 26 dB |
| | Detection rate | 500 – 1,700 a.u. | 1,700 a.u. |

Experiments were firstly performed using the camera-based devices: microscope and smartphone (Figure 32). Illumination was critical because image quality changed due to the reflective and scattering processes on the chip surface (polycarbonate). The circular configuration of the LED sources in the USB digital microscope restricted the focused area by limiting the microarray slide zone to a few square-millimeters that gave comparable data. Excessively high light intensity provided lower spot signals and a higher percentage of statured pixels due to reflection problems.

For smartphone-based measurements, direct frontal lighting by the camera's LED flash was not possible because this configuration (0º between capturing and illumination) compromised spot discrimination due to a high

reflection rate (signal-to-noise ratios < 3). Consequently, an external broadband light source was used to illuminate chips, which provided more versatility and control to take measurements with adequate light power. Depending on the light source angle, light reflection and shadowing effects were more relevant, with the variation between the spot and background decreasing. A 20 W compact cold light source and a 90º illumination angle were selected to generate the indirect lighting of the chip surface through the chamber internal walls, which was generated more reproducible and distinguishable signals.

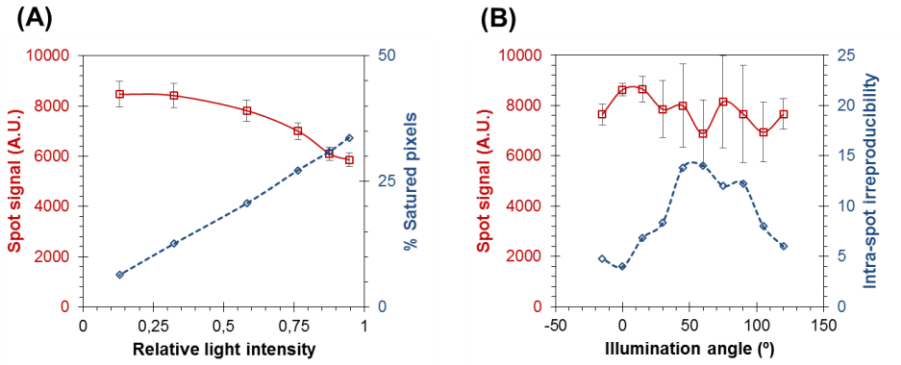


**Figure 32.** (A) Effect of illumination power on spot signal (continuous line) and the percentage of statured pixels due to light reflection (dashed line) for the microscope. (B) Effect of illumination angle on the spot signal (continuous line) and intra-spot irreproducibility (dashed line) for the smartphone. Spot diameter = 400 μm. Replicates = 9.

In both camera-based devices, the separation between the detector and assay chip affected the optical system performances, expressed as a maximum signal and ratio between the spot signal and the background signal (Figure 33). For smartphone capturing, the distance was also critical for the image resolution and poorly focused images resulted when capturing from

less than 4 cm. The most sensitive results were achieved at 5 cm for both instruments. Finally, the image processing effect was evaluated depending on the color scale. Reliable data results were obtained with the RGB analysis (red channel) and greyscale, and positive spots were clearly differentiable from negative ones. Considering the highest relative intensity between the positive and negative spots, direct black/white acquisition or greyscale conversion was selected and used for the subsequent measurements.

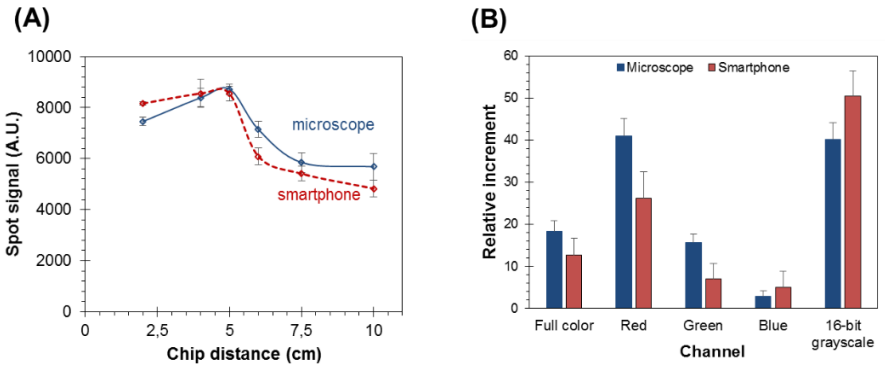


**Figure 33.** (A) Effect of chip distance on the spot signal for the microscope and smartphone. (B) Relative signal variation (%) between the positive and negative spots depending on the image color scale for both CMOS-based devices. Spot diameter = 400 µm. Replicates = 9.

In this desktop scanner, a white light on a motorized belt progressively illuminated the reference chips, and a CCD sensor measured the intensity and color of the light reflected from the sample. If hybridization was positive, the blue precipitate attenuated the captured optical density (reflection-mode detection), as shown in Figure 34. The flatbed scanner was less flexible regarding reading conditions than the other explored devices as it was possible to vary only the imaging mode and scanning resolution. The captured image was better defined (higher pixel density per spot) by

increasing the scanning resolution, which led to correct spot segmentation. At a resolution of 1,600 dpi, signal intensity was adequate and spot heterogeneity was minimal.

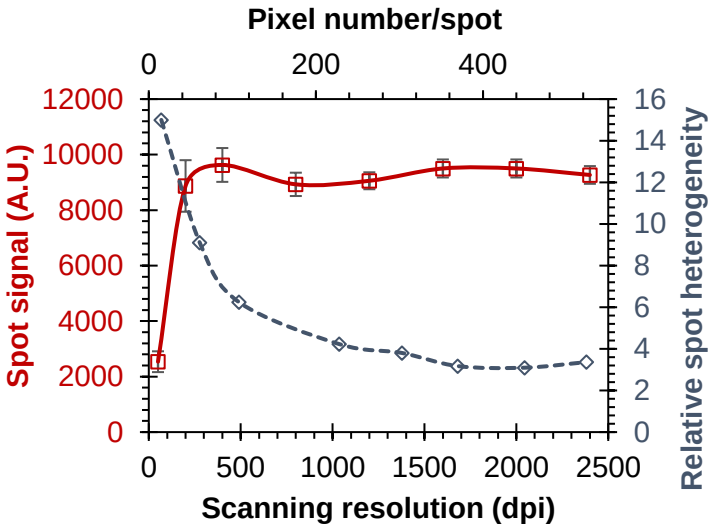


**Figure 34.** Effect of scanning resolution on the spot signal (continuous line) and the relative spot heterogeneity (dashed line) for the flatbed scanner. Spot diameter = 400 μm. Replicates = 9.

With the compact disc reader, the selected detection principle was the reflection at the DVD multi-layer system and scattering/absorption by the array spots since the laser wavelength (650 nm) fitted the absorption spectrum of the blue precipitates. During the disc's laser scanning process, the light from the pickup unit passed through the bottom surface of the polycarbonate layer and was reflected on the upper reflective layer (0.6 mm). Tight focusing at the DVD track guaranteed robust measurements. After making the inverse path, light intensity was recorded on the photodetector. The assay was

performed on the disc bottom layer that allowed the hybridization yield to be monitored by attenuating the reflected light by the formed products. Then each pixel corresponded to a specific disc coordinate which, in turn, corresponded to the pickup unit position (disc radius and rotation angle). Software treatment converted the measured pixel-to-pixel signals at the different disc radii into digital spot images, which were subsequently analyzed by grey-scale quantifications. The scanning conditions of DVD surface were studied to obtain better optical performance (Figure 35). Regarding the rotation rates (up to 16×), although comparable intensity results were recorded at all the tested speeds (t-test, $p < 0.05$), a slower rotation favored correct disc reading. Consequently, a 4× rate was selected with a total scanning duration of 13 minutes. The effect of the sampling rates was also evaluated and, as expected, it affected image resolution. In detail, more pixels per spot were displayed by increasing the sampling rate (2,000 mega samples per second). The photodiode gain also affected detection sensitivity and, consequently, the working range, expressed as the number of amplification product copies in the hybridization assay. Considering the highest spot intensities and the dynamic range, gain was adjusted to 27 dB.

In short, these four low-cost devices were capable of quantifying the microarray spot intensities resulting from a DNA recognition process performed in polycarbonate chips, which is a thermopolymeric substrate suitable for mass production. This approach works on a low scale in terms of the amount of reagent, cost and waste.

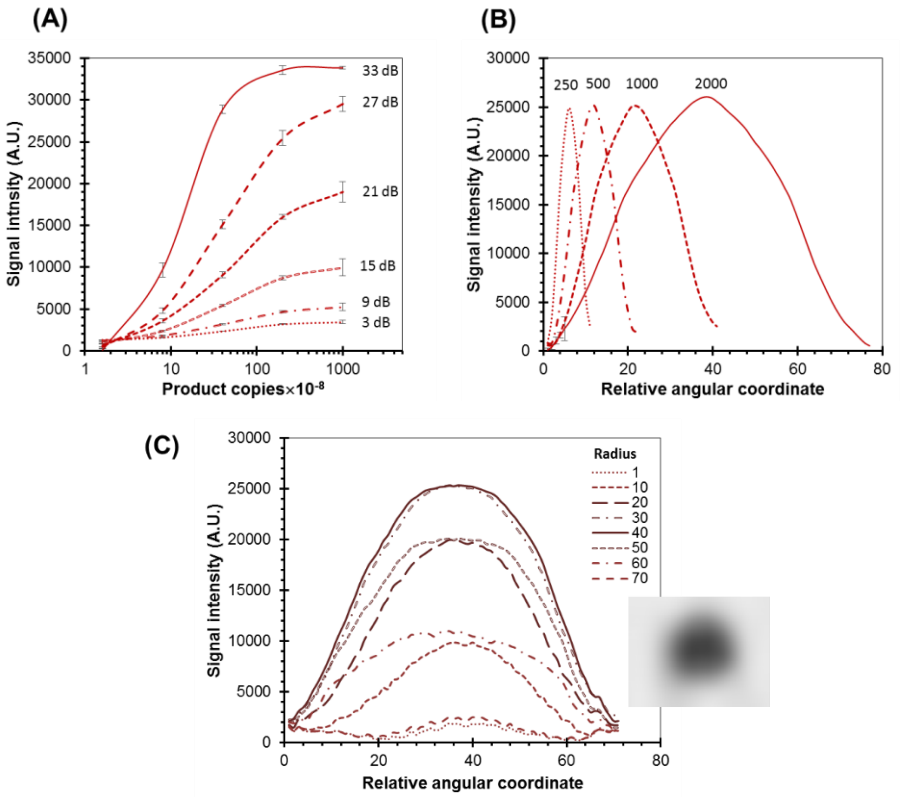


**Figure 35.** (A) Signal intensity collected along the DVD track during the scanning process at different sampling rates (mega-samples per second). (B) Signal intensity collected at different photodiode gain values. (C) Signal intensity collected along the DVD track during the scanning process at different disc radii (radial step = 5.8 μm). Insert: Generated image. Spot diameter = 400 μm. Replicates = 9.

## Comparison of imaging approaches

The selection of an imaging technique for POC genetic detection requires a precise evaluation its features as an analytical instrument (*28*). Model DNA chips were measured after incubating a wild-type amplification product on 4×4 arrays (spot diameter: 450 μm). Supplementary Material

reports some examples of a reference array image that was captured using the four studied devices. The evaluation of the read-out system is summarized in Table 9.

The first examined parameter was the measured area. Due to its reading configuration of USB microscope, the imaged area was restricted to a single microarray per reading (6 mm × 6 mm), which required 10 captures per chip. The rest of devices recorded the entire chip (or DVD disc) in a single measurement. Optical resolution, expressed as the distance between two points that can still be distinguished as separate entities, was compared. The measured pixel width was 17 μm for the smartphone, 10 μm for the digital microscope, 10 μm for the scanner and 10 μm for the DVD reader, which meant a similar resolution for all the equipment. An excellent correlation between the optical density of the spots and the printed probe concentration (100-500 nM, data not shown) was obtained in all cases (regression coefficient > 0.95). At the probe concentration selected to perform the hybridization assays (100 nM), an average array spot (400 μm diameter) was found to contain between 450 pixels (smartphone) and 1,250 pixels (the other devices). Another important aspect of the capturing process was data compression. While the microscope, scanner and DVD reader generate uncompressed TIFF-format images, smartphones usually save images in the JPG format, which lead to data losses and can distort the analytical signal in some cases.

**Table 9.** Comparison of the studied consumer electronic devices used as DNA array readers.

| Device | Microscope | Smartphone | Office Scanner | DVD reader |
|---|---|---|---|---|
| |  |  |  |  |
| Dimensions | 16 × 6 × 6 cm | 13 × 6.6 × 1.2 cm | 44 × 29 × 10 cm | 27.0 × 11.7 × 5.6 cm |
| Weight | 100 g | 143 g | 4500 g | 2700 g |
| Acquisition software | DinoCapture2.0 | Android 4.3 | Epson | Home-made |
| Connectivity | Laptop - USB port | Direct | Laptop - USB port | Laptop - USB port |
| Energy requirements | USB supply (2 W) | Phone battery (2070 mAh, ~8W) | External power supply (200W) | External power supply (12V/4A, 48W) |
| Reading area | 6 mm × 6 mm (0.36 $cm^2$) | 25 mm × 75 mm (19 $cm^2$) | 216 mm × 296 mm (640 $cm^2$) | ∅120 mm-disc (83 $cm^2$) |
| Reading process | Manual, 10 min | Manual, 0.5 min | Automatic, 7 min | Automatic, 13 min |
| Samples per chip | 10 | 10 | 10 | 36 |

**Table 9 (cont.).** Comparison of the studied consumer electronic devices used as DNA array readers.

| Device | Microscope | Smartphone | Office Scanner | DVD reader |
|---|---|---|---|---|
| Measurements per chip [a] | 10 | 1 | 1 | 1 |
| Resolution (pixel width) | 10 μm | 17 μm | 10 μm | 10 μm |
| Scan-to-scan variation [b] | 0.1% | 3.2% / 0.4% | 0.1% | 0.8% |
| Spot location variation [b] | 3.6% | 5.2% / 0.6% | 0.5% | 2.5% |
| Inter-spot variation [c] | 4.6% | 9.8% | 2.9% | 8.0% |
| Background variation | 3.2% | 4.0% | 1.1% | 3.2% |
| DNA sensitivity [d] | 100 copies | 100 copies | 100 copies | 100 copies |
| Detector prize | €150 | €100 | €100 | €350 (prototype) |

[a] Required measurements to read the entire chip; [b] replicates = 3, smartphone values with/without a color palette; [c] replicates = 5; [d] Minimal copy number of the genomic template employed for the LAMP-hybridization method needed to generate a signal-to-noise ratio above 3.

Images were also evaluated in terms of mean dot intensities. A perfect-match interaction (LAMP product/probe) produced signals that ranged from 43,000 (office scanner) to 56,000 (smartphone). Meanwhile, the chip background values ranged from 500 (USB-microscope) to 7,000 (smartphone). The lowest negative signals (negative control and mismatched probe) were obtained using the USB microscope, while the highest positive signals (positive control and perfect-match probe) were achieved with the scanner and DVD reader. Any statistical significance was calculated by a Student's *t*-test. The *t*-statistic values varied from 4.66 for the smartphone to 20.61 for the USB microscope (p-values $<0.05$). For all the devices, the signal-to-noise ratios were higher than 10. Although the resolution and signal-to-noise ratios were worse than those of a fluorescent scanner, the achieved values were still sufficient for a reliable microarray analysis and quality assurance.

Measurement reproducibility was compared by considering the variation of the signal intensities between different readings, depending on the spot location in the chip. The calculated values, expressed as relative standard deviation, varied between 0.1% and 5.2%. The systems based on imaging and external illumination (microscope and smartphone) reported the least robust results. Inter-spot precision ranged between 90.2% and 97.1%, which implies that the most important contributions to signal variations were related to the discrimination assay, such as probe printing, hybridization and staining reaction, besides instrumental features. The signal-to-background ratio was calculated to assess the systems' sensitivities. The detection limit, estimated from the consecutive dilutions of a genomic DNA template, was 100 copies, where positive spots were clearly differentiable from the background (signal-to-noise ratio higher than 3). These precision and

sensitivity values were better or comparable to previous approaches for POC methods (*2*, *6*, *11*, *23–29*).

Regarding the operational characteristics for POC applications in remote scenarios, the smartphone presented the best features: lightweight, small size, internal data processing, direct connectivity and low-energy. Nevertheless, compact disc drives and scanners also have an important potential, with commercially available portable external slim units (USB power supply) and handheld scanners, respectively. Despite its excellent optical performance, the USB microscope offers limited applications in low-resource environments.

Several authors have coupled optical elements to exploit consumer electronics as instruments for more sophisticated detection principles, such as bright-field microscopy, or as electrochemical, fluorescence or cytometric analyses (*6*, *9*, *30*). According to our experience, unmodified commercial technology has its advantages, such as robustness, continuous updating, is affordable, and offers high-working tolerance, familiarity and minimal maintenance. In this study, we demonstrated the optical capacities of unmodified readers, such as 10 μm pixel resolution, being adequate for detecting micrometer-size spots (100 μm diameter) dispensed using contactless nanoprinters. There are a wide range of optical potential applications, especially the integration of the studied devices with microfluidic platforms (*31*).

**Application to pharmacogenomics**

The analytical performances showed that these technologies can support healthcare decentralization to become ubiquitous, such as a doctor's office, remote locations, emergency needs and low-resource health systems.

Pharmacogenetics is a candidate field for the developed POC methods because the discrimination of specific nucleotide changes can enable personalized patient management. In this context, the performance of all our systems was tested for the specific genotyping of the rs1954787 variants in human buccal samples (change thymine>cytosine). This SNP is located in the *GRIK4* gene, which encodes a glutamatergic receptor, and it associated with the effectiveness of anti-depressant drugs (*32*, *33*). The array layout was composed by four probes (positive control, negative control, wild-type probe and mutant probe).

In all devices, the recorded spot signals depended on the probe/product pair (Figure 36). The biggest differences between the perfect-match and mismatched probes were achieved with the office scanner and DVD reader. Despite the differences, a clear genotype assignation was achieved for all the samples because positive and negative recognition events were discriminated (Student's *t*-test, p-values < 0.05). Homozygous wild-type (TT), heterozygous genotype (CT) and mutant homozygous (CC) were identified for three, six and six patients, respectively. The results obtained with the four studied devices agreed with those obtained by a reference method (Sanger sequencing).

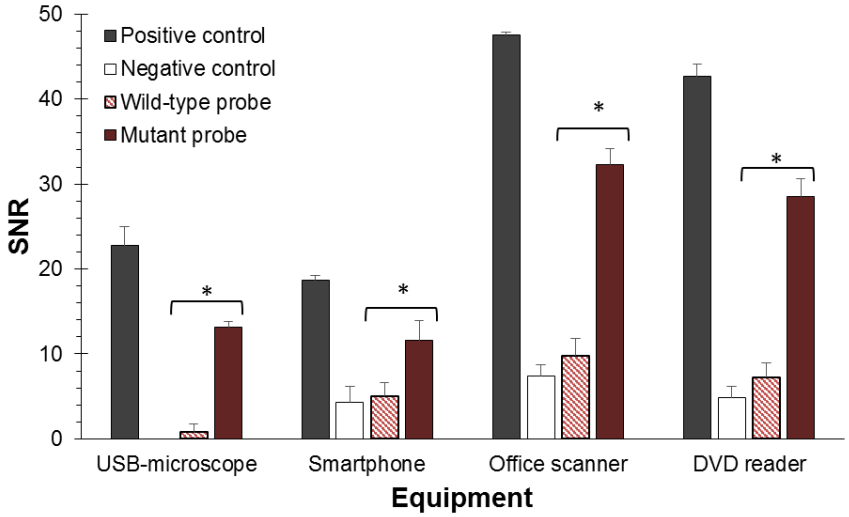


**Figure 36.** Signal-to-noise ratio recorded for genotyping microarray images using the studied consumer electronic devices. Sample: mutant homozygous individual (CC). All the data are shown as mean±standard deviation. * p-value < 0.05

From a simple oral swab, genetic information about the expected efficacy of an antidepressant drug was obtained. Indeed, the presence of a wild-type allele in nine patients indicated a higher risk of non-response treatment (*32*). Considering the performance in this evaluation study, the LAMP-based method combined to consumer electronic devices showed the potential for reliable POC analyses. The total duration of the assay (6 samples) was 140 min, which corresponded to a 15-minute DNA extraction, a 50-minute amplification, a 45-minute hybridization and a 30-minute colorimetric staining. The estimated cost per assay was €9 (excluding personnel, instruments and power). Assay repeatability, expressed as the relative deviation between assay replicates, was lower than 15%. These results confirmed that the approaches studied herein would be suitable as competitive diagnostic tools of single nucleotide changes.

## 3.23 Conclusions

As demonstrated herein, some consumer electronic technologies are appropriate biosensing readers if adequately combined with an assay with good sensitivity, selectivity and robustness. DNA arrays are a powerful technique, which is due mainly to their multiplexing capabilities and their reduced sample and reagent uses. This research endorses the excellent features of LAMP combined with allele-specific hybridization in array format. The high amplification yield of this isothermal amplification reaction and the compatible colorimetric staining reagents of on-chip DNA complexes are two important properties for combinations with imaging devices.

We demonstrated that the four studied devices, based on different optical reading principles (camera capturing or scanning), fulfilled the requirements of array detectors. But integration is not direct as there are several experimental factors that influence image quality. For instance, illumination conditions are essential because heterogeneous intensity distribution over the plastic chip reduces both image contrast and spot-to-spot reproducibility. Apart from their low-cost, these devices also present several advantages, like good availability, portability, the ability to transmit data and having a user-friendly interface. The selection criteria of a specific technology depends on the specific application. Sample number, power supply requirements, availability of equipment, personnel training, turnaround time and hands-on time are some factors that influence which device is to be chosen.

The potential as molecular diagnostic platform is high. Our study demonstrated that the robust, effective and highly specific genotyping of a relevant pharmacogenomics biomarker was achieved in human samples collected by a minimally invasive method. Thus, access to specific genetic

information (polymorphisms or point-mutations) can be achieved by overcoming the important technological barriers associated with sequencing techniques and providing information to support a tailored therapy.

**Acknowledgements**

The authors acknowledge the financial support received from the Generalitat Valenciana (GVA-PROMETEOII/2014/040 Project and GRISOLIA/2014/024 PhD grant) and the Spanish Ministry of Economy and Competitiveness (MINECO CTQ2016-75749-R project) by U. E. FEDER funds. The authors also thank J. Carrascosa for supporting the DVD reader measurements.

## 3.24 References

1. C. F. Woolley, M. A. Hayes, *Analyst.* **139**, 2277–2288 (2014).
2. M. Zarei, *TrAC - Trends Anal. Chem.* **91**, 26–41 (2017).
3. S. K. Vashist, P. B. Luppa, L. Y. Yeo, A. Ozcan, J. H. T. Luong, Emerging Technologies for Next-Generation Point-of-Care Testing. *Trends Biotechnol.* **33** (2015), pp. 692–705.
4. S. Nayak, N. R. Blumenfeld, T. Laksanasopin, S. K. Sia, *Anal. Chem.* **89**, 102–123 (2017).
5. K. Grudpan, S. D. Kolev, S. Lapanantnopakhun, I. D. McKelvie, W. Wongwilai, Applications of everyday IT and communications devices in modern analytical chemistry: A review. *Talanta*. **136** (2015), pp. 84–94.
6. A. Roda *et al.*, Smartphone-based biosensors: A critical review and perspectives. *TrAC - Trends Anal. Chem.* **79** (2016), pp. 317–325.
7. K. V. Oskolok, E. V. Shults, O. V. Monogarova, A. A. Chaplenko, *Talanta*. **178**, 377–383 (2018).
8. E. Petryayeva, W. R. Algar, *RSC Adv.* **5**, 22256–22282 (2015).
9. D. Quesada-González, A. Merkoçi, *Biosens. Bioelectron.* **92**, 549–562 (2017).
10. A. Maquieira, in *Biosensors and molecular technologies for cancer diagnostics*, K. Herold, E. Rasooly, Eds. (CRC Press, 2012), pp. 417–440.
11. L. A. Tortajada-Genaro, S. Santiago-Felipe, M. Amasia, A. Russom, Á. Maquieira, *RSC Adv.* **5**, 29987–29995 (2015).
12. H. Z. Yu, Y. Li, L. M. L. Ou, *Acc. Chem. Res.* **46**, 258–268 (2013).

13. S. Santiago-Felipe, L. A. Tortajada-Genaro, S. Morais, R. Puchades, Á. Maquieira, *Sensors Actuators, B Chem.* **204**, 273–281 (2014).
14. A. Niemz, T. M. Ferguson, D. S. Boyle, Point-of-care nucleic acid testing for infectious diseases. *Trends Biotechnol.* **29** (2011), pp. 240–250.
15. S. E. McCalla, A. Tripathi, *Annu. Rev. Biomed. Eng.* **13**, 321–343 (2011).
16. F. Ahmad, S. A. Hashsham, Miniaturized nucleic acid amplification systems for rapid and point-of-care diagnostics: A review. *Anal. Chim. Acta*. **733** (2012), pp. 1–15.
17. H. Deng, Z. Gao, Bioanalytical applications of isothermal nucleic acid amplification techniques. *Anal. Chim. Acta*. **853** (2015), pp. 30–45.
18. M. Safavieh *et al.*, *ACS Biomater. Sci. Eng.* **2**, 278–294 (2016).
19. A. Ozcan, *Lab Chip*. **14**, 3187–3194 (2014).
20. S. C. Liao *et al.*, *Sensors Actuators, B Chem.* **229**, 232–238 (2016).
21. T. H. Wu, C. C. Chang, J. Vaillant, A. Bruyant, C. W. Lin, *Lab Chip*. **16**, 4527–4533 (2016).
22. S. Kanchi, M. I. Sabela, P. S. Mdluli, Inamuddin, K. Bisetty, Smartphone based bioanalytical and diagnosis applications: A review. *Biosens. Bioelectron.* **102** (2018), pp. 136–149.
23. R. D. Stedtfeld *et al.*, *Biomed. Microdevices*. **17** (2015), doi:10.1007/s10544-015-9994-1.
24. E. S. Yamanaka, L. A. Tortajada-Genaro, N. Pastor, Á. Maquieira, *Biosens. Bioelectron.* **109** (2018), doi:10.1016/j.bios.2018.03.008.
25. F. M. Walker, K. M. Ahmad, M. Eisenstein, H. T. Soh, *Anal. Chem.* **86**, 9236–9241 (2014).
26. L. A. Tortajada-Genaro *et al.*, *Anal. Bioanal. Chem.* **408**, 2339–2345 (2016).
27. N. Nakamura *et al.*, *Anal Chem*. **79**, 9484–9493 (2007).
28. N. Nakamura *et al.*, *Clin. Biochem.* **42**, 1158–1161 (2009).
29. M. Schäferling, S. Nagl, Optical technologies for the read out and quality control of DNA and protein microarrays. *Anal. Bioanal. Chem.* **385** (2006), pp. 500–517.
30. K. Yang, H. Peretz-Soroka, Y. Liu, F. Lin, Novel developments in mobile sensing based on the integration of microfluidic devices and smartphones. *Lab Chip*. **16** (2016), pp. 943–958.
31. S. Sharma, J. Zapatero-Rodríguez, P. Estrela, R. O'Kennedy, *Biosensors*. **5**, 577–601 (2015).
32. S. Paddock *et al.*, *Am. J. Psychiatry*. **164**, 1181–1188 (2007).
33. D. M. Kawaguchi, S. J. Glatt, *Pharmacogenomics*. **15**, 1451–1459 (2014).

# 4 RESULTS DISCUSSION

As presented in this thesis, the development of new DNA biosensors is essential to solve the current demand for less complex and costly support technologies for application in pharmacogenetics. In the work developed in this thesis, we aimed to create novel genotyping systems to be used in low-specialization contexts, using isothermal enzymatic reactions for increasing sensitivity and selectivity; and consumer electronic devices to achieve competitive qualities for POC application. Herein we discuss the main features and observations regarding the developed genotyping systems.

RPA showed a great selectivity for SNPs and a high amplification speed, producing significant amounts of cDNA in only 5 to 30 min, being faster than the majority of amplification techniques. Its oligonucleotide design and format are very similar to PCR, using a single pair of primers per target, which facilitates the adaptation of PCR-based methods to an isothermal format. We demonstrated for the first time that RPA is capable of performing single-base-specific amplification of primers in genomic DNA samples, with great efficiency, also being an effective support reaction to other discrimination strategies, such as the oligonucleotide ligation. The allele-discrimination was also improved by the use of short primers and locked-nucleic acid (LNA) oligonucleotides, that made the genotyping assay more consistent and selective. Moreover, RPA required a very low operation temperature, which could allow genetic analysis with wearable devices, using corporal heat as energy source for amplification, as presented in other studies (*1, 2*). These features make RPA one of the most promising isothermal amplification reactions, although it has much more to be explored. Nevertheless, the crowding agents necessary for allowing recombination and extension make difficult to apply the reaction with multiple primer pairs and

hinder the detection of amplification products with standard methods such as fluorescent intercalants.

We also demonstrated in this thesis that the enzymatic ligation is an effective solution for increasing the multiplex capacities of RPA-based methods, from low to medium-high levels. The reaction is known to present a very high selectivity (*3*), which was verified in this thesis work. It showed a remarkable ability for ligating matched single base polymorphisms, with low signals for mismatched bases. The ligase also maintained activity and selectivity even when working with multiple polymorphisms (six simultaneous probe pairs) or with low amounts of target DNA (10 copies per assay). The reaction occurs rapidly, with a total duration of 25 minutes: 15 min for ligation and 5 min for both thermal aperture and enzyme denaturation steps. By coupling the ligation of multiple probes to isothermal amplification of shared common primers, the method provided the simplicity for performing a multiplex analysis of SNPs.

The LAMP is one of the most studied and widespread techniques for isothermal amplification. This popularity can be related mostly with the very high amplification yields obtained from the reaction (about $10^8$ replicates per template), which allows the indirect detection of the amplicons by diverse methods. This versatility was well exploited in this thesis, since the LAMP products were detected in homogeneous phase, by naked-eye (magnesium pyrophosphate precipitate), colorimetry (HNB magnesium indicator) and fluorescence (DNA intercalant dye); as well as in heterogeneous formats, such as microarrays and electrophoresis. Therefore, the amplification by LAMP has presented a high potential for point-of-care testing solutions, with the capacity for being incorporated in commercial technologies. However, it must be noticed that the unspecific amplification with the absence of DNA templates

was a major problem encountered in our experience. These events can probably be related to the high number of primers employed, which could generate non-specific annealing and amplification. These problems were managed by a careful design of the oligonucleotides and controlling the medium conditions, with the addition of betaine. Therefore, although the LAMP is a very powerful and versatile technique, the adequate control of the reaction parameters is essential for achieving the correct selectivity in SNP-genotyping assays.

The chosen method for analyzing multiple analytes at once was the oligonucleotide probe microarray. As main advantages, this format provided gene-specific or base-specific results, allowing the detection of several SNPs simultaneously. Nevertheless, it is known that this format can be employed for a scale of thousands of simultaneous polymorphisms, with an adequate optimization for avoiding cross hybridization (*4*). Therefore, the multiplex capacity of a microarray-based technology is mostly limited to the previous steps before performing hybridization. We found that the selectivity for correctly detecting the target amplification products was associated mainly to the oligonucleotide design and medium stringency, which was controlled by adjusting the ionic strength and the concentration of a formamide, ssDNA stabilizing agent. The signal calibration with negative and positive control probes was also essential for correcting the intensities while performing multi-sample analysis.

In this thesis, we also exploited antibody-based strategies to recognize products labeled with digoxigenin, which has a simpler manufacturing process than other haptens, such as biotin (*5*), and presented adequate capacities for recognizing immobilized hybridization products. On the other hand, the indirect colorimetric detection of LAMP products using hydroxynaphtol blue

has also shown to be a reliable method for optically detecting amplification products, since the measurements can be carried out directly in the reaction vials, avoiding sample contamination by tube aperture and integrating amplification and detection in a single step. This can be an interesting option for performing real-time colorimetric detection, which was already studied by our group (*6*). Both immunostaining and colorimetric methods provided rapid and versatile solutions for achieving simple and reproducible detection.

Regarding the application of consumer electronics for point-of-care detection, this strategy contributed for reducing the complexity costs related to assay reading. While the cost of a fluorescence microarray scanner can reach up from $40,000 to $100,000 (*7*), the price of a mid-range equipment studied in this thesis is in the scale of the hundreds of dollars. On another hand, although the imaging resolution of smartphone cameras, scanners and disc drives are very high, there are repeatability issues associated to the detection of genotyping assays with these technologies. For this reason, the detection parameters, such as lighting intensity and angle, imaging distance and disc reading conditions, must be carefully controlled, in order to ensure a reproducible assay detection. Among the studied equipment, the smartphone showed to be the most integrated reading platform, as it can perform the imaging, data analysis and result transmission.

In Tables 10 and 11 we summarize and compare the main features and advantages of each genotyping system developed in this thesis. In a general perspective, all methods presented a very high selectivity, which was the main challenge and objective while developing single nucleotide polymorphism discrimination technologies. On another hand, a low equipment requirement was also presented by all systems, allowing their application in low-resource environments. In system 1 we highlight the capacity of RPA to perform allele-

specific amplification, which was superficially studied until now, and the 3D-printed amplification platform, making possible to integrate it with different detection and automation platforms. In system 2, the remarkable feature was its multiplex capacity, by combining ligation and universal RPA, while the potential of this technique for genotyping more SNPs is yet to be explored. We also highlight the assay speed and integration of system 3, which performs the genotype analysis in only 70 minutes, combining amplification and detection. Finally, system 4 presented a reliable strategy for genotyping multiple genes with the aid of consumer electronics, reducing assay costs and complexity.

These performances allow the developed methods to be applied in applications in pharmacogenetics, which were demonstrated by genotyping genes of clinical relevance, related to smoking addiction, major depression disorder and blood-clotting cardiovascular disorders. As these systems are meant to be employed in primary healthcare, the simplicity, speed and assay costs for determining a small group of SNPs are more critical than an extremely high throughput or base-call accuracy, found in NGS and SNP discovery methods. Our methods showed an excellent selectivity in all cases, employing human genomic samples at femtomolar-scale concentrations and using simple genotype-call criteria. Regarding multiplex capacity, although we worked with a maximum of three parallel SNP, the ligation-RPA system could be probably adjusted to discriminate more simultaneous polymorphisms.

**Table 10.** Summary of the developed genotyping biosensors

| **Analytical feature** | **System** | | | |
|---|---|---|---|---|
| | **Allele-specific RPA** | **Allele-specific ligation and universal RPA** | **Allele-specific LAMP** | **Generic LAMP and allele-specific hybridization** |
| Detection | Microarray | Microarray | Colorimetry | Microarray |
| Assay support | PLA chip<br>PC chip | Blu-ray disc | PP vial | PC chip |
| Assay time (min) | 130 | 155 | 70 | 140 |
| Oligonucleotides per SNP | 4 | 8 | 3 | 4 |
| Assay steps | 4 | 5 | 2 | 4 |
| Temperature (°C) | 37 | 54 (L)<br>37 (A) | 65 | 65 |
| Sensitivity (template copies) | 50 | 10 | 100 | 50 |
| RSD (%) | 13 – 17 | 6.0 - 19 | 3.4 – 4.0 | 2.9 – 9.8 |
| Throughput (simultaneous samples) | 36 | 36 | 1 | 36 |
| Multiplex gene capacity | 3 | 3 | 1 | 3 |

PLA: polylactic acid; PC: polycarbonate; PP: polypropylene

L: ligation; A: amplification

**Table 11.** Technological advantages of the developed biosensors for point-of-care application

| **Feature** | **System** | | | |
|---|---|---|---|---|
| | **Allele-specific RPA** | **Allele-specific ligation and universal RPA** | **Allele-specific LAMP** | **Generic LAMP and allele-specific hybridization** |
| Multiplex analysis | ++ | +++ | + | ++ |
| Throughput | ++ | ++ | + | ++ |
| Assay speed | ++ | + | +++ | ++ |
| Assay cost | ++ | + | +++ | ++ |
| Reproducibility | + | ++ | ++ | ++ |
| Sensitivity | ++ | +++ | + | ++ |
| Selectivity | ++ | +++ | ++ | + |
| Portability | ++ | + | +++ | ++ |
| Ease of use | ++ | ++ | +++ | ++ |
| Energy requirement | +++ | + | ++ | ++ |
| Equipment requirement | ++ | ++ | ++ | ++ |
| Integration level | + | + | +++ | ++ |

## REFERENCES

1. A. Tricoli, N. Nasiri, S. De, *Adv. Funct. Mater.* **27**, 1–19 (2017).
2. J. Tu *et al.*, *Adv. Funct. Mater.* **1906713**, 1–30 (2019).
3. A. A. Gibriel, O. Adel, *Mutat. Res. - Rev. Mutat. Res.* **773**, 66-90 (2017).
4. G. C. Kennedy *et al.*, *Nat. Biotechnol.* **21**, 1233–1237 (2003).
5. T. McCreery, *Appl. Biochem. Biotechnol. - Part B Mol. Biotechnol.* **7**, 121-124 (1997).
6. S. Santiago-Felipe *et al.*, *Biosens. Bioelectron.* **79**, 300–306 (2016).
7. S. Yatsushiro *et al.*, *PLoS One*. **5**, e13179 (2010).

# 5 GENERAL CONCLUSIONS

The main challenge for popularizing genetic analysis and pharmacogenetics is to overcome the technical and economic barriers present in DNA analysis and clinical procedures validation. Our main goal was to surpass these obstacles by employing a new generation of DNA biosensing systems for POC detection, including isothermal reactions, integrated platforms and consumer electronics to create precise, rapid and affordable genotyping techniques.

The recombinase polymerase amplification and loop-mediated isothermal amplification showed to be effective alternatives to PCR-based genotyping methods, since they reduce the assay equipment requirements, energy consumption and turnover times. While the RPA presented a simpler primer design, lower temperature and faster amplification, the LAMP presented a higher amplification efficiency and a more versatile detection protocol. On the other hand, although it must be combined with an amplification step, the enzymatic ligation was a suitable solution for selectively discriminating SNPs, while allowing the analysis of multiple analytes simultaneously.

The most critical factors to achieve the adequate selectivity were the assay format, enzyme error rates, primer/probe design, assay temperature and medium stringency, by addition of destabilizing agents, such as formamide and betaine. Regarding the detection conditions, antibody concentration was the predominant factor for selectively staining the correct microarray spots.

Performing the amplification in solution and capturing the products using DNA microarrays combined the efficiency of a homogenous reaction and the multiplex capacities of a heterogeneous one. Concerning the analyte labelling, modified primers presented a higher selectivity, whereas the modified dUTP is more versatile and cheap solution. The immunoenzymatic

staining was very reliable, selective and fast, being an interesting solution for reading microarray assays with colorimetry.

The indirect colorimetric detection, combined with RGB analysis, was suitable for performing the semiquantitative analysis of the discrimination products. As main advantages, this technique showed the simplicity and repeatability, while paired with common and affordable instruments, like camera-based devices.

An important conclusion of this thesis was that consumer electronic devices are very promising tools for detecting DNA assays at a low cost and high flexibility. The disc-drive provided fast reading times and integrated data analysis. Those based on higher energy lasers, such as Blu-ray discs, were capable of reading smaller microarrays, due to the higher resolution capability, showing an increased throughput. On the other hand, CMOS-based devices like the flatbed scanner and smartphone cameras, presented a simpler and more rapid reading times, at the cost of a reduced reproducibility. This issue can be attenuated by controlling the detection conditions, such as capture distance, illumination intensity and angle, as well as employing calibration steps with controls. When compared with CCD cameras, CMOS-based cameras present a lower sensitivity and higher noise levels. However, this is compensated by higher capture speed and digital output, making it compatible with daily-use devices. Moreover, while in the developed methods the signal intensity was amplified by enzymatic reactions, sensitivity was not considered a main issue. We also conclude that among the studied consumer electronic devices, smartphones have the greatest potential for POC analytical applications, since they integrate assay reading, processing, data analysis and transmission in a single equipment.

Regarding the application to pharmacogenetics, our aim was to evaluate the developed systems for performing genotyping assays associated with significant relevant polymorphisms of pharmacogenetic application. Our methods showed a high degree of selectivity, being capable of discriminating SNPs in human DNA samples, in reduced times and with much lower technical requirements than the commercially available genotyping technologies, which employ PCR and expensive fluorescence scanners to perform the assay.

This thesis has also opened a background for future improvements in DNA biosensing, isothermal amplification, SNP detection and POC detection. Using the methods developed in this work as a basis, higher multiplex and throughput capacities could be achieved, by performing multiple primers and probe optimization studies, as well as clinical studies to provide the pharmacogenomic association background. Among the developed systems, the allele-specific ligation combined with universal RPA shows the highest potential for multiplex assays. Also, the integration level of DNA analysis can be improved in the developed systems, by combining two or more steps, such as ligation and amplification or amplification and hybridization. Much more can be made to improve the assay platforms as well, by employing microfabricated structures and other 3D-printed supports to carry out the assays, enhancing the integration, miniaturization and reproducibility. Thus, although much effort must be made to convert them into commercial technologies, the developed systems represent a viable solution to the current genotyping PCR-based or very-high-throughput technologies available at the present time.

In summary, the results obtained in this work contribute for the creation of more practical, simple and affordable DNA POC genotyping tools

to support pharmacogenetics. This opens another path for spreading these procedures to a more democratized level, by performing genetic analysis tests in an affordable and practical way, extending the use of these technologies for daily routine clinical practices. Nevertheless, the knowledge generated in this research could be also applied in other branches of personalized medicine, for instance, in the prediction of genetic risks, diagnosis and prognosis, which still do not show an expressive level of use in the standard healthcare procedures; as well as for other DNA biosensing demands, such as in environmental and industrial applications.

# 6 ANNEXES

In this final section we present information that is complementary to the support the discussions carried out in this thesis. Annex 1 presents the publications generated from the results of this research work, along with the contributions of the author to each one of these articles. Moreover, we list the communications in conferences made during the research period.

Annex 2 has the supplementary material from Chapter 1, while Annexes 3 and 4 contain the supplementary information from Chapters 3 and 4, respectively.

## 6.1 Annex 1

## RESULT DISSEMINATION

**PUBLICATIONS**

Yamanaka, Eric Seiti; Tortajada-Genaro, Luis Antonio; Maquieira, Ángel. Low-cost genotyping method based on allele-specific recombinase polymerase amplification and colorimetric microarray detection. **Microchimica Acta**, v. 184, n. 5, p. 1453-1462. (Thesis chapter 1)

Personal contribution:

- Evaluation of the 3D-printed and polycarbonate chip platforms;
- Condition selection for RPA, hybridization and detection
- Analytical performance evaluation
- Sample collection and extraction
- Genomic DNA sample analysis
- Manuscript writing

Yamanaka, Eric Seiti; Maquieira, Ángel; Tortajada-Genaro, Luis Antonio. Triplex allele discrimination by ligation, universal recombinase polymerase amplification and optical array detection. (in writing phase) (Thesis chapter 2)

Personal contribution:

- Oligonucleotide evaluation for ligation and amplification
- Labelling and detection condition selection
- Ligation and universal RPA set-up
- Analytical performance evaluation

- Manuscript writing

Yamanaka, Eric Seiti; Tortajada-Genaro, Luis Antonio; Pastor, Nuria; Maquieira, Ángel. Polymorphism genotyping based on loop-mediated isothermal amplification and smartphone detection. **Biosensors and Bioelectronics**, 2018, v. 109, p. 177-183. (Thesis chapter 3)

Personal contribution:

- LAMP condition selection and set-up
- Selectivity optimization and evaluation
- Smartphone detection set-up and evaluation
- Genomic DNA sample analysis
- Manuscript writing

Tortajada-Genaro, Luis Antonio; Yamanaka, Eric Seiti; Maquieira, Ángel. Consumer electronic devices for DNA genotyping based on loop-mediated isothermal amplification and array hybridisation. **Talanta**, 2019, v. 198, p. 424-431. (Thesis chapter 4).

Personal contribution:

- Genotyping assay development
- Evaluation of smartphone capturing distance and illumination
- Data analysis evaluation
- Method comparison and patient analysis

## COMMUNICATIONS IN CONFERENCES

Yamanaka, Eric Seiti; Tortajada-Genaro, Luis Antonio; Maquieira, Ángel. Sistema de análisis farmacogenético direccionado al tratamiento personalizado de la adicción al tabaco. II Encuentro de Estudiantes de Doctorado de la UPV. 2015, June 25, Universitat Politècnica de València, Valencia, Spain.

Yamanaka, Eric Seiti; Tortajada-Genaro, Luis Antonio; Puchades, Rosa.; Maquieira, Ángel. SNP genotyping method base on solid-phase recombinase polymerase amplification. IX International Workshop on Sensors and Molecular Recognition. 2015, July 6-7, Universitat Politècnica de València, Valencia, Spain.

Tortajada Genaro, Luis Antonio; Yamanaka, Eric Seiti; Puchades, Rosa; Maquieira, Ángel. Solid-phase amplification on optical disks for genotyping of polymorphisms applied to pharmacogenomics. XIII Europtrode – Conference on Optical Chemical Sensors and Biosensors. 2016, March 20-23, Graz, Austria, p. 273.

Yamanaka, Eric Seiti; Tortajada Genaro, Luis Antonio; Puchades, Rosa.; Maquieira, Ángel. Evaluation of loop-mediated isothermal amplification as a tool for point-of-care diagnostics in the pharmacogenetic field. X International Workshop on Sensors and Molecular Recognition. 2016, July 7-8, Universitat de València, Valencia, Spain. ISBN: 978-84-617-5330-7, p. 270-273.

Yamanaka, Eric Seiti; Tortajada-Genaro, Luis Antonio; Maquieira, Ángel. Biosensores de ADN para aplicación en el tratamiento personalizado con

antidepresivos. IV Encuentro de Estudiantes de Doctorado de la UPV. 2017, June 1, Universitat Politècnica de València, Valencia, Spain.

Tortajada Genaro, Luis Antonio; Yamanaka, Eric Seiti; Martorell Tejedor, Sara; Lázaro Zaragoza, Ana; Puchades, Rosa; Maquieira, Ángel. Estabilidad de ácidos nucleicos: análisis termodinámico para el bio-reconocimiento de mutaciones y polimorfismos. XXXVI Reunión Bienal de la Real Sociedad Española de Química. 2017, June 25-29, Sitges, Spain.

Sanchón-Sánchez, Paula; Yamanaka, Eric Seiti; Tortajada-Genaro, Luis Antonio; Maquieira, Ángel. Detección de polimorfismos de un único nucleótido como herramienta farmacogenética para la administración de anticoagulantes orales. XI International Workshop on Sensors and Molecular Recognition. 2017, July 6-7, Universitat Politècnica de València, Valencia, Spain. ISBN: 978-84-697-5069-8, p. 262-266.

Yamanaka, Eric Seiti; Tortajada-Genaro, Luis Antonio; Puchades, Rosa.; Maquieira, Ángel. Smartphones as sensing elements in point-of-care DNA genotyping assays. XI International Workshop on Sensors and Molecular Recognition. 2017, July 6-7, Universitat Politècnica de València, Valencia, Spain. ISBN: 978-84-697-5069-8, p. 284-287.

Yamanaka, Eric Seiti; Tortajada-Genaro, Luis Antonio; Puchades, Rosa; Maquieira, Ángel. Dispositivos electrónicos como elementos de detección en ensayos genómicos de interés clínico. XXI Reunión de la Sociedad Española de Química Analítica. 2017, September 5-7, Valencia, Spain.

Tortajada-Genaro, Luis Antonio; Yamanaka, Eric Seiti; Morais, Sergi; Maquieira, Ángel. Compact disc reactors for the monitoring of isothermal amplification applied to polymorphism genotyping. XXVIII World Congress on Biosensors. 2018, June 12-15, Miami, United States.

Lázaro-Zaragoza, Ana; Yamanaka, Eric Seiti; Tortajada-Genaro, Luis Antonio; Maquieira, Ángel. Blu-ray technology for classifying patients with cardiovascular diseases. XII International Workshop on Sensors and Molecular Recognition. 2018, July 5, Universitat de València, València, Spain. ISBN 978-84-09-05881-5.

## 6.2 Annex 2

# Electronic Supplementary Material

### Low-cost genotyping method based on allele-specific recombinase polymerase amplification and colorimetric microarray detection

Eric Seiti Yamanaka, Luis A. Tortajada-Genaro, Ángel Maquieira

**Target SNPs**

Several clinical studies have related SNPs to the drug effect in smoking cessation and the highly addictive properties of nicotine (*1–4*). in particular, research efforts have focused on the genes involved in neurotransmitter pathways for the brain reward system and on those genes that alter nicotine metabolism. As proof of concept, this study was applied to the simultaneous genotyping of rs4680, rs1799971, rs1800497 and rs16969968 (Table S1). Nevertheless, these polymorphisms are involved in the pharmacogenomics of other diseases and drug effects. Tables S2 and S3 summarize the information collected in the PharmGKB database (*5*).

**Table S1**: Description of the studied polymorphisms

| | rs4680 | rs1799971 | rs1800497 | rs16969968 |
|---|---|---|---|---|
| Genes | *COMT* | *OPRM1* | *ANKK1,DRD2* | *CHRNA3,CHRNA5* |
| Primary Locus | chr22:19951271 | chr6:154360797 | chr11:113270828 | chr15:78882925 |
| Allele change | G > A | A > G | G > A | G > A |
| Amino acid change | p.V158M | p.N40D | p.E713K | p.D398N |
| Protein | catechol-O-methyltransferase | opioid receptor, mu 1 | ankyrin repeat and kinase domain containing 1 dopamine D2 receptor DRD2 gene | cholinergic receptor, nicotinic, alpha 3/5 |

Table S4 lists the oligonucleotides used for the amplification and hybridization assays, including targeted genes and controls. In order to monitor the DNA extraction and amplification processes, the *ACTB* gene was selected as the human endogenous gene. Then a conventional RPA reaction was run and the product was mixed with AS-RPA products prior to incubation on the chip. To check the hybridization steps, two controls were included. A double labelled oligonucleotide (5′-biotin and 5′-digoxigenin) was spotted on chip as the positive control of the immobilization process. Single-strand DNA (5′-digoxigenin-labelled oligonucleotide complementary to a control probe) was used as the positive hybridization control.

**Table S2**: Diseases related with the studied polymorphisms. Data from the PharmGKB database

| | rs4680 | rs1799971 | rs1800497 | rs1696996 | | rs4680 | rs1799971 | rs1800497 | rs1696996 |
|---|---|---|---|---|---|---|---|---|---|
| Alcoholism | | x | x | x | Hyperprolactinemia | x | | x | |
| Anxiety Disorders | x | x | x | | Kidney Transplantation | x | | | |
| Attention Deficit Disorder with Hyperactivity | x | | | | Narcolepsy | x | | | |
| Autism Spectrum Disorder | x | | | | Nausea | | x | | |
| Bipolar Disorder | x | | x | | Neonatal Abstinence Syndrome | x | x | | |
| Breast Neoplasms | x | | | | Neoplasms | x | x | | |
| Cessation | x | | x | x | Neuropathic pain | | x | | |
| Cocaine-Related Disorders | | | x | | Neurotoxicity Syndromes | | | x | |
| Constipation | | x | | | Obsessive-Compulsive Disorder | x | | | |
| Depression | | | x | | Opioid-Related Disorders | x | x | x | |
| Depressive Disorder | x | | | | Pain | x | | | x |
| Depressive Disorder, Major | x | x | | | Panic Disorder | x | | | |
| Diastolic blood pressure | x | | | | Parkinson Disease | x | | | |
| Drug Toxicity | | | x | | Schizophrenia | x | | x | x |
| Dry mouth | | x | | | Substance Withdrawal Syndrome | x | | | |
| Epilepsy | | | x | | Substance-Related Disorders | x | | | x |
| Gastrointestinal toxicity | | | x | | Systolic blood pressure | x | | | |
| Headache | | | x | | Tardive dyskinesia | x | | x | |
| Headache Disorders | x | x | | | **Tobacco Use Disorder** | **x** | **x** | **x** | **x** |
| Heroin Dependence | | x | x | | Weight gain | | | x | |

**Table S3**: Drug effects related with the studied polymorphisms. Data from the PharmGKB database

| | rs4680 | rs1799971 | rs1800497 | rs16969968 | | rs4680 | rs1799971 | rs1800497 | rs16969968 |
|---|---|---|---|---|---|---|---|---|---|
| Acetaminophen | | x | | | Lithium | x | | x | |
| Alfentanil | | x | | | Methadone | x | x | x | |
| Amisulpride | | | x | | Methylphenidate | x | | | |
| Analgesics | x | x | | | Modafinil | x | | | |
| Antidepressants | x | | | | Morphine | x | x | | |
| Antiinflammatory agents, non-steroids | x | x | | | Naloxone | | x | | |
| Antipsychotics | x | | x | | Naltrexone | | x | | |
| Aripiprazole | | | x | | Nemonapride | | | x | |
| Benztropine | x | | | | **Nicotine** | x | x | x | x |
| Bupropion | | | x | | Olanzapine | x | | | |
| Clomipramine | x | | | | Olanzapine | | | x | |
| Clozapine | x | | x | | Opioids | x | x | | |
| Codeine | | x | | | Opioids | | | | |
| Cotinine | | | | x | Opium alkaloids and derivatives | | | | x |
| Disulfiram | | | x | | Oxycodone | x | x | | |
| **Drugs used in nicotine dependence** | x | x | x | x | Paroxetine | x | | | |
| Drugs used in opioid dependence | | x | | | Quetiapine | x | | x | |
| Entacapone | x | | | | Risperidone | x | | x | |
| Ergot alkaloids | x | x | | | Sertraline | x | | | |
| Ethanol | | x | x | x | Sumatriptan | x | x | | |
| Fentanyl | | x | | | Tacrolimus | x | | | |
| Fluoxetine | x | | | | Tolcapone | x | | | |
| Fluvoxamine | x | | | | Tramadol | x | x | | |
| Glucose | x | | | | Trihexyphenidyl | x | | | |
| Haloperidol | x | | x | | Valproic acid | x | | x | |
| Heroin | x | x | x | | Varenicline | | | | x |
| Hydrocodone | | x | | | Venlafaxine | x | x | x | |

**Table S4**: List of oligonucleotides. WT-FP: wild-type forward primer, M-FP: mutant forward primer. RP: reverse primer, Ci: immobilization controls, Ch: hybridization control.

| Gene | Use | Sequence 5'-3' | Length | %GC | Tm | Product |
|---|---|---|---|---|---|---|
| *COMT* rs4680 | WT-FP | ATGGTGGATTTCGCTGGCG | 19 | 58 | 59,5 | 69 bp |
| | M-FP | ATGGTGGATTTCGCTGGCA | 19 | 53 | 57,5 | |
| | RP | Dig-CCCTTTTTCCAGGTCTGACA | 20 | 50 | 58,4 | |
| | Pr | Bt-Tg-T10-ACAAGGTGTGCATGCCTGACCCGTT | 25 | 56 | 69,1 | |
| *OPRM1* rs1799971 | WT-FP | CTTGTCCCACTTAGATGGCA | 20 | 50 | 58,4 | 175 bp |
| | M-FP | CTTGTCCCACTTAGATGGCG | 20 | 55 | 60,5 | |
| | RP | Dig-GACCAGGAAGTTTCCGAAGA | 20 | 50 | 58,4 | |
| | Pr | Bt-Tg-T10-GCAGTCCCTCCATGATCACGGCCATCA | 27 | 59 | 72,7 | |
| *ANKK1* rs1800497 | WT-FP | CATCCTCAAAGTGCTGGTCG | 20 | 55 | 60,5 | 125 bp |
| | M-FP | CATCCTCAAAGTGCTGGTCA | 20 | 50 | 58,4 | |
| | RP | Dig-CCTTGCCCTCTAGGAAGGAC | 20 | 60 | 62,5 | |
| | Pr | Bt-Tg-T10-TGGAGTGAGCTGCACACCCCTGCAACTG | 28 | 61 | 74,6 | |
| *CHRNA5* rs16969968 | WT-FP | ACATTGGAAGCTGCGCTCG | 19 | 58 | 59,5 | 110 bp |
| | M-FP | ACATTGGAAGCTGCGCTCA | 19 | 53 | 57,5 | |
| | RP | Dig-TGGAAGAAGATCTGCATTTGT | 21 | 38 | 55,4 | |
| | Pr | Bt-Tg-T10-GAAGGAAAATGATGTCCGTGAGGTCTG | 27 | 48 | 68,2 | |
| *ACTB* Endogenous gene | FP | AATCTGGCACCACACCTTCTAC | 22 | 50 | 62,1 | 170 bp |
| | RP | Dig-ATAGCACAGCCTGGATAGCAAC | 22 | 50 | 62,1 | |
| | Pr | Bt-Tg-T10-CAACCGCGAGAAGATGACCCAGATCA | 26 | 54 | 69,5 | |
| Array controls | Ci+ | Dig-GTCATGGGCCTCGTGTCGGAAAACC-Tg-Bt | 25 | 60 | 70,7 | |
| | Ch+ | Bt-Tg-T10-GAACCTTTCGCTTCACCGGCCGATC | 25 | 60 | 70,7 | |
| | Ch+ | Dig-TATCTCTTCCCTGTTTGGATCGGCCGGTGAAGCGAAAGGTTC | 42 | 52 | 80,7 | |

Bt-Tg: Biotin with a triethylene glycol spacer; T10: Thymine tail (10 nucleotides); Dig: digoxigenin.

**Effect of the PLA printing conditions**

The prototypes were fabricated with different layer thicknesses (up to 0.2 mm). Subsequently, the printed structures were cleaned in a 30-minute ultrasonic bath and dried with compressed air. The fabrication quality of the PLA-chips was monitored by optical microscopy imaging. Surface pictures were captured (1.2x magnification) using an Olympus SZ61 stereo microscope (Olympus Co., Japan). Images were analyzed with the Image J software by providing an estimated roughness per sample (Figure S1).

The contact angle data of the deionized water droplets were registered using a Dino-Lite Digital Microscope (AnMo Electronics Co., Taiwan) at the 1.3-megapixel resolution (Figure S2).

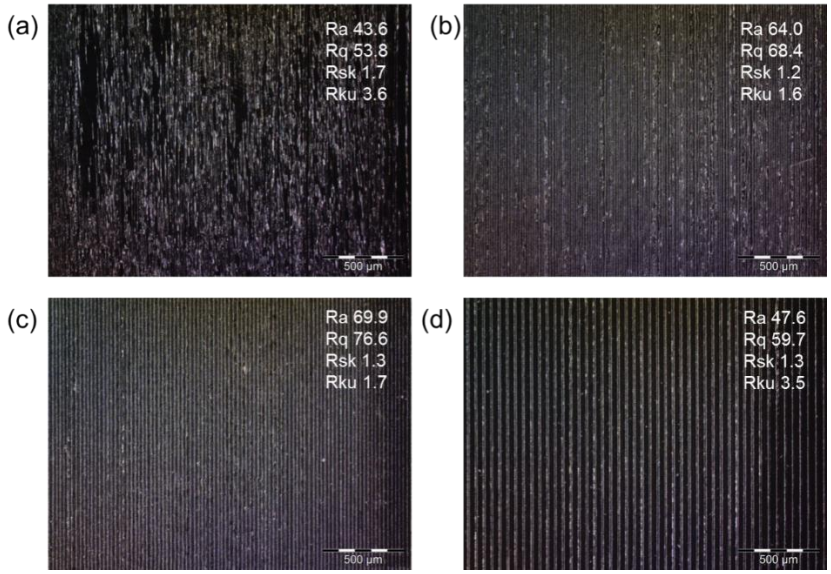


**Figure S1**: Microscopy images from the PLA chip walls with variable layer heights. a) 0.02 mmb) 0.06 mm c) 0.1 mm d) 0.2 mm. Parameters of the assessed profile (units: µm) according to international standards (ISO 4288): Ra, arithmetic mean deviation; Rq, root square deviation; RSk, skewness; Rku, kurtosis.

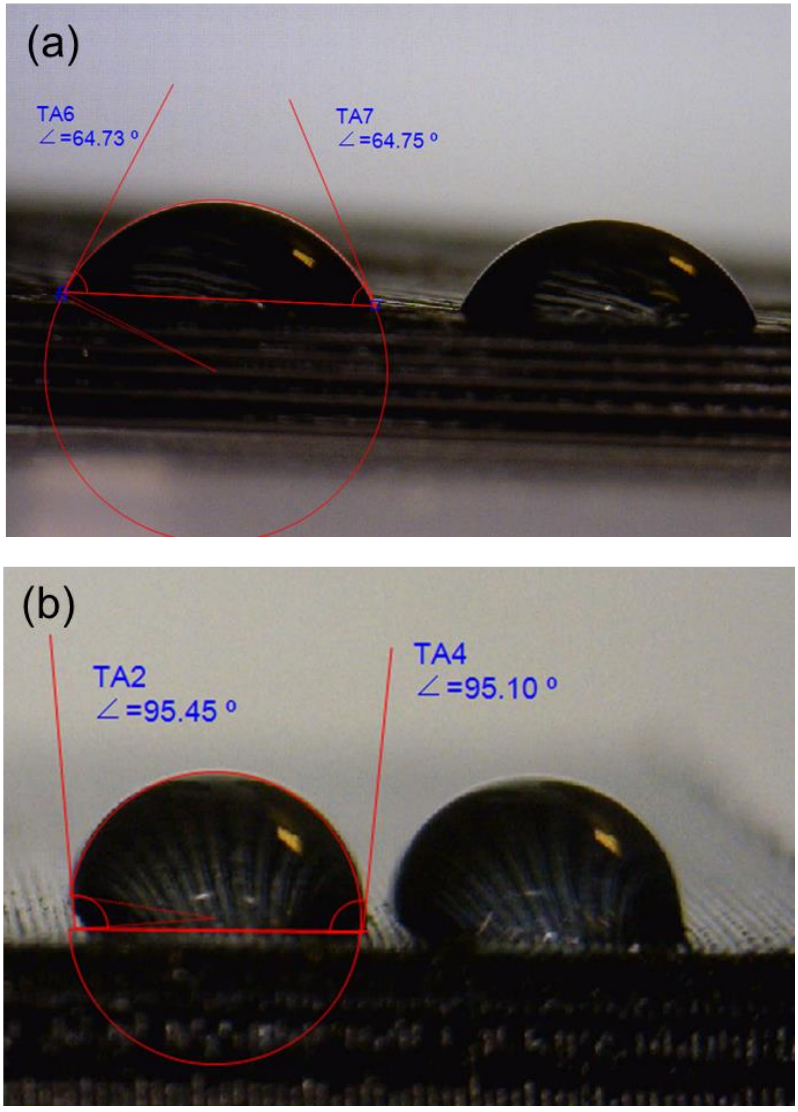


**Figure S2**: Contact angle measurement images for PLA-chip: (a) bottom surface and (b) wall surface

**Patient's genotypes**

A representative example of the hybridization chip images captured by a documental scanner is shown in Figure S3. The qualitative analysis indicates that the patient is heterozygote for rs4680 and rs 1799971, with the wild-type homozygote for rs1800497 and 5. rs16969968.

Table S5 lists the discrimination factors of the AS-RPA method for the samples of validation set. These values were calculated from the mean spot signal of the wild-type (WT) and mutant (MUT) variants according to the equation (WT − MUT)/(WT + MUT). The heterozygous genotypes produced an intermediate discrimination factor (between -0.3 and +0.3), whereas the homozygous ones led to discrimination factors above 0.3 (wild-type) and under -0.3 (mutant), respectively. The table also reports the genotype assignments obtained by the reference method.

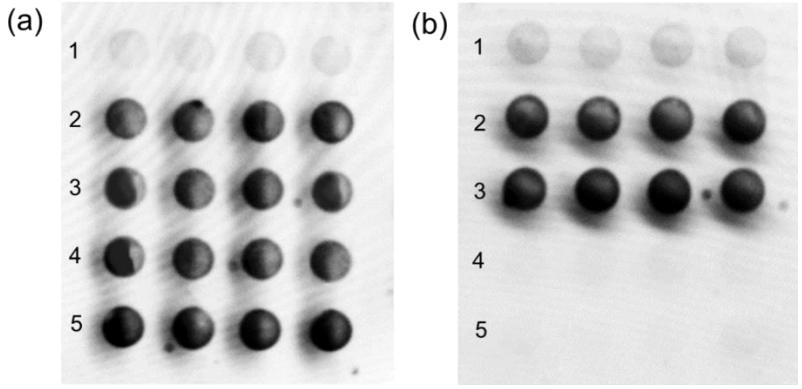


**Figure S3**: Arrays generated by the hybridization of the wild-type (a) and mutant (b) mixtures of four allele-specific RPA products. Probes: 1. Positive control, 2. rs4680, 3. rs1799971, 4. rs1800497, 5. rs16969968.

**Table S5**: Genotyping results obtained by both the AS-RPA and the reference methods (three replicates per patient).

| | AS-RPA | | | | | | | | Reference method | | | |
|---|---|---|---|---|---|---|---|---|---|---|---|---|
| | Discrimination factor | | | | Assignments | | | | Assignments | | | |
| | rs4680 | rs1799971 | rs1800497 | rs16969968 | rs4680 | rs1799971 | rs1800497 | rs16969968 | rs4680 | rs1799971 | rs1800497 | rs16969968 |
| Patient | *COMT* | *OPRM1* | *ANKK1* | *CHRNA5* | *COMT* | *OPRM1* | *ANKK1* | *CHRNA5* | *COMT* | *OPRM1* | *ANKK1* | *CHRNA5* |
| 1 | 0.03 | 0.82 | -0.10 | 0.55 | AG | AA | AG | GG | AG | AA | AG | GG |
| 2 | -0.58 | 0.42 | 0.42 | 0.81 | AA | AA | GG | GG | AA | AA | GG | GG |
| 3 | -0.23 | 0.05 | 0.73 | 0.59 | AG | AG | GG | GG | AG | AG | GG | GG |
| 4 | -0.16 | 0.07 | -0.03 | -0.01 | AG | GG | AG | AG | AG | GG | AG | AG |
| 5 | -0.03 | 0.04 | 0.71 | 0.60 | AG | AG | GG | GG | AG | AG | GG | GG |
| 6 | -0.04 | 0.23 | 0.59 | -0.63 | AG | AG | GG | AA | AG | AG | GG | AA |
| 7 | 0.64 | 0.72 | 0.91 | 0.00 | GG | AA | GG | AG | GG | AA | GG | AG |
| 8 | 0.86 | -0.37 | 0.86 | 0.10 | GG | AG | GG | AG | GG | AG | GG | AG |
| 9 | -0.31 | 0.09 | 0.02 | 0.54 | AG | AG | AG | GG | AG | AG | AG | GG |
| 10 | -0.55 | 0.79 | 0.90 | -0.69 | AA | AA | GG | GG | AA | AA | GG | GG |
| 11 | 0.54 | 0.30 | -0.04 | -0.02 | GG | AA | AG | AG | GG | AA | AG | AG |
| 12 | 0.72 | 0.81 | 0.92 | 0.34 | GG | AA | GG | GG | GG | AA | GG | GG |
| 13 | -0.87 | 0.50 | 0.15 | 0.16 | AG | AA | AG | AG | AG | AA | AG | AG |
| 14 | -0.30 | 0.06 | -0.04 | 0.55 | AG | AG | AG | GG | AG | AG | AG | GG |
| 15 | -0.14 | -0.83 | 0.16 | -0.34 | AG | GG | AG | AA | AG | GG | AG | AA |
| 16 | 0.34 | 0.60 | 0.93 | 0.76 | GG | AA | GG | GG | GG | AA | GG | GG |
| 17 | 0.45 | 0.00 | 0.93 | 0.51 | AG | AG | GG | GG | AG | AG | GG | GG |

## References

1. L. J. Bierut *et al.*, *Hum. Mol. Genet.* **16**, 24–35 (2007).
2. M. K. Ho, R. F. Tyndale, *Pharmacogenomics J.* **7**, 81–98 (2007).
3. M. J. Carpenter *et al.*, *Drugs*. **73**, 407-426 (2013).
4. M. Mamoun *et al.*, *CNS Drugs*. **29**, 359-369 (2015).
5. C. F. Thorn, T. E. Klein, R. B. Altman, *Methods Mol. Biol.* **1015**, 311–320 (2013).

## 6.3 Annex 3

## SUPPLEMENTARY INFORMATION

# Polymorphism genotyping based on loop-mediated isothermal amplification and smartphone detection

Eric Seiti Yamanaka, Luis A. Tortajada-Genaro, Nuria Pastor, Ángel Maquieira

### DESCRIPTION OF LAMP FORMATS

**LAMP.** In a typical LAMP reaction, four primers are designed to recognize 6 different regions of a target sequence and a polymerase with high strand displacement activity (Bst polymerase) is employed for amplification (*1*). The forward and backward outer primers (F3 and B3) initiate strand displacement DNA synthesis (copy of the original target sequence). The annealing and extension of the forward and backward inner primers (FIP and BIP) generate specific sequences in which the central and external regions are self-complementary, producing stem-loop structures after strand displacement by the outer primers. The formed stem-loop can act as a self-primered structure that generates a second concatenated copy of itself after extension. Additionally, the inner primers can also extend by targeting the 5' of the loop, creating another single copy of the original structure. This process occurs exponentially, producing amplicons with different lengths, varying with the number of repetitions of the original sequence.

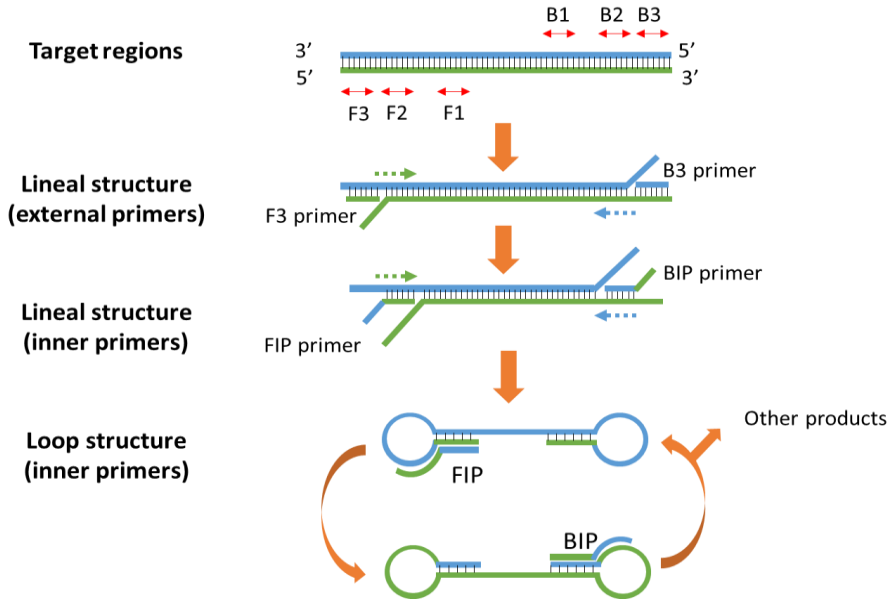


**Figure S6.** General scheme of LAMP reaction

**LAMP-ASO**. The technique is based on the combination of this isothermal DNA amplification and allele selective hybridization in a solid-phase format. The primers (FIP and BIP) are designed with the objective of positioning the target polymorphism in the loop of the LAMP product. Later, a selective hybridization is achieved using allele-specific probes (single-base mismatch) immobilized on a chip. Therefore, a heterozygous patient leads to positive hybridization for both probes: wild-type (WT) and mutant (MUT). A homozygous patient yields positive hybridization only for the corresponding probe (perfect match).

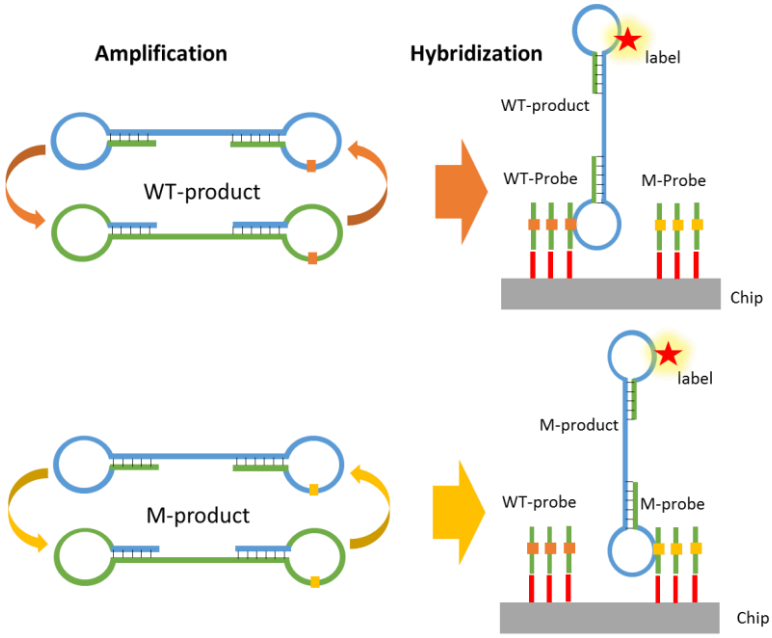


**Figure S7.** Scheme of LAMP-ASO method. SNP position is indicated for wild-type variant (orange) and mutant (yellow).

**AS-LAMP-3'**. An allele-specific LAMP is induced by adding an allele-specific primer to each reaction mixture. In this case, the SNP is located at the 3' end of the forward inner primer (FIP), with an additional mismatched nucleotide at the penultimate position. Therefore, the stem-loop structure formation is highly dependent on the perfect alignment of the primer 3' end, meaning that amplification should not occur in the absence of the target SNP.

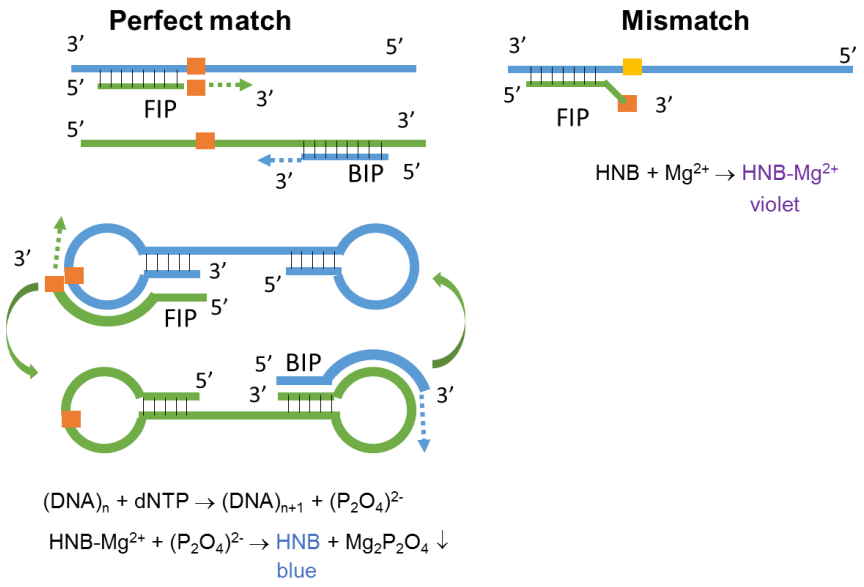


**Figure S8.** Scheme of AS-LAMP-3'method. SNP position is indicated for wild-type variant (orange) and mutant (yellow).

**AS-LAMP-5'**. In this case, the SNP is located between the F1 and B1c regions of the loop sequence. Both FIP and BIP primers are design with complementary nucleotides at their 5' ends, with a mismatched penultimate nucleotide at the BIP. After primer alignment and strand displacing by the Bst polymerase, the resulting stem-loop product would have two possible structures: one with matched bases at the central SNP and 5' and 3' ends, and another with mismatched nucleotides between these regions. DNA synthesis from the dumbbell-like starting structure depends on the complementarity of primer. Thus, the presence of the target SNP would form a matched product, triggering its self-priming ability and allowing the exponential amplification. On the other hand, the presence of a non-complementary sequence would form an open loop, preventing its self-extension.

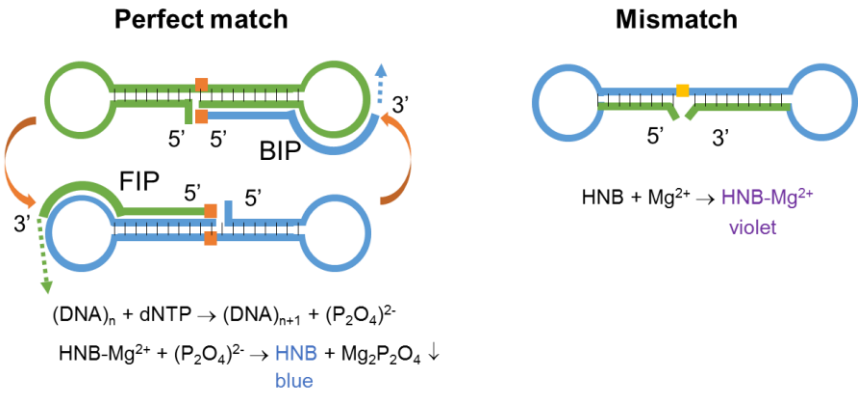


**Figure S9.** Scheme of AS-LAMP-5'method

## PRIMER DESIGN

The target polymorphism is rs1954787 located in GRIK4 gene (Assembly: GRCh38.p7 Primary Locus: chr11: 120792654) that codifies the glutamate receptor, ionotropic, kainate 4. The allele change is T (wild-type) to C (mutant).

According to the PharmGKB database (https://www.pharmgkb.org), diseases associated to the studied polymorphism are depression, depressive disorder and major depressive disorder. Drugs related to *GRIK4* gene are carbamazepine, citalopram, fluoxetine, fluvoxamine, among others (*2*, *3*).

Following the design strategies described in the previous sections, a different set of primers was selected for each of the three studied methods. A LAMP reaction requires several restrictions as it is described in the first paper about this isothermal reaction (*2*). They include melting temperature, length of primers and distances between them. For genotyping approaches, additional restrictions were considered. According to our strategy for LAMP-ASO method, the stem-loop product was designed to have the SNP at its loop region and the probes contained the polymorphism at their center position.

The design of allele-specific amplifications was more complex because there were fewer candidate oligonucleotides than for the ASO-approach (*4*). In 3' AS-LAMP, two forward inner primers with the SNP at their 3' end were selected. In 5' AS-LAMP, both forward and reversed inner primers were complementary to the polymorphism SNPs at their 5' ends. An additional deliberate mismatch at the penultimate base of AS primers to increase the reaction specificity (*5*–*7*). Based on the results of a thermodynamic study, this nucleotide substitution was selected for introducing the strongest destabilizing effect.

Table S6 lists the oligonucleotides used for the amplification and hybridization assays, including targeted genes and controls. A double labelled oligonucleotide (5'-biotin-Tg-T10TTGTCATGGGCCTCGTGTCGGAAAACC-digoxigenin-3') was spotted on chip as the positive control. The negative control probe sequence was 5'-biotin-Tg-T10CAACCGCGAGAAG ATGACCCAGATCA-3'. The table also includes the oligonucleotides used in the reference methods (ASA-PCR and Sanger sequencing). Table S7 shows the specific products obtained depending on the discrimination method.

**Table S6**: List of oligonucleotides for wild-type (WT) and mutant (M) discrimination. FP: forward primer, RP: reverse primer.

| Method | Function | Sequence (5'-3') |
|---|---|---|
| LAMP-ASO | FIP | CATCGTGCCTTCACCCAAT-GAGGAAGTACAACCAAAAGCA |
| | BIP | GTAGCTGGTGCTGCTATTAAC-AACCCACCTCTTCCCTCCTA |
| | F3 | AAGAAGTGGACTGGTTTGAGAA |
| | B3 | GCAGAGCATCTCAAATTTAGG |
| | WT-Probe | [BtnTg]-T10-AGACTGGTTATTGGAAGGTGCGG |
| | M-Probe | [BtnTg]-T10-AGACTGGTTATCGGAAGGTGCGG |
| AS-LAMP-3' | WT-FIP1 | CATCGTGCCTTCACCCAAT-AGCAATTGGAGACTGGTTAGT |
| | M-FIP1 | CATCGTGCCTTCACCCAAT-AGCAATTGGAGACTGGTTAGC |
| | BIP | GTAGCTGGTGCTGCTATTAAC-AACCCACCTCTTCCCTCCTA |
| | F3 | AAGAAGTGGACTGGTTTGAGAA |
| | B3 | GCAGAGCATCTCAAATTTAGG |
| | Probe | [BtnTg]-T10-GATTCTTCCTGTTAACATTCCTACG |
| AS-LAMP-5' | WT-FIP2 | AATAACCAGTCTCCAATTG-ATTTTGAGGAAGTACAACC |
| | M-FIP2 | GATAACCAGTCTCCAATTG-ATTTTGAGGAAGTACAACC |
| | WT-BIP | TAGAAGGTGCGGAATTGGG-AGTTAATAGCAGCACCAGCT |
| | M-BIP | CAGAAGGTGCGGAATTGGG-AGTTAATAGCAGCACCAGCT |
| | F3 | AAGAAGTGGACTGGTTTGAGAA |
| | B3 | GCAGAGCATCTCAAATTTAGG |
| AS-PCR | WT-FP | AAGCAATTGGAGACTGGTTATT |
| | M-FP | AAGCAATTGGAGACTGGTTATC |
| | RP | AACCCACCTCTTCCCTCCTA |
| | Probe | [BtnTg]-T10-GATTCTTCCTGTTAACATTCCTACG |
| Sequencing | FP | AAGAAGTGGACTGGTTTGAGAA |
| | RP | GCAGAGCATCTCAAATTTAGG |
| | Marker | GCAGAGCATCTCAAATTTAGG |

Red color: SNP position; blue color: additional mismatch
[Btn-Tg]: Biotin with a triethylene glycol spacer; T10: Thymine tail (10 nucleotides); [Dig]: digoxigenin

**Table S7**. Sense strand sequence of the LAMP product structures. Polymorphisms are indicated in IUPAC code (Y= C or T and R = A or G). Red color: SNP position; blue color: additional mismatch.

| | |
|---|---|
| **LAMP-ASO** | CATCGTGCCTTCACCCAATGAGGAAGTACAACCAAAAGCAATTGGAGAC TGGTTATYGG AAGGTGCGGAATTGGGTGAAGGCACGATGCCTGGGTAGCTGGTGCTGCT ATTAACTAAA CGTAGGAATGTTAACAGGAAGAATCTAGGAGGGAAGAGGTGGGTTGTTA ATAGCAGCA CCAGCTAC (184 nt) |
| **3' AS-LAMP** | CATCGTGCCTTCACCCAATAGCAATTGGAGACTGGTTATYGGAAGGTGCG GAATTGGGT GAAGGCACGATGCCTGGGTAGCTGGTGCTGCTATTAACTAAACGTAGGA ATGTTAACAG GAAGAATCTAGGAGGGAAGAGGTGGGTTGTTAATAGCAGCACCAGCTAC (167 nt) |
| **5' AS-LAMP** | RATAACCAGTCTCCAATTGATTTTGAGGAAGTACAACCAAAAGCAATTG GAGACTGGTT ATYGGAAGGTGCGGAATTGGGTGAAGGCACGATGCCTGGGTAGCTGGTG CTGCTATTAA CTCCCAATTCCGCACCTTCTR (139 nt) |

## LAMP-ASO METHOD. COMPLEMENTARY EXPERIMENTS

In the real-time experiments, assays were carried out in a 7500 Real-time PCR System (Applied Biosystems, USA) using 2x SYBR Safe as the reporter dye (502 nm/530 nm) and ROX as the reference dye (575 nm/602 nm). Fluorescence measures were taken at 2-minute intervals during a total time of 90 min and at a constant temperature of 62ºC. The results were expressed in ΔRn terms, calculated as the reporter signal normalized with the reference signal and corrected with the baseline.

Amplification conditions were also studied by end-point fluorescence, varying the reagents concentrations (primers, enzyme, nucleotides and buffer ions) and incubation temperature. Figure S10 shows the signals registered in each case. The selected conditions were 0.2 µM outer primers, 1.2 µM inner primers, 8 mM $MgSO_4$, 1.2 mM dNTPs, 4 Bst polymerase units (0.32 U/µL) and incubation temperature of 62 °C.

False-positives were frequently observed in the absence of DNA template, when the conditions were not adequately selective. In order to verify the correct formation of the designed stem-loop structures, a subsequent nested-like PCR was carried out using diluted LAMP products as template. For that, false-positive, negative and positive amplification products were diluted (dilution factor of $10^6$ to $10^8$) and added to a PCR mixture containing a forward (5'-GAGGAAGTACAACCAAAAGCA-3') and reverse primer (5'AACCCACCTCTTCCCTCCTA-3'). End-point fluorescence was applied to analyze the resulting products. A positive fluorescent response after the addition of an intercalant dye (post-amplification detection) was registered for all cases.

In the electrophoresis analysis, products were diluted in a loading buffer and transferred to an agarose gel (3%). After applying a 110 V potential

for 30 min, the gel was stained with a fluorescent dye (Real Safe staining, Durviz, Spain) and bands were observed in a 312 nm transilluminator (ECX-F20.M, Vilber, Germany).

A single band of 184 pb was observed for PCR products from LAMP amplifications under selective conditions (Figure S11). This length corresponds to the expected PCR product according to the sequence of the loop-structure for the GRIK4 gene. In case of false-positive LAMP products (non-optimal conditions), an unspecific band (about 90 pb) was detected. This band was associated to the formation of primer dimer complexes. Under the chosen conditions, no band was observed, confirming the amplification selectivity.

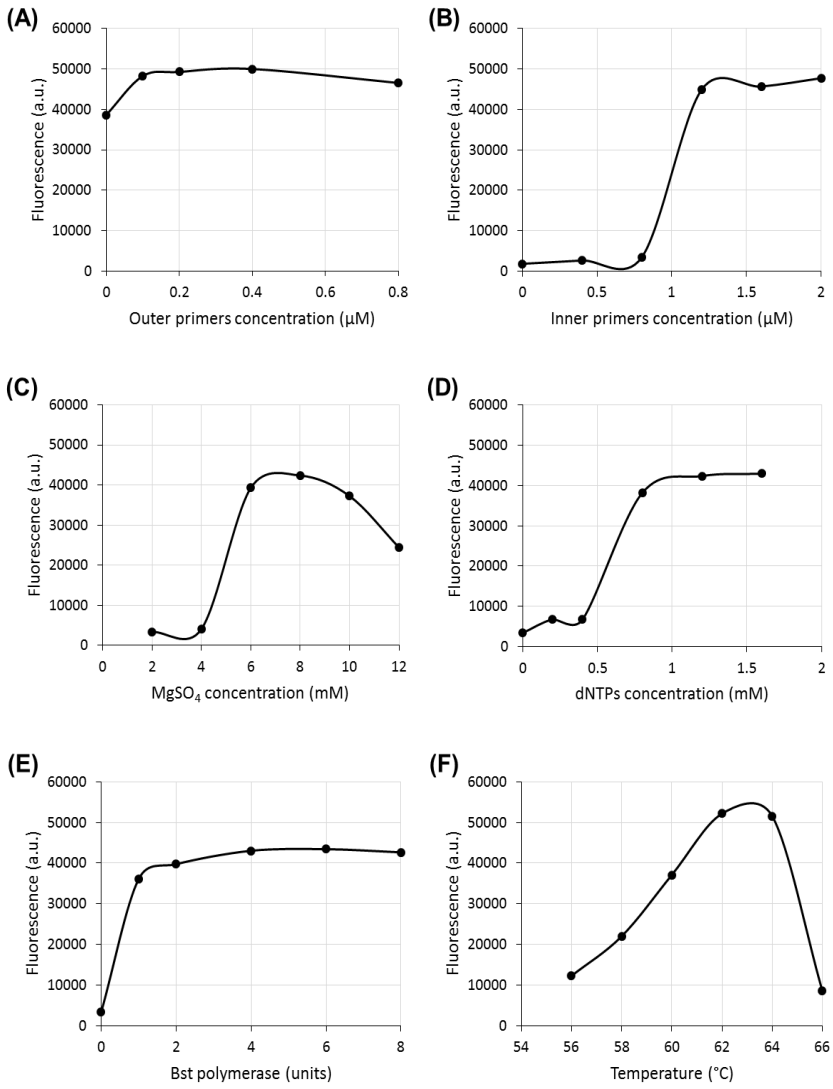


**Figure S10.** Effect of reaction composition on the amplification measured as fluorescence signal at end-point. (A) Outer primers concentration. (B) Inner primer concentration. (C) $MgSO_4$ concentration. (D) dNTPs concentration. (E) Enzyme amount. (F) Amplification temperature.

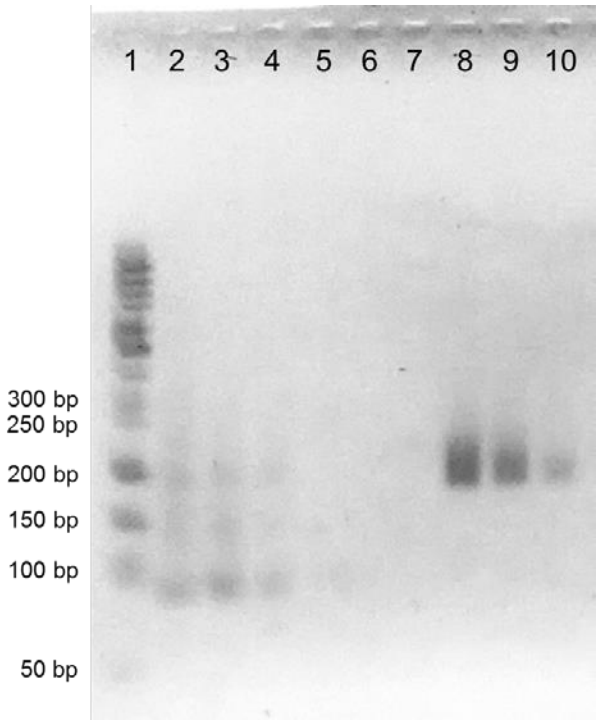


**Figure S11.** Image of agarose gel electrophoresis of post-amplification of LAMP products. Lane 1: DNA ladder standard; Lanes 2-4: negative samples amplified under non-selective conditions, Lane 5-7: negative samples amplified under selective conditions, Lanes 8-10: patient samples ($10^6$ to $10^4$ copies).

The end-point colorimetric detection of amplification products was performed by hybridization assay on a chip. Two formats were assayed depending on the post-amplification treatment, with or without thermal denaturation before the incubation on array. Statistical tests (paired test t) indicated that the spot signals were comparable for wild-type (t = -0.45, p-value = 0.66) and mutant samples (t = 0.57, p-value = 0.58). These results confirmed that the denaturation of LAMP products was unnecessary because the hybridization sequence is located in a single strand region of loop-products.

The final protocol starts with the dilution of LAMP products in a hybridization mix composed by formamide (30 %) and Denhardt's reagent (2.5×, Thermo Fisher Scientific, USA) in a sodium saline citrate buffer (SSC 1×: NaCl 150 mM, sodium citrate 15 mM at pH 7). Sessile droplets (15 µL) of each solution were directly dispensed over the chip microarrays and incubated at 37 °C for 60 min. The non-immobilized products were washed by gradually diluted SSC (0.1× and 0.01×) solutions and the chip was dried by centrifugation and submitted to the staining protocol.

For detecting the hybridized products of the LAMP-ASO method, an immunoassay followed by enzymatic staining was used. A recognition solution was made by diluting a sheep anti-digoxigenin primary antibody and an anti-sheep secondary antibody conjugated to horse radish peroxidase in phosphate buffered saline (phosphate 10 mM, NaCl 150 mM, 0.05 % Tween 20, pH 7.4). A fraction of this solution (15 µL) was then dispensed over each microarray and incubated at room temperature for 30 min. After washing with phosphate buffer and distilled water, 1 mL of a high sensitivity 3,3′,5,5′-tetramethylbenzidine substrate was spread over the chip surface and incubated for 2 min at room temperature, forming a blue precipitate over the positive spots. The chip was then washed with distilled water and dried by centrifugation (Figure S12). Therefore, specific molecular recognition was facilitated by the probe and product design.

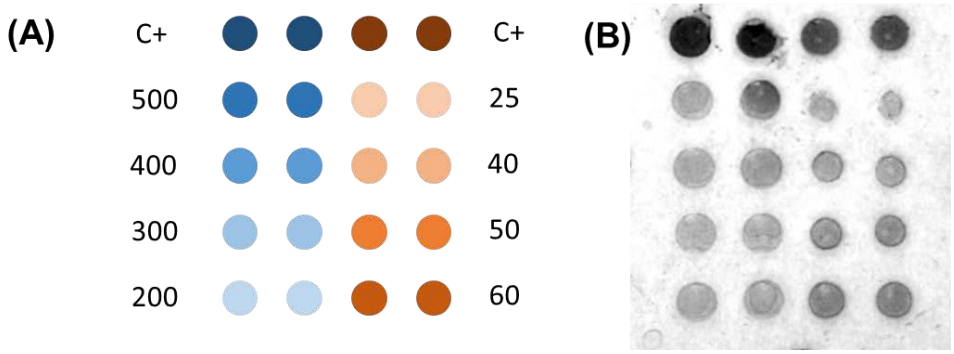


**Figure S12.** Colorimetric microarray detection of LAMP product. (A) Layout scheme: probe concentration (200-500 nM) and spot volume (25-60 nL). (B) Captured image.

## AS-LAMP METHODS. COMPLEMENTARY EXPERIMENTS

The isothermal nature of the LAMP mechanism makes the reaction selectivity highly dependent on the reaction conditions (*1*). In PCR approaches, an adequate design of allele specific primers can regulate the relative increment of copy number (*2*). For that, the set-up of allele specific amplification involved an exploration of experimental conditions. Wild-type and mutant DNA templates were amplified in reaction mixtures containing allele specific BIP and FIP primers (wild-type or mutant). The method optimization was based on the fluorescence response measurements, including a fluorescent intercalant dye in the reaction mixture (SYBR Safe, excitation 502 nm, emission 530 nm). The concentration of inner primers and enzyme produced an important variation on amplification yields. In addition, we observed that the increase on both variables led to a less selective assay. For instance, the amplification of a wild-type DNA template produced a similar signal for both reaction mixtures (Figure S13).

A selective fluorescent response was obtained for a primer concentration of 1.2 μM and 4 Bst polymerase units.

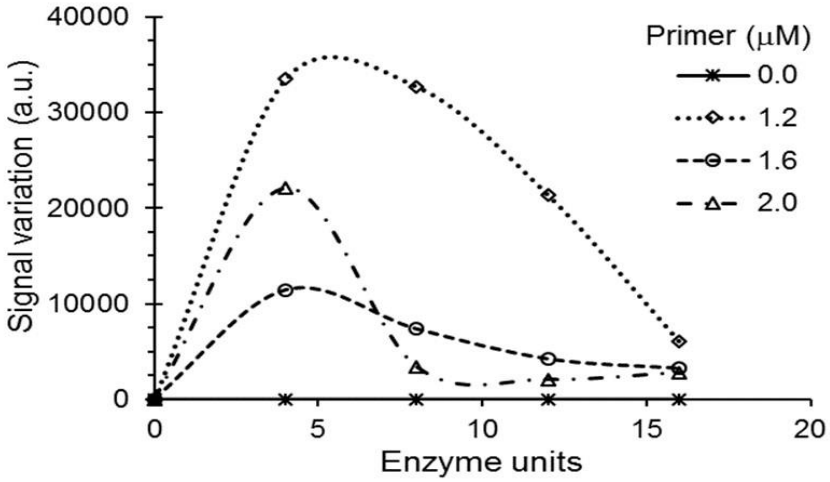


**Figure S13.** Effect of the Bst polymerase (enzyme units) and inner primer concentration (μM) on 5' LAMP selectivity. The signal represents the increment of fluorescence signal between a wild-type and mutant primer. Wild-type DNA template: 1,300 copies.

For ameliorating the assay selectivity, betaine was added to the reaction mixture. The objective was to reduce the formation of secondary structures that interfere in the selective amplification process. Low concentration of betaine produced false-positives (positive signal in negative controls). At concentrations higher than 1.5 M, only vials containing target alleles yielded a detectable amplification. For 5' AS-LAMP, high betaine concentrations also inhibited correct target template amplification, generating false-negatives. This effect could be related to the double allele-specific primers, and also to the unstable stem-loop structure required for this format, that is more susceptible to modifications on the medium conditions.

The next experiments were focused on the colorimetric detection LAMP products. The studied option was the color change of a magnesium indicator, concretely hydroxynaphtol blue (HNB). In the initial LAMP reaction mixture, the magnesium ions formed a complex with deoxynucleotides (dNTPs) and with HNB (violet). The elongation process produced pyrophosphate ($P_2O_7^{4-}$), which precipitated with magnesium ions, releasing HNB as a free-solution species (blue). Therefore, the system was based on the relative formation of three complexes: $Mg^{2+}$/HNB, $Mg^{2+}$/dNTPs and $Mg^{2+}$/pyrophosphate.

The concentration of reagents was examined, varying up to 12 mM of Mg salt and up to 2 mM of dNTPs (Figure S14). Under the selected conditions (8 mM and 1.2 mM, respectively), the amplification of target genes produced a sky-blue solution, distinguished from the violet solutions (initial reaction mixture). The HNB concentration was studied for improving the discrimination capability (Figure S15). Using concentrations higher than 60 µM, positive samples were identified by naked eye. Nevertheless, higher concentrations (> 300 µM) provided better results for smartphone detection.

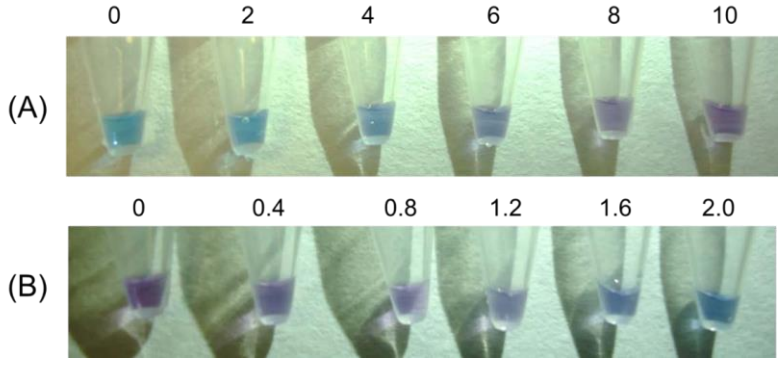


**Figure S14.** Effect of reagents concentration on the LAMP solution colour with hydroxynaphtol blue magnesium indicator: a) added $MgSO_4$ (mM) and b) dNTPs (mM).

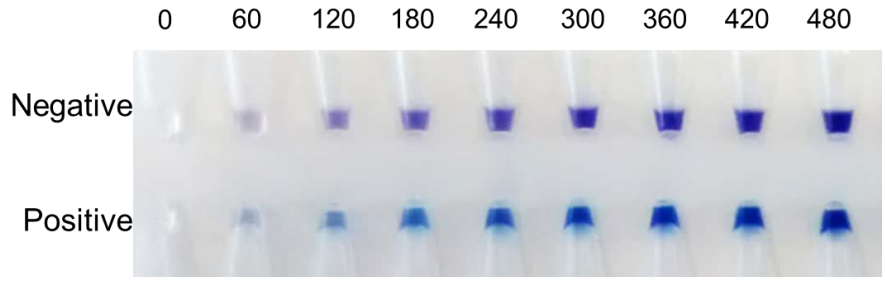


**Figure S15.** Effect of colorimetric dye concentration (μM) on negative (mismatch) and positive (perfect-match) samples.

**COMPARISON OF LAMP-BASED METHODS**

The estimated product sizes of the shorter products were 92, 139, 233 and 374 bp for ASO-LAMP; 84, 122, 208 and 322 bp for 3' AS-LAMP; and 70, 101, 170 and 271 bp for 5' AS-LAMP. In order to confirm the product formation, an agarose gel electrophoresis was performed (Figure S16). The image shows a different ladder-like band profile depending on the amplification approach. In a typical LAMP reaction, a base stem-loop is formed, whose size depends on FIP/BIP distance. In addition, the strand displacement activity and subsequent extensions produce some longer products. Therefore, a ladder-like profile is usually observed when analyzing the LAMP products by electrophoresis.

All the predicted bands were detected in the electrophoresis analysis, except for 84 and 70 bp bands for 3' and 5' AS-LAMP, respectively, indicating that in those formats the generation of higher size structures is favored.

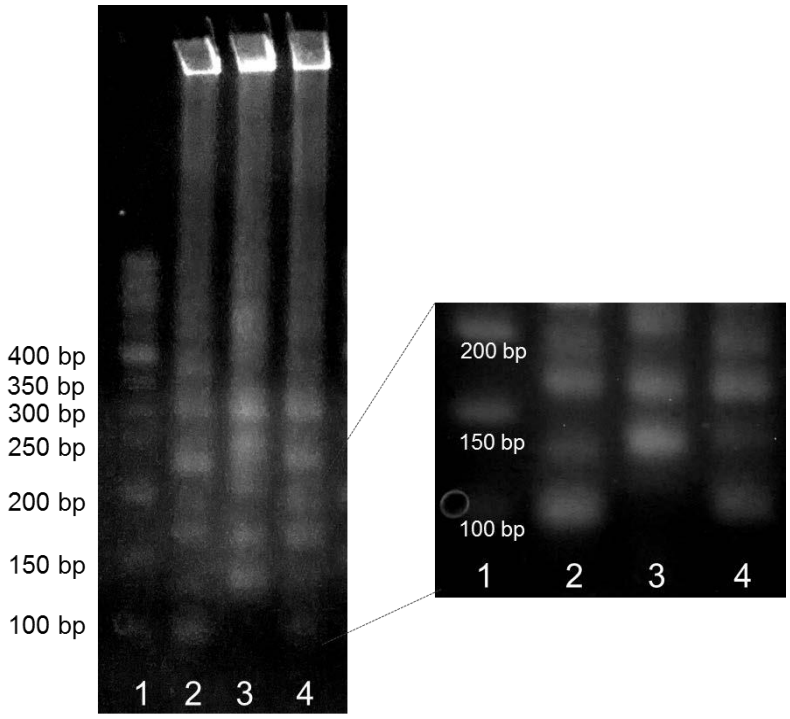


**Figure S16.** Image of agarose gel electrophoresis captured by the smartphone at normal zoom and with macro lens. Fluorescent dye: SYBR Safe. Lanes: 1. DNA ladder standard, 2. LAMP-ASO product, 3. 3' AS-LAMP product, 4. 5' AS-LAMP product. DNA template: 1,300 copies.

## SMARTPHONE DETECTION

The smartphone is a consumer electronic equipment for everyday use. The conversion of this electronic device into a DNA detection platform required to review their capabilities and to exploit the feasibility of their components (*8*, *9*). A reading assembly was designed and fabricated (Figure S17).

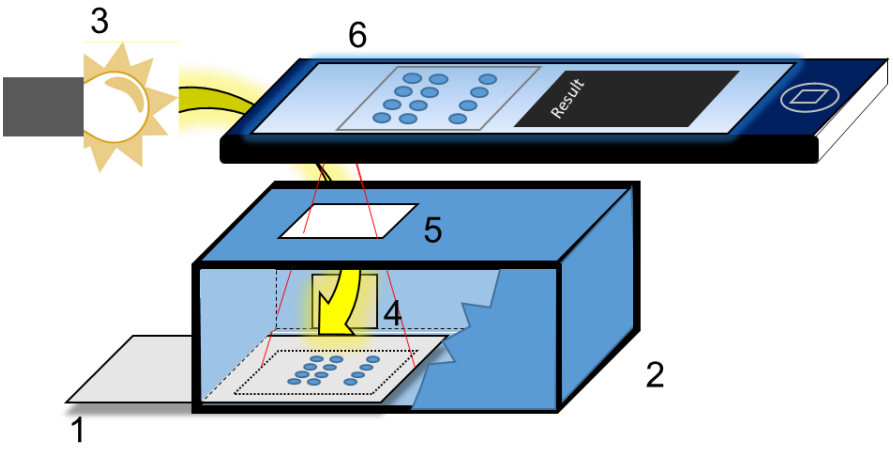


**Figure S17.** Detection assembly: 1. Assay chip, 2. Capture chamber, 3. Cold light source, 4. Illumination entrance, 5. Capture entrance, and 6. Smartphone. Drawing not to scale.

Following the guidelines of previous research (*6*, *7*), the experimental conditions of imagining were studied. A tailored assembly was designed for capturing the digital photography. Illumination conditions and chip distance were the most critical variables. Since the array support has a high reflectivity, direct frontal lighting by the smartphone LED was not possible without compromising the image quality. In this case, a cold light source was chosen at 20 W power and lateral angle (about 45 º). Several chip distances were assayed (3.0 – 8.0 cm). The best results were obtained at a distance of 5 cm. Regarding the direct colorimetric measurement, allele-specific LAMP products were repeatedly photographed with the smartphone camera. The imaging quality was evaluated in terms of channel intensities (red, green and blue channel) as function of light saturation (50 - 100%). A significant difference between negative and positive samples was observed in the red channel, while green and blue maintained a similar level in most cases. In

order to avoid negative signal differences, the red/green and red/blue ratios were used as the reference signal. A 75% light saturation produced the highest differences, reaching a 39.5 and 40.4 % variation for R/G and R/B ratios, respectively (Figure S18). For evaluating the reading robustness, the detection precision was determined by three measurements (3 replicates each) of negative and positive standards, carried out in three different days. The inter-sample and inter-day errors were similar (4.0 and 3.3 %, respectively). The results revealed that the measurement using smartphone camera was highly stable and precise, under the selected conditions.

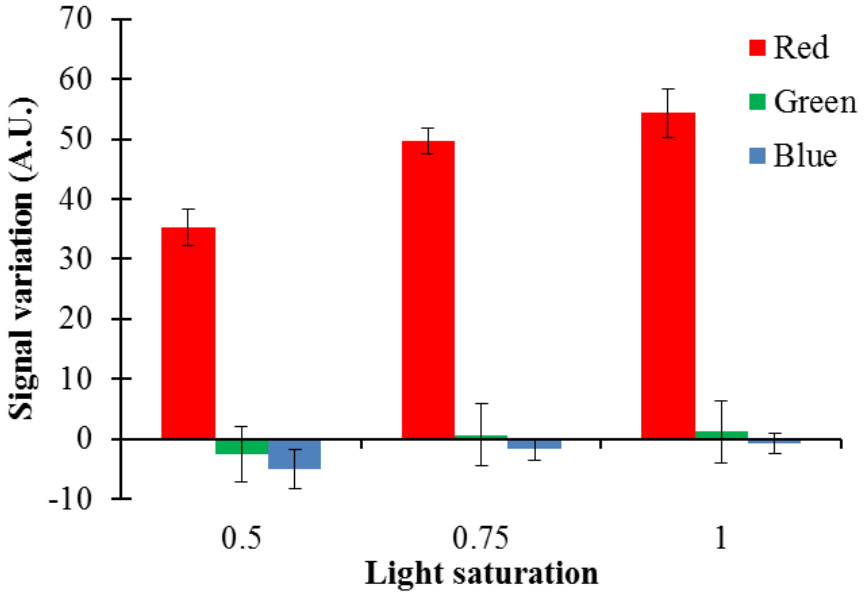


**Figure S18.** Signal variation for RGB channel varying the light saturation.

## REFERENCES


1. T. Notomi *et al.*, *Nucleic Acids Res.* **28**, e63 (2000).
2. D. M. Kawaguchi, S. J. Glatt, *Pharmacogenomics*. **15**, 1451–1459 (2014).
3. S. Paddock *et al.*, *Am. J. Psychiatry*. **164**, 1181–1188 (2007).
4. L. A. Tortajada-Genaro, R. Puchades, Á. Maquieira, *J. Pharm. Biomed. Anal.* **136**, 14–21 (2017).
5. J. I. Ruiz-Sanz *et al.*, *Mol. Cell. Probes*. **21**, 202–207 (2007).
6. S. Ikeda *et al.*, *Pathol. Int.* **57**, 594–599 (2007).
7. A. Badolo *et al.*, *Malar. J.* **14**, 1–8 (2015).
8. D. Erickson *et al.*, *Lab Chip*. **14**, 3159–3164 (2014).
9. F. M. Walker *et al.*, *Anal. Chem.* **86**, 9236–9241 (2014).

## 6.4 Annex 4
## SUPPLEMENTARY INFORMATION

# Consumer electronics devices for DNA genotyping based on loop-mediated isothermal amplification and array hybridization

Luis A. Tortajada-Genaro, Eric Seiti Yamanaka, Ángel Maquieira

### PRIMER DESIGN

The target polymorphism is rs1954787 located in the GRIK4 gene (Assembly: GRCh38.p7 Primary Locus: chr11:120792654) that codifies the glutamate receptor, ionotropic, kainate 4. The allele change is thymine (wild-type) to cytosine (mutant) (*1*).

The design of a LAMP reaction introduces several restrictions, as described in the first paper about this isothermal reaction (*2*, *3*). They include melting temperature, length and distances between primers. In order to develop a genotyping approach based on the LAMP-ASO method, additional restrictions were considered. The stem-loop product was designed to have the SNP in its loop region. Figure S19 shows the target regions for primer binding. Table S8 compares the recommended parameters for the LAMP primer design and the selected ones.

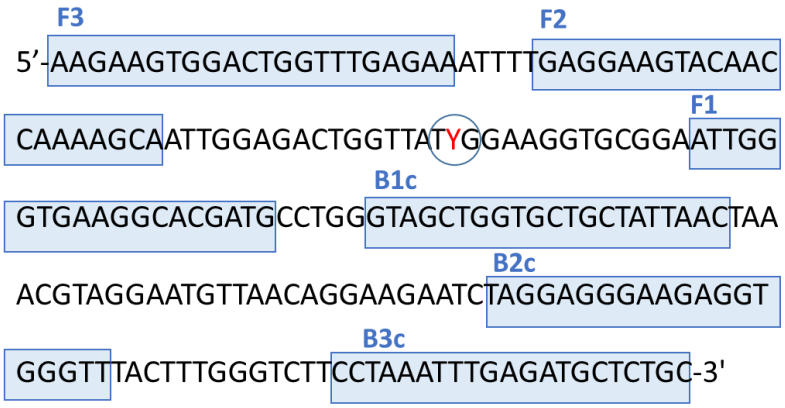


**Figure S19.** Partial sequence of the GRIK4 gene (direct strand). SNP position and LAMP recognition sites are indicated.

**Table S8.** Properties of the LAMP primers designed for the selective amplification of the GRIK4 gene.

| | | Recommended | Selected set |
|---|---|---|---|
| Length (nucleotides) | F1 and B1 | 18-22 | 19 and 21 |
| | F2 and B2 | 18-22 | 21 and 20 |
| | F3 and B3 | 19-22 | 22 and 21 |
| Melting temperature (ºC) | F1 and B1 | 50-66 | 57.5 and 59.5 |
| | F2 and B2 | 50-62 | 57.5 and 60.5 |
| | F3 and B3 | 50-60 | 58.0 and 57.5 |
| Distance (nucleotides) | F3-F2 and B3-B2 | 0-20 | 5 and 5 |
| | F2-F1 and B2-B1 | 20-40 | 29 and 29 |
| | F1-B1 | 0-20 | 5 |
| | F2-B2 | 100-160 | 103 |

Finally, probes were designed to hybridize the stem-loop product by its loop structure. The polymorphism was positioned at a central position to increase selectivity. To improve hybridization yields and to reduce the surface effect, a poly-thymine tail was incorporated into the 5’-end of the allele-specific probes.

Table S9 lists the oligonucleotides used for the amplification and hybridization assays, including the targeted genes and controls. A double labelled oligonucleotide was employed as the positive control. A negative control probe, with no complementarity to the amplification products, was also present in the array. The table includes the oligonucleotides used in the reference method (Sanger sequencing).

**Table S9**: List of the oligonucleotides for the wild-type (WT) and mutant (M) discriminations.

| **Method** | **Function** | **Sequence (5'-3')** |
|---|---|---|
| LAMP-ASO | FIP | CATCGTGCCTTCACCCAAT-GAGGAAGTACAACCAAAAGCA |
| | BIP | GTAGCTGGTGCTGCTATTAAC-AACCCACCTCTTCCCTCCTA |
| | F3 | AAGAAGTGGACTGGTTTGAGAA |
| | B3 | GCAGAGCATCTCAAATTTAGG |
| | WT-Probe | [BtnTg]-T10-AGACTGGTTAT-**T**-GGAAGGTGCGG |
| | M-Probe | [BtnTg]-T10-AGACTGGTTAT-**C**-GGAAGGTGCGG |
| | C+ | [BtnTg]-T10-TTGTCATGGGCCTCGTGTCGGAAAACC-Dig |
| | C- | [BtnTg]-T10-CAACCGCGAGAAGATGACCCAGATCA |
| Sequencing | FP | AAGAAGTGGACTGGTTTGAGAA |
| | RP | GCAGAGCATCTCAAATTTAGG |
| | Marker | GCAGAGCATCTCAAATTTAGG |

FIP: Forward inner primer; BIP: Backward inner primer; [Btn-Tg]: Biotin with a triethylene glycol spacer; T10: Thymine tail (10 nucleotides); [Dig]: Digoxigenin; C+: Positive control; C-: Negative control; FP: Forward primer, RP: Reverse primer.

## DNA AMPLIFICATION AND ON-CHIP HYBRIDIZATION

The reference assay was DNA array from the allele-specific hybridization of loop-mediated amplification method (LAMP) products. This technique is based on combining this isothermal DNA amplification and allele selective probes immobilized in a solid-phase format. The development experiments were divided into (1) assay optimization for isothermal DNA

amplification (LAMP), (2) allele-selective hybridization in a solid-phase format (DNA array) for discriminating nucleotide changes in the target sequence, and (3) a staining setup.

Isothermal amplification. As a typical LAMP reaction, four primers were used to recognize six different regions of a target sequence. An extension and strand displacement formed a stem-loop sequence, which acted as a self-primered structure that generated a second concatenated copy of itself. The inner primers were extended from the 5'-end of the loop by creating another single copy of the original structure. This process occurred exponentially at a constant temperature (62ºC) in a simple heating system. The electrophoretic separation of products confirmed the reliable amplification of the target region, and the shorter product length was 184 bp. The negative controls (no template and no human DNA) produced background yields (Student's *t*-test, $p<0.05$). As the polymerase (Bst polymerase) had a high processivity and turnover rate, the amplification yield rated $10^8$ times, independently of the wild-type or mutant allele. Real-time measurements confirmed the similar kinetic behavior for both templates, with saturation reached in 60 min (2,000 copies).

Verification of LAMP products. Amplification products were characterized by gel electrophoresis and real-time fluorescence. In the electrophoresis analysis, products were diluted in a loading buffer and transferred to agarose gel (3%). After applying a 110 V potential for 30 min, gel staining with fluorescent dye (Real Safe staining, Durviz, Spain) was employed and bands were observed in a 312 nm transilluminator (ECX-F20.M, Vilber, Germany). In the real-time experiments, assays were carried out in a 7500 Real-time PCR System (Applied Biosystems, USA) using 2x SYBR Safe as the reporter dye (502 nm/530 nm) and ROX as the reference dye (575 nm/602 nm). Fluorescence measurements were taken at 2-minute

intervals for a total time of 90 min at a constant temperature of 62ºC. The results were expressed in terms of ΔRn, calculated as the reporter signal normalized with the reference signal, corrected with the baseline.

Chip fabrication. Allele-specific probes (single-base mismatch) were anchored to the chip surface via streptavidin/biotin chemistry. Experiments showed that appropriate results were obtained by immobilizing the streptavidin/allele-specific probe complexes at a concentration of 10 mg/L and 100 nM, respectively. The selected microarray format had a spot diameter of 450 μm, a center-to-center distance of 1 mm and 4 replicates/probe.

Chip hybridization. In order to improve the signal-to-noise ratios, the recognition of LAMP products to on-chip probes was enhanced in relation to the conventional array approaches. Primers were designed by considering the dumbbell-like structure of the LAMP product by locating the target polymorphism in a single strand loop region (between regions F2 and F1). The hybridization experiments of these amplification products showed a higher response (20%) compared to the conventional approach. Furthermore, the intermediate thermal denaturalization step was not required, which implied a 15-minute faster method.

Chip staining. The selected approach was based on labelling LAMP products during amplification, and on the hybridization complexes being recognized with peroxidase-conjugated antibodies. A sensitive peroxidase substrate was employed to produce blue stable precipitates ($\lambda_{max}$ = 650 nm) over 450 μm array spots in less than 2 minutes.

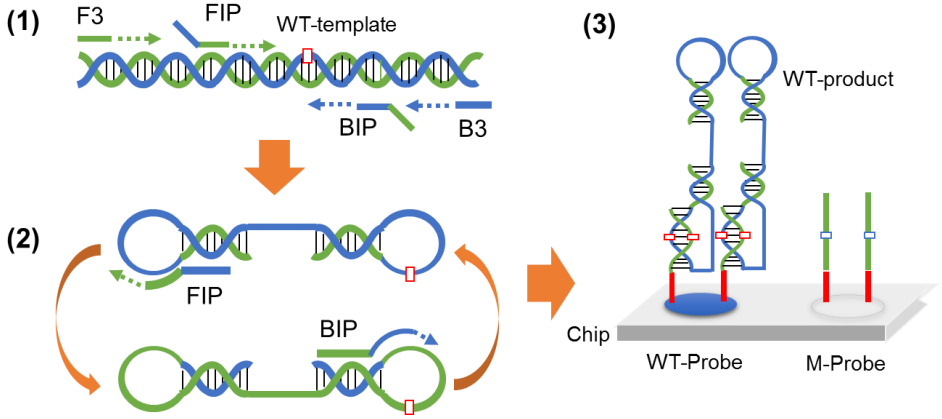


**Figure S20.** Scheme of the ASO-LAMP method. (1) The forward and backward outer primers (F3 and B3) are used to displace the inner-extended sequences (FIP and BIP primers). (2) The generated stem-loop structures are further duplicated by additional reaction cycles. (3) The LAMP product hybridizes to the allele-specific probe immobilized on the chip surface.

## READING PRINCIPLE OF THE CHIP ARRAY SENSORS

Four consumer electronic technologies were examined to image the DNA arrays: Portable microscope, smartphone, documental flatbed scanner and DVD drive (Figure S21).

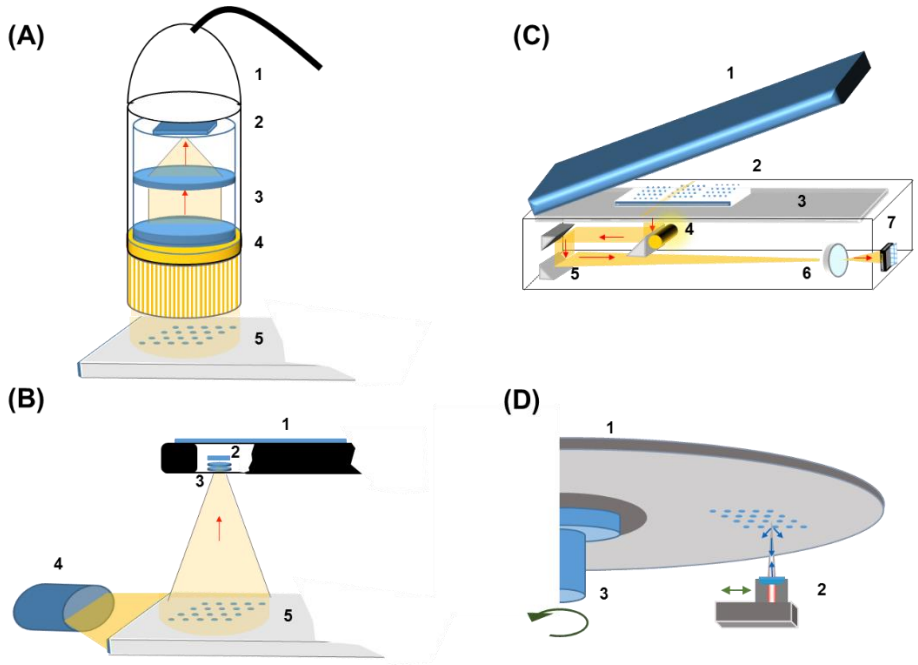


**Figure S21.** Reading schemes by sensing devices (not on scale): (A) Portable microscope: 1. USB connection; 2. CMOs chip; 3. Internal lens; 4. Illumination ring; 5. Assay chip. (B) Smartphone reading stand: 1. Smartphone screen; 2. CMOs chip; 3. Internal lens; 4. External illumination; 5. Assay chip. (C) Documental flatbed scanner: 1. Cover lid; 2. Assay chip; 3. Glass screen; 4. Lamp; 5. Mirrors; 6. Lens; 7. CCD chip. (D) DVD drive: 1. Disc with array on bottom layer; 2. DVD pick-up; 3. Rotor.

Applying the optimized protocol to patient samples, a chip with a specific hybridization profile was obtained. A heterozygous patient leads to positive spots for both probes: wild-type (WT) and mutant (M). A homozygous patient yields positive spots only for the corresponding probe (perfect match). Following the guidelines of previous research and the results of our own studies (*4*, *5*), the detection conditions were examined to capture the images of the microarrays on chips. Model chips were prepared for the hybridization of different amounts of LAMP products on the chip surface. Figure S22 shows the assay images displayed by the different reading devices.

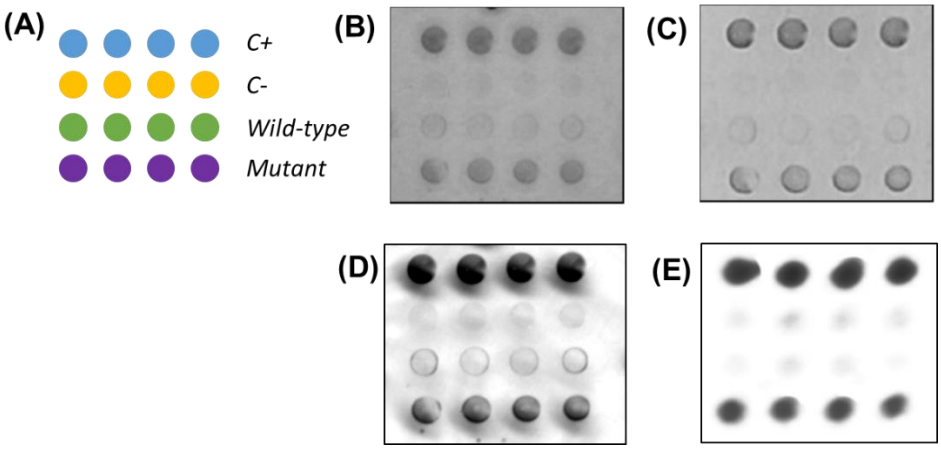


**Figure S22.** Captured chip images: (a) microarray layout, (b) USB digital-microscope, (c) smartphone, (d) flatbed scanner and (e) DVD reader.

## REFERENCES

1. E. Milanesi *et al.*, *Genet. Res. (Camb).* **97**, e14 (2015).
2. T. Notomi *et al.*, *Nucleic Acids Res.* **28**, e63 (2000).
3. L. A. Tortajada-Genaro, R. Puchades, Á. Maquieira, *J. Pharm. Biomed. Anal.* **136**, 14–21 (2017).
4. F. M. Walker *et al.*, *Anal. Chem.* **86**, 9236–9241 (2014).
5. L. A. Tortajada-Genaro *et al.*, *RSC Adv.* **5**, 29987–29995 (2015).